The only thing that will redeem mankind is cooperation.

– Bertrand Russell, 1954.

University of Alberta

Performance Evaluation and Protocol Design of Fixed-Rate and Rateless Coded Relaying Networks

by

Reza Nikjah

A thesis submitted to the Faculty of Graduate Studies and Research
in partial fulfillment of the requirements for the degree of

Doctor of Philosophy

in

Communications

Department of Electrical and Computer Engineering

Spring 2011
Edmonton, Alberta

Examining Committee

Norman C. Beaulieu, Electrical and Computer Engineering

Andreas F. Molisch, Electrical Engineering, University of Southern California

Byron Schmuland, Mathematical and Statistical Sciences

Chintha Tellambura, Electrical and Computer Engineering

Yindi Jing, Electrical and Computer Engineering

Dedicated to

my beloved parents and sisters.

Abstract

The importance of cooperative relaying communication in substituting for, or complementing, multiantenna systems is described, and a brief literature review is presented.

Amplify-and-forward (AF) and decode-and-forward (DF) relaying are investigated and compared for a dual-hop relay channel. The optimal strategy, source and relay optimal power allocation, and maximum cooperative gain are determined for the relay channel. It is shown that while DF relaying is preferable to AF relaying for strong source-relay links, AF relaying leads to more gain for strong source-destination or relay-destination links.

Superimposed and selection AF relaying are investigated for multirelay, dual-hop relaying. Selection AF relaying is shown to be globally strictly outage suboptimal. A necessary condition for the selection AF outage optimality, and an upper bound on the probability of this optimality are obtained. A near-optimal power allocation scheme is derived for superimposed AF relaying.

The maximum instantaneous rates, outage probabilities, and average capacities of multirelay, dual-hop relaying schemes are obtained for superimposed, selection, and orthogonal DF relaying, each with parallel channel cooperation (PCC) or repetition-based cooperation (RC). It is observed that the PCC over RC gain can be as much as 4 dB for the outage probabilities and 8.5 dB for the average capacities. Increasing the number of relays deteri-

orates the capacity performance of orthogonal relaying, but improves the performances of the other schemes.

The application of rateless codes to DF relaying networks is studied by investigating three single-relay protocols, one of which is new, and three novel, low complexity multirelay protocols for dual-hop networks. The maximum rate and minimum energy per bit and per symbol are derived for the single-relay protocols under a peak power and an average power constraint. The long-term average rate and energy per bit, and relay-to-source usage ratio (RSUR), a new performance measure, are evaluated for the single-relay and multirelay protocols. The new single-relay protocol is the most energy efficient single-relay scheme in most cases. All the multirelay protocols exhibit near-optimal rate performances, but are vastly different in the RSUR.

Several future research directions for fixed-rate and rateless coded cooperative systems, and frameworks for comparing these systems, are suggested.

Acknowledgments

I would like to offer my sincere thanks to my supervisor, Dr. Norman C. Beaulieu, for his valuable support and advice in the course of my Ph.D. program. I learned and gained enormously from his wide knowledge and experience.

I would also like to thank Dr. Andreas F. Molisch, Dr. Byron Schmuland, Dr. Chintha Tellambura, and Dr. Yindi Jing for accepting to be a member of the examining committee and review my thesis.

Many thanks are dedicated to all my colleagues and friends in the Informatics Circle of Research Excellence (*i*CORE) Wireless Communications Laboratory (*i*WCL), who helped me in my academic endeavors and provided a motivating research environment.

Last but not least, I would like to express my deepest gratitude for all the encouragement and devotion I received from my loving parents and sisters.

This thesis was financially supported by the Alberta Ingenuity Fund and the *i*CORE Graduate Student Scholarship Award.[†]

[†]Alberta Ingenuity and *i*CORE are now part of Alberta Innovates - Technology Futures.

Table of Contents

1 Introduction **1**

1.1 Cooperative Communication 1

1.2 Literature Review: Pioneering Research 3

1.3 Subject and Scope 4

1.4 Contributions and Outline 5

2 Basic AF and DF Relaying Strategies **9**

2.1 Introduction 9

2.2 Dual-Hop AF and DF Relaying 11

2.2.1 The AF Relaying Case 13

2.2.2 The DF Relaying Case 15

2.2.3 Numerical Examples 17

2.3 Benefits of Relaying and CG 18

3 Dual-Hop AF Relaying Networks **24**

3.1 Introduction 24

3.2 System Model and Problem Formulation 27

3.3 Selection AF Suboptimality 32

3.4 Proposed Suboptimal Scheme 33

4 Dual-Hop DF Relaying Networks **38**

4.1 Introduction 38

4.2 System Model 40

4.2.1 Complexity Issues 44

4.3 Maximum Achievable Instantaneous Rates 45

4.3.1 Superimposed Relaying . . . 45
4.3.2 Selection Relaying . . . 48
4.3.3 Orthogonal Relaying . . . 49
4.4 Capacity Analysis . . . 50
4.4.1 General Fading Case . . . 51
4.4.2 Rayleigh Fading Case . . . 54
4.5 Numerical Results . . . 66

5 Rateless Coded Relaying: Single-Relay Case 73
5.1 Introduction . . . 73
5.2 Channel Model and Definitions . . . 75
5.3 Rateless Coded Protocols . . . 78
5.3.1 The DT Scheme . . . 79
5.3.2 The P-1 Scheme . . . 81
5.3.3 The P-2 Scheme . . . 82
5.3.4 The P-3 Scheme . . . 84
5.4 Feedback Requirements and Effects . . . 85
5.5 Power Fairness . . . 86
5.6 Energy Efficiency . . . 86
5.6.1 Minimum Energy per Bit Under the PPC . . . 87
5.6.2 Maximum Rate Under the APC . . . 88
5.7 Long-Term Average Behavior . . . 90
5.7.1 Long-Term Average Rate . . . 91
5.7.2 Long-Term Average Energy per Bit . . . 92
5.7.3 The RSUR . . . 92
5.8 Numerical Examples . . . 94
5.8.1 Discussion on Rate and Energy Efficiency . . . 100

6 Rateless Coded Relaying: Multirelay Case 101
6.1 Introduction . . . 101
6.2 System Model . . . 103
6.3 Rateless Coded Selection Strategies . . . 104
6.3.1 General Description . . . 104

6.3.2 Mathematical Description . . . 105
6.3.2.1 The P-n Scheme . . . 105
6.3.2.2 The P-γ Scheme . . . 106
6.3.2.3 The P-t Scheme . . . 106
6.4 Performance Analysis . . . 108
6.4.1 The P-n Scheme . . . 109
6.4.2 The P-γ Scheme . . . 110
6.4.3 The P-t Scheme . . . 111
6.4.4 The P-o Scheme . . . 111
6.4.5 Single-Relay Case . . . 112
6.4.6 Optimal Parameters . . . 113
6.4.6.1 Experimental Steepest-Descent Optimization . . . 113
6.4.6.2 Analytical Optimization: Large SNR Approximations . . . 114
6.5 Numerical Examples . . . 115
6.5.1 Numerical Optimization of the Parameters . . . 117
6.5.2 Performance Comparison . . . 121
6.6 Design and Performance Implications . . . 124

7 Conclusions and Future Research Directions 125
7.1 Conclusions . . . 125
7.2 Possibilities for Future Research . . . 130
7.2.1 Multisource Cooperation . . . 130
7.2.2 Small and Large SNR Characterization . . . 131
7.2.3 Opportunistic Rateless Coded Relaying . . . 132
7.2.4 Comparing Fixed-Rate and Rateless Coded Relaying Networks . . . 132
7.2.5 Optimal Power Allocation . . . 133
7.2.6 Rateless Coded Multihop Relaying Networks . . . 134

References 135

Appendix A Maximum Likelihood Detection in Dual-Hop DF Relaying 140

Appendix B Proof of Theorem 2.1 (Best Strategy and CG in Dual-Hop AF/DF Relaying) 143

Appendix C Proof of Theorem 3.1 (Necessary Condition for Selection AF Optimality) 148

Appendix D Proof of Theorem 3.2 (Selection AF Asymptotically Strict Suboptimality) 149

Appendix E Average Capacities of DF Relaying Networks for Rayleigh Fading 152

E.1 Superimposed Relaying 153

E.2 Selection Relaying 155

E.3 Orthogonal Relaying 156

Appendix F Maximum Rates in P-1, P-2, and P-3 Under the APC 160

F.1 The P-1 Scheme 160

F.2 The P-2 Scheme 163

F.3 The P-3 Scheme 165

Appendix G Expected Values of the Transmission Times in P-n, P-γ, and P-t 169

G.1 The P-n Scheme 169

G.2 The P-γ Scheme 170

G.3 The P-t Scheme 172

List of Tables

4.1 Maximum Instantaneous Rates in Multirelay, Dual-Hop, DF Relaying Networks 46

4.2 Outage Probability for Superimposed Relaying in the Rayleigh Fading Case 58

4.3 Average Capacity for Superimposed Relaying in the Rayleigh Fading Case 59

4.4 Outage Probability for Selection Relaying in the Rayleigh Fading Case . . . 60

4.5 Average Capacity for Selection Relaying in the Rayleigh Fading Case 61

4.6 Outage Probability for Orthogonal Relaying With the SD Link in the Rayleigh Fading Case 62

4.7 Average Capacity for Orthogonal Relaying With the SD Link in the Rayleigh Fading Case 63

4.8 Outage Probability for Orthogonal Relaying With No SD Link in the Rayleigh Fading Case 64

4.9 Average Capacity for Orthogonal Relaying With No SD Link in the Rayleigh Fading Case 65

5.1 Different Transmission Schemes With Their Average Rates and Energies per Symbol 79

5.2 Features of the Different Transmission Schemes 80

List of Figures

2.1 A dual-hop diversity relay channel. 10
2.2 The effect of power optimization in AF and DF relaying. 18
2.3 The error floor in DF relaying. 19
2.4 Time-bandwidth dimensionality for cooperative transmission and DT, and the corresponding link SNRs. 20
2.5 Cooperative gain versus the SD full-power SNR, and the optimal relaying strategies. 22
2.6 Cooperative gain versus the SR full-power SNR, and the optimal relaying strategies. 22
2.7 Cooperative gain versus the RD full-power SNR, and the optimal relaying strategies. 23

3.1 The network configuration and corresponding channel complex gains. 25
3.2 The outage probability versus the number of relays for selection and optimal superimposed AF relaying for a symmetric case in Rayleigh fading channels. 33
3.3 The outage probability versus the fading severity for selection and optimal superimposed relaying for Nakagami fading channels. 34
3.4 The outage probability versus the number of relays for the selection, optimal superimposed, and proposed schemes for a symmetric case in Rayleigh fading channels. 36

4.1 The system model, and the corresponding SNRs of the links. 40
4.2 The relaying protocols. 42

4.3 The outage probability versus the average SD SNR for the different protocols and two-relay case. 67
4.4 The average capacity versus the average SD SNR for the different protocols and two-relay case. 68
4.5 The outage probability versus the SR distance for the different protocols and a linear network topology in the symmetric case. 70
4.6 The average capacity versus the SR distance for the different protocols and a linear network topology in the symmetric case. 70
4.7 The outage probability versus the number of relays for the different protocols in the symmetric case. 71
4.8 The average capacity versus the number of relays for the different protocols in the symmetric case. 72

5.1 The rate region for the multiaccess channel from the source and relay to the destination. 83
5.2 The long-term average rate under the PPC versus the average SD SNR for DT, P-1, P-2, and P-3. 95
5.3 The long-term average energy per bit under the PPC versus the average SD SNR for DT, P-1, P-2, and P-3. 96
5.4 The long-term average rate under the APC versus the average SD SNR for DT, P-1, P-2, and P-3. 96
5.5 The RSUR versus the average SD SNR for P-1, P-2, and P-3. 97
5.6 The long-term average rate under the PPC versus the SR distance for DT, P-1, P-2, and P-3, and a linear network topology. 98
5.7 The long-term average energy per bit under the PPC versus the SR distance for DT, P-1, P-2, and P-3, and a linear network topology. 99
5.8 The long-term average rate under the APC versus the SR distance for DT, P-1, P-2, and P-3, and a linear network topology. 99
5.9 The RSUR versus the SR distance for P-1, P-2, and P-3, and a linear network topology. 100

6.1 The optimal parameters of P-γ and P-t versus the average SD SNR. 116

6.2 The optimal parameter of the P-n scheme versus the average SR and RD SNRs. 118
6.3 The optimal parameter of the P-n scheme versus the number of relays and average SD SNR. 118
6.4 The optimal parameter of the P-γ scheme versus the average SR and RD SNRs. 119
6.5 The optimal parameter of the P-γ scheme versus the number of relays and average SD SNR 119
6.6 The optimal parameter of the P-t scheme versus the average SR and RD SNRs. 120
6.7 The optimal parameter of the P-t scheme versus the number of relays and average SD SNR. 120
6.8 The average transmission rate versus the average SD SNR for DT, P-n, P-γ, P-t, and P-o. 122
6.9 The RSUR versus the average SD SNR for P-n, P-γ, P-t, and P-o. 122
6.10 The average transmission rate versus the number of relays for P-n, P-γ, P-t, and P-o. 123
6.11 The RSUR versus the number of relays for P-n, P-γ, P-t, and P-o. 123

F.1 The ranges of branches of the Lambert W-function. 162

List of Symbols

$(\cdot)^*$	The complex conjugate.	15
$(\cdot)^{\mathrm{H}}$	The conjugate transpose.	26
$(\cdot)^{\mathrm{T}}$	The transpose.	26
$\succ$	Componentwise inequality for vectors, and positive or negative definiteness for matrices.	27
$\succeq$	Componentwise inequality for vectors, and nonnegative or nonpositive definiteness for matrices.	27
$\lvert\cdot\rvert$	The cardinality operator for a set.	56
$\lvert\cdot\rvert$	The componentwise absolute value for vectors.	26
$\mathbf{A}$	A matrix defined by (3.10).	30
$\mathcal{A}^{\mathrm{c}}$	Complement of $\mathcal{A}$ with respect to $\{1, \cdots, M\}$.	56
$\mathbf{a}$	A vector defined in (3.9).	29
α	The path loss exponent.	69
B_i	The source's ith message or the rateless encoded block for the ith message.	78
$\mathbf{b}$	A vector defined in (3.9).	29
b_1	Data bit 1 of a QPSK symbol from the source.	13
$\hat{b}_1$	The decision that the relay makes about b_1.	15
b_2	Data bit 2 of a QPSK symbol from the source.	13
$\hat{b}_2$	The decision that the relay makes about b_2.	15
β	The relay amplification gain in an AF single-relay network.	13
β_m	The amplification gain at R_m.	28
$\mathcal{C}(\cdot)$	A function defined by (5.7e).	77
$C(\gamma)$	Capacity per 2-D DoF of a single-hop AWGN link with SNR γ.	104

C_0	Capacity of the SD link.	77
C_1	Capacity of the SR link.	77
C_2	Capacity of the RD link.	77
C_{m}	Sum-rate capacity of the multiaccess channel from the source and relay to the destination.	77
$\mathbf{D}$	A matrix defined by (3.11).	30
$\mathcal{D}(t)$	Set of the indices of all decoding relays at time t, in rateless coded relaying.	105
$\acute{\mathbf{D}}$	A matrix defined by (3.16c).	31
$\mathbf{d}$	Vector $(\sqrt{k_1}, \cdots, \sqrt{k_M})$.	29
d_{RD}	The RD distance.	69
d_{SD}	The SD distance.	69
d_{SR}	The SR distance.	69
$\delta(\cdot)$	The Dirac delta function.	55
$\mathrm{diag}\{\cdot\}$	An operator mapping a vector $\mathbf{w}$ to a diagonal matrix whose main diagonal vector is $\mathbf{w}$.	26
E	The total energy expended per 2-D DoF in a CR in rateless coded relaying.	77
$\mathrm{E}\{\cdot\}$	The expectation operator.	13
$\mathcal{E}$	The energy per 2-D DoF at any node in rateless coded relaying.	76
$\mathcal{E}_0$	Total energy budget of the source and relay per transmission.	12
$\mathcal{E}_{\mathrm{R}}$	The (aggregate) energy per transmission at the relay(s).	12
$\mathcal{E}_{\mathrm{S}}$	The energy per transmission at the source.	12
$\mathbf{e}_i$	A vector having 1 at the ith component and zero elsewhere.	27
$\epsilon_{(m)\mathrm{D}}$	The $\epsilon_{i\mathrm{D}}$ corresponding to $\epsilon_{\mathrm{S}(m)}$.	114
$\epsilon_{m\mathrm{D}}$	The value x obtained by solving (6.33) for $\mu_{\mathrm{sub}} = \mu_{m\mathrm{D}}$.	114
$\epsilon_{\mathrm{S}(m)}$	The mth smallest among $\epsilon_{\mathrm{S}1}, \ldots, \epsilon_{\mathrm{S}M}$.	114
ϵ_{SD}	The value x obtained by solving (6.33) for $\mu_{\mathrm{sub}} = \mu_{\mathrm{SD}}$.	114
$\epsilon_{\mathrm{S}m}$	The value x obtained by solving (6.33) for $\mu_{\mathrm{sub}} = \mu_{\mathrm{S}m}$.	114
ϵ_{sub}	The point x at which $u_{\mathrm{sub}}(x)$ reaches its maximum.	114
EB	The short-term average energy per bit in a CR.	78
$\mathrm{EB}_{\mathrm{avg}}$	The long-term average energy per bit in rateless coded relaying.	78

$\mathrm{EB}_{\min}$	The minimum possible EB in a CR.	78
$\mathrm{EB}_{\min}[i]$	The $\mathrm{EB}_{\min}$ realized in the ith CR.	92
$F_{1+Y\text{-prod}}(\cdot)$	The CDF of $\prod_{m=1}^{M}(1+Y_m)$.	157
$F_{\mathcal{A}\text{-RD}}(\cdot)$	The CDF of $\sum_{m\in\mathcal{A}}\gamma_{m\mathrm{D}}$.	159
$F_{\ln 1+Y\text{-sum}}(\cdot)$	The CDF of $\sum_{m=1}^{M}\ln(1+Y_m)$.	53
$F_{m\text{-RD}}(\cdot)$	The CDF of the sum of m different $\gamma_{i\mathrm{D}}$'s.	154
$F_{m\mathrm{D}}(\cdot)$	The CDF of $\gamma_{m\mathrm{D}}$.	54
$F_{\mathrm{RD}}(\cdot)$	The CDF of γ_{RD}.	55
$F_{\mathrm{SD}}(\cdot)$	The CDF of γ_{SD}.	54
$F_{\mathrm{S}m}(\cdot)$	The CDF of $\gamma_{\mathrm{S}m}$.	54
$F_{\mathrm{SR}}(\cdot)$	The CDF of γ_{SR}.	55
$F_{Y\text{-sum}}(\cdot)$	The CDF of $\sum_{m=1}^{M}Y_m$.	52
$F_{Y_m}(\cdot)$	The CDF of Y_m.	53
$f_{\mathrm{SD}}(\cdot)$	The PDF of γ_{SD}.	52
$g(\cdot;\cdot,\cdot,\cdot)$	A definite integral defined by (4.68).	57
$G_{\mathrm{S}m}$	A value defined by (3.6b) or (3.6c).	28
$\Gamma(\cdot)$	The gamma function.	56
$\Gamma(\cdot,\cdot)$	The upper incomplete gamma function.	56
g_0	Complex gain of the SD link in a single-relay network.	11
g_1	Complex gain of the SR link in a single-relay network.	11
g_2	Complex gain of the RD link in a single-relay network.	11
$g_{m\mathrm{D}}$	Complex gain of the link $\mathrm{R}_m\mathrm{D}$.	27
$g_{\mathrm{S}m}$	Complex gain of the link SR_m.	27
γ	A channel-gain-independent SNR defined by (5.6).	76
$\boldsymbol{\gamma}$	The channel state $(\gamma_{\mathrm{SD}},\gamma_{\mathrm{S1}},\ldots,\gamma_{\mathrm{S}M},\gamma_{1\mathrm{D}},\ldots,\gamma_{M\mathrm{D}})$.	43
$\gamma_{(m)\mathrm{D}}$	The RD SNR corresponding to $\gamma_{\mathrm{S}(m)}$.	45
γ_0	The SD full-power SNR.	14
γ_1	The SR full-power SNR.	14
γ_2	The RD full-power SNR.	14
γ_{eq}	The equivalent SNR per symbol between the source and destination in AF relaying.	13

$\gamma_{\mathrm{eq,b}}$	The equivalent SNR per bit between the source and destination in AF relaying. 13
$\gamma_{m\mathrm{D}}$	The SNR associated to the link R$_m$D. 33
γ_{RD}	The RD SNR per symbol. 13
$\gamma_{\mathrm{RD,b}}$	The RD SNR per bit. 13
$\gamma_{\mathrm{S}(m)}$	The mth largest SNR among $\gamma_{\mathrm{S}1}, \ldots, \gamma_{\mathrm{S}M}$. 45
γ_{SD}	The SD SNR per symbol. 13
$\gamma_{\mathrm{SD,b}}$	The SD SNR per bit. 13
$\gamma_{\mathrm{S}m}$	The SNR associated to the link SR$_m$. 32
γ_{SR}	The SR SNR per symbol. 13
$\gamma_{\mathrm{SR,b}}$	The SR SNR per bit. 13
γ_{th}	Parameter of P-γ. 106
$\gamma_{\mathrm{th,opt}}$	Optimal value of γ_{th}. 114
H	Entropy of the source message. 75
$\mathrm{H}(\cdot)$	The Heaviside step function. 114
$h(\cdot;\cdot,\cdot)$	A definite integral defined by (4.67). 56
$\mathcal{I}_{\cdot}(\cdot,\cdot,\cdot,\cdot)$	A definite integral defined by (4.64). 56
$\mathcal{I}_{\cdot}(\cdot,\cdot,\cdot,\cdot,\cdot)$	A definite integral defined by (4.63). 56
$I_{\mathrm{DL}}(R)$	The maximum downlink MI in DF relaying that the destination can gather when the source's rate is R. 43
$\mathbf{I}_M$	The identity matrix of order M. 31
$I_{\max}$	The maximum achievable instantaneous MI between the source and destination. 19
$\overline{I_{\max}}$	The average capacity, or expectation of $I_{\max}$ with respect to the channel state $\boldsymbol{\gamma}$. 42
$\mathrm{Im}\{\cdot\}$	The imaginary part. 16
K	A parameter defined in (2.35). 20
k_m	Power allocation ratio of the mth relay. 28
$k_{\mathrm{opt}}^{(\mathrm{AF})}$	The OPA ratio between the source and relay in an AF single-relay network. 14
$k_{\mathrm{opt}}^{(\mathrm{DF})}$	The OPA ratio between the source and relay in a DF single-relay network. 145

L	Parameter of P-n.	105
L_1	A parameter defined in (2.33).	20
L_2	A parameter defined in (2.34).	20
L_{opt}	Optimal value of L.	114
$\mathbf{\Lambda}$	A matrix defined by (3.29c).	35
M	Number of relays in a multirelay network.	27
$M_{\ln 1+Y\text{-sum}}(\cdot)$	The MGF of $\sum_{m=1}^{M} \ln(1+Y_m)$.	54
$M_{m\text{D}}(\cdot)$	The MGF of $\gamma_{m\text{D}}$.	54
$M_{Y\text{-sum}}(\cdot)$	The MGF of $\sum_{m=1}^{M} Y_m$.	54
μ_0	Mean of γ_0.	77
μ_1	Mean of γ_1.	77
μ_2	Mean of γ_2.	77
$\mu_{\mathcal{A}\text{D}}$	A value defined by (4.61).	56
$\mu_{m\text{D}}$	Mean of $\gamma_{m\text{D}}$.	54
μ_{RD}	Mean of γ_{RD}.	55
$\mu_{\text{S}\mathcal{A}}$	A value defined by (4.60).	56
$\mu_{\text{S}\mathcal{B}}$	A value defined by (4.60).	63
μ_{SD}	Mean of γ_{SD}.	54
$\mu_{\text{S}m}$	Mean of $\gamma_{\text{S}m}$.	54
μ_{SR}	Mean of γ_{SR}.	55
μ_{sub}	Mean of γ_{sub}.	114
N_0	One-sided PSD of the AWGN, common to all channels.	77
N_{D}	One-sided PSD of n_{D}.	29
N_m	One-sided PSD of n_m.	28
N_{SD}	Variance of n_{SD}.	13
N_{SR}	Variance of n_{SR}.	13
n_{D}	The AWGN at the destination from the transmissions of AF relays.	29
n_m	The AWGN at R$_m$.	28
n_{RD}	The noise term at the destination from the relay transmission.	13
n_{SD}	The noise term at the destination from the source transmission.	13
n_{SR}	The noise term at the relay.	13

ν	A parameter defined by (4.39b).	51
P	Power of each node in a multirelay network.	76
$P(\cdot,\cdot)$	The regularized lower incomplete gamma function.	56
P_{e}	The BER.	16
$P_{\mathrm{e}}^{(\mathrm{SR})}$	The BER at the relay.	15
P_{out}	The outage probability.	32
P_{R}	Aggregate power of the relays.	28
$\Pr\{\cdot\}$	The probability operator.	15
$\mathrm{Q}(\cdot)$	The standard Gaussian Q-function.	16
R	The rate per 2-D DoF in a CR in rateless coded relaying.	76
$\mathcal{R}(\cdot,\cdot,\cdot)$	A definite integral defined by (4.66).	56
$\mathcal{R}(\cdot,\cdot,\cdot,\cdot,\cdot)$	A definite integral defined by (4.65).	56
R_{avg}	The long-term average rate per 2-D DoF in rateless coded relaying.	77
R_m	The mth relay.	27
$R_{\max}$	The maximum possible R in a CR.	77
r_{RD}	The signal received at the destination from the relay.	13
r_{SD}	The signal received at the destination from the source.	12
r_{SR}	The signal received at the relay.	12
$\mathrm{Re}\{\cdot\}$	The real part.	16
$\mathcal{S}(\cdot)$	A function defined by (4.69).	57
T	Duration of a CR in rateless coded relaying.	76
$\mathcal{T}(\cdot,\cdot)$	A function defined by (4.70).	57
$T[i]$	Value of T in the ith CR.	90
T_{DL}	The downlink duration (duration of Phase II) in rateless coded relaying.	108
T_{R}	Duration of the relay transmission in a CR in rateless coded relaying.	90
$T_{\mathrm{R}}[i]$	Value of T_{R} in the ith CR.	90
T_{R_m}	Duration of the R_m transmission in a CR in rateless coded relaying.	109

T_{S} Duration of the source transmission in a CR in rateless coded relaying. 90

$T_{\mathrm{S}}[i]$ Value of T_{S} in the ith CR. 90

T_{UL} The uplink duration (duration of the source broadcasting) in rateless coded relaying. 105

t_0 Parameter of P-t. 106

$t_{0,\mathrm{opt}}$ Optimal value of t_0. 114

$\tau_{m\mathrm{D}}$ A notation defined by (6.4). 109

τ_{RD} A notation defined by (6.4). 112

$\tau_{\mathrm{S}(m)}$ In rateless coded relaying, the time duration in the uplink after which the mth relay decodes. 106

τ_{SD} The DT time, defined by (6.4). 106

$\tau_{\mathrm{S}m}$ A notation defined by (6.4). 109

τ_{SR} A notation defined by (6.4). 111

τ_{sub} A notation defined by (6.4). 104

τ_{th} A notation defined by (6.4). 110

$\tau_{\mathrm{th,opt}}$ Optimal value of τ_{th}. 114

$\tau_{X\mathrm{D}}$ A notation defined by (6.4). 107

$\Theta_{\cdot}(\cdot)$ A function defined in (6.11). 107

$U_{m\mathrm{D}}(\cdot)$ The CDF of $\tau_{m\mathrm{D}}$. 109

$U_{\mathrm{SD}}(\cdot)$ The CDF of τ_{SD}. 109

$U_{\mathrm{S}m}(\cdot)$ The CDF of $\tau_{\mathrm{S}m}$. 109

$U_{\mathrm{sub}}(\cdot)$ The CDF of τ_{sub}. 114

$u_{m\mathrm{D}}(\cdot)$ The PDF of $\tau_{m\mathrm{D}}$. 109

$u_{\mathrm{SD}}(\cdot)$ The PDF of τ_{SD}. 109

$u_{\mathrm{S}m}(\cdot)$ The PDF of $\tau_{\mathrm{S}m}$. 109

$u_{\mathrm{sub}}(x)$ The PDF of γ_{sub}. 114

W The system bandwidth. 27

$W(\cdot)$ The (zeroth branch of the) Lambert W-function. 161

$\mathrm{W}_k(\cdot)$ The kth branch of the Lambert W-function. 89

$\mathbf{w}^+$ Vector $(\max\{w_1, 0\}, \cdots, \max\{w_M, 0\})^{\mathrm{T}}$. 27

x_{S} A source's 2-D symbol. 28

ξ	A value defined by (5.39c).	89
Y_m	Effective cascaded link SNR of the mth branch in a dual-hop DF relaying system.	51
y_{D}	The signal received at the destination from the transmissions of AF relays.	29
y_m	The signal received at R_m	28

List of Abbreviations

2-D	two-dimensional	12
ACK	acknowledgment signal	80
AF	amplify-and-forward	2
APC	average power constraint	74
AT	above-threshold	106
AWGN	additive white Gaussian noise	12
BER	bit error rate	10
BPSK	binary phase shift keying	12
CDF	cumulative distribution function	52
CDMA	code division multiple access	4
CF	compress-and-forward	2
CG	cooperative gain	11
CR	cooperation round	12
CSCG	circularly symmetric complex Gaussian	13
CSI	channel state information	5
DF	decode-and-forward	2
DoF	degree of freedom	19
DSTC	distributed space-time coding	4
DT	direct transmission	2
EB	energy per bit	78
FISC	fixed-rate coded selection cooperation	133
LT	Luby-transform	73
MAI	multiaccess interference	4
MGF	moment generating function	54

MI	mutual information	3
MIMO	multi-input, multi-output	1
ML	maximum likelihood	6
MRC	maximal ratio combining	6
MUD	multiuser detection	80
OPA	optimal power allocation	6
PCC	parallel channel cooperation	39
PDF	probability density function	52
PPC	peak power constraint	74
PSD	power spectral density	28
QPSK	quadrature phase shift keying	11
R_mD	R_m-destination	27
RC	repetition-based cooperation	39
RD	relay-destination	11
RSUR	relay-to-source usage ratio	90
RV	random variable	13
SD	source-destination	11
SNR	signal-to-noise ratio	6
SR	source-relay	11
SR_m	source-R_m	27

Chapter 1

Introduction

1.1 Cooperative Communication

Multimedia services of seamless fourth-generation wireless communication networks require larger data rates and better sustainable qualities of service. This necessitates more prudent economical use of network resources such as time, bandwidth, energy, and space. On the other hand, the capacity of multiaccess wireless channels is mostly restricted by the transmitter power, channel impairments, and interference. Utilizing multiple, almost independent, receptions of a transmitted signal, widely known as diversity, is a recognized way of overcoming these limitations.

Diversity is implemented in a variety of forms including time, frequency, and multipath diversities. Spatial diversity in multiantenna or multi-input, multi-output (MIMO) systems is possibly one of the most brilliant kinds of diversity ever devised. It makes use of different independent paths in free space, which is abundantly available to communicating parties, to provide multireception at the receiver.

Spatial diversity can be easily coupled with other kinds of diversity to enhance the capacity without much additional complexity. However, while it offers spatial diversity, conventional MIMO communication contends with a number of deficiencies. First, it cannot overcome severe shadowing between the transmitter and receiver as all the physical antennas that make the communication feasible are concentrated at either the transmitter or the receiver. Second, MIMO systems leave the everlasting crucial demand for light and small mobile communicating equipment almost unanswered since they basically require mobile devices to accommodate more than one transmitting/receiving antenna. Although

the numerous advantages of MIMO systems may sometimes outweigh these deficiencies, devising substitute methods for attaining nearly the same benefits, while also combating shadowing and avoiding actual multiantenna equipment in a node, sounds promising. Cooperative communication has been proposed to achieve this objective.

Relaying channels are the building blocks of cooperative communication. The classic relay channel consists of a source, a destination, and a relay that assists the source, e.g. by relaying its message to the destination. Depending on whether the relay amplifies and forwards, decodes and forwards, or quantizes/compresses and forwards, the information received, the relaying is called amplify-and-forward (AF), decode-and-forward (DF), or compress-and-forward (CF) relaying, respectively. General relay channels are more complex and exploit several relays to assist one or more sources by passing their messages.

Relays can also have their own messages to send, and become sources of information. What essentially happens in these situations is that several sources pool their resources to reliably send each other's messages to the corresponding destinations. In fact, two or more nodes share their antennas to form a virtual array and imitate MIMO systems.

The important role of relaying in ad hoc networks is prevalent and undeniable since the nodes themselves act as switches and routers for each other. Relays can be utilized equally well in cellular networks and sensor networks where power consumption is a concern.

One of the main rationales behind relaying is to create a new form of diversity, called distributed spatial diversity or user cooperative diversity. Cooperative diversity is the natural result of benefiting from other users' antennas, which can provide the destination with fresh replicas of the transmitting signal. Besides the inherent diversity gain, other benefits of relaying, directly or indirectly brought about by cooperative diversity, include economical power consumption by multihop routing, and combating shadowing effects in the channel between the transmitter and receiver.

Resilience against shadowing is a key difference between multinode cooperative systems and conventional MIMO communication, and represents one of the important motivations behind cooperation. As explained above, conventional MIMO systems are susceptible to severe direct-link shadowing. Severe shadowing can hamper conventional single-hop communication such that neither multiantenna transmission nor coding can improve direct transmission (DT) substantially. However in cooperation, if the direct link is blocked, the communication may be still feasible through distributed relaying nodes. Indeed, if the

quality of service has to be sustained under severe shadowing, collaborative transmission appears to be an inevitable solution, rather than a mere substitute or complement to multi-antenna systems.

Cooperative relaying communication also becomes more persuasive and appealing if the use of multiple antennas in the system is prohibited by hardware physical limitation.

In contrast to MIMO schemes, one major challenge in cooperative networks is the noisy fading channel among distributed shared antennas of different nodes. Therefore, MIMO systems may be considered as ideal collaborative networks, whereas collaborative networks can be regarded as distributed MIMO systems.

It may first seem on the surface that cooperation incurs increased power consumption due to sources sending each other's messages as well as their own. However, it has paradoxically been demonstrated that energy can be considerably saved in the system owing to the dominance of the cooperative diversity gain. In fact, it has been confirmed that two major benefits brought about by cooperation in different channel scenarios include larger data rates and less sensitivity to channel variations. Therefore, cooperative diversity has the potential of being exploited in lieu of or along with MIMO spatial diversity. One drawback of cooperation is its unavoidable signal processing delay. However, it may be argued that for most practical purposes this delay is tolerable and outweighed by the cooperative gain.

1.2 Literature Review: Pioneering Research

While Meulen introduced the concept of relaying by analyzing a three-terminal network and obtaining bounds on the mutual information (MI) flow among the nodes [1], [2], Cover and El Gamal were first to introduce and comprehensively analyze the classic relay channel [3]. The development in [3] embraced many ideas that appeared later in the literature. The authors analyzed their relay scheme in a static channel from an information-theoretic viewpoint, and derived upper and lower bounds on the capacity of the relay channel, and in some limited cases, found the exact capacity. It was assumed that the relay assistance takes the form of facilitation, cooperation, or observation.

Some achievable rates for multirelay scenarios with DF and CF relaying were derived in [4]. The authors also developed some DF and CF strategies for relay channels, multi-access relay channels, and broadcast relay channels. In [5], a three-node relay channel in

a Rayleigh fading environment was examined, and, partly by invoking the results in [3], several upper and lower bounds on the outage and ergodic capacities were derived.

Cooperative networks were first considered and analyzed for cellular environments in [6], [7], where the merit of cooperation was demonstrated in achieving significantly larger rates than conventional DT, and less sensitivity to channel variations. The authors considered a generalized feedback model, introduced in [8], for a two-user cooperation and obtained maximum achievable rates for the partners. They also proposed a code division multiple access (CDMA) framework for collaboration. Cooperation in ad hoc networks was considered in [9], [10], where several novel cooperative protocols based on AF and DF relaying were proposed, and their outage probabilities and diversity orders were obtained. It was assumed that each node is allotted one of available orthogonal time or frequency channels so that multiaccess interference (MAI) is avoided.

Coding techniques in relaying constitute another important part of advancement in the theory of cooperative communication. In fact, collaboration gain on the one hand, and immense coding gain on the other hand, motivated many researchers into devising efficient schemes and strategies for applying coding to cooperation. Some of these techniques and protocols include distributed space-time coding (DSTC) [9], [11]–[14], dynamic DF relaying [15], coded cooperation [12], [16]–[19], parity forwarding [20], and rateless coded cooperation [21], [22].

Research in the area of cooperative communication has been very active, leading to a myriad of results, insights, and novel designs in addition to the aforementioned. Other literature reviews relevant to the topic of the thesis are presented in the introduction sections of the subsequent chapters.

1.3 Subject and Scope

The topic of the dissertation is restricted in scope to the following:

- We only consider dual-hop AF or DF relaying, where there is a source of information, a destination, and one or more relays that can assist the source by communicating its message to the destination in dual-hop links using an AF or a DF operation. Note that cooperative networks can be considerably large and complex. Dual-hop networks can be viewed as one of the building blocks of larger networks. They have cheaper

and less complex network coordination, implementation, and routing, and provide distributed spatial diversity, described in Section 1.1. Also, AF and DF relaying have attracted major attention to date owing to their simplicity and/or performance approaching the channel capacity in some cases.

- Only half-duplex relays are considered; i.e. relays that cannot simultaneously transmit and receive on the same frequency band. The possibility of full-duplex operation, i.e. simultaneous transmission and reception on the same band, for small communication devices is implausible due to current practical radio limitations, including insufficient isolation between the transmitting and receiving circuitries [6], [7], [23].

- Physical layer performance evaluation, protocol design, and network routing techniques constitute the topics investigated in the dissertation. Other functionalities and issues in other communication layers, such as the problem of cooperative partner selection, network traffic management and scheduling, the network lifetime, and cross-layer design, are not considered.

- We assume for simplicity that relays do not have or transmit messages of their own. In other words, multisource scenarios are not discussed. Nonetheless, many schemes and protocols considered and proposed in the thesis can be straightforwardly extended to multisource cases.

1.4 Contributions and Outline

The thesis has seven chapters, where the last chapter is devoted to a summary of the results and contributions in the thesis, as well as suggestions for future research. In Chapters 2–4, relaying networks with so-called *fixed-rate* codes are considered, while Chapters 5 and 6 are devoted to DF relaying networks with so-called *rateless* codes. Fixed-rate coding refers to conventional coding schemes in which the code rate is predetermined or preset at the transmitter. In contrast, rateless codes, which represent a fairly new approach to the concept of coding, do not have a preset rate at the transmitter. The realized rate is automatically adapted to the channel condition even if the transmitter does not have channel state information (CSI). Rateless coding has been shown to have great potential for integrating with DF relaying. Note that the term “fixed-rate” used in the literature to contrast with the term

"rateless" does not imply that the transmitter cannot or does not change the code rate. It only means that the transmitter presets and knows the code rate before transmission.

A summary of the material and contributions presented in Chapters 2–6 is outlined in order as follows:

- In Chapter 2, a single-relay AF/DF relaying network is considered. It is shown that AF relaying may outperform DF relaying under either an unreliable source-relay (SR) link or a suboptimal power allocation between the source and relay. Otherwise, DF relaying is superior. In DF relaying, a maximal ratio combining (MRC) receiver at the destination, which is not a maximum likelihood (ML) structure in this application, has an error floor at large signal-to-noise ratios (SNRs). True ML detection at the destination can remove this error floor, but cannot always make the performance of DF relaying surpass that of AF relaying. The exact optimal power allocation (OPA) is also obtained for dual-hop AF relaying. Conditions under which AF or DF relaying, under a short-term power constraint, increases the achievable MI between the source and destination are derived. The optimal strategy, the OPA ratio between the source and relay, and the maximum cooperative gain are determined for each case. It is shown that DF relaying is preferable to AF relaying in the case of a strong SR link, whereas the AF operation leads to more collaborative gain in the case of strong source-destination or relay-destination links. The cooperative gain provides a quantitative measure for choosing the best relay among a set of available candidate relays.

- The problem of relay power optimization in superimposed AF relaying is investigated in Chapter 3. In superimposed AF relaying, the source transmission is orthogonal to the relay transmissions but the relay transmissions are nonorthogonal and superimposed. The power optimization problem is formulated as a nonconcave fractional program. Selection AF relaying is a possible power allocation strategy, which allocates the whole available power to a single relay in each cooperation round. A necessary condition for the optimality of the selection AF power allocation is derived in terms of instantaneous channel coefficients, based on which, an upper bound on the selection AF optimality probability is calculated. The upper bound approaches zero exponentially as the number of relays increases, showing that selection AF relaying is asymptotically strictly suboptimal. Selection AF relaying has been previously shown

to be optimal under the constraints of localized channel information at the relays and a constant relay power allocation template. A suboptimal power allocation, which is significantly superior to the selection AF algorithm in terms of outage performance, is also proposed for superimposed AF relaying.

- In Chapter 4, the average achievable rate of multirelay, dual-hop, DF relaying networks is analyzed for block fading channels. Different cases of superimposed, selection, and orthogonal DF relaying are investigated. Parallel channel cooperation (PCC) and repetition-based cooperation (RC) are considered for each case. Closed-form expressions for the instantaneous achievable rates in each case are obtained. The outage probabilities and average rates of the different schemes are derived for Rayleigh fading. Also, the PCC over RC gain and the effect of increasing the number of relays on the performances are investigated.

- In Chapter 5, rateless coded, dual-hop DF single-relay networks are explored. Rateless codes do not have a preset rate at the transmitter, in contrast to fixed-rate codes, and have great potential for integrating with DF relaying. Three single-relay schemes, called P-1, P-2, and P-3, are introduced, where P-1 and P-2 are taken from prior research, but P-3 is proposed here, based upon P-1 and P-2 and opportunistic communication. The P-3 scheme is simpler and generally has better energy efficiency compared to its predecessors. We derive the maximum instantaneous achievable rate and minimum instantaneous energy per symbol of the protocols. It is observed that greater rates are achieved at the cost of larger energy expenditure. To compare the protocols fairly on a power basis, two new techniques are developed; 1) comparison between the minimum energies per bit of the protocols; and 2) comparison of the achievable rates under an average power constraint (APC). Both minimum energy per bit, and maximum rate under the APC are derived for the three protocols. Also, to examine the long-term behavior of the protocols we consider the long-term average rate and energy per bit, as well as a newly developed metric, relay-to-source usage ratio (RSUR), showing the amount of relay usage relative to source usage. We derive expressions for calculating the average rate and the RSUR. Our numerical results show that P-3 exhibits superior energy efficiency compared to P-1 and P-2 in most cases. We also study the optimal positioning of the relay in the different protocols

that yields the best rate or energy performances for a linear network topology.

- In Chapter 6, we extend P-3 of Chapter 5 to three novel, low complexity, multirelay protocols, denoted P-n, P-γ, and P-t. The protocols, each having a single design parameter, rely on selection cooperation, and are differentiated based on their stopping strategies for the source broadcasting period. They all become P-3 in the single-relay case, if used with their optimal parameters which are trivially obtained. The protocols are generally rate suboptimal, except for the single-relay case where they can reduce to P-3. We derive a rate optimal protocol, P-o, from P-3, and use it as a baseline for performance comparison. We also derive analytical expressions for the average transmission time of the source and each of the relays, from which the average rate and the RSUR of the protocols can be calculated. Based on the analysis developed, large SNR approximations to the optimal parameters of the protocols that maximize the average rate are obtained. The approximations are good for large SNR scenarios, and satisfactory for small and medium values of SNR. The optimal parameters are also numerically studied for a wide range of the numbers of relays and the link qualities. We use the average rate and the RSUR to study the long-term behavior of the protocols. It is observed that the rate performances of the suboptimal protocols are close to the optimal behavior, with P-γ performing slightly better than the others. However, the RSUR performances vastly differ. We observe that P-o and P-n have the largest and smallest source usage relative to relay usage, respectively. Also, in all the protocols the source is less utilized for medium values of SNR.

Chapter 2

Basic AF and DF Relaying Strategies[1]

2.1 Introduction

Fig. 2.1 illustrates a dual-hop relaying scheme where the relay, Node R, assists the source, Node S, in communicating its message to the destination, Node D. This scheme is considered a diversity relay channel as the destination utilizes both signals received from the source and relay. In this chapter, we consider AF and repetition DF relaying [10] in which the relay forwards the source's whole message, either a noisy version or a regenerated one.

In recent years, much research has been devoted to devising efficient protocols capable of best exploiting the inherent synergy and diversity gain of relaying [4], [6], [7], [9]–[11], [16], [19], [24]–[29]. Several collaborative protocols based on AF relaying, DF relaying, and DSTC were proposed in [9], [10]. It was shown that even with basic relaying operations, considerable gain can be achieved. Also, various adaptive and hybrid relaying protocols based on AF relaying, DF relaying, and code combining were proposed in [26], and their capacity regions were derived and compared. In [11], based on varying the nodes involved in the broadcast and multiple access portions of the relay channel, three cooperative protocols employing an AF or DF relay were examined, and their performances were compared in terms of the ergodic capacity, outage capacity, and spatial diversity.

Many researchers investigated and compared AF and DF relaying in various scenarios

[1] *A version of this chapter has been published in the Proceedings of the IEEE Global Telecommunications Conference (GLOBECOM), 2006.*

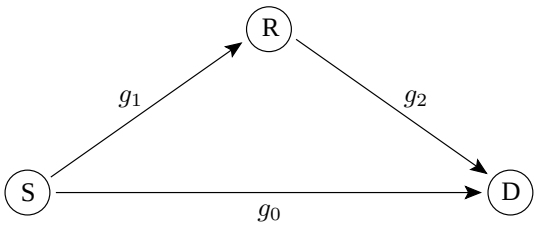

Fig. 2.1. A dual-hop diversity relay channel.

[27], [30]–[34]. Multihop relaying with and without diversity was investigated in [27]. It was found that AF relaying excels in fading diversity relay channels. Moreover, in fading relay channels without diversity, power optimized AF relaying can outperform power-suboptimal DF relaying [30]. Also, in fading nondiversity channels DF relaying is superior to AF relaying in terms of the average bit error rate (BER) and outage probability at small average values of SNR, but both exhibit similar performances at large average values of SNR [31]. In [32], it was shown that AF relaying generally outperforms or performs as well as repetition DF relaying in terms of network coding gain. In [33], the authors pointed out that AF and DF relaying can offer similar benefits. They demonstrated their results in a particular scenario. In [34], the impact of the relay location on the system capacity and outage probability was examined for AF and DF relaying. It was found that each of AF and DF relaying can outperform the other depending on the relay location. Favorable relay positionings for AF and DF relaying were also discussed.

Meanwhile, proper resource allocation in cooperative networks has been shown to significantly improve gain, especially for resource constrained networks such as sensor networks, and has received considerable attention in the literature [30], [35]–[40]. A comprehensive survey of power optimization and its importance in cooperative networks was presented in [35]. Optimal power allocation for Rayleigh fading multihop relay channels was examined in [30] with the outage probability as the optimization criterion, and the enormous gain of power optimization was established for highly asymmetric link strengths or a large number of hops. In [36], based on an asymptotic analysis of the outage probability for large values of SNR, OPA for the multirelay protocols introduced in [9] was derived in terms of mean channel gains. Moreover, the importance of the direct link between the source and destination in power allocation, and the significant asymptotic gain brought about by power optimization were demonstrated [36]. The large SNR gain of OPA or near-optimal power allocation over equal power allocation in dual-hop diversity relay networks was shown in

[37], where SNR maximizing power allocation schemes were developed for AF and DF, uncoded and coded, systems. In [38], a utility maximization framework for jointly optimizing relay selection, relaying strategy, and the allocation of power, bandwidth, and rate in a cellular network with AF or DF relaying was proposed. In the framework proposed, a pricing structure was used to decompose the cross-layer optimization problem into application layer and physical layer subproblems. In [39], a numerical power optimization for AF and DF relaying for maximizing instantaneous equivalent SNR between the source and destination was performed. Also in [40], relay OPA and optimal bandwidth allocation for maximizing the total system rate under a total network power budget were derived for AF and DF multirelay scenarios and static channels. The two cases of shared bandwidth and orthogonal channels for the relays were considered.

In this chapter, it is shown in Section 2.2 that guaranteeing the superiority of DF relaying over AF relaying in terms of the equivalent SNR requires both source-relay (SR) link reliability and power optimization between the source and relay. Otherwise, AF relaying may outperform DF relaying. Moreover, it is shown for DF relaying and quadrature phase shift keying (QPSK) modulation that ML detection can gracefully remove the error floor experienced with MRC at the destination. It is well known that MRC is not an ML detection in this application [6], [7], [24], [41] and the cause of the error floor at large values of SNR is shown to be the MRC detection at the destination. However, it is shown that with an unreliable SR link, even ML detection may not make DF relaying surpass AF relaying in the error-floor region. The exact OPA for maximizing the instantaneous end-to-end SNR in dual-hop AF relaying is also derived.

Subsequently, exact quantitative conditions under which AF or DF relaying is advantageous are obtained in Section 2.3. The communication strategy and power allocation are jointly optimized, and the maximum cooperative gain (CG), under a total power constraint and under the condition that three options for communication are available, DT, AF relaying, and DF relaying, is derived.

2.2 Dual-Hop AF and DF Relaying

Consider Fig. 2.1 where the source-destination (SD), SR, and relay-destination (RD) links have complex gains of g_0, g_1, and g_2, respectively. We consider the case of fixed channel

gains. This case is widely considered in the literature [5], [37], [40], and leads to tractable, closed-form solutions.[2]

Motivated by the enormous potential of collaboration in energy-limited networks with simple nodes such as sensor networks [4], [9], [25], [35], [42]–[46], we assume that the source and relay have a total energy budget of $\mathcal{E}_0$ per transmission, and that the relay is half-duplex (see Section 1.3). We also assume that

$$\mathcal{E}_{\mathrm{S}} = k\,\mathcal{E}_0 \tag{2.1}$$

and

$$\mathcal{E}_{\mathrm{R}} = (1-k)\,\mathcal{E}_0 \tag{2.2}$$

where $\mathcal{E}_{\mathrm{S}}$ and $\mathcal{E}_{\mathrm{R}}$ are the energies per transmission at the source and relay, respectively, and $k \in (0, 1]$ is a power allocation ratio.

The transmission scheme is based on orthogonal relaying as in [10], in which the cooperation round (CR) is split into two consecutive equal time slots. During the first slot, the source broadcasts its message to the relay and destination, and during the second slot, the relay assists the source by relaying the source's message using an AF or DF scheme.

Throughout, two-dimensional (2-D) symbols are assumed for transmission. In this section, and only for illustration, we consider QPSK modulation at the source and relay.[3] Channel state information is only available to the corresponding receivers, and, therefore, no beamforming is performed at the transmitters. Also, all transmissions are narrowband, and distorted by flat fading and additive white Gaussian noise (AWGN). Now, the baseband equivalent signals received at the relay and destination from the source can be written as

$$r_{\mathrm{SR}} = g_1\sqrt{\frac{\mathcal{E}_{\mathrm{S}}}{2}}\,(b_1 + j\,b_2) + n_{\mathrm{SR}} \tag{2.3}$$

and

$$r_{\mathrm{SD}} = g_0\sqrt{\frac{\mathcal{E}_{\mathrm{S}}}{2}}\,(b_1 + j\,b_2) + n_{\mathrm{SD}} \tag{2.4}$$

[2]It should be noted that all results excluding BER expressions can be directly applied to slowly fading channels if instantaneous quantities per cooperation round (CR) are desirable and if the duration of one CR is exceeded by the channel coherence time. For example, the OPA derived can be regarded as the power allocation that maximizes the instantaneous SNR in a CR; or, the optimal relaying strategy obtained can be utilized as the strategy yielding maximum instantaneous CG in a given CR. As for BER derivations in this chapter, numerical averaging over channel fading statistics can be used to extend the results to the case of block fading channels.

[3]The results can also be applied to the case of binary phase shift keying (BPSK) modulation after appropriate replacement of parameters, as explained later in this section.

respectively, where b_1 and b_2 are the transmitted data bits of a symbol which are independent uniform random variables (RVs) over $\{-1, +1\}$, and where $n_{\rm SR}$ and $n_{\rm SD}$ are independent, circularly symmetric complex Gaussian (CSCG) zero-mean RVs with variances

$$\mathrm{E}\left\{|n_{\rm SR}|^2\right\} \triangleq N_{\rm SR} \tag{2.5}$$

and

$$\mathrm{E}\left\{|n_{\rm SD}|^2\right\} \triangleq N_{\rm SD}. \tag{2.6}$$

2.2.1 The AF Relaying Case

In AF relaying, the relay amplifies $r_{\rm SR}$ with a gain equal to [24]

$$\beta \triangleq \sqrt{\frac{\mathcal{E}_{\rm R}}{|g_1|^2\,\mathcal{E}_{\rm S} + N_{\rm SR}}} \tag{2.7}$$

such that the received signal at the destination from the relay is given by

$$r_{\rm RD} = g_2\,\beta\,r_{\rm SR} + n_{\rm RD} \tag{2.8}$$

where $n_{\rm RD}$ is a CSCG zero-mean RV with variance $N_{\rm RD}$, and is independent of $n_{\rm SD}$ and $n_{\rm SR}$. The destination combines $r_{\rm SD}$ and $r_{\rm RD}$ to detect b_1 and b_2, the transmitted bits from the source. It has been shown under the above model that the equivalent SNR per symbol between the source and destination is [25]

$$\gamma_{\rm eq} \triangleq \gamma_{\rm SD} + \frac{\gamma_{\rm SR}\,\gamma_{\rm RD}}{\gamma_{\rm SR} + \gamma_{\rm RD} + 1} \tag{2.9a}$$

where

$$\gamma_{\rm SD} \triangleq \frac{\mathcal{E}_{\rm S}\,|g_0|^2}{N_{\rm SD}} \tag{2.9b}$$

$$\gamma_{\rm SR} \triangleq \frac{\mathcal{E}_{\rm S}\,|g_1|^2}{N_{\rm SR}} \tag{2.9c}$$

and

$$\gamma_{\rm RD} \triangleq \frac{\mathcal{E}_{\rm R}\,|g_2|^2}{N_{\rm RD}} \tag{2.9d}$$

are the SD, SR, and RD SNRs per symbol. Eq. (2.9) can be used for any 2-D modulation. However, for one-dimensional modulations, such as BPSK and pulse amplitude modulation, the relay can perform noise reduction before amplification [47]. The result is that

$$\gamma_{\rm eq,b} = \gamma_{\rm SD,b} + \frac{\gamma_{\rm SR,b}\,\gamma_{\rm RD,b}}{\gamma_{\rm SR,b} + \gamma_{\rm RD,b} + \frac{1}{2}} \tag{2.10}$$

where the subscript "b" denotes per-bit SNRs. Note that (2.9) becomes (2.10) after each per-symbol γ is replaced with two times its corresponding per-bit γ, which shows that BPSK modulation with noise reduction AF relaying and QPSK modulation exhibit the same equivalent SNR per bit. It can be shown that all of the results in this chapter also hold for the case of BPSK modulation after changing per-symbol SNRs (or energies) to the equivalent per-bit SNRs (or energies).

The BER minimizing power allocation ratio $k_{\rm opt}^{(\rm AF)}$ maximizes $\gamma_{\rm eq}$ in (2.9). After some algebraic manipulations and defining

$$\gamma_0 \triangleq \frac{\mathcal{E}_0 \left|g_0\right|^2}{N_{\rm SD}} \tag{2.11}$$

$$\gamma_1 \triangleq \frac{\mathcal{E}_0 \left|g_1\right|^2}{N_{\rm SR}} \tag{2.12}$$

and

$$\gamma_2 \triangleq \frac{\mathcal{E}_0 \left|g_2\right|^2}{N_{\rm RD}} \tag{2.13}$$

we obtain the novel result[4]

$$k_{\rm opt}^{(\rm AF)} = \begin{cases} \dfrac{(\gamma_0+\gamma_1)\gamma_2+\gamma_0}{(\gamma_0+\gamma_1)\gamma_2-\gamma_0\gamma_1+\sqrt{\gamma_1\gamma_2[(\gamma_0+\gamma_1)\gamma_2-\gamma_0\gamma_1]\frac{\gamma_1+1}{\gamma_2+1}}}, & \gamma_0 < \dfrac{\gamma_1\gamma_2}{\gamma_1+1} \\ 1, & \gamma_0 \geq \dfrac{\gamma_1\gamma_2}{\gamma_1+1} \end{cases}. \tag{2.14}$$

Note that $k_{\rm opt}^{(\rm AF)} = 1$ means that the relay should not be used. In this chapter, we refer to γ_0, γ_1, and γ_2 as the SD, SR, and RD full-power SNRs, respectively. In contrast to $\gamma_{\rm SD}$, $\gamma_{\rm SR}$, and $\gamma_{\rm RD}$, the parameters γ_0, γ_1, and γ_2 principally represent the quality of the SD, SR, and RD links independently of the power allocation ratio, k. Also, note that combining (2.1), (2.2), (2.9b)–(2.9d), and (2.11)–(2.13), we can write

$$\gamma_{\rm SD} = k\,\gamma_0 \tag{2.15}$$

$$\gamma_{\rm SR} = k\,\gamma_1 \tag{2.16}$$

[4]The results [37, eqs. (21)–(29)] and [48, Theorem 5], which give the OPA ratio for the same scenario, are incomplete or incorrect. A counterexample for [37, eqs. (21)–(29)] is to set $P\left|h_{sd}\right|^2/\sigma_N^2 = 40$, $P\left|h_{sr,1}\right|^2/\sigma_N^2 = 45$, and $P\left|h_{rd,1}\right|^2/\sigma_N^2 = 10$. The calculation in [37] fails and yields a complex-valued ratio (neither the modulus, real part, or imaginary part is the correct answer). However, (2.2.1) gives the correct answer $k_{\rm opt}^{(\rm AF)} = 1$. A counterexample for [48, Theorem 5] is to set $A_0 = 10$, $A_i = 30$, and $B_i = 20$. Then, [48, Theorem 5] gives an incorrect OPA ratio $\rho = 1$ which leads to the end-to-end SNR $\gamma_r = 10$. However, our formula gives the correct answer $k_{\rm opt}^{(\rm AF)} \approx 0.695$ which yields $\gamma_{\rm eq} \approx 11.5$, greater than 10.

and

$$\gamma_{\mathrm{RD}} = (1-k)\,\gamma_2. \tag{2.17}$$

2.2.2 The DF Relaying Case

In DF relaying, the relay makes a decision about b_1 and b_2, denoted $\hat{b}_1$ and $\hat{b}_2$, respectively, using r_{SR}, and sends it to the destination. Then, the baseband equivalent signal received at the destination is

$$r_{\mathrm{RD}} = g_2\sqrt{\frac{\mathcal{E}_{\mathrm{R}}}{2}}\,\left(\hat{b}_1 + j\,\hat{b}_2\right) + n_{\mathrm{RD}} \tag{2.18}$$

where n_{RD} is the noise term as used in (2.8). The destination combines r_{SD} in (2.4) with r_{RD} in (2.18) in some manner to detect the data bits b_1 and b_2. Unlike the case of AF relaying, in this case MRC and ML detection at the destination are not the same and represent two different detectors at the destination. In the former, the destination assumes that $\hat{b}_1 = b_1$ and $\hat{b}_2 = b_2$, whereas in the latter, the destination takes into account the probability of erroneous detection at the relay,

$$P_{\mathrm{e}}^{(\mathrm{SR})} \triangleq \Pr\left\{\hat{b}_1 \neq b_1\right\}. \tag{2.19}$$

Note from the symmetry in (2.3) that

$$\Pr\left\{\hat{b}_1 \neq b_1\right\} = \Pr\left\{\hat{b}_2 \neq b_2\right\}. \tag{2.20}$$

Let x_{SD} and x_{RD} be defined as

$$x_{\mathrm{SD}} \triangleq \frac{\sqrt{2\mathcal{E}_{\mathrm{S}}}}{N_{\mathrm{SD}}}\,r_{\mathrm{SD}}\,g_0^* \tag{2.21}$$

and

$$x_{\mathrm{RD}} \triangleq \frac{\sqrt{2\mathcal{E}_{\mathrm{R}}}}{N_{\mathrm{RD}}}\,r_{\mathrm{RD}}\,g_2^* \tag{2.22}$$

where "$*$" denotes the complex conjugate. In MRC detection, the destination calculates

$$y = x_{\mathrm{SD}} + x_{\mathrm{RD}} \tag{2.23}$$

and decides on the values of b_1 and b_2 based on y. It can be verified from (2.4), (2.18), (2.21), and (2.22) that T_1 and T_2 defined as

$$T_1 \triangleq \mathrm{Re}\{y\} \tag{2.24}$$

and

$$T_2 \triangleq \mathrm{Im}\{y\} \tag{2.25}$$

where $\mathrm{Re}\{\cdot\}$ and $\mathrm{Im}\{\cdot\}$ denote the real and imaginary parts, are independent functions of b_1 and b_2, and hence, are sufficient statistics of y relative to b_1 and b_2, respectively. Considering only b_1, we have

$$T_1 = \gamma_{\mathrm{SD}}\, b_1 + \gamma_{\mathrm{RD}}\, \hat{b}_1 + n_{\mathrm{SRD}} \tag{2.26a}$$

where

$$n_{\mathrm{SRD}} \triangleq \mathrm{Re}\left\{ \frac{g_0^* \sqrt{2\mathcal{E}_{\mathrm{S}}}}{N_{\mathrm{SD}}}\, n_{\mathrm{SD}} + \frac{g_2^* \sqrt{2\mathcal{E}_{\mathrm{R}}}}{N_{\mathrm{RD}}}\, n_{\mathrm{RD}} \right\} \tag{2.26b}$$

is a zero-mean Gaussian RV with variance $\gamma_{\mathrm{SD}} + \gamma_{\mathrm{RD}}$. The destination compares T_1 with 0 to detect b_1. Using (2.26) and considering the different cases that $b_1 = \hat{b}_1$ and $b_1 \neq \hat{b}_1$, the BER is derived as[5]

$$P_{\mathrm{e}} = \left(1 - P_{\mathrm{e}}^{(\mathrm{SR})}\right) \mathrm{Q}\left(\sqrt{\gamma_{\mathrm{SD}} + \gamma_{\mathrm{RD}}}\right) + P_{\mathrm{e}}^{(\mathrm{SR})}\, \mathrm{Q}\left(\frac{\gamma_{\mathrm{SD}} - \gamma_{\mathrm{RD}}}{\sqrt{\gamma_{\mathrm{SD}} + \gamma_{\mathrm{RD}}}} \right) \tag{2.27a}$$

where

$$P_{\mathrm{e}}^{(\mathrm{SR})} \triangleq \mathrm{Q}(\sqrt{\gamma_{\mathrm{SR}}}) \tag{2.27b}$$

is the error probability at the relay and where $\mathrm{Q}(\cdot)$ is the standard Gaussian Q-function [50, eq. (2.3–10)]. The same BER given in (2.27) is also obtained for b_2.

Inspection of (2.27) reveals that if the SD and SR SNRs are fixed but the RD SNR improves, an error floor in the performance is experienced, as expected. But more interestingly, if the SR SNR is fixed but the SD and RD links improve such that $\gamma_{\mathrm{SD}} - \gamma_{\mathrm{RD}}$ is almost unchanging, then another error floor is encountered at $P_{\mathrm{e}} = P_{\mathrm{e}}^{(\mathrm{SR})}/2$. These two observations imply that the performance of the relay channel with DF relaying and MRC detection at the destination is limited by the SR link, as noted previously [6], [7].

In ML combining, the detection rule for b_1 is obtained in Appendix A. The result is that

$$\tanh(\mathrm{Re}\{x_{\mathrm{SD}}\}) + \left(1 - 2P_{\mathrm{e}}^{(\mathrm{SR})}\right) \tanh(\mathrm{Re}\{x_{\mathrm{RD}}\}) \underset{-1}{\overset{+1}{\gtrless}} 0 \tag{2.28}$$

where x_{SD} and x_{RD} are given by (2.21) and (2.22). Note that (2.28) can be rewritten such that it agrees with the results given in [24], [41]. However, (2.28) is more amenable

[5] A similar expression for the BER was derived in [49].

to obtaining the exact BER, which, after some manipulation detailed in Appendix A, is obtained as

$$P_{\mathrm{e}} = \mathrm{Q}\left(\frac{p+\gamma_{\mathrm{SD}}}{\sqrt{\gamma_{\mathrm{SD}}}}\right) + \frac{1}{2\sqrt{2\pi\gamma_{\mathrm{SD}}}}\int_{-p}^{p}\mathrm{d}x\left[(1+\tanh p)\,\mathrm{Q}\left(\frac{\tanh^{-1}(\frac{\tanh x}{\tanh p})+\gamma_{\mathrm{RD}}}{\sqrt{\gamma_{\mathrm{RD}}}}\right)\right.$$
$$\left. + (1-\tanh p)\,\mathrm{Q}\left(\frac{\tanh^{-1}(\frac{\tanh x}{\tanh p})-\gamma_{\mathrm{RD}}}{\sqrt{\gamma_{\mathrm{RD}}}}\right)\right]\mathrm{e}^{-(x-\gamma_{\mathrm{SD}})^2/(2\gamma_{\mathrm{SD}})} \tag{2.29a}$$

where

$$p \triangleq \tanh^{-1}\left(1-2P_{\mathrm{e}}^{(\mathrm{SR})}\right) \tag{2.29b}$$

for $0 < P_{\mathrm{e}}^{(\mathrm{SR})} < 0.5$. Note from (2.27b) that $P_{\mathrm{e}}^{(\mathrm{SR})}$ is bounded by 0 and 0.5. The exact BER given in (2.29) is a new result.[6] The BER at the destination is an increasing function of the BER at the relay. This implies that P_{e} can be bounded above by its value when $P_{\mathrm{e}}^{(\mathrm{SR})} = 0.5$, which is shown to equal $\mathrm{Q}(\sqrt{\gamma_{\mathrm{SD}}})$. Consequently, the BER in ML detection is not subject to any error floor, in sharp contrast to the case experienced in MRC detection.

The BER minimizing power allocation ratio in the DF case with MRC and ML detection cannot be obtained explicitly as in the AF case. Instead, we perform numerical optimization for (2.27) and (2.29) (after applying the replacements (2.15)–(2.17)) with respect to $k \in (0, 1]$ to obtain the OPA ratio. Nonetheless, in Section 2.3 the OPA ratio, leading to the maximum MI between the source and destination, is explicitly given for each case.

2.2.3 Numerical Examples

Fig. 2.2 shows the importance of power optimization in DF relaying. In this figure, the performances of several AF and DF relaying schemes are depicted versus the SD full-power SNR per bit, $\gamma_{0,\mathrm{b}}$, which is half of the corresponding SNR per symbol, γ_0. Power-suboptimal systems in this figure use $k = 0.5$ as their power allocation ratio. As shown in the figure, all of the relaying schemes perform better than DT. The power optimized DF relaying with either MRC detection or ML combining at the destination surpasses the power optimized AF relaying. However, even with ML detection at the destination, the power-suboptimal DF relaying is inferior to the power optimized AF relaying. Also, the performance of the power-suboptimal AF relaying appears to be slightly better than that

[6] Previously, only approximate expressions for the BER for noncoherent and coherent binary modulations with ML demodulation were derived in [41] and [51], respectively, based on a piecewise-linear approximation of the ML operation.

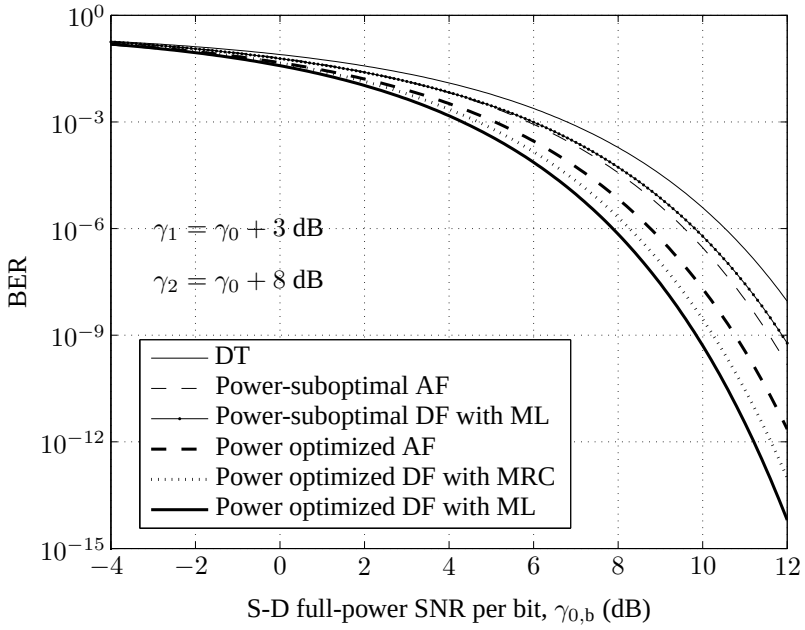

Fig. 2.2. The effect of power optimization in AF and DF relaying.

of the power-suboptimal DF relaying with ML detection for medium values of SNR. Note that the simple power optimized DF relaying with MRC detection outperforms the power optimized AF relaying, the power-suboptimal AF relaying, and DT by as much as 0.5 dB, 1.5 dB, and 2.5 dB, respectively. This figure indicates that DF relaying and ML detection at the destination are not sufficient conditions to guarantee the best performance; the power allocation ratio also plays a major role.

Fig. 2.3 indicates the impact of trusting the SR link in DF relaying with MRC detection at the destination. All of the schemes in this figure are power optimized. As explained before, an error floor is expected when γ_{SR} is fixed. As shown in the figure, ML detection at the destination removes the error floor since the cause of the error floor is suboptimal (i.e. non-ML) detection. However, with an unreliable SR link even using ML detection may not make DF relaying outperform AF relaying for large values of SNR.

2.3 Benefits of Relaying and CG

In this section, we derive joint optimization of the relaying strategy and power allocation ratio for maximizing the overall MI between the source and destination, and quantify the maximum CG under a total power constraint, all in terms of the instantaneous channel coefficients. The underlying assumption is the availability of only three communication

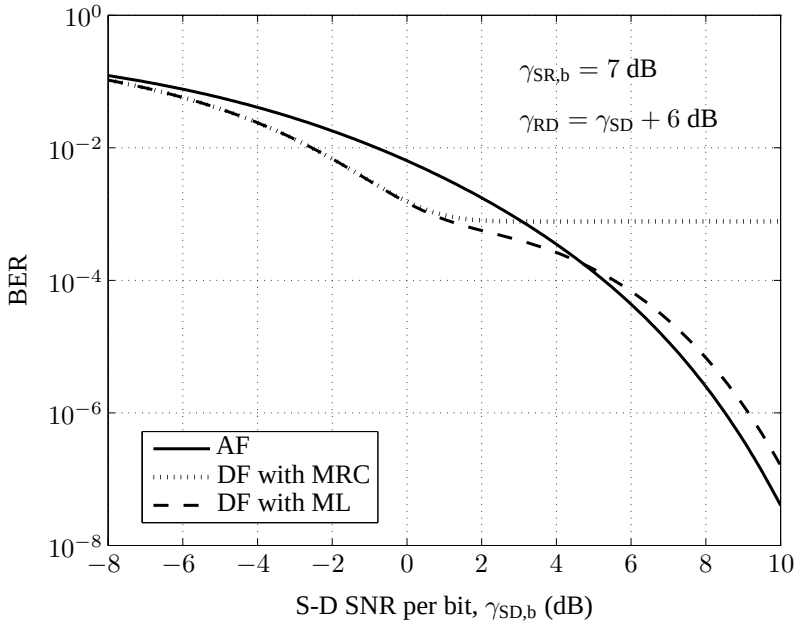

Fig. 2.3. The error floor in DF relaying.

options (strategies), DT, AF relaying, and DF relaying.

Fig. 2.4 shows how a fair comparison on a power basis between the relaying and DT schemes can be made. One 2-D symbol is transmitted in every degree of freedom (DoF). In the relaying scheme, N DoFs, in time or frequency, are available for each of the source and relay. In the DT case, the source takes up all available $2N$ DoFs. Also, using the same notations as in Section 2.2, we assume that in the relaying case, the source and relay have a total energy budget of $\mathcal{E}_0$ per DoF. Therefore, a total energy of $N\mathcal{E}_0$ is available for the period of cooperation. The source uses energy $\mathcal{E}_{\rm S}$ given in (2.1), and the relay uses energy $\mathcal{E}_{\rm R}$ defined in (2.2), per DoF. As shown in this figure, the SNRs of the SD, SR, and RD links per DoF are $\gamma_{\rm SD}$, $\gamma_{\rm SR}$, and $\gamma_{\rm RD}$, respectively, with the definitions given in (2.9b)–(2.9d). In DT, the source uses energy $\mathcal{E}_0/2$ per DoF, and therefore, the SNR in the SD link becomes $\gamma_0/2$, where γ_0 is defined in (2.11).

If the maximum achievable MI between the source and destination in cooperative or DT transmission is $I_{\max}$ nats per 2-D symbol, then we define the CG as

$$\mathrm{CG} \triangleq 10\log_{10}\left(\frac{\mathrm{e}^{I_{\max}}-1}{\mathrm{e}^{I_{\max}^{(\mathrm{DT})}}-1}\right) \ \text{dB} \tag{2.30}$$

where $I_{\max}^{(\mathrm{DT})}$ is the maximum achievable MI in DT. In fact, the CG shows the amount of gain in the equivalent SNR from the source to the destination with respect to DT. Note that

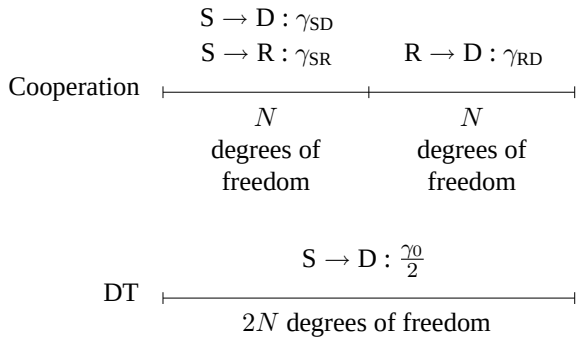

Fig. 2.4. Time-bandwidth dimensionality for cooperative transmission and DT, and the corresponding link SNRs.

if the best option for the source is not to use the relay, then

$$\mathrm{CG} = 0 \ \text{dB}. \tag{2.31}$$

The results for the best strategy for the source to maximize the CG, the OPA ratio k, and the maximum CG are summarized in Theorem 2.1. In this theorem, we employ the definitions of γ_0, γ_1, γ_2, $k_{\mathrm{opt}}^{(\mathrm{AF})}$, and CG given in (2.11)–(2.13), (2.2.1), and (2.30).

Theorem 2.1 (Best Strategy and CG in Dual-Hop AF/DF Relaying). Assume that the only available options for the source are either not to use the relay (i.e. to use DT), or to use AF or DF relaying at the relay, and that DF relaying is adopted if and only if the relay is capable of successfully decoding. Successful decoding at a node operating at a rate R nats per 2-D symbol is considered to be attainable if and only if the received value of SNR exceeds the limit,

$$10\log_{10}\left(\mathrm{e}^R - 1\right) + 10\log_{10}\rho \ \text{dB} \tag{2.32}$$

for some $\rho \geq 1$. Define

$$L_1 \triangleq 1 - \frac{\gamma_0^2}{4\rho(\gamma_2 - \gamma_0)} \tag{2.33}$$

$$L_2 \triangleq \frac{\gamma_2}{\gamma_1 + \gamma_2 - \gamma_0} \tag{2.34}$$

and

$$K \triangleq \left\{ \frac{(\gamma_0 + \gamma_1)\gamma_2 + \gamma_0}{\sqrt{[(\gamma_0 + \gamma_1)\gamma_2 - \gamma_0\gamma_1]\,(\gamma_2 + 1)} + \sqrt{\gamma_1\gamma_2(\gamma_1 + 1)}} \right\}^2. \tag{2.35}$$

Then, if

$$\gamma_2 \leq \gamma_0 + \frac{\gamma_0^2}{4\rho} \tag{2.36}$$

the relaying is not beneficial and

$$\mathrm{CG} = 0 \text{ dB}. \tag{2.37}$$

Otherwise, we have the following possible cases with the best strategy given in each case:

i) $L_1 \leq L_2$ and $\gamma_0 \geq \gamma_1\gamma_2/(\gamma_1+1)$: No cooperation; $\mathrm{CG} = 0$ dB.

ii) $L_1 \leq L_2$ and $K \leq \gamma_0 + \gamma_0^2/(4\rho)$: No cooperation; $\mathrm{CG} = 0$ dB.

iii) $L_1 \leq L_2$, $\gamma_0 < \gamma_1\gamma_2/(\gamma_1+1)$, and $K > \gamma_0 + \gamma_0^2/(4\rho)$: AF relaying.

iv) $L_1 > L_2$, $\gamma_0 < \gamma_1\gamma_2/(\gamma_1+1)$, and $K \geq L_2\gamma_1$: AF relaying.

v) $L_1 > L_2$ and $K < L_2\gamma_1$: DF relaying.

vi) $L_1 > L_2$ and $\gamma_0 \geq \gamma_1\gamma_2/(\gamma_1+1)$: DF relaying.

In the case of AF relaying, the OPA ratio is $k_{\mathrm{opt}}^{(\mathrm{AF})}$, and one has

$$\mathrm{CG} = 10\log_{10}\left[\frac{2\rho}{\gamma_0}\left(\sqrt{1+\frac{K}{\rho}}-1\right)\right] \text{ dB}. \tag{2.38}$$

In the case of DF relaying, the OPA ratio is L_2, and one has

$$\mathrm{CG} = 10\log_{10}\left[\frac{2\rho}{\gamma_0}\left(\sqrt{1+\frac{L_2\gamma_1}{\rho}}-1\right)\right] \text{ dB}. \tag{2.39}$$

Note that (2.32) is, in fact, the decoding threshold for a capacity-approaching code operating at a rate R nats per 2-D symbol. Theorem 2.1 stipulates the decoding SNR threshold at a node as a function of the transmission rate. The first term in (2.32) is the Shannon limit, and the second term is a margin depending on the code block length, the structure of the code, and weakly on the rate R. This margin can be around 1 dB for low density parity check codes [52].

Proof. A proof is given in Appendix B. ■

Figs. 2.5–2.7 show the CG and optimal strategies in collaborative transmission for several scenarios. In all cases, the decoding margin,

$$10\log_{10}\rho \tag{2.40}$$

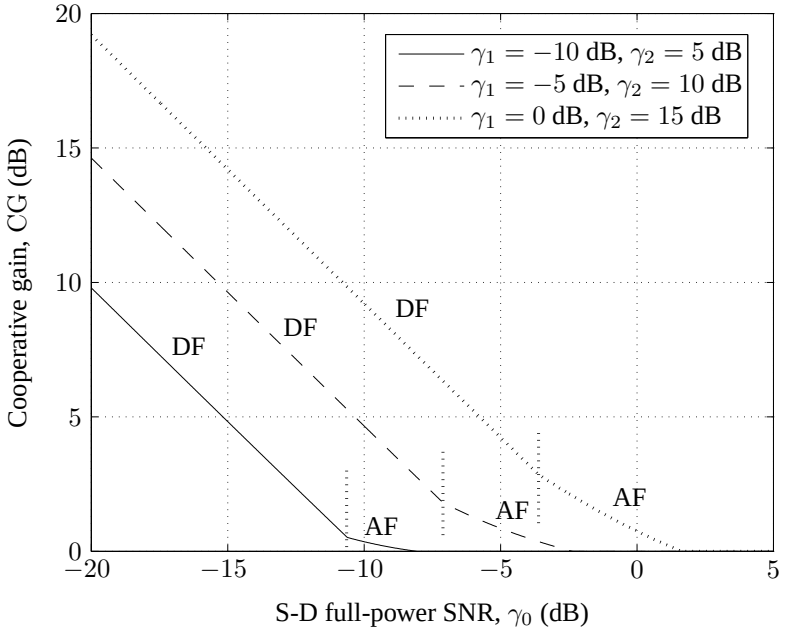

Fig. 2.5. Cooperative gain versus the SD full-power SNR, and the optimal relaying strategies.

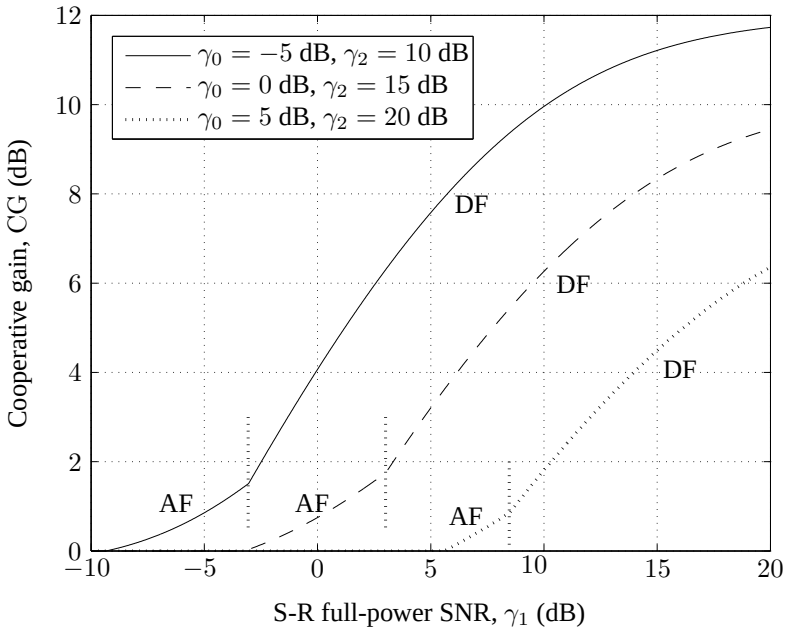

Fig. 2.6. Cooperative gain versus the SR full-power SNR, and the optimal relaying strategies.

has been set to 1 dB. Observe in Fig. 2.5 that the CG is as much as 19.2 dB when the SD link is very weak. In fact, the CG increases when the SR and RD links improve or the SD link deteriorates.

Note that in Figs. 2.6 and 2.7, there is a saturation effect as γ_1 or γ_2 increases. This expected phenomenon is because an increase in γ_1 effectively makes the relaying system

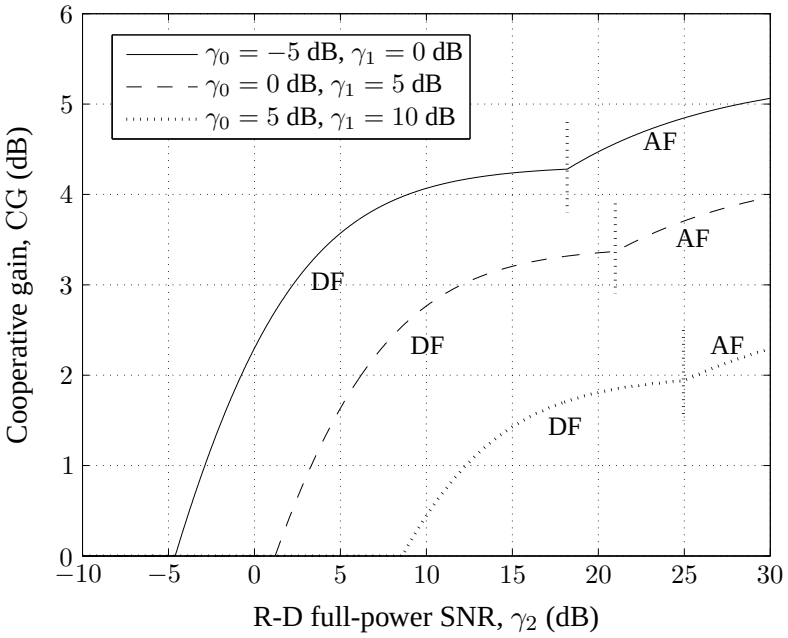

Fig. 2.7. Cooperative gain versus the RD full-power SNR, and the optimal relaying strategies.

approach a two-transmitting-antenna scheme having a fixed gain over single-antenna DT. Also, as γ_2 improves, the relaying system imitates a two-receiving-antenna scheme.

Fig. 2.6 indicates that DF relaying is favorable at large γ_1. This is explained by the relay's higher chance of decoding successfully at larger rates as the SR link improves.[7] A more interesting observation from Figs. 2.5 and 2.7 is that a strong SD or RD link persuades the relay to execute AF relaying. This persuasion is overshadowed by sufficient improvement of the SR link.

[7]The superiority of DF relaying over AF relaying in the case of strong SR links has been reported in the literature for other scenarios and other figures of merit [10], [25], [27], [34], [49].

Chapter 3

Dual-Hop AF Relaying Networks[1]

3.1 Introduction

In a multirelay, dual-hop AF relaying network, such as the one depicted in Fig. 3.1, the relays cooperate with the source by amplifying and forwarding its message to the destination. In such a network, the source and relays can be assigned orthogonal channels. This constitutes *orthogonal AF* relaying. An alternate scheme is to have the source transmission be orthogonal to relay transmissions but to let relay transmissions overlap in time and frequency, constituting *superimposed AF* scheme. Yet another scheme, which can be subsumed under superimposed relaying as will be explained in this section, is *selection AF* relaying, where in each CR, a single relay is chosen for the cooperation.

Orthogonal relaying suffers from orthogonalization loss [9], which is avoided in superimposed relaying at the expense of greater receiver complexity [15]. Recall from Section 1.3 or 2.2 that half-duplex relaying, which is the common mode of operation compared to the full-duplex mode, requires separation, similar to orthogonalization, between transmitting and receiving signals. However, it was shown in [15] that the inefficacy of conventional half-duplex schemes is due to the use of orthogonal subspaces, rather than the half-duplex operation. In [53], the problems of minimizing the BER subject to a total energy constraint, and minimizing the energy consumption under a BER constraint were investigated as a linear 0-1 knapsack problem for orthogonal AF relaying. In [48], it was shown that orthogonal AF relaying is always inferior to the selection AF scheme, and the source and relay

[1] *A version of this chapter has been published in the Proceedings of the IEEE Global Telecommunications Conference (GLOBECOM), 2008, and in part in the IEEE Transactions on Communications, vol. 57, no. 10, pp. 2918–2922, Oct. 2009.*

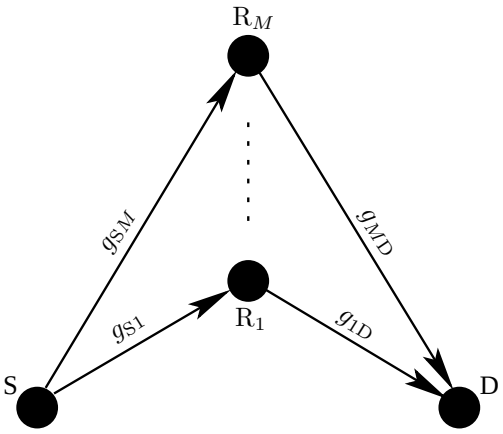

Fig. 3.1. The network configuration and corresponding channel complex gains.

OPA ratios for orthogonal and selection AF relaying were derived. In this chapter, we only consider and study superimposed and selection AF relaying.

Superimposed AF relaying was first introduced and studied in [11], [40]. The superimposed AF scheme considered in this chapter is similar to the schemes in [40], [54], [55], and comprises two phases of equal duration. In the first phase, the source broadcasts, and in the second phase, relays amplify and simultaneously forward the source data, received from the first phase, to the destination, using the same frequency band.

The importance of proper power allocation in relaying was explained in Chapter 2, and demonstrated for a simple network. Here, we formulate and examine the relay OPA in superimposed AF relaying, and investigate the optimality of the selection AF power allocation scheme. The selection AF power allocation [48], [54] can be considered a special case of the superimposed AF scheme, in which the entire available aggregate relay power is allocated to a single relay in each CR. The single relay is selected such that the overall outage probability is minimized. The selection is revised for each CR.

It was shown in [54] that selection AF relaying is optimal among all superimposed AF schemes for Rayleigh fading channels under the conditions that the relays can only access their local channel state information, and that the relay power allocation template is constant. In [40], optimal relay power and bandwidth allocation for maximizing the total system rate under a total network power budget for orthogonal and superimposed AF and DF schemes were derived for the case where the baseband link coefficients are real-valued, i.e. where links only suffer path loss. This assumption leads to closed-form solutions for the

OPA, and is different from our more realistic assumption that the baseband link coefficients are generally complex-valued. In [55], source and relay OPA for superimposed relaying was obtained when the relays use beamforming in each CR and when each relay has its own power constraint. Here, we consider a similar superimposed AF relaying problem but with a relay aggregate power constraint and without beamforming which can increase the overall complexity and implementation cost.

In [56], the authors considered a generalized selection AF relaying problem where relays have knowledge of their local channels and use beamforming, and where in general, more than one relay can transmit simultaneously to the destination. It was assumed in [56] that each relay either does not transmit or transmit with its full power. The diversity order of several AF single-relay selection schemes was derived, and several multirelay selection schemes were proposed. In this chapter, we only consider best-relay (single-relay) selection schemes [48], [54], which do not need interrelay synchronization used in multirelay selection protocols, and compare them with superimposed AF relaying for SNR optimality.

We show that the superimposed AF OPA can be formulated as a so-called nonconcave fractional program, consisting of globally maximizing the ratio of two positive semidefinite quadratic forms over the nonnegative orthant. We then proceed to derive a necessary condition for the selection AF power allocation optimality in terms of instantaneous channel coefficients. We show that as the number of relays increases, the selection AF power allocation is less likely to be outage optimal, such that the probability of optimality decays exponentially with the number of relays. We then develop a closed-form, outage suboptimal power allocation solution whose outage performance closely follows that of the optimal scheme, and noticeably outperforms that of the selection AF scheme.

Throughout, upright boldface small letters represent vectors, while an upright boldface capital letter denotes a matrix. Also, we use the following notations:

- Superscripts "T" and "H" denote the transpose and conjugate transpose, respectively.
- Operator $\mathrm{diag}\,\{\cdot\}$ maps a vector $\mathbf{w}$ to a diagonal matrix whose diagonal vector is $\mathbf{w}$.
- Vector $|\mathbf{w}|$, where

$$\mathbf{w} = (w_1, \cdots, w_M)^{\mathrm{T}} \tag{3.1}$$

  is defined as,

$$(|w_1|, \cdots, |w_M|)^{\mathrm{T}}. \tag{3.2}$$

- Vector $\mathbf{w}^+$, where $\mathbf{w}$ is a real-valued vector as in (3.1), is defined as,

$$(\max\{w_1, 0\}, \cdots, \max\{w_M, 0\})^{\mathrm{T}}. \tag{3.3}$$

- Vector $\mathbf{e}_i$ represents a vector having 1 at the ith component and zero elsewhere.

- The notations $\succ$ and $\succeq$ for vectors represent componentwise inequalities, and for matrices represent (non)positive or (non)negative definiteness.

The remainder of the chapter is organized as follows. The system model is described in Section 3.2, and the problem is introduced and formulated. Section 3.3 provides a necessary condition for the selection AF optimality, and demonstrates the selection AF asymptotically strict suboptimality. Finally, a suboptimal superimposed AF relay power allocation scheme is developed in Section 3.4.

3.2 System Model and Problem Formulation

Consider the relay channel depicted in Fig. 3.1 with a source (Node S), a destination (Node D), and M AF half-duplex relays $\mathrm{R}_1, \ldots, \mathrm{R}_M$, where the destination can only receive from the relays. In fact, we assume that the direct SD link is blocked, e.g. due to severe shadowing [30], [57]–[59]. Collaboration is particularly appealing to such a scenario, as conventional communication cannot help, and cooperation appears to be the only remedy.

One CR is split into two equal-length phases, in the first of which the source broadcasts a number of symbols, and in the second of which the relays, each with a preassigned power, simultaneously amplify and forward the source's message from the first phase. Therefore, the destination receives relay superimposed signals in the second phase.

All source and relay transmissions are oblivious to CSI, and occupy the same frequency band of baseband width W. Also, the transmissions are narrowband and distorted by quasistatic flat fading and AWGN. The channel complex baseband coefficients of the source-R_m (SR_m), and R_m-destination (R_mD) links are denoted $g_{\mathrm{S}m}$ and $g_{m\mathrm{D}}$, respectively. The channels are assumed to be independent and to remain constant during one CR, but to change independently over consecutive CRs.

It is assumed that the source and R_m transmit with energies per 2-D symbol $\mathcal{E}_{\mathrm{S}}$ and

$k_m \mathcal{E}_{\mathrm{R}}$, where $\mathcal{E}_{\mathrm{S}}$ and $\mathcal{E}_{\mathrm{R}}$ are two constants and where $k_1, \ldots, k_M$ represent relay power allocation ratios, which are nonnegative and sum to 1. Note that the output powers of the source and R_m are obtained as $W \mathcal{E}_{\mathrm{S}}$ and $k_m W \mathcal{E}_{\mathrm{R}}$. It is also assumed for technical considerations that each relay can sustain a maximum continuous power no less than $W \mathcal{E}_{\mathrm{R}}$.

The problem is to find $k_1, \ldots, k_M$ such that the outage probability is minimized. Outage is defined as the event that the maximum achievable rate between the source and destination is exceeded by a fixed target rate r. The ratios $k_1, \ldots, k_M$ are allowed to be functions of the link instantaneous coefficients $g_{\mathrm{S}m}$ and $g_{m\mathrm{D}}$. Therefore, irrespective of r and the link statistics, the relay power allocation ratios that minimize the outage probability are the same as those that maximize the overall instantaneous achievable rate. Note that $k_m = 0$ in a CR means that R_m is not utilized in the CR. Also, $k_m = 1$ (and therefore, $k_i = 0$ for $i \neq m$) indicates the solitary use of the mth relay. Therefore, the selection AF algorithm that allocates the entire aggregate power P_{R} to a single relay in each CR in order to minimize the outage probability, amounts to finding an m, in a CR, for which the instantaneous rate resulting from $k_m = 1$ equals or exceeds the rate resulting from $k_i = 1$ for any $i \neq m$.

Assume that the source transmits a 2-D symbol x_{S}, where

$$\mathrm{E}\left\{|x_{\mathrm{S}}|^2\right\} = \mathcal{E}_{\mathrm{S}}. \tag{3.4}$$

This symbol is received at Node R_m as

$$y_m \triangleq g_{\mathrm{S}m}\, x_{\mathrm{S}} + n_m \tag{3.5}$$

where n_m is the AWGN with one-sided power spectral density (PSD) N_m. Node R_m amplifies y_m with the factor

$$\beta_m \triangleq \sqrt{\frac{k_m \mathcal{E}_{\mathrm{R}}}{G_{\mathrm{S}m} \mathcal{E}_{\mathrm{S}} + N_m}} \tag{3.6a}$$

where

$$G_{\mathrm{S}m} \triangleq |g_{\mathrm{S}m}|^2 \tag{3.6b}$$

or

$$G_{\mathrm{S}m} \triangleq \mathrm{E}\left\{|g_{\mathrm{S}m}|^2\right\} \tag{3.6c}$$

depending on whether we need

$$\mathrm{E}\left\{|\beta_m\, y_m|^2 \;\middle|\; g_{\mathrm{S}m}\right\} = k_m\, \mathcal{E}_{\mathrm{R}} \tag{3.6d}$$

corresponding to an instantaneous or short-term power constraint for R_m, or

$$\mathrm{E}\left\{|\beta_m\, y_m|^2\right\} = k_m\, \mathcal{E}_{\mathrm{R}} \tag{3.6e}$$

indicating an ergodic or long-term power constraint based on averaging over different realizations of $g_{\mathrm{S}m}$.[2] Now, the signal received at the destination in the second phase is

$$y_{\mathrm{D}} \triangleq \sum_{m=1}^{M} g_{m\mathrm{D}}\, \beta_m\, y_m + n_{\mathrm{D}} = \left(\sum_{m=1}^{M} \beta_m\, g_{\mathrm{S}m}\, g_{m\mathrm{D}}\right) x_{\mathrm{S}} + \sum_{m=1}^{M} \beta_m\, g_{m\mathrm{D}}\, n_m + n_{\mathrm{D}} \tag{3.7}$$

where n_{D} is the AWGN at the destination with one-sided PSD N_{D}. Conditioned on the channel coefficients, the maximum MI in nats between x_{S} and y_{D} can then be written as,

$$\ln\left(1 + \gamma_{\mathrm{eq}}\right) \tag{3.8a}$$

where

$$\gamma_{\mathrm{eq}} \triangleq \frac{\mathcal{E}_{\mathrm{S}} \left|\sum_{m=1}^{M} \beta_m\, g_{\mathrm{S}m}\, g_{m\mathrm{D}}\right|^2}{\sum_{m=1}^{M} \beta_m^2\, |g_{m\mathrm{D}}|^2\, N_m + N_{\mathrm{D}}} \tag{3.8b}$$

is the equivalent SNR from the source to the destination. Eq. (3.8b) can be rewritten, after some manipulations using (3.6a), as

$$\gamma_{\mathrm{eq}} = \frac{\left|\mathbf{d}^{\mathrm{T}}\mathbf{a}\right|^2}{1 + \left\|\mathbf{d}^{\mathrm{T}}\mathrm{diag}\left\{\mathbf{b}\right\}\right\|^2} = \frac{\mathbf{d}^{\mathrm{T}}\mathbf{a}\,\mathbf{a}^{\mathrm{H}}\mathbf{d}}{1 + \mathbf{d}^{\mathrm{T}}\mathrm{diag}\left\{\mathbf{b}\right\}\mathrm{diag}\left\{\mathbf{b}\right\}^{\mathrm{H}}\mathbf{d}} \tag{3.9a}$$

where

$$\mathbf{d} \triangleq \left(\sqrt{k_1},\, \cdots,\, \sqrt{k_M}\right)^{\mathrm{T}} \tag{3.9b}$$

is the square-root power allocation ratio vector, and where

$$\mathbf{a} \triangleq \left(a_1,\, \cdots,\, a_M\right)^{\mathrm{T}} \tag{3.9c}$$

$$\mathbf{b} \triangleq \left(b_1,\, \cdots,\, b_M\right)^{\mathrm{T}} \tag{3.9d}$$

$$a_m \triangleq \sqrt{\frac{\mathcal{E}_{\mathrm{S}}\, \mathcal{E}_{\mathrm{R}}}{N_{\mathrm{D}}}}\, \frac{g_{\mathrm{S}m}\, g_{m\mathrm{D}}}{\sqrt{G_{\mathrm{S}m}\, \mathcal{E}_{\mathrm{S}} + N_m}} \tag{3.9e}$$

and

$$b_m \triangleq \sqrt{\frac{\mathcal{E}_{\mathrm{R}}\, N_m}{N_{\mathrm{D}}}}\, \frac{g_{m\mathrm{D}}}{\sqrt{G_{\mathrm{S}m}\, \mathcal{E}_{\mathrm{S}} + N_m}}. \tag{3.9f}$$

[2] Both approaches have been considered in the literature [9], [54].

The optimization problem is to find $(k_1, \cdots, k_M)$ that maximizes γ_{eq}. Therefore, using the definitions

$$\mathbf{A} \triangleq \mathbf{a}\,\mathbf{a}^{\text{H}} \tag{3.10}$$

and

$$\mathbf{D} \triangleq \text{diag}\,\{\mathbf{b}\}\ \text{diag}\,\{\mathbf{b}\}^{\text{H}} \tag{3.11}$$

and from (3.9), one can rewrite the problem as,

$$\underset{\mathbf{d}}{\text{argmax}}\ \frac{\mathbf{d}^{\text{T}}\mathbf{A}\,\mathbf{d}}{1+\mathbf{d}^{\text{T}}\mathbf{D}\,\mathbf{d}} \tag{3.12a}$$

subject to the constraints

$$\mathbf{d} \succeq \mathbf{0} \tag{3.12b}$$

and

$$\mathbf{d}^{\text{T}}\mathbf{d} = 1 \tag{3.12c}$$

(see the notations defined in Section 3.1). Any global solution to (3.12) is equivalent to an OPA strategy. Based on the selection AF description in this section, the selection AF algorithm solves (3.12) when,

$$\mathbf{d} \in \{\mathbf{e}_1, \cdots, \mathbf{e}_M\} \tag{3.13}$$

where $\mathbf{e}_m$ has been defined in Section 3.1. This amounts to solving,

$$\underset{m}{\text{argmax}}\ \frac{\mathbf{A}_{mm}}{1+\mathbf{D}_{mm}} \tag{3.14}$$

or

$$\underset{m}{\text{argmax}}\ \frac{|a_m|^2}{1+|b_m|^2}. \tag{3.15}$$

Therefore, selection AF relaying is optimal whenever a global solution to (3.12) is one of the M extreme vectors $\mathbf{e}_1, \cdots, \mathbf{e}_M$ of the constraint set.

To further simplify the problem, one can show that (3.12) is equivalent to,

$$\underset{\mathbf{d}}{\text{argmax}}\ \frac{\mathbf{d}^{\text{T}}\mathbf{A}\,\mathbf{d}}{\mathbf{d}^{\text{T}}\acute{\mathbf{D}}\,\mathbf{d}} \tag{3.16a}$$

subject to the constraint

$$\mathbf{d} \succeq \mathbf{0} \tag{3.16b}$$

where

$$\acute{\mathbf{D}} \triangleq \mathbf{D} + \mathbf{I}_M \tag{3.16c}$$

and where $\mathbf{I}_M$ is the identity matrix of order M, in the sense that any global solution to (3.12) is a global solution to (3.16), and for any global solution $\mathbf{d}$ to (3.16), $\mathbf{d}/\|\mathbf{d}\|$ is a global solution to (3.12). Problem (3.16) is advantageous over problem (3.12) in that it consists of the ratio of two convex quadratic functions with a closed-set, convexity constraint. Note that the constraint set in (3.12) is closed, but not convex. Such a global optimization problem, a so-called nonconcave fractional programming, may arise in realistic applications [60]. The problem in general lacks a closed-form solution. Nonetheless, some global optimization algorithms have been developed for its solution (e.g., see [61], [62], and the references therein).

Observe from (3.9)–(3.12) and (3.16c) that the objective function in (3.16),

$$\frac{\mathbf{d}^{\mathrm{T}} \mathbf{A}\, \mathbf{d}}{\mathbf{d}^{\mathrm{T}} \acute{\mathbf{D}}\, \mathbf{d}} \tag{3.17}$$

actually equals γ_{eq} when the square-root power allocation ratio vector is given by

$$(\sqrt{k_1},\, \cdots,\, \sqrt{k_M})^{\mathrm{T}} = \frac{\mathbf{d}}{\|\mathbf{d}\|}. \tag{3.18}$$

This obviously shows that (3.17) is upper bounded, and, therefore, the global optimization problem (3.16) has a solution.

The boundedness of (3.17) can be verified via another approach which also yields an interesting upper bound on γ_{eq}. If

$$\boldsymbol{\eta} \triangleq \sqrt{\mathcal{E}_{\mathrm{S}}} \left(\frac{g_{\mathrm{S}1}}{\sqrt{N_1}},\, \cdots,\, \frac{g_{\mathrm{S}M}}{\sqrt{N_M}} \right)^{\mathrm{T}} \tag{3.19}$$

where N_m is the PSD of n_m (see (3.5)), we obtain

$$\mathbf{a} = \mathrm{diag}\,\{\mathbf{b}\}\, \boldsymbol{\eta} \tag{3.20}$$

from (3.9). Meanwhile, one has

$$\|\mathbf{z}\|^2\, \mathbf{I}_M \succeq \mathbf{z}\, \mathbf{z}^{\mathrm{H}} \tag{3.21}$$

for any complex M-tuple vector $\mathbf{z}$. Combining these facts, we can show that

$$\acute{\mathbf{D}} \succ \frac{\mathbf{A}}{\|\boldsymbol{\eta}\|^2} \succeq \mathbf{0} \tag{3.22}$$

and consequently,

$$0 \leq \frac{\mathbf{d}^{\mathrm{T}} \mathbf{A}\, \mathbf{d}}{\mathbf{d}^{\mathrm{T}} \acute{\mathbf{D}}\, \mathbf{d}} = \gamma_{\mathrm{eq}} < \|\boldsymbol{\eta}\|^2 = \gamma_{\mathrm{S}1} + \cdots + \gamma_{\mathrm{S}M} \tag{3.23a}$$

where

$$\gamma_{\mathrm{S}m} \triangleq \frac{\mathcal{E}_{\mathrm{S}} \left|g_{\mathrm{S}m}\right|^2}{N_m} \tag{3.23b}$$

is the SNR realized at R_m.

3.3 Selection AF Suboptimality

In this section, the deviation of the selection AF algorithm from optimality in relay power allocation is examined. We start with a necessary condition for the selection AF optimality.

Theorem 3.1 (Necessary Condition for Selection AF Optimality). If the selection AF algorithm is optimal for relay power allocation, then we have

$$\exists i,\ \forall j,\ j \neq i:\ \mathrm{Re}\left\{g_{\mathrm{S}i}\, g_{i\mathrm{D}}\, g_{\mathrm{S}j}^{*}\, g_{j\mathrm{D}}^{*}\right\} \leq 0. \tag{3.24}$$

Proof. A proof is given in Appendix C. ■

Next, we prove that selection AF relaying is asymptotically strictly suboptimal.

Theorem 3.2 (Selection AF Asymptotically Strict Suboptimality). The probability of the selection AF outage optimality approaches zero exponentially as M increases, independently of the fading model except that different links suffer independent fading with uniformly distributed phase distortion.

Proof. A proof is given in Appendix D. ■

The upper bound (D-15) from the proof of Theorem 3.2 shows that $\Pr\{E\} < 10^{-2}$ for $M > 11$; i.e. for more than 11 available relays, selection AF relaying is suboptimal with a probability greater than 99%. Note that the independent fading and uniformly distributed phase assumptions stipulated in the theorem are common in the literature.

The increasing divergence of the selection AF protocol from outage optimality is illustrated by numerical examples in Fig. 3.2, where the outage probabilities of the selection AF and optimal schemes versus the number of relays are depicted for two rates r in Rayleigh fading channels. Recall that the outage probability P_{out} at rate r bits is given as

$$P_{\mathrm{out}} = \Pr\{\ln(1 + \gamma_{\mathrm{eq}}) < r \ln 2\} \tag{3.25}$$

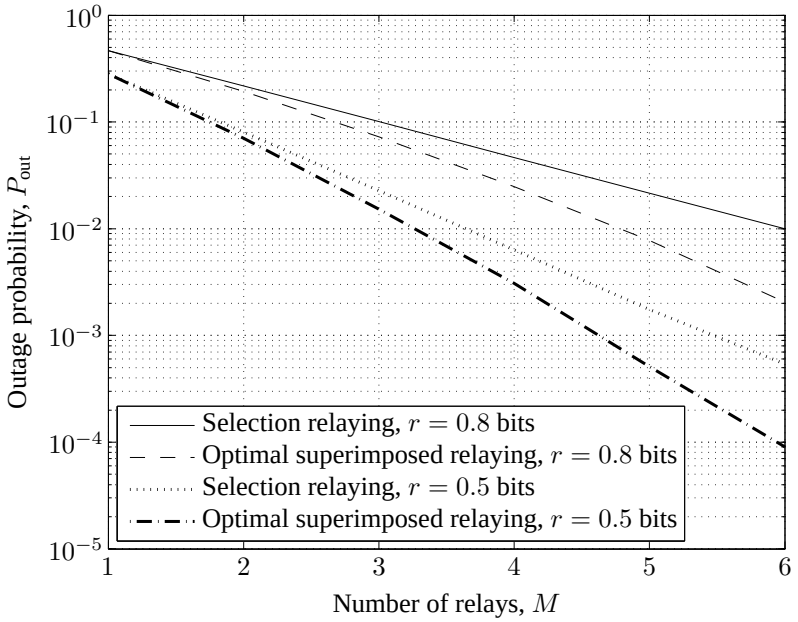

Fig. 3.2. The outage probability versus the number of relays for selection and optimal superimposed AF relaying in Rayleigh fading channels, when $\gamma_{\mathrm{S}m} = 7$ dB and $\gamma_{m\mathrm{D}} = 15$ dB for $m = 1, \cdots, 6$.

where γ_{eq} is given by (3.8b). The outage probabilities in Fig. 3.2 have been obtained by 10^5-iteration Monte Carlo simulation. In this figure, a symmetrical case has been considered in which $\gamma_{\mathrm{S}m} = 7$ dB and $\gamma_{m\mathrm{D}} = 15$ dB, where $\gamma_{\mathrm{S}m}$ is defined by (3.23b) and where

$$\gamma_{m\mathrm{D}} \triangleq \frac{\mathcal{E}_{\mathrm{R}} \left| g_{m\mathrm{D}} \right|^2}{N_{\mathrm{D}}} \tag{3.26}$$

is the SNR at the destination if only R_m transmits. One can observe that as M increases, the selection AF scheme diverges more from optimality. For example, when $M = 6$, P_{out} for the selection AF scheme is almost 5 times that of the optimal scheme for both rates r.

Fig. 3.3 exhibits P_{out} versus fading severity, parameter m in a Nakagami-m distribution, for a typical example when $M = 5$. It is observed that the selection AF deviation from optimality is also susceptible to fading severity, intensified as the fading moderates.

3.4 Proposed Suboptimal Scheme

The optimal superimposed AF scheme is too complex to be implemented in practical networks. In fact, the branch and bound algorithms presented in [61], [62] for solving nonconcave fractional global optimization programs are general with indeterministic convergence time and computational load. In this section, motivated by the exact optimal solution for the

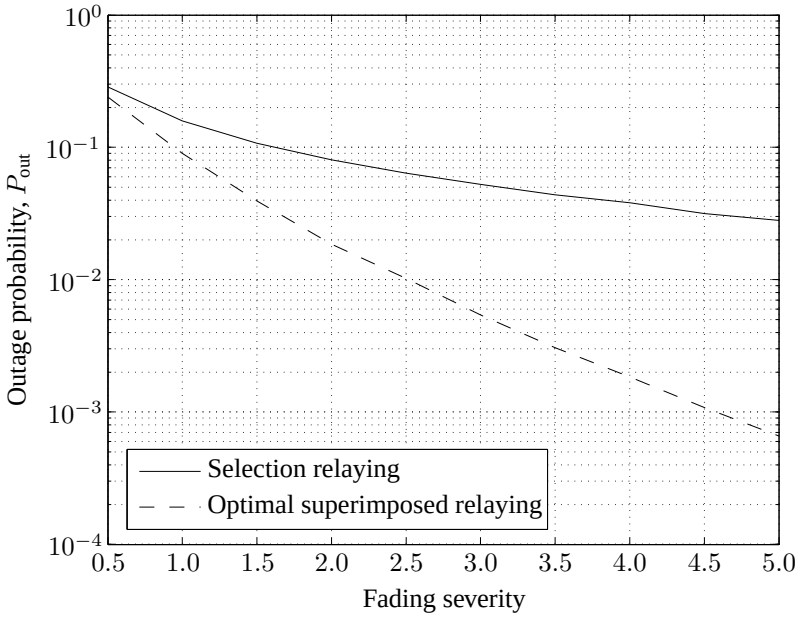

Fig. 3.3. The outage probability versus the fading severity for selection and optimal superimposed relaying in the case of five relays for a Nakagami fading channel, when $r = 0.6$ bits and $(\gamma_{\mathrm{S}1}, \gamma_{1\mathrm{D}}) = (8, 3)$ dB, $(\gamma_{\mathrm{S}2}, \gamma_{2\mathrm{D}}) = (3, 7)$ dB, $(\gamma_{\mathrm{S}3}, \gamma_{3\mathrm{D}}) = (8, 6)$ dB, $(\gamma_{\mathrm{S}4}, \gamma_{4\mathrm{D}}) = (5, 3)$ dB, and $(\gamma_{\mathrm{S}5}, \gamma_{5\mathrm{D}}) = (5, 7)$ dB.

case of $M = 2$ as will be explained, we propose a suboptimal power allocation scheme. We develop a closed-form suboptimal solution to (3.16), which does not involve convergence issues or indefinite search.

First, note that (3.16) can be converted to the equivalent problem,

$$\underset{\mathbf{u}}{\operatorname{argmax}} \; \frac{\mathbf{u}^{\mathrm{T}} \acute{\mathbf{D}}^{-1/2} \mathbf{A} \acute{\mathbf{D}}^{-1/2} \mathbf{u}}{\mathbf{u}^{\mathrm{T}} \mathbf{u}} \tag{3.27a}$$

subject to the constraint

$$\mathbf{u} \succeq \mathbf{0} \tag{3.27b}$$

where

$$\mathbf{u} = \acute{\mathbf{D}}^{1/2} \mathbf{d} \tag{3.27c}$$

or

$$\mathbf{d} = \acute{\mathbf{D}}^{-1/2} \mathbf{u}. \tag{3.27d}$$

It can be shown that,

$$\acute{\mathbf{D}}^{-1/2} \mathbf{A} \acute{\mathbf{D}}^{-1/2} \tag{3.28}$$

is Hermitian and nonnegative definite. However, (3.27) is not a typical quadratic form

maximization problem due to the constraint (3.27b). Also, note that expression (3.28) is complex-valued, whereas the optimization is performed over real values. While this is not of concern in general, for the purposes of this section we equivalently convert (3.27) to,

$$\underset{\mathbf{u}}{\operatorname{argmax}} \ \frac{\mathbf{u}^{\mathrm{T}} \mathbf{\Lambda}\, \mathbf{u}}{\mathbf{u}^{\mathrm{T}} \mathbf{u}} \tag{3.29a}$$

subject to the constraint

$$\mathbf{u} \succeq \mathbf{0} \tag{3.29b}$$

where

$$\mathbf{\Lambda} \triangleq \acute{\mathbf{D}}^{-1/2} \left(\mathbf{A} + \mathbf{A}^{\mathrm{T}}\right) \acute{\mathbf{D}}^{-1/2} \tag{3.29c}$$

is a nonnegative definite, symmetric, real-valued matrix. Note that for a given $\mathbf{u}$ satisfying (3.29b) and any positive ℓ, $\ell\, \mathbf{u}$ is componentwise nonnegative and leads to the same value of the objective function in (3.29). Therefore, if $\mathbf{u}$ is globally optimal, then $\ell\, \mathbf{u}$ is globally optimal for any $\ell > 0$. Also, note that based on quadratic form maximization results [63], if corresponding to its maximum eigenvalue, $\mathbf{\Lambda}$ has an eigenvector

$$\mathbf{v} \triangleq (v_1, \cdots, v_M)^{\mathrm{T}} \tag{3.30}$$

such that $\mathbf{v} \succeq \mathbf{0}$ or $-\mathbf{v} \succeq \mathbf{0}$, then a globally optimal solution to (3.29) is

$$\mathbf{u}_{\mathrm{opt}} = |\mathbf{v}| \tag{3.31}$$

where the notation $|\cdot|$ for a vector has been defined in Section 3.1.

Our proposed suboptimal solution to (3.29), $\mathbf{u}_{\text{s-opt}}$, is as follows, and can be proved through differentiation to be optimal for $M = 2$ (and trivially for $M = 1$), and which in fact, is the generalization of the optimal solution for $M = 2$ to the case of an arbitrary M. Assume that the maximum eigenvalue of $\mathbf{\Lambda}$, $\lambda_{\max}$, has multiplicity t, and that $\mathbf{v}_1, \cdots, \mathbf{v}_t$ are the eigenvectors corresponding to $\lambda_{\max}$. Now, if for any $j \in \{1, \cdots, t\}$ one has $\mathbf{v}_j \succeq \mathbf{0}$ or $-\mathbf{v}_j \succeq \mathbf{0}$, then

$$\mathbf{u}_{\text{s-opt}} \triangleq |\mathbf{v}_j|. \tag{3.32}$$

Note that in this case, $\mathbf{u}_{\text{s-opt}}$ is globally optimal. Otherwise,

$$\mathbf{u}_{\text{s-opt}} \triangleq \underset{\mathbf{u} \in \left\{\mathbf{v}_1^+, (-\mathbf{v}_1)^+, \cdots, \mathbf{v}_t^+, (-\mathbf{v}_t)^+, \mathbf{e}_1, \cdots, \mathbf{e}_M\right\}}{\operatorname{argmax}} \ \frac{\mathbf{u}^{\mathrm{T}} \mathbf{\Lambda}\, \mathbf{u}}{\mathbf{u}^{\mathrm{T}} \mathbf{u}} \tag{3.33}$$

where we have used the notations defined in Section 3.1. Note that (3.33) only involves

search over a finite set of size $2t + M$, and that for $\mathbf{u} = \mathbf{e}_m$, the objective function in (3.33) simply reduces to Λ_{mm}.

To summarize the proposed suboptimal relay power allocation scheme, first, vectors $\mathbf{a}$ and $\mathbf{b}$ from (3.9e) and (3.9f) are calculated. Then, the expressions

$$\mathbf{A} = \mathbf{a}\,\mathbf{a}^{\mathrm{H}} \tag{3.34}$$

$$\acute{\mathbf{D}} = \mathrm{diag}\,\{\mathbf{b}\}\,\mathrm{diag}\,\{\mathbf{b}\}^{\mathrm{H}} + \mathbf{I}_M \tag{3.35}$$

and

$$\mathbf{\Lambda} = \acute{\mathbf{D}}^{-1/2}\left(\mathbf{A} + \mathbf{A}^{\mathrm{T}}\right)\acute{\mathbf{D}}^{-1/2} \tag{3.36}$$

are evaluated. Finally, the suboptimal solution to (3.29), $\mathbf{u}_{\text{s-opt}}$, is obtained from (3.32) or (3.33), which then translates to the square-root power allocation ratio vector

$$\mathbf{d}_{\text{s-opt}} \triangleq \frac{\acute{\mathbf{D}}^{-1/2}\,\mathbf{u}_{\text{s-opt}}}{\|\acute{\mathbf{D}}^{-1/2}\,\mathbf{u}_{\text{s-opt}}\|}. \tag{3.37}$$

Fig. 3.4 shows the superiority of the proposed scheme over the selection AF protocol in terms of the outage probability, and that the proposed suboptimal scheme performs almost as well as the optimal scheme. The outage probabilities have been obtained by Monte-Carlo

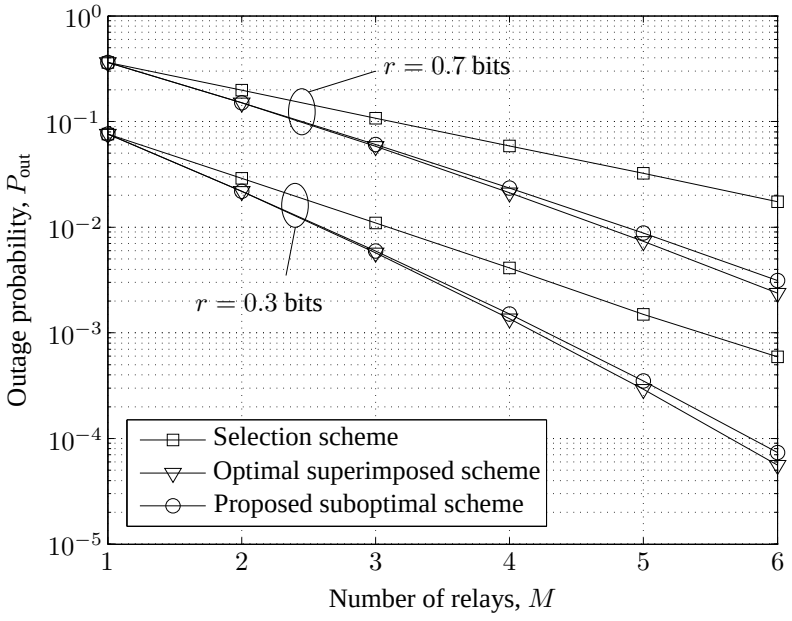

Fig. 3.4. The outage probability versus the number of relays for the selection, optimal superimposed, and proposed schemes in Rayleigh fading channels, when $\gamma_{\mathrm{S}m} = 15$ dB and $\gamma_{m\mathrm{D}} = 10$ dB for $m = 1, \cdots, 6$.

simulating and solving (3.12), for the selection AF and optimal superimposed AF schemes, and (3.33), for the proposed scheme. The superiority of the optimal or proposed suboptimal schemes over the selection AF scheme is increased as M is raised, and reaches about 0.88 and 0.76 decades smaller outage probabilities at $M = 6$ for $r = 0.3$ bits and $r = 0.7$ bits, respectively. It can be argued that the proposed scheme can be implemented with almost the same complexity requirements as those required for a centralized implementation of the selection AF scheme.

Chapter 4

Dual-Hop DF Relaying Networks[1]

As explained in Chapter 1, several ideas for basic relay operations were developed in [1], [3], which were later termed AF [9], DF [4], [9], and CF [4] relaying. In Chapter 3, we investigated superimposed and selection AF relaying. In this chapter, we consider fixed DF relaying, in which relays, under constant time/frequency allocation, attempt to fully decode the source's message, prior to forwarding.

4.1 Introduction

The DF relaying protocol and its capacity evaluation have been the main topics of a vast body of research [4], [5], [9]–[11], [26], [57]–[59], [64]–[75]. In the seminal work [9], [10], the diversity-multiplexing tradeoff and outage probability of different single-relay and multirelay AF and DF protocols were derived. The capacity regions of various protocols based on AF and DF relaying were derived and compared for static channels in [26]. The ergodic capacity, outage capacity, and spatial diversity gain of three AF and DF relaying protocols for a three-node relay channel were derived in [11]. In [5], lower and upper bounds on the instantaneous, outage, and ergodic capacities of a three-node relay channel with perfect CSI at the transmitters were derived for Rayleigh fading and full-duplex/time division and synchronized/asynchronous transceiver models [5].

In another major progress, capacity bounds were derived for several multirelay DF and CF strategies [4]. It was shown that the DF strategy achieves the ergodic capacity with some

[1] *A version of this chapter has been published in part in the Proceedings of the IEEE Global Telecommunications Conference (GLOBECOM), 2009.*

topological and fading phase assumptions. The development in [66] optimized multirelay selection and power allocation for the best capacity in a dual-hop multisource network with full CSI at the nodes. In a similar system setup, bounds on the ergodic capacity of a multisource, dual-hop, orthogonal DF relaying network with global CSI were derived assuming Rayleigh fading, random relay positionings, and a short-term power constraint [67]. In [70], the ergodic capacity of a three-node relaying network was studied for AF and DF relaying with adaptive modulation. In [73], closed-form expressions were derived for the symbol error rate and average capacity for a DF relay selection scheme without the SD link in the Rayleigh fading and dissimilar links case. In [71], [72], closed-form expressions for the error probability and average capacity of dual-hop selection relaying, based on choosing the relay with the strongest link to the destination among a decoding set, were derived. In [59], the ergodic capacities of multirelay, dual-hop, reactive and proactive selection DF relaying were derived for Rayleigh fading. Also, the ergodic capacities of single-relay, multihop AF and DF relaying were studied for Rayleigh fading in [57]. It was shown that DF relaying is superior to AF relaying in this scenario.

In this chapter, we consider the multirelay, dual-hop DF relaying network depicted in Fig. 4.1, and answer the question of what the maximum possible average rate of communication from the source to the destination, referred to as the average capacity, is, under the assumptions detailed in Section 4.2. In contrast to single-relay, multihop DF relaying networks where the maximum achievable rate is simply determined by the capacity of the poorest hop [57], a multibranch, dual-hop scheme has more complex achievable rate expressions as will be observed in Sections 4.3 and 4.4. The average rate is calculated here as the expectation of the maximum instantaneous, nonoutage rate of the system. This maximum rate is independent of any given operating rate, and, therefore, is different from the realized MI evaluated at an operating rate, such as the rates given in [9], [10], [68], [76].

We consider three protocols, called superimposed, selection, and orthogonal relaying, respectively referring to the strategies where different relay transmissions are superimposed [9], [40], [64], [77], where only the best relay is utilized [58], [68], [74], and where the relays transmit in their dedicated orthogonal channels [9], [40], [69], [77], [78]. We also consider two cooperation strategies in each case, called parallel channel cooperation (PCC) and repetition-based cooperation (RC) [9], [75]. These protocols and cooperation strategies have been frequently employed in the literature (with slight variations in some cases). How-

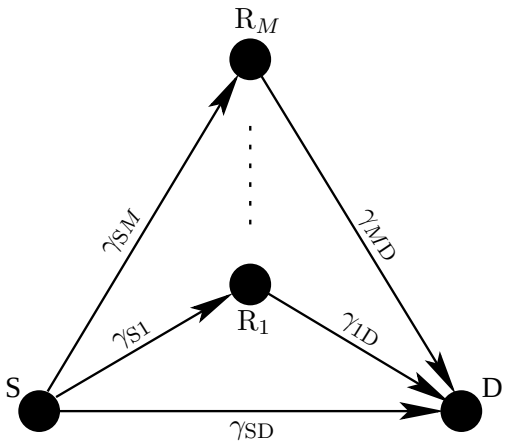

Fig. 4.1. The system model, and the corresponding SNRs of the links.

ever, no result has been reported for the capacity performance of the general network in Fig. 4.1 under the above mentioned protocols and strategies. In the analysis performed here, the average capacity is calculated through the outage probability. Therefore, the outage probability of the different schemes is also derived as a side result of our analysis. Although the outage performance of DF relaying schemes has received more attention with more results in the literature compared to the capacity performance, our analysis reveals new results for outage probabilities. We mention both new and overlapping results for completeness and cite the relevant references.

The remainder of the chapter is organized as follows. Section 4.2 details the system model and assumptions, and complexity issues. Maximum achievable instantaneous rates are derived in Section 4.3, and an average capacity analysis is executed in Section 4.4. Finally in Section 4.5, several numerical examples are studied.

4.2 System Model

Consider the system depicted in Fig. 4.1, including a source node S, a destination node D, and M half-duplex DF relays $\mathrm{R}_1, \ldots, \mathrm{R}_M$. Feasible communication links and the direction of transmissions are shown by arrows in Fig. 4.1.

It is assumed that the transmissions are narrowband, and suffer AWGN and quasistatic flat fading. The channel complex gains are assumed to remain constant during one CR, defined as the duration needed for communicating a message from the source to the destination, but to change independently from one CR to another. Amplitude and phase in-

formation of a link AB is perfectly estimated by, and available to, receiver B for coherent detection. The instantaneous SNRs associated with the links SD, SR_m, and $\mathrm{R}_m\mathrm{D}$ are denoted γ_{SD}, $\gamma_{\mathrm{S}m}$, and $\gamma_{m\mathrm{D}}$, respectively, as shown in Fig. 4.1. It is assumed that the SNRs of the different links are independent [9], [11], [30], [58], [68], [69], [74]–[76].

No optimization for resource (power, time, bandwidth) allocation is considered; the nodes are assumed to transmit with constant power and bandwidth in fixed durations of time during a CR. This assumption is for simplicity as the optimization of resource allocation in cooperative networks, e.g. explored in [5], [30], [64], [67], [69], [75], is generally computationally demanding and least amenable to closed-form solutions, especially when there are more than one relay in the network.

We consider three relaying protocols, superimposed, selection, and orthogonal relaying, and two cooperation strategies, PCC and RC [9], [75]. The two cooperation strategies are opposite extremes in the sense that in PCC, all transmissions from different nodes in a CR utilize different, independent codebooks, while in RC, the same codebook is used for all the transmissions. In fact, in PCC, transmissions from the source to a relay and from a relay to the destination contain fresh MI. Consequently, the resulting MI accumulated at the destination equals the sum of the MI received from orthogonal subspaces [9], [10], [22], viz. parallel subchannels [79, Section 9.4]. In contrast, in the RC case, transmissions convey repeated information such that the destination *accumulates energy*, rather than MI, from different transmissions [22] and that the resulting SNR at the destination equals the sum of the SNRs from source and relay transmissions [9], [10].

One CR is divided into two phases as depicted in Fig. 4.2a. In phase I, which lasts T_0 seconds, in any relaying protocol, the source broadcasts its message to the destination and the relays, which attempt to decode the message fully at the end of Phase I. A relay successful in decoding is called a decoding relay. The three protocols are distinguished in Phase II, where only the source and the decoding relays participate, as illustrated in Figs. 4.2b–4.2d and described in the following.

In superimposed relaying, the source and decoding relays, simultaneously transmit to the destination for T_0 seconds. The destination can execute serial interference cancellation [80] or space-time decoding [9], [11]–[14] for detection if the transmissions are simply superimposed [80] or if the transmissions are distributed-space-time-coded [9], [11]–[14], respectively. The latter is only for the RC case, and needs stringent internode synchroniza-

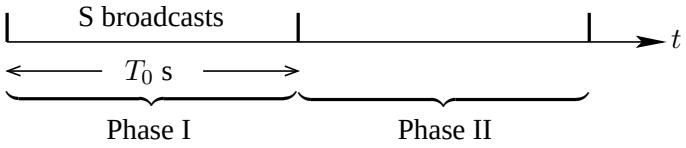

(a) Different phases of the protocols. The protocols differ in Phase II.

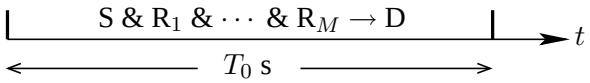

(b) Phase II for superimposed relaying.

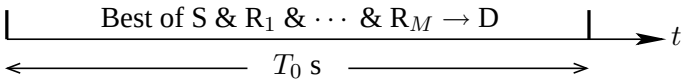

(c) Phase II for selection relaying.

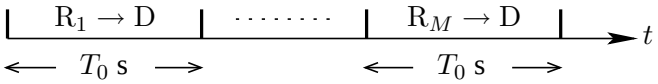

(d) Phase II for orthogonal relaying.

Fig. 4.2. The relaying protocols. A right arrow shows the direction of transmission. A relay transmits only if it has decoded the message. Otherwise, it remains silent.

tion at the symbol level. In selection relaying [58], [68], [74], only the best of the source and decoding relays (i.e. the one with the strongest link to the destination) transmits to the destination in Phase II, which again, lasts T_0 seconds. In orthogonal relaying [9], all relays are assigned orthogonal (time or frequency) channels, each containing as many degrees of freedom as the channel devoted to the source in Phase I.[2] In Fig. 4.2d, only the case of time division multiplexing for the relays has been depicted. The message is retransmitted only by decoding relays in their dedicated channels.

As stipulated earlier, a CR experiences one channel fading block. This assumption best suits delay-sensitive applications.[3] In this chapter, we focus on determining $I_{\max}$, the maximum instantaneous end-to-end MI rate per CR, and $\overline{I_{\max}}$, the expectation of $I_{\max}$ with

[2] A channel of baseband bandwidth W Hz and duration T_0 seconds contains $W\,T_0$ 2-D DoFs [79].

[3] In contrast, in delay-unlimited applications, the CR and codewords can span a large number of independent fading blocks [4], [5], [11], [64] such that the source can benefit from larger ergodic rates.

respect to the channel state

$$\boldsymbol{\gamma} \triangleq (\gamma_{\mathrm{SD}}, \gamma_{\mathrm{S1}}, \ldots, \gamma_{\mathrm{S}M}, \gamma_{\mathrm{1D}}, \ldots, \gamma_{M\mathrm{D}}). \tag{4.1}$$

We refer to $\overline{I_{\max}}$ as the *average capacity*. Using [81, eq. (5-53)], we calculate $\overline{I_{\max}}$ as

$$\overline{I_{\max}} = \int_0^\infty \mathrm{d}r \, [1 - \Pr\{I_{\max} < r\}]. \tag{4.2}$$

To rigorously define $I_{\max}$, first let $I_{\mathrm{DL}}(R)$ be defined as the maximum downlink MI that the destination can gather from Phases I and II when the source's rate is R. A given rate R determines which relays can decode, from which $I_{\mathrm{DL}}(R)$ can be obtained. For example, in selection relaying with PCC, if for a source rate R only Relays 1 and 2 can decode, then $I_{\mathrm{DL}}(R)$ becomes,

$$\frac{1}{2}\ln(1+\gamma_{\mathrm{SD}}) + \frac{1}{2}\ln(1+\max\{\gamma_{\mathrm{SD}}, \gamma_{\mathrm{1D}}, \gamma_{\mathrm{2D}}\}) \tag{4.3}$$

where the first and second summands are the amounts of MI received at the destination from Phases I and II, respectively. The rate R is realizable and does not cause outage if $R \leq I_{\mathrm{DL}}(R)$. Many examples of downlink rates $I_{\mathrm{DL}}(R)$ can be found in [9], [10], [68], [76], where MI is typically used to evaluate outage. Now, we define $I_{\max}$ as

$$I_{\max} = \max_{R \leq I_{\mathrm{DL}}(R)} R. \tag{4.4}$$

Therefore, $I_{\max}$ is the maximum instantaneous, sustainable (nonoutage) rate, or the instantaneous capacity of the system, and thus, important to evaluate. Note that the outage probability at rate R considered in the literature [9], [10], [68], [76], is actually given by

$$P_{\mathrm{out}}(R) \triangleq \Pr\{I_{\mathrm{DL}}(R) < R\} \tag{4.5}$$

rather than by $\Pr\{I_{\max} < R\}$.[4] Although $\Pr\{I_{\max} < R\}$ is equal to $P_{\mathrm{out}}(R)$ for all cases that we consider, the equality does not hold in general, as will be explained in Section 4.4. While the outage performance of relaying networks has received much attention, only limited results are available on $I_{\max}$ and $\overline{I_{\max}}$ for dual-hop DF relaying networks in the literature, e.g. in [59], [70]. Existing results relate to different or simpler networks, and will be compared to our results in Sections 4.3 and 4.4.

[4]Note that $I_{\max}$ is independent of, and can be smaller than, equal to, or greater than, a *given* source rate R.

4.2.1 Complexity Issues

The value $\overline{I_{\max}}$, defined in Section 4.2, has different interpretations for, and implications on the CSI available at the different nodes as follows. The interpretation of $\overline{I_{\max}}$, which is a function of only the channel state $\boldsymbol{\gamma}$, as will be observed in Section 4.4, depends on the source's knowledge of $I_{\max}$ in a CR. If the source is oblivious to $I_{\max}$, outage is always a possibility.[5] In this case, $\overline{I_{\max}}$ is not realizable, but still can serve to compare two systems.

However, if the source can obtain $\boldsymbol{\gamma}$ in each CR via feedback links almost instantly, it can calculate, and adaptively transmit with rate $I_{\max}$ such that no outage occurs. In this case, $\overline{I_{\max}}$ equals the (long-term) average rate. The rate $I_{\max}$ can also be calculated at another node and quickly fed back to the source. For example, it may be practically easier for the destination to obtain $\boldsymbol{\gamma}$ and calculate $I_{\max}$, because the components γ_{SD}, $\gamma_{1\mathrm{D}}, \ldots, \gamma_{M\mathrm{D}}$ of $\boldsymbol{\gamma}$ are estimated at the destination anyway for coherent detection.

Also, independently of the source lacking or obtaining knowledge of $I_{\max}$ for adaptive transmission, the different schemes introduced in Section 4.2 demand different amounts of signaling feedback for their operation, as follows. In superimposed relaying, the decoding relays should declare their successful decoding and participation in Phase II to the destination. In selection relaying, again these success feedbacks from the relays are needed. Additionally, the destination needs to broadcast a designating feedback to determine which node is best to transmit next. In orthogonal relaying, no success or designating feedbacks are required given that the destination can realize which relay is or is not transmitting, by monitoring their dedicated channels.

Note that all the above mentioned CSI and signaling feedbacks entail additional overhead usage and need dedicated time slots or frequency channels, which cause some loss of spectral efficiency. Nevertheless, the assumption of having CSI or feedback at the transmitters is common in the literature of cooperation. Previous research has shown that feedback information can significantly enhance the performance of cooperative networks and is more critical to relaying than DT [3], [10], [23], [58], [68]. The impact of imperfect CSI feedback or feedback delay on the rate performance is worth investigating, but beyond the scope of the investigation here.

[5] Note that in delay-limited scenarios, the source cannot encode over more than one channel fading block.

4.3 Maximum Achievable Instantaneous Rates

In this section, evaluating R and $I_{\mathrm{DL}}(R)$, defined in Section 4.2, and using (4.4) in each case, we derive $I_{\max}$ for the different protocols described in Section 4.2. We assume that both R and $I_{\mathrm{DL}}(R)$ are normalized by the entire period of the CR. We utilize the following notations in our derivations. Assume that the SR SNRs $\gamma_{\mathrm{S}1}, \ldots, \gamma_{\mathrm{S}M}$ are sorted in decreasing order as $\gamma_{\mathrm{S}(1)}, \ldots, \gamma_{\mathrm{S}(M)}$. Let the RD SNR corresponding to $\gamma_{\mathrm{S}(m)}$ be denoted $\gamma_{(m)\mathrm{D}}$. Note that $\gamma_{(1)\mathrm{D}}, \ldots, \gamma_{(M)\mathrm{D}}$ are generally unordered. We also define

$$\gamma_{\mathrm{S}(0)} \triangleq \gamma_{(0)\mathrm{D}} \triangleq \gamma_{\mathrm{SD}} \tag{4.6}$$

and

$$\gamma_{\mathrm{S}(M+1)} \triangleq \gamma_{(M+1)\mathrm{D}} \triangleq 0 \tag{4.7}$$

for convenience, by misuse of notation, as $\gamma_{\mathrm{S}(0)}$ is out of order with $\gamma_{\mathrm{S}(1)}, \ldots, \gamma_{\mathrm{S}(M)}$.

All the achievable rates derived in the following are new and summarized in Table 4.1. The corresponding results for the achievable rates in the single-relay case with fixed resource allocation can be found in [3], [11], [23], [26].

4.3.1 Superimposed Relaying

If the source transmits with rate R_{S} nats per channel use such that

$$\ln\left(1+\gamma_{\mathrm{S}(i+1)}\right) < R_{\mathrm{S}} \leq \ln\left(1+\gamma_{\mathrm{S}(i)}\right) \tag{4.8}$$

for an $i \in \{1, \ldots, M\}$, then only i relays can decode. In this case, denoting $I_{\mathrm{DL}}(R)$ for the PCC and RC cases by $I_{\mathrm{DL}}^{(\mathrm{sup},\,\mathrm{PCC})}(R)$ and $I_{\mathrm{DL}}^{(\mathrm{sup},\,\mathrm{RC})}(R)$, respectively, we obtain

$$R = \frac{R_{\mathrm{S}}}{2} \tag{4.9}$$

$$I_{\mathrm{DL}}^{(\mathrm{sup},\,\mathrm{PCC})}(R) = \frac{1}{2}\left[\ln(1+\gamma_{\mathrm{SD}}) + \ln\left(1+\sum_{m=0}^{i}\gamma_{(m)\mathrm{D}}\right)\right] \tag{4.10}$$

and

$$I_{\mathrm{DL}}^{(\mathrm{sup},\,\mathrm{RC})}(R) = \frac{1}{2}\ln\left(1+\gamma_{\mathrm{SD}}+\sum_{m=0}^{i}\gamma_{(m)\mathrm{D}}\right) \tag{4.11}$$

where all the divisions by 2 are for normalization. This normalization is similar to that employed in [10], [11], [26] due to the CR comprising two equal-size phases. The derivation of

TABLE 4.1
MAXIMUM INSTANTANEOUS RATES IN NATS
ACHIEVABLE IN MULTIRELAY, DUAL-HOP, DF RELAYING NETWORKS

Superimposed relaying with PCC	$\frac{1}{2}\max\left\{2\ln(1+\gamma_{\mathrm{SD}}), \min\left\{\ln\left(1+\gamma_{\mathrm{S}(1)}\right), \ln(1+\gamma_{\mathrm{SD}})+\ln\left(1+\sum_{m=0}^{1}\gamma_{(m)\mathrm{D}}\right)\right\}, \ldots, \min\left\{\ln\left(1+\gamma_{\mathrm{S}(M)}\right), \ln(1+\gamma_{\mathrm{SD}})+\ln\left(1+\sum_{m=0}^{M}\gamma_{(m)\mathrm{D}}\right)\right\}\right\}$
Superimposed relaying with RC	$\frac{1}{2}\max\left\{\ln(1+2\gamma_{\mathrm{SD}}), \min\left\{\ln\left(1+\gamma_{\mathrm{S}(1)}\right), \ln\left(1+\gamma_{\mathrm{SD}}+\sum_{m=0}^{1}\gamma_{(m)\mathrm{D}}\right)\right\}, \ldots, \min\left\{\ln\left(1+\gamma_{\mathrm{S}(M)}\right), \ln\left(1+\gamma_{\mathrm{SD}}+\sum_{m=0}^{M}\gamma_{(m)\mathrm{D}}\right)\right\}\right\}$
Selection relaying with PCC	$\frac{1}{2}\max\Big\{2\ln(1+\gamma_{\mathrm{SD}}), \min\big\{\ln(1+\gamma_{\mathrm{S1}}), \ln(1+\gamma_{\mathrm{SD}})+\ln(1+\gamma_{1\mathrm{D}})\big\}, \ldots, \min\big\{\ln(1+\gamma_{\mathrm{S}M}), \ln(1+\gamma_{\mathrm{SD}})+\ln(1+\gamma_{M\mathrm{D}})\big\}\Big\}$
Selection relaying with RC	$\frac{1}{2}\max\Big\{\ln(1+2\gamma_{\mathrm{SD}}), \min\big\{\ln(1+\gamma_{\mathrm{S1}}), \ln(1+\gamma_{\mathrm{SD}}+\gamma_{1\mathrm{D}})\big\}, \ldots, \min\big\{\ln(1+\gamma_{\mathrm{S}M}), \ln(1+\gamma_{\mathrm{SD}}+\gamma_{M\mathrm{D}})\big\}\Big\}$
Orthogonal relaying with PCC	$\frac{1}{M+1}\max\left\{\ln(1+\gamma_{\mathrm{SD}}), \min\left\{\ln\left(1+\gamma_{\mathrm{S}(1)}\right), \sum_{m=0}^{1}\ln(1+\gamma_{(m)\mathrm{D}})\right\}, \ldots, \min\left\{\ln\left(1+\gamma_{\mathrm{S}(M)}\right), \sum_{m=0}^{M}\ln(1+\gamma_{(m)\mathrm{D}})\right\}\right\}$
Orthogonal relaying with RC	$\frac{1}{M+1}\max\left\{\ln(1+\gamma_{\mathrm{SD}}), \min\left\{\ln\left(1+\gamma_{\mathrm{S}(1)}\right), \ln\left(1+\sum_{m=0}^{1}\gamma_{(m)\mathrm{D}}\right)\right\}, \ldots, \min\left\{\ln\left(1+\gamma_{\mathrm{S}(M)}\right), \ln\left(1+\sum_{m=0}^{M}\gamma_{(m)\mathrm{D}}\right)\right\}\right\}$

(4.10) and (4.11) relies on the facts that the channels from the source to the destination and from the decoding relays to the destination are two independent parallel Gaussian channels [79, Section 9.4], [9], [10], and that the channel from the decoding relays to the destination is a multiaccess channel [79, Section 15.3], [50, Section 16.2].

In PCC, the MI terms from the first and second phases are added, because the transmission in the first phase is orthogonal to the transmissions in the second phase, and because the codebooks used in the different transmissions are independent. However, in the second phase, although different transmissions use independent codebooks, the SNRs, rather than the MI terms, are added because the transmissions are not orthogonal and are simply superimposed. Indeed, in the second phase, the sum-rate capacity according to the multiaccess-channel rate region [79, Section 15.3] is achieved.

In RC, as the codebooks used for all the transmissions in both phases are identical, all the SNRs from Phases I and II are added to give the resulting SNR at the destination.

However, if the source transmits with rate R_{S} nats such that $R_{\mathrm{S}} \geq \ln(1+\gamma_{\mathrm{S}(1)})$, no relays can decode. In this case, one has

$$R = \frac{R_{\mathrm{S}}}{2} \tag{4.12}$$

$$I_{\mathrm{DL}}^{(\mathrm{sup,\,PCC})}(R) = \ln(1+\gamma_{\mathrm{SD}}) \tag{4.13}$$

and

$$I_{\mathrm{DL}}^{(\mathrm{sup,\,RC})}(R) = \frac{1}{2}\ln(1+2\gamma_{\mathrm{SD}}). \tag{4.14}$$

Combining (4.4)–(4.14), we obtain

$$\begin{aligned} I_{\max}^{(\mathrm{sup,\,PCC})} = \frac{1}{2}\max\Bigg\{2\,\ln(1+\gamma_{\mathrm{SD}}), \min\Bigg\{\ln\big(1+\gamma_{\mathrm{S}(1)}\big), \ln(1+\gamma_{\mathrm{SD}})+\ln\Big(1+\sum_{m=0}^{1}\gamma_{(m)\mathrm{D}}\Big)\Bigg\}, \\ \cdots, \min\Bigg\{\ln\big(1+\gamma_{\mathrm{S}(M)}\big), \ln(1+\gamma_{\mathrm{SD}}) + \ln\Big(1+\sum_{m=0}^{M}\gamma_{(m)\mathrm{D}}\Big)\Bigg\}\Bigg\} \end{aligned} \tag{4.15}$$

and

$$\begin{aligned} I_{\max}^{(\mathrm{sup,\,RC})} = \frac{1}{2}\max\Bigg\{\ln(1+2\gamma_{\mathrm{SD}}), \min\Bigg\{\ln\big(1+\gamma_{\mathrm{S}(1)}\big), \ln\Big(1+\gamma_{\mathrm{SD}}+\sum_{m=0}^{1}\gamma_{(m)\mathrm{D}}\Big)\Bigg\}, \\ \cdots, \min\Bigg\{\ln\big(1+\gamma_{\mathrm{S}(M)}\big), \ln\Big(1+\gamma_{\mathrm{SD}}+\sum_{m=0}^{M}\gamma_{(m)\mathrm{D}}\Big)\Bigg\}\Bigg\} \end{aligned} \tag{4.16}$$

where superscripts “sup”, “PCC”, and “RC” denote superimposed relaying, PCC, and RC.

4.3.2 Selection Relaying

In this case, it can be observed that all expressions given in Section 4.3.1 hold after every $\sum_{m=0}^{i}\{\cdot\}$ is replaced with $\max_{m=0,\ldots,i}\{\cdot\}$, as the only difference here is that in Phase II; only the best of the source and decoding relays, rather than all of them, transmits to the destination. Therefore, one can write, in a manner similar to (4.15) and (4.16),

$$I_{\max}^{(\mathrm{sel,\,PCC})}=\frac{1}{2}\max\Big\{2\ln(1+\gamma_{\mathrm{SD}}),\min\Big\{\ln\big(1+\gamma_{\mathrm{S}(1)}\big),\ln(1+\gamma_{\mathrm{SD}})+\ln\Big(1+\max_{m=0,1}\gamma_{(m)\mathrm{D}}\Big)\Big\},$$
$$\cdots,\ \min\Big\{\ln\big(1+\gamma_{\mathrm{S}(M)}\big),\ln(1+\gamma_{\mathrm{SD}})+\ln\Big(1+\max_{m=0,\ldots,M}\gamma_{(m)\mathrm{D}}\Big)\Big\}\Big\} \quad (4.17)$$

and

$$I_{\max}^{(\mathrm{sel,\,RC})}=\frac{1}{2}\max\Big\{\ln(1+2\gamma_{\mathrm{SD}}),\min\Big\{\ln\big(1+\gamma_{\mathrm{S}(1)}\big),\ln\Big(1+\gamma_{\mathrm{SD}}+\max_{m=0,1}\gamma_{(m)\mathrm{D}}\Big)\Big\},\ \ldots,$$
$$\min\Big\{\ln\big(1+\gamma_{\mathrm{S}(M)}\big),\ln\Big(1+\gamma_{\mathrm{SD}}+\max_{m=0,\ldots,M}\gamma_{(m)\mathrm{D}}\Big)\Big\}\Big\} \quad (4.18)$$

where superscript "sel" represents selection relaying. However, we can obtain expressions simpler than (4.17) and (4.18) for $I_{\max}^{(\mathrm{sel,\,PCC})}$ and $I_{\max}^{(\mathrm{sel,\,RC})}$ by taking an alternate approach as follows.

In selection relaying, only one node leading to the largest rate transmits in Phase II. Therefore, the rates resulting from the different nodes transmitting in Phase II can be obtained and compared to see which one is the largest. If the source transmits in Phase II, the resulting rates for PCC and RC are given as,

$$\ln(1+\gamma_{\mathrm{SD}}) \quad (4.19)$$

and

$$\frac{1}{2}\ln(1+2\gamma_{\mathrm{SD}}) \quad (4.20)$$

respectively. Also, if R_i transmits in the downlink, the rates,

$$\min\big\{\ln(1+\gamma_{\mathrm{S}i}),\ln(1+\gamma_{\mathrm{SD}})+\ln(1+\gamma_{i\mathrm{D}})\big\} \quad (4.21)$$

and

$$\min\big\{\ln(1+\gamma_{\mathrm{S}i}),\ln(1+\gamma_{\mathrm{SD}}+\gamma_{i\mathrm{D}})\big\} \quad (4.22)$$

are realizable for PCC and RC, respectively. Therefore, we can write

$$I_{\max}^{(\mathrm{sel,\,PCC})} = \frac{1}{2}\max\Big\{2\ln(1+\gamma_{\mathrm{SD}}), \min\big\{\ln(1+\gamma_{\mathrm{S1}}), \ln(1+\gamma_{\mathrm{SD}})+\ln(1+\gamma_{\mathrm{1D}})\big\}, \ldots, \min\big\{\ln(1+\gamma_{\mathrm{S}M}), \ln(1+\gamma_{\mathrm{SD}})+\ln(1+\gamma_{M\mathrm{D}})\big\}\Big\} \quad (4.23)$$

and

$$I_{\max}^{(\mathrm{sel,\,RC})} = \frac{1}{2}\max\Big\{\ln(1+2\gamma_{\mathrm{SD}}), \min\big\{\ln(1+\gamma_{\mathrm{S1}}), \ln(1+\gamma_{\mathrm{SD}}+\gamma_{\mathrm{1D}})\big\}, \ldots, \min\big\{\ln(1+\gamma_{\mathrm{S}M}), \ln(1+\gamma_{\mathrm{SD}}+\gamma_{M\mathrm{D}})\big\}\Big\}. \quad (4.24)$$

Note that (4.23) and (4.24) can be directly shown to be equivalent to (4.17) and (4.18), respectively. In fact, if one has

$$\max_{m=0,\ldots,j} \gamma_{(m)\mathrm{D}} = \gamma_{(i)\mathrm{D}} \quad (4.25)$$

for given integers i and j satisfying $0 \le i < j \le M$, then

$$\min\Big\{\ln\big(1+\gamma_{\mathrm{S}(j)}\big), \ln(1+\gamma_{\mathrm{SD}})+\ln\Big(1+\max_{m=0,\ldots,j}\gamma_{(m)\mathrm{D}}\Big)\Big\} \le \begin{cases} 2\ln(1+\gamma_{\mathrm{SD}}), & i=0 \\ \min\big\{\ln\big(1+\gamma_{\mathrm{S}(i)}\big), \ln(1+\gamma_{\mathrm{SD}})+\ln\big(1+\gamma_{(i)\mathrm{D}}\big)\big\}, & i>0 \end{cases} \quad (4.26)$$

and

$$\min\Big\{\ln\big(1+\gamma_{\mathrm{S}(j)}\big), \ln\Big(1+\gamma_{\mathrm{SD}}+\max_{m=0,\ldots,j}\gamma_{(m)\mathrm{D}}\Big)\Big\} \le \begin{cases} \ln(1+2\gamma_{\mathrm{SD}}), & i=0 \\ \min\big\{\ln\big(1+\gamma_{\mathrm{S}(i)}\big), \ln\big(1+\gamma_{\mathrm{SD}}+\gamma_{(i)\mathrm{D}}\big)\big\}, & i>0 \end{cases}. \quad (4.27)$$

This obviously shows that in (4.17) and (4.18), we can safely replace,

$$\max_{m=0,\ldots,j} \gamma_{(m)\mathrm{D}} \quad (4.28)$$

with $\gamma_{(j)\mathrm{D}}$ for any j ranging from 1 to M. Making these replacements in (4.17) and (4.18), one can readily reach (4.23) and (4.24).

4.3.3 Orthogonal Relaying

First assume that the source transmits with rate R_{S} satisfying (4.8). Then, only i relays decode, and one has, like (4.9),

$$R = \frac{R_{\mathrm{S}}}{M+1} \quad (4.29)$$

where the division by $M+1$ is because the CR comprises $M+1$ equal-size orthogonal channels. Also, we can write

$$I_{\mathrm{DL}}^{(\mathrm{ort,\,PCC})}(R) = \frac{1}{M+1}\sum_{m=0}^{i}\ln\left(1+\gamma_{(m)\mathrm{D}}\right) \tag{4.30}$$

and

$$I_{\mathrm{DL}}^{(\mathrm{ort,\,RC})}(R) = \frac{1}{M+1}\ln\left(1+\sum_{m=0}^{i}\gamma_{(m)\mathrm{D}}\right) \tag{4.31}$$

where superscript "ort" denotes orthogonal relaying, using the fact that the destination can accumulate MI in the PCC case, and energy in the RC case from the $M+1$ orthogonal channels. Note that in (4.30), contrary to (4.10), we have sums of SNR logarithms, i.e. sums of MI terms, rather than logarithms of SNR sums, for the MI created in Phase II. This is because orthogonal relaying constitutes independent parallel Gaussian channels for the downlink [79, Section 9.4], while superimposed relaying employs an interference-limited multiaccess channel [79, Section 15.3].

If R_{S} is greater than $\ln(1+\gamma_{\mathrm{S}(1)})$ (i.e. if (4.8) is not satisfied), no relays can decode. This leads to the same PCC and RC schemes with the realized MI rate

$$I_{\mathrm{DL}}^{(\mathrm{ort,\,PCC})}(R) = I_{\mathrm{DL}}^{(\mathrm{ort,\,RC})}(R) = \frac{1}{M+1}\ln(1+\gamma_{\mathrm{SD}}). \tag{4.32}$$

Now, combining (4.4) and (4.29)–(4.32) yields

$$I_{\max}^{(\mathrm{ort,\,PCC})} = \frac{1}{M+1}\max\left\{\ln(1+\gamma_{\mathrm{SD}}), \min\left\{\ln\left(1+\gamma_{\mathrm{S}(1)}\right), \sum_{m=0}^{1}\ln\left(1+\gamma_{(m)\mathrm{D}}\right)\right\}, \ldots, \min\left\{\ln\left(1+\gamma_{\mathrm{S}(M)}\right), \sum_{m=0}^{M}\ln\left(1+\gamma_{(m)\mathrm{D}}\right)\right\}\right\} \tag{4.33}$$

and

$$I_{\max}^{(\mathrm{ort,\,RC})} = \frac{1}{M+1}\max\left\{\ln(1+\gamma_{\mathrm{SD}}), \min\left\{\ln\left(1+\gamma_{\mathrm{S}(1)}\right), \ln\left(1+\sum_{m=0}^{1}\gamma_{(m)\mathrm{D}}\right)\right\}, \ldots, \min\left\{\ln\left(1+\gamma_{\mathrm{S}(M)}\right), \ln\left(1+\sum_{m=0}^{M}\gamma_{(m)\mathrm{D}}\right)\right\}\right\}. \tag{4.34}$$

4.4 Capacity Analysis

As shown in (4.2), to obtain the average capacity, we first calculate $\Pr\{I_{\max} < r\}$ at any r. However, deriving this probability directly from the $I_{\max}$ expressions given in Table 4.1

is intricate. Instead, note from (4.4) that for a positive r satisfying $r \leq I_{\mathrm{DL}}(r)$, one has $r \leq I_{\max}$. Therefore, we have

$$\Pr\{I_{\max} < r\} \leq \Pr\{I_{\mathrm{DL}}(r) < r\}. \tag{4.35}$$

Also, $I_{\mathrm{DL}}(r)$ is a decreasing function of r for all the protocols considered, a result obtainable by intuition or by inspecting the rate expressions listed in Table 4.1. Combining this fact with (4.4), we conclude that for a positive r satisfying $r \leq I_{\max}$, we can write

$$r \leq I_{\max} \leq I_{\mathrm{DL}}(I_{\max}) \leq I_{\mathrm{DL}}(r) \tag{4.36}$$

and, therefore,

$$\Pr\{I_{\max} < r\} \geq \Pr\{I_{\mathrm{DL}}(r) < r\}. \tag{4.37}$$

Combining (4.35) and (4.37) yields

$$\Pr\{I_{\max} < r\} = \Pr\{I_{\mathrm{DL}}(r) < r\} \tag{4.38}$$

for all the protocols considered here.[6] The probability $\Pr\{I_{\mathrm{DL}}(r) < r\}$ (which equals $P_{\mathrm{out}}(r)$ from (4.5)) is easier to calculate than $\Pr\{I_{\max} < r\}$ as $I_{\mathrm{DL}}(r)$ can be written as a sum of RVs using the cascaded link technique introduced in [76]. In the sequel, we utilize (4.38) and the cascaded link methodology [76] to calculate $\Pr\{I_{\max} < r\}$.

4.4.1 General Fading Case

Let

$$Y_m \triangleq \begin{cases} \gamma_{m\mathrm{D}}, & \gamma_{\mathrm{S}m} \geq \mathrm{e}^{\nu r} - 1 \\ 0, & \gamma_{\mathrm{S}m} < \mathrm{e}^{\nu r} - 1 \end{cases} \tag{4.39a}$$

where

$$\nu \triangleq \begin{cases} 2, & \text{superimposed or selection relaying} \\ M+1, & \text{orthogonal relaying} \end{cases}. \tag{4.39b}$$

In fact, Y_m is the effective cascaded link SNR of the mth branch at the normalized operating rate r. Now, from the description of the protocols in Section 4.2 and the results derived in

[6] An example where $I_{\mathrm{DL}}(r)$ is not a decreasing function of r and where (4.38) does not hold is as follows. Imagine the orthogonal relaying scheme in this paper, with only one difference that in Phase II, whenever a relay has not decoded, the source substitutes for the relay. In this new scheme, it can be verified that if the SD SNR is larger than at least one RD SNR, $I_{\mathrm{DL}}(r)$ is no more a decreasing function of r, and that (4.37) and (4.38) fail to hold (but (4.35) is still valid).

Section 4.3, one obtains

$$I_{\mathrm{DL}}^{(\mathrm{sup,\,PCC})}(r) = \frac{1}{2}\left[\ln(1+\gamma_{\mathrm{SD}}) + \ln\left(1+\gamma_{\mathrm{SD}}+\sum_{m=1}^{M} Y_m\right)\right] \tag{4.40}$$

$$I_{\mathrm{DL}}^{(\mathrm{sup,\,RC})}(r) = \frac{1}{2}\ln\left(1+2\gamma_{\mathrm{SD}}+\sum_{m=1}^{M} Y_m\right) \tag{4.41}$$

$$I_{\mathrm{DL}}^{(\mathrm{sel,\,PCC})}(r) = \frac{1}{2}\left[\ln(1+\gamma_{\mathrm{SD}}) + \ln\left(1+\max\{\gamma_{\mathrm{SD}}, Y_1, \ldots, Y_M\}\right)\right] \tag{4.42}$$

$$I_{\mathrm{DL}}^{(\mathrm{sel,\,RC})}(r) = \frac{1}{2}\ln\left(1+\gamma_{\mathrm{SD}}+\max\{\gamma_{\mathrm{SD}}, Y_1, \ldots, Y_M\}\right) \tag{4.43}$$

$$I_{\mathrm{DL}}^{(\mathrm{ort,\,PCC})}(r) = \frac{1}{M+1}\left[\ln(1+\gamma_{\mathrm{SD}}) + \sum_{m=1}^{M}\ln(1+Y_m)\right] \tag{4.44}$$

and

$$I_{\mathrm{DL}}^{(\mathrm{ort,\,RC})}(r) = \frac{1}{M+1}\ln\left(1+\gamma_{\mathrm{SD}}+\sum_{m=1}^{M} Y_m\right) \tag{4.45}$$

where superscripts "sup", "sel", and "ort" respectively denote superimposed, selection, and orthogonal relaying.

Then, using (4.38), (4.40), and the theorem of total probability [81, p. 103] we obtain

$$\begin{aligned}\Pr\left\{I_{\max}^{(\mathrm{sup,\,PCC})} < r\right\} &= \int_0^{\infty} \mathrm{d}\gamma\; F_{Y\text{-sum}}\left(\frac{\mathrm{e}^{2r}}{1+\gamma} - 1 - \gamma\right) f_{\mathrm{SD}}(\gamma) \\ &= \int_0^{\mathrm{e}^r-1} \mathrm{d}\gamma\; F_{Y\text{-sum}}\left(\frac{\mathrm{e}^{2r}}{1+\gamma} - 1 - \gamma\right) f_{\mathrm{SD}}(\gamma)\end{aligned} \tag{4.46}$$

and

$$\begin{aligned}\Pr\left\{I_{\max}^{(\mathrm{sup,\,RC})} < r\right\} &= \int_0^{\infty} \mathrm{d}\gamma\; F_{Y\text{-sum}}\left(\mathrm{e}^{2r} - 1 - 2\gamma\right)\right] f_{\mathrm{SD}}(\gamma) \\ &= \int_0^{\frac{\mathrm{e}^{2r}-1}{2}} \mathrm{d}\gamma\; F_{Y\text{-sum}}\left(\mathrm{e}^{2r} - 1 - 2\gamma\right) f_{\mathrm{SD}}(\gamma)\end{aligned} \tag{4.47}$$

where $F_{Y\text{-sum}}(\cdot)$ is the the cumulative distribution function (CDF) of,

$$\sum_{m=1}^{M} Y_m \tag{4.48}$$

and where $f_{\mathrm{SD}}(\cdot)$ is the probability density function (PDF) of γ_{SD}. The second equalities in (4.46) and (4.47) are obtained using the fact that for γ greater than a limit, $F_{Y\text{-sum}}(\cdot)$

vanishes as its argument becomes negative. Similarly, we have

$$\begin{aligned}\Pr\left\{I_{\max}^{(\text{sel, PCC})} < r\right\} &= \int_0^{\infty} \mathrm{d}\gamma \ \Pr\left\{ \max\{\gamma, Y_1, \ldots, Y_M\} < \frac{\mathrm{e}^{2r}}{1+\gamma} - 1 \right\} f_{\text{SD}}(\gamma) \\ &= \int_0^{\mathrm{e}^r - 1} \mathrm{d}\gamma \ \Pr\left\{ \max\{Y_1, \ldots, Y_M\} < \frac{\mathrm{e}^{2r}}{1+\gamma} - 1 \right\} f_{\text{SD}}(\gamma) \\ &= \int_0^{\mathrm{e}^r - 1} \mathrm{d}\gamma \ \prod_{m=1}^{M} F_{Y_m}\left(\frac{\mathrm{e}^{2r}}{1+\gamma} - 1 \right) f_{\text{SD}}(\gamma) \end{aligned} \tag{4.49}$$

and

$$\begin{aligned}\Pr\left\{I_{\max}^{(\text{sel, RC})} < r\right\} &= \int_0^{\infty} \mathrm{d}\gamma \ \Pr\left\{ \max\{\gamma, Y_1, \ldots, Y_M\} < \mathrm{e}^{2r} - 1 - \gamma \right\} f_{\text{SD}}(\gamma) \\ &= \int_0^{\frac{\mathrm{e}^{2r}-1}{2}} \mathrm{d}\gamma \ \Pr\left\{ \max\{Y_1, \ldots, Y_M\} < \mathrm{e}^{2r} - 1 - \gamma \right\} f_{\text{SD}}(\gamma) \\ &= \int_0^{\frac{\mathrm{e}^{2r}-1}{2}} \mathrm{d}\gamma \ \prod_{m=1}^{M} F_{Y_m}\left(\mathrm{e}^{2r} - 1 - \gamma \right) f_{\text{SD}}(\gamma) \end{aligned} \tag{4.50}$$

where $F_{Y_m}(\cdot)$ is the CDF of Y_m and where the fact that the Y_m's are independent has been used (cf. (4.39) and the channel assumptions made in Section 4.2). The second equalities in (4.49) and (4.50) are obtained using the facts that the max terms exceed $\mathrm{e}^{2\,r}/(1+\gamma) - 1$ and $\mathrm{e}^{2\,r} - 1 - \gamma$ for γ greater than $\mathrm{e}^r - 1$ and $(\mathrm{e}^{2\,r} - 1)/2$, respectively. We also obtain

$$\begin{aligned}\Pr\left\{I_{\max}^{(\text{ort, PCC})} < r\right\} &= \int_0^{\infty} \mathrm{d}\gamma \ F_{\ln 1+Y\text{-sum}}\big((M+1)r - \ln(1+\gamma)\big) \, f_{\text{SD}}(\gamma) \\ &= \int_0^{\mathrm{e}^{(M+1)r}-1} \mathrm{d}\gamma \ F_{\ln 1+Y\text{-sum}}\big((M+1)r - \ln(1+\gamma)\big) \, f_{\text{SD}}(\gamma) \end{aligned} \tag{4.51}$$

and

$$\begin{aligned}\Pr\left\{I_{\max}^{(\text{ort, RC})} < r\right\} &= \int_0^{\infty} \mathrm{d}\gamma \ F_{Y\text{-sum}}\Big(\mathrm{e}^{(M+1)r} - 1 - \gamma\Big) \, f_{\text{SD}}(\gamma) \\ &= \int_0^{\mathrm{e}^{(M+1)r}-1} \mathrm{d}\gamma \ F_{Y\text{-sum}}\Big(\mathrm{e}^{(M+1)r} - 1 - \gamma\Big) \, f_{\text{SD}}(\gamma) \end{aligned} \tag{4.52}$$

where $F_{\ln 1+Y\text{-sum}}(\cdot)$ is the CDF of,

$$\sum_{m=1}^{M} \ln(1+Y_m). \tag{4.53}$$

The second equalities in (4.51) and (4.52) are obtained by considering the values of γ at which the arguments of $F_{\ln 1+Y\text{-sum}}(\cdot)$ and $F_{Y\text{-sum}}(\cdot)$ become zero.

To calculate the probabilities (4.46)–(4.52), we first need to calculate $F_{Y_m}(\cdot)$, $F_{Y\text{-sum}}(\cdot)$, and $F_{\ln 1+Y\text{-sum}}(\cdot)$. A general approach to meet this objective, applicable to any fading

model[7] and number of relays, is as follows. The CDF $F_{Y_m}(\cdot)$ can be written from (4.39) as

$$F_{Y_m}(y) = F_{\mathrm{S}m}(\mathrm{e}^{\nu\, r} - 1) + \left[1 - F_{\mathrm{S}m}(\mathrm{e}^{\nu\, r} - 1)\right] F_{m\mathrm{D}}(y) \tag{4.54}$$

where $F_{\mathrm{S}m}(\cdot)$ and $F_{m\mathrm{D}}(\cdot)$ are the CDFs of $\gamma_{\mathrm{S}m}$ and $\gamma_{m\mathrm{D}}$, respectively, and where ν is defined by (4.39b). Also, $F_{Y\text{-sum}}(\cdot)$ and $F_{\ln 1+Y\text{-sum}}(\cdot)$ can be directly represented by the approximate Fourier series in [82] in terms of the moment generating functions (MGFs) of $\sum_{m=1}^{M} Y_m$ and $\sum_{m=1}^{M} \ln(1+Y_m)$, denoted $M_{Y\text{-sum}}(\cdot)$ and $M_{\ln 1+Y\text{-sum}}(\cdot)$, respectively. These MGFs can be written from (4.39) as

$$M_{Y\text{-sum}}(s) = \prod_{m=1}^{M} \mathrm{E}\{\mathrm{e}^{sY_m}\} = \prod_{m=1}^{M} \left\{F_{\mathrm{S}m}(\mathrm{e}^{\nu\, r}-1) + \left[1-F_{\mathrm{S}m}(\mathrm{e}^{\nu\, r}-1)\right] M_{m\mathrm{D}}(s)\right\} \tag{4.55}$$

where $M_{m\mathrm{D}}(\cdot)$ is the MGF of $\gamma_{m\mathrm{D}}$, and

$$\begin{aligned} M_{\ln 1+Y\text{-sum}}(s) &= \prod_{m=1}^{M} \mathrm{E}\{(1+Y_m)^s\} \\ &= \prod_{m=1}^{M} \left\{F_{\mathrm{S}m}(\mathrm{e}^{\nu\, r} - 1) + \left[1 - F_{\mathrm{S}m}(\mathrm{e}^{\nu\, r} - 1)\right]\mathrm{E}\{(1+\gamma_{m\mathrm{D}})^s\}\right\}. \end{aligned} \tag{4.56}$$

Now, (4.2) can be calculated by evaluating the expressions (4.46)–(4.52) using (4.54)–(4.56). However, note that this general method is involved with double integrals over infinite series, that lack a closed-form solution and are difficult to compute with high precision. Next, we specialize the analysis to the Rayleigh fading case.

4.4.2 Rayleigh Fading Case

In this case, not using the MGF approach explained in Section 4.4.1, we can directly evaluate the outage probabilities (4.46)–(4.52) and apply the results to (4.2). The final results for the outage probabilities and average capacities of the different schemes with PCC and RC for Rayleigh fading and any number of relays have been listed in Tables 4.2–4.9. Note that for Rayleigh fading, γ_{SD}, $\gamma_{\mathrm{S}m}$, and $\gamma_{m\mathrm{D}}$ are exponentially distributed with mean values denoted μ_{SD}, $\mu_{\mathrm{S}m}$, and $\mu_{m\mathrm{D}}$, and CDFs denoted $F_{\mathrm{SD}}(\cdot)$, $F_{\mathrm{S}m}(\cdot)$, and $F_{m\mathrm{D}}(\cdot)$. The derivation steps have been summarized in Appendix E. All the results obtained are exact except for orthogonal relaying with PCC and $M > 1$ where only lower and upper bounds are presented due to mathematical intractability. The bounds presented become the corresponding exact values when $M = 1$. In the derivations for any of the schemes, we have considered two

[7] The channel gains are always assumed to be independent in any fading model.

cases of asymmetric and symmetric links, each with and without considering the SD link. These cases and the notations and functions used in the tables are explained next.[8]

The case of asymmetric links for superimposed and orthogonal relaying refers to the situation where μ_{SD}, the $\mu_{\mathrm{S}m}$'s, and the $\mu_{m\mathrm{D}}$'s can take any value except that the $\mu_{m\mathrm{D}}$'s must be unequal. However, this case for selection relaying refers to the most general scenario where μ_{SD}, the $\mu_{\mathrm{S}m}$'s, and the $\mu_{m\mathrm{D}}$'s can have any value. The analysis of the most general scenario for superimposed and orthogonal relaying is very intricate; one can use the general MGF approach, mentioned in Section 4.4.1, in such a scenario instead.

In the symmetric case, considered for analytical simplicity and practical insight [9], [59], we assume that

$$\mu_{\mathrm{S}1} = \cdots = \mu_{\mathrm{S}M} \triangleq \mu_{\mathrm{SR}} \tag{4.57}$$

and

$$\mu_{1\mathrm{D}} = \cdots = \mu_{M\mathrm{D}} \triangleq \mu_{\mathrm{RD}}. \tag{4.58}$$

We also denote the CDFs of the SR and RD SNRs by $F_{\mathrm{SR}}(\cdot)$ and $F_{\mathrm{RD}}(\cdot)$. Note that in selection relaying the results for the symmetric case are simply a special case of those in the asymmetric case. However, in superimposed and orthogonal relaying, the symmetric case is not subsumed under the case of asymmetric links, as in the latter, we assume that the $\mu_{m\mathrm{D}}$'s are unequal. Also, note that the cases of asymmetric and symmetric links for a given scheme coincide when $M = 1$, i.e. when only one relay is available. The single-relay case has been the focus of much research owing to its combined simplicity and offer of diversity [3], [5], [10], [11], [26], [65], [75].

The no SD-link case corresponds to the scenario considered in Chapter 3 and depicted in Fig. 3.1, where the SD link is blocked [30], [57]–[59] such that γ_{SD} can be approximated by zero, or equivalently, the PDF of γ_{SD} can be assumed to be

$$f_{\mathrm{SD}}(\gamma) = \delta(\gamma) \tag{4.59}$$

where $\delta(\cdot)$ is the Dirac delta function. The expressions given in Tables 4.2–4.5, 4.8, and 4.9 for the no SD-link case are not always readily obtainable from those for the cases with

[8]The results given in Tables 4.2, 4.4, 4.6, and 4.8 for the outage probabilities in the RC case can be found in the literature in equivalent forms; e.g. see [9], [68], [72], [74], [83]–[85]. Also, the results for the average capacity of selection relaying with no SD link given in Table 4.5 can be found in [59], [73]. All other results in Tables 4.2–4.9 are new. Here, we list all results for coherence and completeness.

the SD link, which is why we have also presented the results for the no SD-link case in these tables. Inspection of the results in Table 4.1 or Tables 4.2–4.9 reveals that in the no SD-link case, the PCC and RC schemes are identical under either superimposed or selection relaying, but not under orthogonal relaying. Moreover, the rate achievable in the orthogonal relaying scheme with RC is exactly $2/(M+1)$ times that achievable in superimposed relaying with PCC or RC.

There are a number of notations and functions used in Tables 4.2–4.9 as follows. The values $\mu_{\mathrm{S}\mathcal{A}}$ and $\mu_{\mathcal{A}\mathrm{D}}$, where $\mathcal{A}$ is a subset of $\{1, \cdots, M\}$ are defined as

$$\mu_{\mathrm{S}\mathcal{A}} \triangleq \left(\sum_{m \in \mathcal{A}} \mu_{\mathrm{S}m}^{-1} \right)^{-1} \tag{4.60}$$

and

$$\mu_{\mathcal{A}\mathrm{D}} \triangleq \left(\sum_{m \in \mathcal{A}} \mu_{m\mathrm{D}}^{-1} \right)^{-1}. \tag{4.61}$$

When $\mathcal{A}$ is empty, $\mu_{\mathrm{S}\mathcal{A}}^{-1}$ and $\mu_{\mathcal{A}\mathrm{D}}^{-1}$ are defined as zero. The operator $|\cdot|$ is the cardinality operator for a set. The set $\mathcal{A}^{\mathrm{c}}$ represents the complement of $\mathcal{A}$ with respect to $\{1, \cdots, M\}$. The functions $P(\cdot,\cdot)$ and $\Gamma(\cdot,\cdot)$ are the regularized lower incomplete gamma [86, eq. 6.5.3] and the upper incomplete gamma [86, eq. 6.5.1] functions, respectively. The former can be written in terms of the latter as

$$P(a,x) = 1 - \frac{\Gamma(a,x)}{\Gamma(a)} \tag{4.62}$$

where $\Gamma(\cdot)$ is the gamma function [86, eq. 6.1.1]. We also use the definite integrals

$$\mathcal{I}_m(k,a,b,c,d) \triangleq \int_1^d \mathrm{d}x \; \frac{x^{k-1}}{b\,c\,x+1} \, \mathrm{e}^{-(ax^m+bx)} \tag{4.63}$$

$$\mathcal{I}_m(k,a,b,c) \triangleq \mathcal{I}_m(k,a,b,c,\infty) \tag{4.64}$$

$$\mathcal{R}(k,\ell,\eta,a,b) \triangleq \int_1^\infty \mathrm{d}x \; \frac{x^k}{(ax+b)^\ell} \, \mathrm{e}^{-\eta\,x} \, \Gamma(\ell, ax^2+bx) \tag{4.65}$$

$\mathcal{R}(\eta,a,b) \triangleq \mathcal{R}(0,0,\eta,a,b)$

$$= \begin{cases} -\Gamma(0,b) + \mathrm{e}^{-b}/b, & \eta = 0, a = 0, b > 0 \\ -\Gamma(0,a+b) + 2\,\mathcal{I}_2(1,a,b,0) & \\ -\frac{b}{a}\,\mathcal{I}_2\Big(0, \frac{(a+b)^2}{a}, -\frac{b(a+b)}{a}, 0\Big), & \eta = 0, a > \max\{-b, 0\} \\ \frac{1}{\eta}\big[\mathrm{e}^{-\eta}\,\Gamma(0,b) - \Gamma(0,\eta+b)\big], & \eta \neq 0, a = 0, \\ & b > \max\{-\eta, 0\} \\ \frac{1}{\eta}\Big[\mathrm{e}^{-\eta}\,\Gamma(0,a+b) - \mathcal{I}_2(0,a,\eta+b,0) & \\ -\mathrm{e}^{\eta\,b/a}\,\mathcal{I}_2\Big(0, \frac{(a+b)^2}{a}, \frac{(\eta-b)(a+b)}{a}, 0\Big)\Big], & \eta \neq 0, a > \max\{-b, 0\} \end{cases} \tag{4.66}$$

$$h(x;\ell,a) \triangleq \frac{1}{(\ell-1)!}\int_0^a \mathrm{d}t\; t^{\ell-1}\,\mathrm{e}^{-x\,t} = \begin{cases} P(\ell,ax)/x^\ell, & x \neq 0 \\ a^\ell/\ell!, & x = 0 \end{cases} \tag{4.67}$$

and

$$g(x;\ell,w,\alpha) \triangleq \int_0^\infty \mathrm{d}t\; (t+1)^{w-1}\,\mathrm{e}^{-\alpha\,t}\,h(x;\ell,t)$$

$$= \begin{cases} \frac{\mathrm{e}^\alpha}{x^\ell}\Big[\frac{\Gamma(w,\alpha)}{\alpha^w} - \frac{1}{(x+\alpha)^w} & \\ \times \sum_{k=0}^{\ell-1}\Big(\frac{x}{x+\alpha}\Big)^k\,\frac{\Gamma(k+w,x+\alpha)\,\Gamma(\ell-k,-x)}{k!\,(\ell-k-1)!}\Big], & x \neq 0 \\ \frac{(-1)^\ell\,\mathrm{e}^\alpha}{\alpha^w}\sum_{k=0}^{\ell}\frac{(-1/\alpha)^k}{k!\,(\ell-k)!}\,\Gamma(k+w,\alpha), & x = 0 \end{cases} . \tag{4.68}$$

The integrals (4.63)–(4.65) lack a closed-form solution in general in terms of standard mathematical functions, but are efficiently numerically computable using standard integration techniques, e.g. presented in [86, Section 25.4]. The integrals (4.66)–(4.68) have been solved using common integration methods, such as change of variables and integration by parts. Further, we define and use the functions

$$\mathcal{S}(x) \triangleq \mathrm{e}^x\,\Gamma(0,x) \tag{4.69}$$

and

$$\mathcal{T}(\alpha,\beta) \triangleq \begin{cases} \frac{\mathcal{S}(\beta)-\mathcal{S}(\alpha)}{\alpha-\beta}, & \alpha \neq \beta \\ \frac{1}{\alpha} - \mathcal{S}(\alpha), & \alpha = \beta \end{cases} \tag{4.70}$$

where $\mathcal{S}(\cdot)$ is given by (4.69), for convenience.

TABLE 4.2
OUTAGE PROBABILITY AT RATE r NATS FOR SUPERIMPOSED RELAYING IN THE RAYLEIGH FADING CASE

Asymmetric case with the SD link with PCC	$1-\mathrm{e}^{(1-\mathrm{e}^{r})/\mu_{\mathrm{SD}}}-\dfrac{\mathrm{e}^{1/\mu_{\mathrm{SD}}}}{\mu_{\mathrm{SD}}}\displaystyle\sum_{m=1}^{M}\mathrm{e}^{(1-\mathrm{e}^{2r})/\mu_{\mathrm{S}m}}\prod_{\substack{k=1\\k\neq m}}^{M}\left(1+\dfrac{\mathrm{e}^{(1-\mathrm{e}^{2r})/\mu_{\mathrm{S}k}}}{\mu_{m\mathrm{D}}/\mu_{k\mathrm{D}}-1}\right)\times\mathcal{I}_{-1}\left(1,\dfrac{\mathrm{e}^{2r}}{\mu_{m\mathrm{D}}},\dfrac{1}{\mu_{\mathrm{SD}}}-\dfrac{1}{\mu_{m\mathrm{D}}},0,\mathrm{e}^{r}\right)$
Asymmetric case with the SD link with RC	$1-\mathrm{e}^{(1-\mathrm{e}^{2r})/(2\,\mu_{\mathrm{SD}})}-\dfrac{1}{2\,\mu_{\mathrm{SD}}}\displaystyle\sum_{m=1}^{M}\mathrm{e}^{(1/\mu_{\mathrm{S}m}+1/\mu_{m\mathrm{D}})(1-\mathrm{e}^{2r})}\times\prod_{\substack{k=1\\k\neq m}}^{M}\left(1+\dfrac{\mathrm{e}^{(1-\mathrm{e}^{2r})/\mu_{\mathrm{S}k}}}{\mu_{m\mathrm{D}}/\mu_{k\mathrm{D}}-1}\right)h\left(\dfrac{1}{2\,\mu_{\mathrm{SD}}}-\dfrac{1}{\mu_{m\mathrm{D}}};1,\mathrm{e}^{2r}-1\right)$
Asymmetric case with no SD link with PCC or RC	$1-\displaystyle\sum_{m=1}^{M}\mathrm{e}^{(1/\mu_{\mathrm{S}m}+1/\mu_{m\mathrm{D}})(1-\mathrm{e}^{2r})}\prod_{\substack{k=1\\k\neq m}}^{M}\left(1+\dfrac{\mathrm{e}^{(1-\mathrm{e}^{2r})/\mu_{\mathrm{S}k}}}{\mu_{m\mathrm{D}}/\mu_{k\mathrm{D}}-1}\right)$
Symmetric case with the SD link with PCC	$1-\mathrm{e}^{(1-\mathrm{e}^{r})/\mu_{\mathrm{SD}}}-\dfrac{\mathrm{e}^{1/\mu_{\mathrm{SD}}}}{\mu_{\mathrm{SD}}}\displaystyle\sum_{m=1}^{M}\sum_{k=0}^{m-1}\sum_{p=0}^{k}\binom{M}{m}\dfrac{(-1)^{k-p}\,\mathrm{e}^{2\,p\,r}}{(k-p)!\,p!\,\mu_{\mathrm{RD}}^{k}}\times\mathrm{e}^{m(1-\mathrm{e}^{2r})/\mu_{\mathrm{SR}}}\left[1-\mathrm{e}^{(1-\mathrm{e}^{2r})/\mu_{\mathrm{SR}}}\right]^{M-m}\times\mathcal{I}_{-1}\left(k-2p+1,\dfrac{\mathrm{e}^{2r}}{\mu_{\mathrm{RD}}},\dfrac{1}{\mu_{\mathrm{SD}}}-\dfrac{1}{\mu_{\mathrm{RD}}},0,\mathrm{e}^{r}\right)$
Symmetric case with the SD link with RC	$1-\mathrm{e}^{(1-\mathrm{e}^{2r})/(2\,\mu_{\mathrm{SD}})}-\dfrac{\mu_{\mathrm{RD}}\,\mathrm{e}^{(1-\mathrm{e}^{2r})/(2\,\mu_{\mathrm{SD}})}}{2\,\mu_{\mathrm{SD}}}\displaystyle\sum_{m=1}^{M}\sum_{k=1}^{m}\binom{M}{m}\times\mathrm{e}^{m(1-\mathrm{e}^{2r})/\mu_{\mathrm{SR}}}\left[1-\mathrm{e}^{(1-\mathrm{e}^{2r})/\mu_{\mathrm{SR}}}\right]^{M-m}h\left(1-\dfrac{\mu_{\mathrm{RD}}}{2\,\mu_{\mathrm{SD}}};k,\dfrac{\mathrm{e}^{2r}-1}{\mu_{\mathrm{RD}}}\right)$
Symmetric case with no SD link with PCC or RC	$\displaystyle\sum_{m=0}^{M}\binom{M}{m}\mathrm{e}^{m(1-\mathrm{e}^{2r})/\mu_{\mathrm{SR}}}\left[1-\mathrm{e}^{(1-\mathrm{e}^{2r})/\mu_{\mathrm{SR}}}\right]^{M-m}P\left(m,\dfrac{\mathrm{e}^{2r}-1}{\mu_{\mathrm{RD}}}\right)$

TABLE 4.3
AVERAGE CAPACITY IN NATS FOR SUPERIMPOSED RELAYING IN THE RAYLEIGH FADING CASE

Asymmetric case with the SD link with PCC	$\mathcal{S}\Big(\frac{1}{\mu_{\mathrm{SD}}}\Big) + \frac{\mathrm{e}^{1/\mu_{\mathrm{SD}}}}{2\,\mu_{\mathrm{SD}}} \sum_{m=1}^{M} \sum_{\mathcal{A}\subset\{1,\cdots,M\}-\{m\}} \frac{\mathrm{e}^{1/\mu_{\mathrm{S}m}+1/\mu_{\mathrm{S}\mathcal{A}}}}{\prod_{k\in\mathcal{A}}\left(\frac{\mu_{m\mathrm{D}}}{\mu_{k\mathrm{D}}}-1\right)} \times \mathcal{R}\Big(\frac{1}{\mu_{\mathrm{SD}}}-\frac{1}{\mu_{m\mathrm{D}}}, \frac{1}{\mu_{\mathrm{S}m}}+\frac{1}{\mu_{\mathrm{S}\mathcal{A}}}, \frac{1}{\mu_{m\mathrm{D}}}\Big)$
Asymmetric case with the SD link with RC	$\frac{1}{2}\,\mathcal{S}\Big(\frac{1}{2\,\mu_{\mathrm{SD}}}\Big) + \frac{1}{4\,\mu_{\mathrm{SD}}} \sum_{m=1}^{M} \sum_{\mathcal{A}\subset\{1,\cdots,M\}-\{m\}} \frac{1}{\prod_{k\in\mathcal{A}}\left(\frac{\mu_{m\mathrm{D}}}{\mu_{k\mathrm{D}}}-1\right)} \times \mathcal{T}\Big(\frac{1}{2\,\mu_{\mathrm{SD}}}+\frac{1}{\mu_{\mathrm{S}m}}+\frac{1}{\mu_{\mathrm{S}\mathcal{A}}}, \frac{1}{\mu_{\mathrm{S}m}}+\frac{1}{\mu_{\mathrm{S}\mathcal{A}}}+\frac{1}{\mu_{m\mathrm{D}}}\Big)$
Asymmetric case with no SD link with PCC or RC	$\frac{1}{2}\sum_{m=1}^{M} \sum_{\mathcal{A}\subset\{1,\cdots,M\}-\{m\}} \frac{\mathcal{S}\left(\frac{1}{\mu_{\mathrm{S}m}}+\frac{1}{\mu_{\mathrm{S}\mathcal{A}}}+\frac{1}{\mu_{m\mathrm{D}}}\right)}{\prod_{k\in\mathcal{A}}\left(\frac{\mu_{m\mathrm{D}}}{\mu_{k\mathrm{D}}}-1\right)}$
Symmetric case with the SD link with PCC	$\mathcal{S}\Big(\frac{1}{\mu_{\mathrm{SD}}}\Big) + \frac{\mathrm{e}^{1/\mu_{\mathrm{SD}}}}{2\,\mu_{\mathrm{SD}}} \sum_{m=1}^{M}\sum_{k=m}^{M}\sum_{p=0}^{m-1}\sum_{q=0}^{p} \frac{(-1)^{q+k-m}\,M!}{(M-k)!\,(k-m)!\,m!} \times \frac{\mathrm{e}^{k/\mu_{\mathrm{SR}}}}{(p-q)!\,q!\,\mu_{\mathrm{RD}}^{p}}\,\mathcal{R}\Big(q, p-q, \frac{1}{\mu_{\mathrm{SD}}}-\frac{1}{\mu_{\mathrm{RD}}}, \frac{k}{\mu_{\mathrm{SR}}}, \frac{1}{\mu_{\mathrm{RD}}}\Big)$
Symmetric case with the SD link with RC	$\frac{1}{2}\,\mathcal{S}\Big(\frac{1}{2\,\mu_{\mathrm{SD}}}\Big) + \frac{M!}{4\,\mu_{\mathrm{SD}}} \sum_{m=1}^{M}\sum_{k=1}^{m}\sum_{p=m}^{M} \frac{(-1)^{p-m}}{(M-p)!\,(p-m)!\,m!\,\mu_{\mathrm{RD}}^{k-1}} \times g\Big(\frac{1}{\mu_{\mathrm{RD}}}-\frac{1}{2\,\mu_{\mathrm{SD}}}; k, 0, \frac{1}{2\,\mu_{\mathrm{SD}}}+\frac{p}{\mu_{\mathrm{SR}}}\Big)$
Symmetric case with no SD link with PCC or RC	$\sum_{m=1}^{M}\sum_{k=m}^{M}\sum_{p=0}^{m-1} \frac{(-1)^{k-m}\,(M!/2)\,\mathrm{e}^{k/\mu_{\mathrm{SR}}}}{(M-k)!\,(k-m)!\,m!\,(m-p-1)!\,p!\,\left(k\frac{\mu_{\mathrm{RD}}}{\mu_{\mathrm{SR}}}+1\right)^{p}} \times \Gamma\Big(m-p, -\frac{1}{\mu_{\mathrm{RD}}}\Big)\,\Gamma\Big(p, \frac{k}{\mu_{\mathrm{SR}}}+\frac{1}{\mu_{\mathrm{RD}}}\Big)$

TABLE 4.4
OUTAGE PROBABILITY AT RATE r NATS FOR SELECTION RELAYING IN THE RAYLEIGH FADING CASE

Asymmetric case with the SD link with PCC	$\dfrac{\mathrm{e}^{1/\mu_{\mathrm{SD}}}}{\mu_{\mathrm{SD}}} \displaystyle\sum_{\mathcal{A}\subset\{1,\cdots,M\}} (-1)^{\lvert\mathcal{A}\rvert}\ \mathrm{e}^{(1-\mathrm{e}^{2r})/\mu_{\mathrm{S}\mathcal{A}}+1/\mu_{\mathcal{A}\mathrm{D}}}\ \mathcal{I}_{-1}\Big(1, \dfrac{\mathrm{e}^{2r}}{\mu_{\mathcal{A}\mathrm{D}}}, \dfrac{1}{\mu_{\mathrm{SD}}}, 0, \mathrm{e}^{r}\Big)$
Asymmetric case with the SD link with RC	$\dfrac{1}{\mu_{\mathrm{SD}}} \displaystyle\sum_{\mathcal{A}\subset\{1,\cdots,M\}} (-1)^{\lvert\mathcal{A}\rvert}\ \mathrm{e}^{(1/\mu_{\mathrm{S}\mathcal{A}}+1/\mu_{\mathcal{A}\mathrm{D}})(1-\mathrm{e}^{2r})} \times h\Big(\dfrac{1}{\mu_{\mathrm{SD}}} - \dfrac{1}{\mu_{\mathcal{A}\mathrm{D}}}; 1, \dfrac{\mathrm{e}^{2r}-1}{2}\Big)$
Asymmetric case with no SD link with PCC or RC	$\displaystyle\prod_{m=1}^{M} \Big[1 - \mathrm{e}^{(1/\mu_{\mathrm{S}m}+1/\mu_{m\mathrm{D}})(1-\mathrm{e}^{2r})}\Big]$
Symmetric case with the SD link with PCC	$\dfrac{\mathrm{e}^{1/\mu_{\mathrm{SD}}}}{\mu_{\mathrm{SD}}} \displaystyle\sum_{m=0}^{M} \binom{M}{m} (-1)^{m}\ \mathrm{e}^{m(1-\mathrm{e}^{2r})/\mu_{\mathrm{SR}}+m/\mu_{\mathrm{RD}}} \times \mathcal{I}_{-1}\Big(1, \dfrac{m\,\mathrm{e}^{2r}}{\mu_{\mathrm{RD}}}, \dfrac{1}{\mu_{\mathrm{SD}}}, 0, \mathrm{e}^{r}\Big)$
Symmetric case with the SD link with RC	$\dfrac{1}{\mu_{\mathrm{SD}}} \displaystyle\sum_{m=0}^{M} \binom{M}{m} (-1)^{m}\ \mathrm{e}^{m(1/\mu_{\mathrm{SR}}+1/\mu_{\mathrm{RD}})(1-\mathrm{e}^{2r})} \times h\Big(\dfrac{1}{\mu_{\mathrm{SD}}} - \dfrac{m}{\mu_{\mathrm{RD}}}; 1, \dfrac{\mathrm{e}^{2r}-1}{2}\Big)$
Symmetric case with no SD link with PCC or RC	$\Big[1 - \mathrm{e}^{(1/\mu_{\mathrm{SR}}+1/\mu_{\mathrm{RD}})(1-\mathrm{e}^{2r})}\Big]^{M}$

TABLE 4.5
AVERAGE CAPACITY IN NATS FOR SELECTION RELAYING IN THE RAYLEIGH FADING CASE

Asymmetric case with the SD link with PCC	$\mathcal{S}\Big(\frac{1}{\mu_{\mathrm{SD}}}\Big) + \frac{1}{2\,\mu_{\mathrm{SD}}} \sum\limits_{\substack{\mathcal{A}\subset\{1,\cdots,M\}\\ \mathcal{A}\neq\varnothing}} (-1)^{\lvert\mathcal{A}\rvert-1} \times \mathrm{e}^{1/\mu_{\mathrm{SD}}+1/\mu_{\mathrm{S}\mathcal{A}}+1/\mu_{\mathcal{A}\mathrm{D}}}\, \mathcal{R}\Big(\frac{1}{\mu_{\mathrm{SD}}}, \frac{1}{\mu_{\mathrm{S}\mathcal{A}}}, \frac{1}{\mu_{\mathcal{A}\mathrm{D}}}\Big)$
Asymmetric case with the SD link with RC	$\frac{1}{2}\,\mathcal{S}\Big(\frac{1}{2\,\mu_{\mathrm{SD}}}\Big) + \frac{1}{4\,\mu_{\mathrm{SD}}} \sum\limits_{\substack{\mathcal{A}\subset\{1,\cdots,M\}\\ \mathcal{A}\neq\varnothing}} (-1)^{\lvert\mathcal{A}\rvert-1} \times \mathcal{T}\Big(\frac{1}{2\,\mu_{\mathrm{SD}}} + \frac{1}{\mu_{\mathrm{S}\mathcal{A}}} + \frac{1}{2\,\mu_{\mathcal{A}\mathrm{D}}}, \frac{1}{\mu_{\mathrm{S}\mathcal{A}}} + \frac{1}{\mu_{\mathcal{A}\mathrm{D}}}\Big)$
Asymmetric case with no SD link with PCC or RC	$\frac{1}{2} \sum\limits_{\substack{\mathcal{A}\subset\{1,\cdots,M\}\\ \mathcal{A}\neq\varnothing}} (-1)^{\lvert\mathcal{A}\rvert-1}\, \mathcal{S}\Big(\frac{1}{\mu_{\mathrm{S}\mathcal{A}}} + \frac{1}{\mu_{\mathcal{A}\mathrm{D}}}\Big)$
Symmetric case with the SD link with PCC	$\mathcal{S}\Big(\frac{1}{\mu_{\mathrm{SD}}}\Big) + \frac{1}{2\,\mu_{\mathrm{SD}}} \sum\limits_{m=1}^{M} \binom{M}{m} (-1)^{m-1} \times \mathrm{e}^{1/\mu_{\mathrm{SD}}+m/\mu_{\mathrm{SR}}+m/\mu_{\mathrm{RD}}}\, \mathcal{R}\Big(\frac{1}{\mu_{\mathrm{SD}}}, \frac{m}{\mu_{\mathrm{SR}}}, \frac{m}{\mu_{\mathrm{RD}}}\Big)$
Symmetric case with the SD link with RC	$\frac{1}{2}\,\mathcal{S}\Big(\frac{1}{2\,\mu_{\mathrm{SD}}}\Big) + \frac{1}{4\,\mu_{\mathrm{SD}}} \sum\limits_{m=1}^{M} \binom{M}{m} (-1)^{m-1} \times \mathcal{T}\Big(\frac{1}{2\,\mu_{\mathrm{SD}}} + \frac{m}{\mu_{\mathrm{SR}}} + \frac{m}{2\,\mu_{\mathrm{RD}}}, \frac{m}{\mu_{\mathrm{SR}}} + \frac{m}{\mu_{\mathrm{RD}}}\Big)$
Symmetric case with no SD link with PCC or RC	$\frac{1}{2} \sum\limits_{m=1}^{M} \binom{M}{m} (-1)^{m-1}\, \mathcal{S}\Big(\frac{m}{\mu_{\mathrm{SR}}} + \frac{m}{\mu_{\mathrm{RD}}}\Big)$

TABLE 4.6
OUTAGE PROBABILITY AT RATE r NATS FOR ORTHOGONAL RELAYING WITH THE SD LINK IN THE RAYLEIGH FADING CASE
(The bounds become the exact values for $M = 1$)

Asymmetric case with PCC, lower bound	$1 - \mathrm{e}^{\left(1-\mathrm{e}^{(M+1)r}\right)/\mu_{\mathrm{SD}}} - \dfrac{\mathrm{e}^{1/\mu_{\mathrm{SD}}}}{\mu_{\mathrm{SD}}} \displaystyle\sum_{\substack{\mathcal{A}\subset\{1,\cdots,M\}\\ \mathcal{A}\neq\varnothing}} \mathrm{e}^{\left(1-\mathrm{e}^{(M+1)r}\right)/\mu_{\mathrm{S}\mathcal{A}}} \times \prod_{m\in\mathcal{A}^{\mathrm{c}}} \left[1 - \mathrm{e}^{\left(1-\mathrm{e}^{(M+1)r}\right)/\mu_{\mathrm{S}m}}\right] \sum_{m\in\mathcal{A}} \dfrac{\mathrm{e}^{\lvert\mathcal{A}\rvert/\mu_{m\mathrm{D}}}}{\prod_{\substack{k\in\mathcal{A}\\ k\neq m}} \left(1 - \frac{\mu_{k\mathrm{D}}}{\mu_{m\mathrm{D}}}\right)} \times \mathcal{I}_{-1/\lvert\mathcal{A}\rvert}\left(1, \dfrac{\lvert\mathcal{A}\rvert\,\mathrm{e}^{(M+1)r/\lvert\mathcal{A}\rvert}}{\mu_{m\mathrm{D}}}, \dfrac{1}{\mu_{\mathrm{SD}}}, 0, \mathrm{e}^{(M+1)r}\right)$
Asymmetric case with PCC, upper bound	$1 - \mathrm{e}^{\left(1-\mathrm{e}^{(M+1)r}\right)/\mu_{\mathrm{SD}}} - \dfrac{\mathrm{e}^{1/\mu_{\mathrm{SD}}}}{\mu_{\mathrm{SD}}} \displaystyle\sum_{\substack{\mathcal{A}\subset\{1,\cdots,M\}\\ \mathcal{A}\neq\varnothing}} \mathrm{e}^{\left(1-\mathrm{e}^{(M+1)r}\right)/\mu_{\mathrm{S}\mathcal{A}}+1/\mu_{\mathcal{A}\mathrm{D}}} \times \prod_{m\in\mathcal{A}^{\mathrm{c}}} \left[1-\mathrm{e}^{\left(1-\mathrm{e}^{(M+1)r}\right)/\mu_{\mathrm{S}m}}\right] \mathcal{I}_{-1/\lvert\mathcal{A}\rvert}\left(1, \dfrac{\mathrm{e}^{(M+1)r/\lvert\mathcal{A}\rvert}}{\mu_{\mathcal{A}\mathrm{D}}}, \dfrac{1}{\mu_{\mathrm{SD}}}, 0, \mathrm{e}^{(M+1)r}\right)$
Asymmetric case with RC, exact value	$1 - \mathrm{e}^{\left(1-\mathrm{e}^{(M+1)r}\right)/\mu_{\mathrm{SD}}} - \displaystyle\sum_{m=1}^{M} \mathrm{e}^{(1/\mu_{\mathrm{S}m}+1/\mu_{m\mathrm{D}})\left(1-\mathrm{e}^{(M+1)r}\right)} \times \prod_{\substack{k=1\\ k\neq m}}^{M} \left[1 + \dfrac{\mathrm{e}^{\left(1-\mathrm{e}^{(M+1)r}\right)/\mu_{\mathrm{S}k}}}{\frac{\mu_{m\mathrm{D}}}{\mu_{k\mathrm{D}}} - 1}\right] h\left(1 - \dfrac{\mu_{\mathrm{SD}}}{\mu_{m\mathrm{D}}}; 1, \dfrac{\mathrm{e}^{(M+1)r} - 1}{\mu_{\mathrm{SD}}}\right)$
Symmetric case with PCC, lower bound	$1 - \mathrm{e}^{\left(1-\mathrm{e}^{(M+1)r}\right)/\mu_{\mathrm{SD}}} - \dfrac{\mathrm{e}^{1/\mu_{\mathrm{SD}}}}{\mu_{\mathrm{SD}}} \displaystyle\sum_{m=1}^{M} \sum_{k=0}^{m-1} \sum_{p=0}^{k} \binom{M}{m} \dfrac{(-1)^{k-p}(m/\mu_{\mathrm{RD}})^k}{(k-p)!\,p!} \times \mathrm{e}^{m\left(1-\mathrm{e}^{(M+1)r}\right)/\mu_{\mathrm{SR}}+m/\mu_{\mathrm{RD}}+(M+1)r\,p/m} \left[1 - \mathrm{e}^{\left(1-\mathrm{e}^{(M+1)r}\right)/\mu_{\mathrm{SR}}}\right]^{M-m} \times \mathcal{I}_{-1/m}\left(1 - \dfrac{p}{m}, \dfrac{m\,\mathrm{e}^{(M+1)r/m}}{\mu_{\mathrm{RD}}}, \dfrac{1}{\mu_{\mathrm{SD}}}, 0, \mathrm{e}^{(M+1)r}\right)$
Symmetric case with PCC, upper bound	$1 - \mathrm{e}^{\left(1-\mathrm{e}^{(M+1)r}\right)/\mu_{\mathrm{SD}}} - \dfrac{\mathrm{e}^{1/\mu_{\mathrm{SD}}}}{\mu_{\mathrm{SD}}} \displaystyle\sum_{m=1}^{M} \binom{M}{m} \mathrm{e}^{m\left(1-\mathrm{e}^{(M+1)r}\right)/\mu_{\mathrm{SR}}+m/\mu_{\mathrm{RD}}} \times \left[1 - \mathrm{e}^{\left(1-\mathrm{e}^{(M+1)r}\right)/\mu_{\mathrm{SR}}}\right]^{M-m} \mathcal{I}_{-1/m}\left(1, \dfrac{m\,\mathrm{e}^{(M+1)r/m}}{\mu_{\mathrm{RD}}}, \dfrac{1}{\mu_{\mathrm{SD}}}, 0, \mathrm{e}^{(M+1)r}\right)$
Symmetric case with RC, exact value	$1 - \mathrm{e}^{\left(1-\mathrm{e}^{(M+1)r}\right)/\mu_{\mathrm{SD}}} - \dfrac{\mu_{\mathrm{RD}}\,\mathrm{e}^{\left(1-\mathrm{e}^{(M+1)r}\right)/\mu_{\mathrm{SD}}}}{\mu_{\mathrm{SD}}} \times \displaystyle\sum_{m=1}^{M} \sum_{k=1}^{m} \binom{M}{m} \mathrm{e}^{m\left(1-\mathrm{e}^{(M+1)r}\right)/\mu_{\mathrm{SR}}} \left[1 - \mathrm{e}^{\left(1-\mathrm{e}^{(M+1)r}\right)/\mu_{\mathrm{SR}}}\right]^{M-m} \times h\left(1 - \dfrac{\mu_{\mathrm{RD}}}{\mu_{\mathrm{SD}}}; k, \dfrac{\mathrm{e}^{(M+1)r} - 1}{\mu_{\mathrm{RD}}}\right)$

TABLE 4.7
AVERAGE CAPACITY IN NATS FOR ORTHOGONAL RELAYING
WITH THE SD LINK IN THE RAYLEIGH FADING CASE
(The bounds become the exact values for $M = 1$)

Asymmetric case with PCC, lower bound	$\frac{1}{M+1}\,\mathcal{S}\Big(\frac{1}{\mu_{\mathrm{SD}}}\Big) + \frac{1}{M+1}\sum_{\substack{\mathcal{A}\subset\{1,\cdots,M\}\\ \mathcal{A}\neq\varnothing}}\sum_{\mathcal{B}\subset\mathcal{A}^{\mathrm{c}}}(-1)^{\lvert\mathcal{B}\rvert}$ $\times\,\mathrm{e}^{1/\mu_{\mathrm{S}\mathcal{A}}+1/\mu_{\mathrm{S}\mathcal{B}}+1/\mu_{\mathcal{A}\mathrm{D}}}\,\mathcal{I}_{1/\lvert\mathcal{A}\rvert}\Big(0,\frac{1}{\mu_{\mathcal{A}\mathrm{D}}},\frac{1}{\mu_{\mathrm{S}\mathcal{A}}}+\frac{1}{\mu_{\mathrm{S}\mathcal{B}}},\mu_{\mathrm{SD}}\Big)$
Asymmetric case with PCC, upper bound	$\frac{1}{M+1}\,\mathcal{S}\Big(\frac{1}{\mu_{\mathrm{SD}}}\Big) + \frac{1}{M+1}\sum_{\substack{\mathcal{A}\subset\{1,\cdots,M\}\\ \mathcal{A}\neq\varnothing}}\sum_{\mathcal{B}\subset\mathcal{A}^{\mathrm{c}}}\sum_{m\in\mathcal{A}}\frac{(-1)^{\lvert\mathcal{B}\rvert}}{\prod_{\substack{k\in\mathcal{A}\\ k\neq m}}\left(1-\frac{\mu_{k\mathrm{D}}}{\mu_{m\mathrm{D}}}\right)}$ $\times\,\mathrm{e}^{1/\mu_{\mathrm{S}\mathcal{A}}+1/\mu_{\mathrm{S}\mathcal{B}}+\lvert\mathcal{A}\rvert/\mu_{m\mathrm{D}}}\,\mathcal{I}_{1/\lvert\mathcal{A}\rvert}\Big(0,\frac{\lvert\mathcal{A}\rvert}{\mu_{m\mathrm{D}}},\frac{1}{\mu_{\mathrm{S}\mathcal{A}}}+\frac{1}{\mu_{\mathrm{S}\mathcal{B}}},\mu_{\mathrm{SD}}\Big)$
Asymmetric case with RC, exact value	$\frac{1}{M+1}\,\mathcal{S}\Big(\frac{1}{\mu_{\mathrm{SD}}}\Big) + \frac{1}{(M+1)\mu_{\mathrm{SD}}}\sum_{m=1}^{M}\sum_{\mathcal{A}\subset\{1,\cdots,M\}-\{m\}}$ $\frac{\mathcal{T}\Big(\frac{1}{\mu_{\mathrm{SD}}}+\frac{1}{\mu_{\mathrm{S}m}}+\frac{1}{\mu_{\mathrm{S}\mathcal{A}}},\frac{1}{\mu_{\mathrm{S}m}}+\frac{1}{\mu_{\mathrm{S}\mathcal{A}}}+\frac{1}{\mu_{m\mathrm{D}}}\Big)}{\prod_{k\in\mathcal{A}}\Big(\frac{\mu_{m\mathrm{D}}}{\mu_{k\mathrm{D}}}-1\Big)}$
Symmetric case with PCC, lower bound	$\frac{1}{M+1}\,\mathcal{S}\Big(\frac{1}{\mu_{\mathrm{SD}}}\Big) + \frac{M!}{M+1}\sum_{m=1}^{M}\sum_{k=m}^{M}\frac{(-1)^{k-m}\,\mathrm{e}^{m/\mu_{\mathrm{RD}}+k/\mu_{\mathrm{SR}}}}{(M-k)!\,(k-m)!\,m!}$ $\times\,\mathcal{I}_{1/m}\Big(0,\frac{m}{\mu_{\mathrm{RD}}},\frac{k}{\mu_{\mathrm{SR}}},\mu_{\mathrm{SD}}\Big)$
Symmetric case with PCC, upper bound	$\frac{1}{M+1}\,\mathcal{S}\Big(\frac{1}{\mu_{\mathrm{SD}}}\Big) + \frac{M!}{M+1}\sum_{m=1}^{M}\sum_{k=m}^{M}\sum_{p=0}^{m-1}\frac{(-1)^{k-m}\,(m/\mu_{\mathrm{RD}})^{p}}{(M-k)!\,(k-m)!\,m!}$ $\times\,\frac{\mathrm{e}^{k/\mu_{\mathrm{SR}}}}{(m-p-1)!\,p!}\,\Gamma\Big(m-p,-\frac{m}{\mu_{\mathrm{RD}}}\Big)\,\mathcal{I}_{1/m}\Big(\frac{p}{m},\frac{m}{\mu_{\mathrm{RD}}},\frac{k}{\mu_{\mathrm{SR}}},\mu_{\mathrm{SD}}\Big)$
Symmetric case with RC, exact value	$\frac{1}{M+1}\,\mathcal{S}\Big(\frac{1}{\mu_{\mathrm{SD}}}\Big) + \frac{M!}{(M+1)\mu_{\mathrm{SD}}}\sum_{m=1}^{M}\sum_{k=1}^{m}\sum_{p=m}^{M}$ $\frac{(-1)^{p-m}}{(M-p)!\,(p-m)!\,m!\,\mu_{\mathrm{RD}}^{k-1}}\,g\Big(\frac{1}{\mu_{\mathrm{RD}}}-\frac{1}{\mu_{\mathrm{SD}}};k,0,\frac{1}{\mu_{\mathrm{SD}}}+\frac{p}{\mu_{\mathrm{SR}}}\Big)$

TABLE 4.8
OUTAGE PROBABILITY AT RATE r NATS FOR ORTHOGONAL RELAYING WITH NO SD LINK IN THE RAYLEIGH FADING CASE
(The bounds become the exact values for $M = 1$)

Asymmetric case with PCC, lower bound	$1 - \sum_{\substack{\mathcal{A}\subset\{1,\cdots,M\} \\ \mathcal{A}\neq\varnothing}} \mathrm{e}^{(1-\mathrm{e}^{(M+1)r})/\mu_{\mathrm{S}\mathcal{A}}} \prod_{m\in\mathcal{A}^{\mathrm{c}}} \left[1 - \mathrm{e}^{(1-\mathrm{e}^{(M+1)r})/\mu_{\mathrm{S}m}}\right] \times \sum_{m\in\mathcal{A}} \frac{\mathrm{e}^{(1-\mathrm{e}^{(M+1)r/\lvert\mathcal{A}\rvert})\lvert\mathcal{A}\rvert/\mu_{m\mathrm{D}}}}{\prod_{\substack{k\in\mathcal{A} \\ k\neq m}} \left(1 - \frac{\mu_{k\mathrm{D}}}{\mu_{m\mathrm{D}}}\right)}$
Asymmetric case with PCC, upper bound	$1 - \sum_{\substack{\mathcal{A}\subset\{1,\cdots,M\} \\ \mathcal{A}\neq\varnothing}} \mathrm{e}^{(1-\mathrm{e}^{(M+1)r})/\mu_{\mathrm{S}\mathcal{A}} + (1-\mathrm{e}^{(M+1)r/\lvert\mathcal{A}\rvert})/\mu_{\mathcal{A}\mathrm{D}}} \times \prod_{m\in\mathcal{A}^{\mathrm{c}}} \left[1 - \mathrm{e}^{(1-\mathrm{e}^{(M+1)r})/\mu_{\mathrm{S}m}}\right]$
Asymmetric case with RC, exact value	$1 - \sum_{m=1}^{M} \mathrm{e}^{(1/\mu_{\mathrm{S}m} + 1/\mu_{m\mathrm{D}})(1-\mathrm{e}^{(M+1)r})} \prod_{\substack{k=1 \\ k\neq m}}^{M} \left[1 + \frac{\mathrm{e}^{(1-\mathrm{e}^{(M+1)r})/\mu_{\mathrm{S}k}}}{\frac{\mu_{m\mathrm{D}}}{\mu_{k\mathrm{D}}} - 1}\right]$
Symmetric case with PCC, lower bound	$\sum_{m=0}^{M} \binom{M}{m} \mathrm{e}^{(1-\mathrm{e}^{(M+1)r})m/\mu_{\mathrm{SR}}} \left[1 - \mathrm{e}^{(1-\mathrm{e}^{(M+1)r})/\mu_{\mathrm{SR}}}\right]^{M-m} \times P\left(m, \frac{m}{\mu_{\mathrm{RD}}}\left[\mathrm{e}^{(M+1)r/m} - 1\right]\right)$
Symmetric case with PCC, upper bound	$1 - \sum_{m=1}^{M} \binom{M}{m} \mathrm{e}^{m(1-\mathrm{e}^{(M+1)r})/\mu_{\mathrm{SR}} + m(1-\mathrm{e}^{(M+1)r/m})/\mu_{\mathrm{RD}}} \times \left[1 - \mathrm{e}^{(1-\mathrm{e}^{(M+1)r})/\mu_{\mathrm{SR}}}\right]^{M-m}$
Symmetric case with RC, exact value	$\sum_{m=0}^{M} \binom{M}{m} \mathrm{e}^{m(1-\mathrm{e}^{(M+1)r})/\mu_{\mathrm{SR}}} \left[1 - \mathrm{e}^{(1-\mathrm{e}^{(M+1)r})/\mu_{\mathrm{SR}}}\right]^{M-m} \times P\left(m, \frac{\mathrm{e}^{(M+1)r} - 1}{\mu_{\mathrm{RD}}}\right)$

TABLE 4.9
AVERAGE CAPACITY IN NATS FOR ORTHOGONAL RELAYING WITH NO SD LINK IN THE RAYLEIGH FADING CASE
(The bounds become the exact values for $M = 1$)

Asymmetric case with PCC, lower bound	$\frac{1}{M+1} \sum\limits_{\substack{\mathcal{A} \subset \{1, \cdots, M\} \\ \mathcal{A} \neq \varnothing}} \sum\limits_{\mathcal{B} \subset \mathcal{A}^{\mathrm{c}}} (-1)^{\lvert\mathcal{B}\rvert} \, \mathrm{e}^{1/\mu_{\mathrm{S}\mathcal{A}} + 1/\mu_{\mathrm{S}\mathcal{B}} + 1/\mu_{\mathcal{A}\mathrm{D}}} \times \mathcal{I}_{1/\lvert\mathcal{A}\rvert}\left(0, \frac{1}{\mu_{\mathcal{A}\mathrm{D}}}, \frac{1}{\mu_{\mathrm{S}\mathcal{A}}} + \frac{1}{\mu_{\mathrm{S}\mathcal{B}}}, 0\right)$
Asymmetric case with PCC, upper bound	$\frac{1}{M+1} \sum\limits_{\substack{\mathcal{A} \subset \{1, \cdots, M\} \\ \mathcal{A} \neq \varnothing}} \sum\limits_{\mathcal{B} \subset \mathcal{A}^{\mathrm{c}}} \sum\limits_{m \in \mathcal{A}} \frac{(-1)^{\lvert\mathcal{B}\rvert} \, \mathrm{e}^{1/\mu_{\mathrm{S}\mathcal{A}} + 1/\mu_{\mathrm{S}\mathcal{B}} + \lvert\mathcal{A}\rvert/\mu_{m\mathrm{D}}}}{\prod_{\substack{k \in \mathcal{A} \\ k \neq m}} \left(1 - \frac{\mu_{k\mathrm{D}}}{\mu_{m\mathrm{D}}}\right)} \times \mathcal{I}_{1/\lvert\mathcal{A}\rvert}\left(0, \frac{\lvert\mathcal{A}\rvert}{\mu_{m\mathrm{D}}}, \frac{1}{\mu_{\mathrm{S}\mathcal{A}}} + \frac{1}{\mu_{\mathrm{S}\mathcal{B}}}, 0\right)$
Asymmetric case with RC, exact value	$\frac{1}{M+1} \sum\limits_{m=1}^{M} \sum\limits_{\mathcal{A} \subset \{1, \cdots, M\} - \{m\}} \frac{\mathcal{S}\left(\frac{1}{\mu_{\mathrm{S}m}} + \frac{1}{\mu_{\mathrm{S}\mathcal{A}}} + \frac{1}{\mu_{m\mathrm{D}}}\right)}{\prod_{k \in \mathcal{A}} \left(\frac{\mu_{m\mathrm{D}}}{\mu_{k\mathrm{D}}} - 1\right)}$
Symmetric case with PCC, lower bound	$\frac{M!}{M+1} \sum\limits_{m=1}^{M} \sum\limits_{k=m}^{M} \frac{(-1)^{k-m} \, \mathrm{e}^{k/\mu_{\mathrm{SR}} + m/\mu_{\mathrm{RD}}}}{(M-k)! \, (k-m)! \, (m-1)!} \mathcal{I}_m\left(0, \frac{k}{\mu_{\mathrm{SR}}}, \frac{m}{\mu_{\mathrm{RD}}}, 0\right)$
Symmetric case with PCC, upper bound	$\frac{M!}{M+1} \sum\limits_{m=1}^{M} \sum\limits_{k=m}^{M} \sum\limits_{p=0}^{m-1} \frac{(-1)^{k-m} \, (m/\mu_{\mathrm{RD}})^p \, \mathrm{e}^{k/\mu_{\mathrm{SR}}}}{(M-k)! \, (k-m)! \, (m-1)! \, (m-p-1)! \, p!} \times \Gamma\left(m-p, -\frac{m}{\mu_{\mathrm{RD}}}\right) \mathcal{I}_m\left(p, \frac{k}{\mu_{\mathrm{SR}}}, \frac{m}{\mu_{\mathrm{RD}}}, 0\right)$
Symmetric case with RC, exact value	$\sum\limits_{m=1}^{M} \sum\limits_{k=m}^{M} \sum\limits_{p=0}^{m-1} \frac{(-1)^{k-m} \, [M!/(M+1)] \, \mathrm{e}^{k/\mu_{\mathrm{SR}}}}{(M-k)! \, (k-m)! \, m! \, (m-p-1)! \, p! \left(k\frac{\mu_{\mathrm{RD}}}{\mu_{\mathrm{SR}}} + 1\right)^p} \times \Gamma\left(m-p, -\frac{1}{\mu_{\mathrm{RD}}}\right) \Gamma\left(p, \frac{k}{\mu_{\mathrm{SR}}} + \frac{1}{\mu_{\mathrm{RD}}}\right)$

4.5 Numerical Results

In this section, some numerical examples are given to verify the analysis performed and to evaluate the performance of the relaying schemes for Rayleigh fading, where the SNRs of the different links are exponentially distributed.

Figs. 4.3 and 4.4 verify the analytical results given in Tables 4.2–4.9, respectively for the outage probability and average capacity, by Monte Carlo simulation for two-relay, asymmetric and symmetric cases. The outage probability has been calculated for the normalized rate $r = 2$ bits, and the average capacity has been expressed in bits. In the asymmetric case, we assume that $\mu_{\mathrm{S1}} = \mu_{\mathrm{SD}} + 25$ dB, $\mu_{\mathrm{1D}} = \mu_{\mathrm{SD}} + 12$ dB, $\mu_{\mathrm{S2}} = \mu_{\mathrm{SD}} + 22$ dB, and $\mu_{\mathrm{2D}} = \mu_{\mathrm{SD}} + 15$ dB. This scenario corresponds to a situation where R_1 and R_2 are closer to the source than to the destination, which is appropriate for DF relaying, and where R_1 is slightly closer to the source than R_2 is. In the symmetric case, we have $\mu_{\mathrm{SR}} = \mu_{\mathrm{SD}} + 27$ dB and $\mu_{\mathrm{RD}} = \mu_{\mathrm{SD}} + 18$ dB which corresponds to the case where both relays are located in a similar position closer to the source than to the destination.

Note that in all cases, the simulation and analytical results are in excellent agreement. In addition, Figs. 4.3e, 4.3f, 4.4e, and 4.4f show that the lower bound on the outage probability and upper bound on the average capacity of orthogonal relaying with PCC are very tight. In fact, this situation exists for many other examples not included here for brevity, such that we only exhibit the outage probability lower and average capacity upper bounds for the performance of orthogonal relaying with PCC in the subsequent figures. In contrast to the lower bound, the upper bound on the outage probability is not satisfactory and degrades as the average SNRs improve. Also, the lower bound on the average capacity is not as tight as the upper bound for small values of SNR, but improves for large SNR regimes. Note from Appendix E that both the lower bound on the outage probability and upper bound on the average capacity of orthogonal relaying with PCC are obtained from a single bound on CDF $F_{\ln 1+Y\text{-sum}}(\cdot)$. Also, the outage probability upper and average capacity lower bounds originate from another bound on $F_{\ln 1+Y\text{-sum}}(\cdot)$.

There are other important observations from Figs. 4.3 and 4.4 as follows. Fig. 4.3 shows that a diversity order of 3 is obtainable from all the schemes in large SNR regimes; i.e., the outage probability is approximately proportional to $1/\mu_{\mathrm{SD}}^3$ for large values of μ_{SD}. Also, the PCC over RC gain in superimposed, selection, and orthogonal relaying, in terms

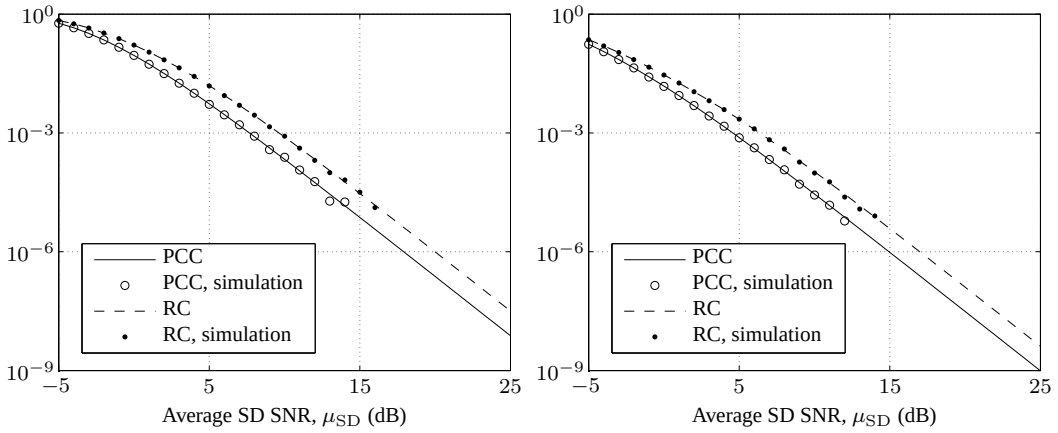

(a) Superimposed relaying, the asymmetric case. (b) Superimposed relaying, the symmetric case.

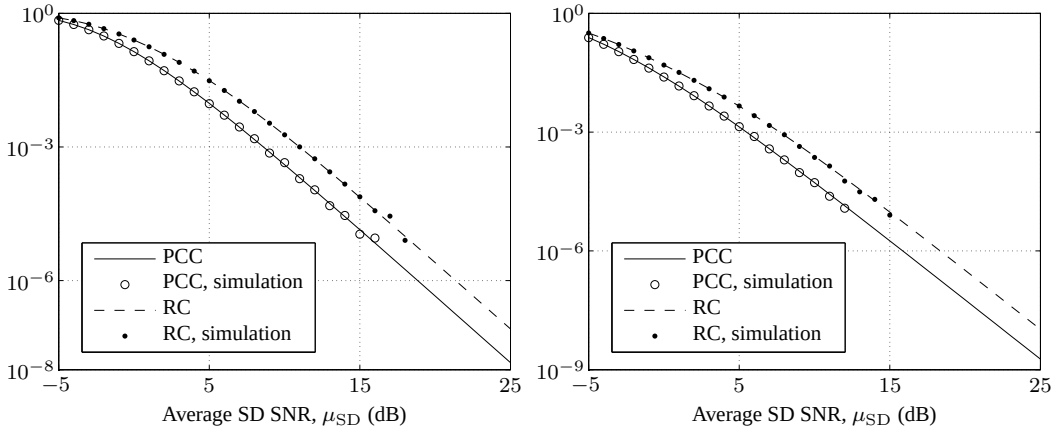

(c) Selection relaying, the asymmetric case. (d) Selection relaying, the symmetric case.

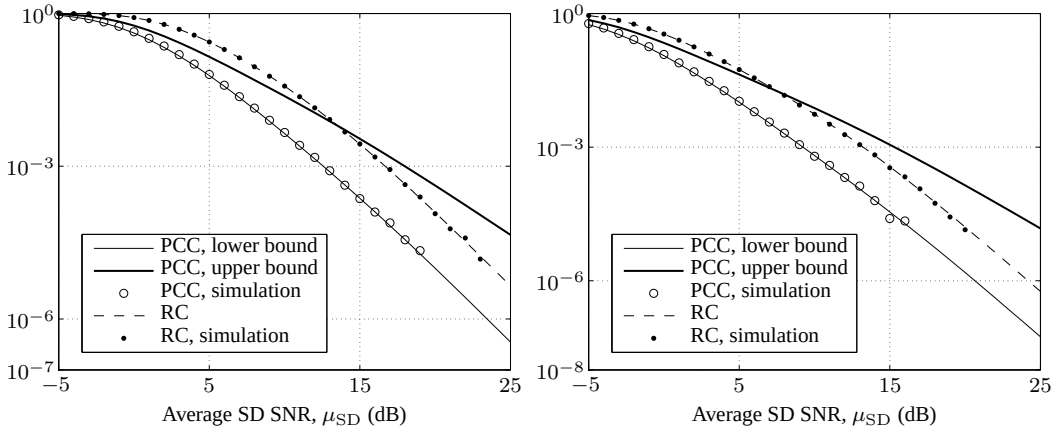

(e) Orthogonal relaying, the asymmetric case. (f) Orthogonal relaying, the symmetric case.

Fig. 4.3. The outage probability at $r = 2$ bits versus the average SD SNR for the different protocols, for asymmetric and symmetric cases when there are two relays available.

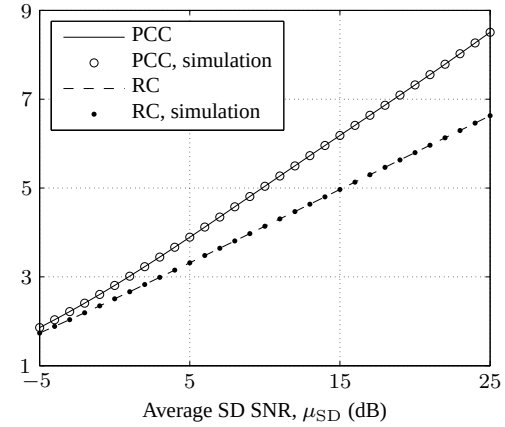

(a) Superimposed relaying, the asymmetric case.

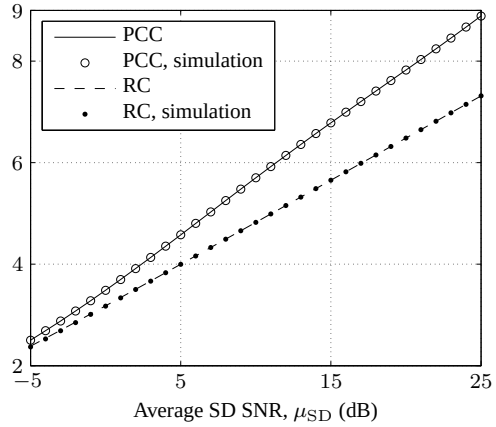

(b) Superimposed relaying, the symmetric case.

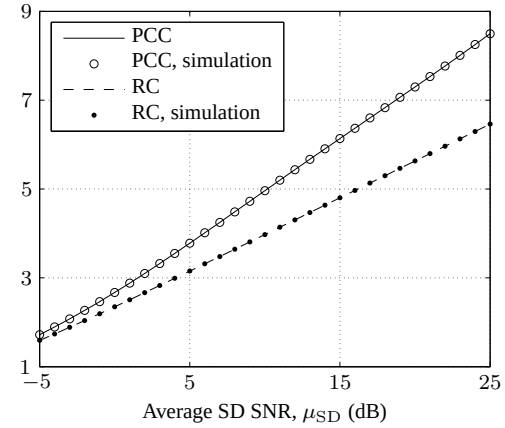

(c) Selection relaying, the asymmetric case.

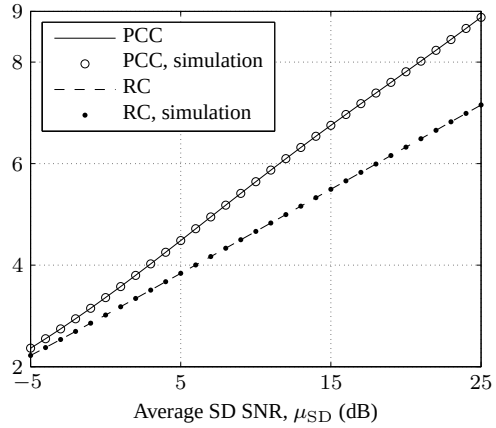

(d) Selection relaying, the symmetric case.

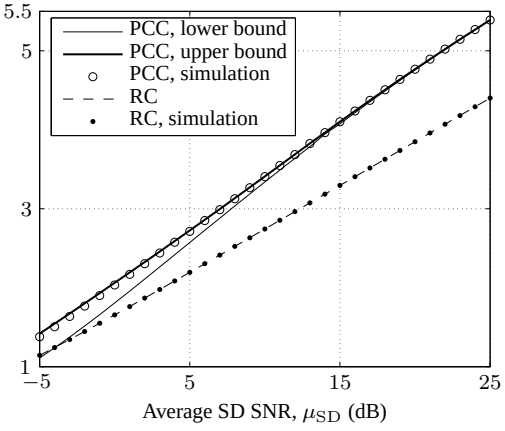

(e) Orthogonal relaying, the asymmetric case.

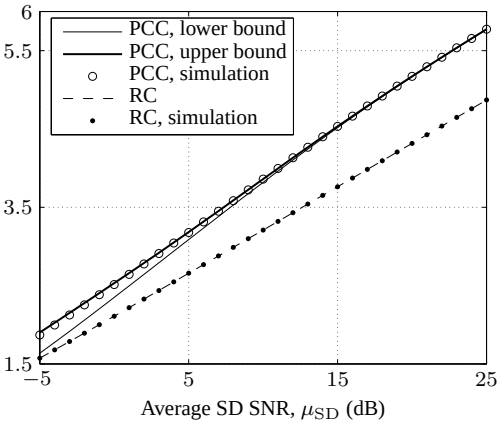

(f) Orthogonal relaying, the symmetric case.

Fig. 4.4. The average capacity in bits versus the average SD SNR for the different protocols, for asymmetric and symmetric cases when there are two relays available.

of the outage performance, can be as much as 2.0 dB, 2.5 dB, and 3.9 dB, respectively. Fig. 4.4 shows that this gain, for the capacity performance, can be larger and up to 8 dB for superimposed relaying, 8.4 dB for selection relaying, and 7.9 dB for orthogonal relaying.

Figs. 4.5 and 4.6 respectively show the outage probability at $r = 1$ bit and average capacity of the different schemes versus the normalized distance of the relays from the source for a linear network topology in the symmetric case when $M = 3$. We assume in this topology that

$$d_{\mathrm{SD}} = d_{\mathrm{SR}} + d_{\mathrm{RD}} \tag{4.71}$$

where d_{SD}, d_{SR}, and d_{RD} are the SD, SR, and RD distances. We also assume that $\mu_{\mathrm{SD}} = 7$ dB, and that, using a simplified path loss model [50, p. 843], [87, Section 2.6],

$$\mu_{\mathrm{SR}} = \mu_{\mathrm{SD}} \left(\frac{d_{\mathrm{SD}}}{d_{\mathrm{SR}}} \right)^{\alpha} \tag{4.72}$$

and

$$\mu_{\mathrm{RD}} = \mu_{\mathrm{SD}} \left(\frac{d_{\mathrm{SD}}}{d_{\mathrm{RD}}} \right)^{\alpha} \tag{4.73}$$

where α is the path loss exponent set to 4 here.[9]

In Figs. 4.5 and 4.6, we have also included the performance of DT as a baseline for comparison. The maximum instantaneous rate for DT is given as [79, Chapter 9]

$$I_{\max}^{(\mathrm{DT})} \triangleq \ln(1 + \gamma_{\mathrm{SD}}) \tag{4.74}$$

nats per 2-D DoF. Therefore, the corresponding outage probability at rate r nats and average capacity in nats for Rayleigh fading are obtained as

$$\Pr\{I_{\max}^{(\mathrm{DT})} < r\} = \Pr\{I_{\max} < \mathrm{e}^{r} - 1\} = 1 - \mathrm{e}^{(1-\mathrm{e}^{r})/\mu_{\mathrm{SD}}} \tag{4.75}$$

and

$$\overline{I_{\max}^{(\mathrm{DT})}} \triangleq \int_0^{\infty} \mathrm{d}\gamma \ \ln(1+\gamma)\, f_{\mathrm{SD}}(\gamma) = \frac{1}{\mu_{\mathrm{SD}}} \int_0^{\infty} \mathrm{d}\gamma \ \ln(1+\gamma)\, \mathrm{e}^{-\gamma/\mu_{\mathrm{SD}}} = \mathcal{S}\left(\frac{1}{\mu_{\mathrm{SD}}}\right) \tag{4.76}$$

where $\mathcal{S}(\cdot)$ is defined by (4.69). Note that despite the relaying schemes for which achievability of the average capacity needs adaptive transmission from the source (as explained in Section 4.2), in DT, $\overline{I_{\max}^{(\mathrm{DT})}}$ is achievable even without CSI at the transmitter [88].

Fig. 4.5 shows that all the relaying schemes significantly outperform DT in terms of

[9] The path loss exponent normally ranges from 1.6 to 6.5 [87, Section 2.6]. A smaller value corresponds to less average signal attenuation in the channel.

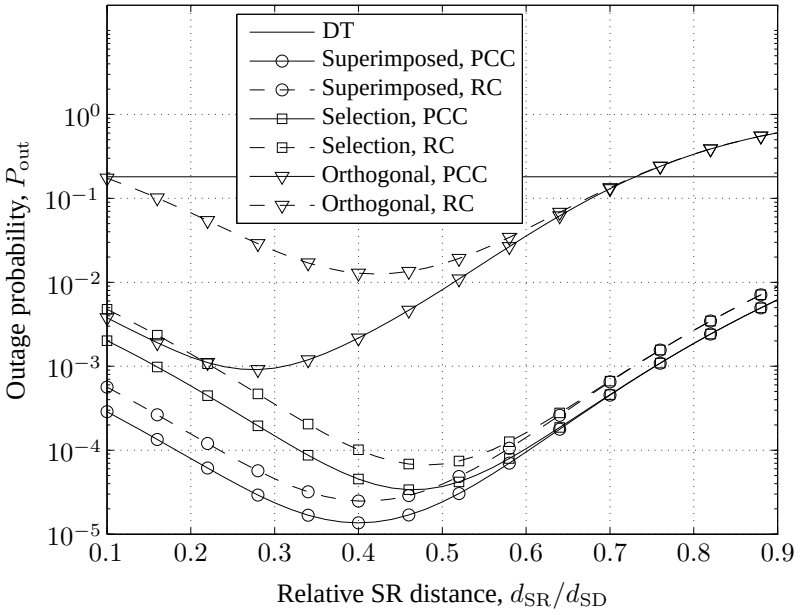

Fig. 4.5. The outage probability at $r = 1$ bit versus the SR distance normalized by the SD distance, for the different protocols and a linear network topology in the symmetric case when $M = 3$ and $\mu_{\text{SD}} = 7$ dB.

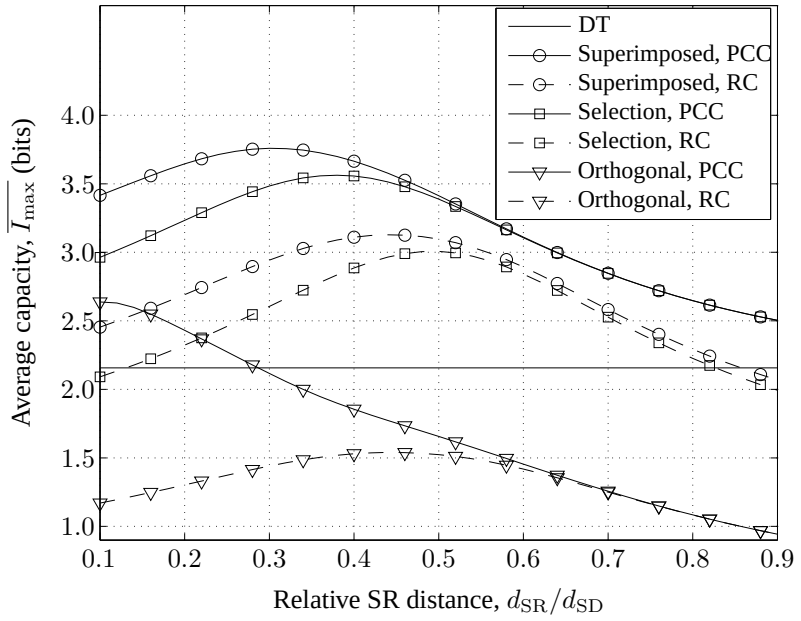

Fig. 4.6. The average capacity in bits versus the SR distance normalized by the SD distance, for the different protocols and a linear network topology in the symmetric case when $M = 3$ and $\mu_{\text{SD}} = 7$ dB.

the outage probability, except for orthogonal relaying when $d_{\text{SR}}/d_{\text{SD}}$ is large. In fact, when $d_{\text{SR}}/d_{\text{SD}}$ is increased, fewer relays decode the message and the performance degrades in all schemes. However, orthogonal relaying is more susceptible in this regard as in this scheme, the time or frequency slot given to a relay is left unused if the relay cannot decode.

Also, note from the figure that superimposed and orthogonal relaying respectively have the best and poorest outage performance for the same cooperation strategy (PCC or RC). Further, it is observed that the relaying schemes have an optimal point of operation in terms of $d_{\mathrm{SR}}/d_{\mathrm{SD}}$. This is expected as when the relays move farther from the source, on the one hand, fewer relays can decode the message, but on the other, their RD links become stronger. The optimal performance occurs at the optimal point of this tradeoff.

Fig. 4.6 presents results with explanations similar to those given for Fig. 4.6, for the average capacity performance of the schemes. However, one major difference here is that except for small values of $d_{\mathrm{SR}}/d_{\mathrm{SD}}$ and its PCC scheme, orthogonal relaying is inferior to DT. Such a poor capacity performance is generally explained by orthogonalization loss, first noted and explained in [9] for the outage performance of an orthogonal relaying system. This loss essentially refers to the diminution of the achievable rate when averaged over several orthogonal channels.

Figs. 4.7 and 4.8 depict the outage and capacity performances of the schemes versus the number of relays in a symmetric case. Fig. 4.7 shows that while the outage performances of superimposed and selection relaying improve as M increases, the outage performance of orthogonal relaying deteriorates for more than 3 relays. Also, Fig. 4.8 shows that in contrast to the average capacity of superimposed and selection relaying which improves

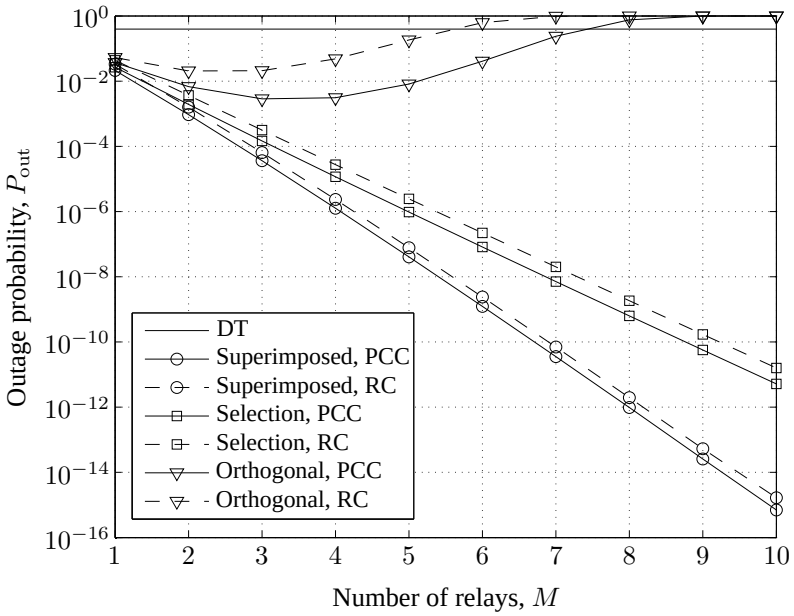

Fig. 4.7. The outage probability at $r = 1$ bit versus the number of relays for the different protocols in the symmetric case when $\mu_{\mathrm{SD}} = 3$ dB, $\mu_{\mathrm{SR}} = 24$ dB, and $\mu_{\mathrm{RD}} = 15$ dB.

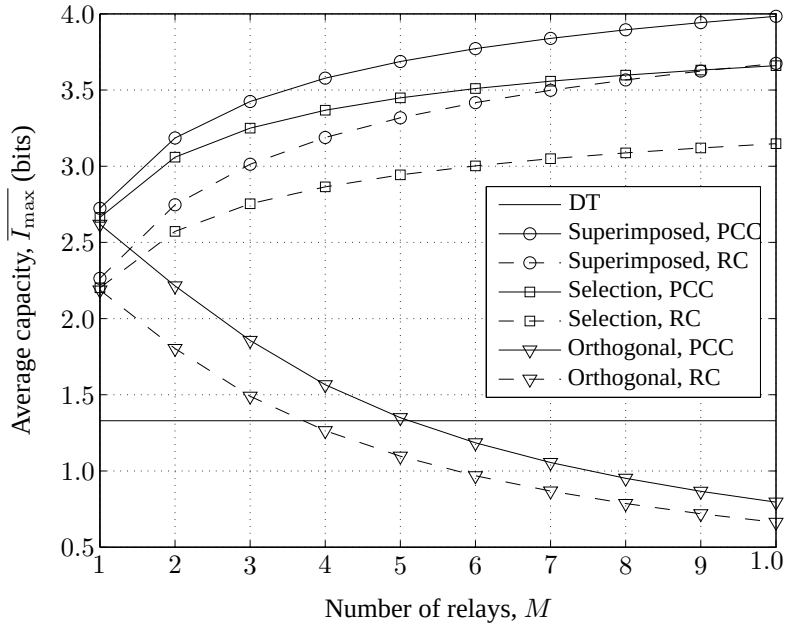

Fig. 4.8. The average capacity in bits versus the number of relays for the different protocols in the symmetric case when $\mu_{\mathrm{SD}} = 3$ dB, $\mu_{\mathrm{SR}} = 24$ dB, and $\mu_{\mathrm{RD}} = 15$ dB.

with increasing M, the average capacity of orthogonal relaying is diminished as M is increased. These deteriorating effects of increasing M on the performance of orthogonal relaying is explained again by orthogonalization loss [9]. Another important observation is that in terms of the outage probability, superimposed relaying benefits more from increasing M than selection relaying does, in the sense that its outage probability decreases more rapidly as M increases. This is in contrast to their capacity performances where the average capacity of both schemes has similar trends and increases with M with diminishing returns.

Chapter 5

Rateless Coded Relaying: Single-Relay Case[1]

5.1 Introduction

Rateless codes, including fountain codes, have garnered considerable interest among coding and communication theorists [22], [89]–[96], since their introduction in [97], [98] and their prevalent use in industrial products as a universal coding solution for erasure channels [99, Chapter 50]. Two common examples of fountain codes include Luby-transform (LT) codes [98] and Raptor codes [100], an improved version of LT codes. In this chapter, it is assumed that transmitters take advantage of rateless coding.

Their value mostly lies in the fact that rateless codes do not have a fixed or predetermined rate at the transmitter, and the source, oblivious to CSI, can generate as many encoding symbols as needed to enable the destination to decode its message. Thus, rateless codes are said to adapt to and follow the channel condition. A one-bit feedback from the receiver can be used to mark the success of the decoding and to signal the transmitter to stop sending more codeletters. Therefore, outage, meaning failure in decoding at the receiver, virtually is not experienced in systems exploiting rateless codes. In fact, the receiver in rateless schemes keeps accumulating MI, rather than energy, from the source until the receiver can decode [22]. These properties best suit DF relaying schemes by having relays

[1] *A version of this chapter has been published in part in the Proceedings of the IEEE International Conference ion Communications (ICC), 2008, pp. 3701–3707, and in the IEEE Transactions on Wireless Communications, vol. 7, no. 11, pp. 4439–4444, Nov. 2008.*

monitor the source *indefinitely*, and having the relay(s) successful in decoding assist the source. Such schemes have been addressed recently in the literature [22], [91], [94]–[96].

Rateless codes are different from fixed-rate codes in several aspects. The authors in [90], [91] were first to propose the use of rateless codes in fading channels, and to show that rateless schemes are capable of simultaneously achieving reliability and efficiency over fading channels. In contrast, fixed-rate systems experience an unavoidable tradeoff between reliability and efficiency [90]. Moreover, to maximize reliability and efficiency at the same time in fixed-rate systems, the transmitter needs full knowledge of the CSI to set the code rate accordingly, provided that it has access to a variable-rate code. However, what is required in a rateless scheme to bring about both reliability and efficiency is at most knowledge of the channel statistics at the transmitter side.

The use of rateless codes in relay networks has been proposed in the literature [22], [91], [94]–[96] as a means to approach the capacity promised for the relaying protocols under study without knowing fully the CSI at the transmitter. We consider using rateless coding and assume that transmitters know the statistics of the channel fading, but are otherwise oblivious to the CSI. Note that if rateless codes are universal over a class of channels, such as erasure channels and AWGN channels, which means that a single code design can be utilized to approach the Shannon capacity of any channel in the class,[2] then the transmitter is relieved of even knowing the channel statistics.

In this chapter, the achievable rates of three single-relay, rateless coded, DF protocols, one of which is proposed here, are investigated under a peak power constraint (PPC) and an average power constraint (APC). The APC provides fair grounds for comparing the protocols in terms of their achievable rates under constant average energy consumption per channel use. In fact, in contrast to DT, cooperative transmission involves transmission from other nodes, i.e. relays. In rateless coded relaying transmission, in one protocol, relays may contribute more time and energy resulting in greater MI between the source and destination, while in another, less energy is spent by the relays and the resulting rate is smaller. Therefore, it is essential to determine which protocol yields larger rates for constant energy consumption. These considerations have been ignored in some previous research [91],

[2]Luby-transform and Raptor codes are universal over erasure channels [99, Chapter 50]. However, the codes lack universality over binary symmetric channels and AWGN channels though exhibiting acceptable performance [92], [93]. No result in the literature precludes the possibility of designing universal rateless codes over non-erasure channels.

[95],[3] leading to unfair comparisons. Along with the maximum rate under the APC, we calculate and use the minimum energy per bit under the PPC for the different protocols, as another performance measure to compare the protocols fairly on the basis of energy consumption. Also, to study and compare the long-term average behaviors of the protocols, we calculate the long-term average rate, the long-term average energy per bit, and a newly defined metric, the relay-to-source usage ratio showing the average amount of relay usage relative to source usage in a protocol. The protocol proposed in this chapter is built upon opportunistic communication [80, Chapter 6] such that although inferior to its predecessors under the PPC, it outperforms them in most cases in energy constrained scenarios.

As is common practice in the literature, it is assumed here that rateless codes, wherever used, can closely approach the Shannon capacity without requiring instantaneous CSI at the transmitter [22], [91], [95]. However, the design of capacity-approaching rateless codes is beyond the scope of this chapter. The accuracy of this assumption has been explained in [22], and demonstrated by numerical examples in [91]. Also, it has been shown that the fountain capacity is the same as the Shannon capacity for memoryless channels [89], and that capacity-approaching rateless codes with low-complexity decoding algorithms exist for AWGN channels [101].

The remainder of the chapter is outlined as follows. In Section 5.2, the system model and definitions are given. In Section 5.3, the different rateless coded protocols are introduced, and the short-term average rate and energy of each scheme are derived. In Section 5.4, the issues and implications of feedback in the protocols are investigated. A discussion on power fairness for the protocols is presented in Section 5.5. In section 5.6, different measures for comparing the protocols fairly on a power basis are examined. The long-term average behavior of the schemes is characterized in Section 5.7. Finally, the chapter is concluded by several numerical examples in Section 5.8.

5.2 Channel Model and Definitions

As depicted in Fig. 2.1, we consider a source, a destination, and an available relay assisting the source in relaying its messages, each of constant entropy H, to the destination. Each

[3] In [9], power normalization is used to take power fairness into account for comparison purposes. However, the model that was considered utilized fixed time or frequency channels. When the amount of network resources used is variable and channel-dependent, as in the case of rateless schemes, a slightly different approach is needed to take account of power fairness.

node has a single transmitting/receiving antenna. A CR is the period over which a message of the source is fully communicated to the destination, and has two phases. In Phase I, the source ratelessly encodes its message and broadcasts the encoding symbols or packets. As soon as the relay successfully decodes the message, Phase II begins where the relay cooperates with the source. It is the method of this collaboration that creates the different cooperation protocols introduced in Section 5.3. Obviously, if in a given CR, the destination can decode the message before the relay can, the CR reduces to DT, i.e. Phase II does not exist and the relay is not used in the CR. Note that the success in decoding at the relay or destination can be assured using an external cyclic redundancy check code [102].

We use system model assumptions similar to those in [22]. We assume that all channels are contaminated with AWGN, and experience independent path loss and flat fading. A block fading model is considered where the SNRs remain constant over a CR [21], [22], [96]. Also, it is assumed that transmissions occupy baseband bandwidth W Hz. Therefore, there are W 2-D DoFs per second available for transmission [9]. In fact, assuming that the duration of a CR is T, one obtains the rate per 2-D DoF realized in the CR, as

$$R = \frac{H}{WT}. \tag{5.1}$$

It is assumed that any node has a continuous-time power P. Therefore, the energy per 2-D DoF is obtained from [9] as

$$\mathcal{E} \triangleq \frac{P}{W}. \tag{5.2}$$

Moreover, we can write the SD, SR, and RD SNRs, respectively as

$$\gamma_0 \triangleq \gamma \left|g_0\right|^2 \tag{5.3}$$

$$\gamma_1 \triangleq \gamma \left|g_1\right|^2 \tag{5.4}$$

and

$$\gamma_2 \triangleq \gamma \left|g_2\right|^2 \tag{5.5}$$

where g_0, g_1, and g_2 are the SD, SR, and RD complex channel coefficients, respectively, and where

$$\gamma \triangleq \frac{\mathcal{E}}{N} = \frac{P}{WN_0} \tag{5.6}$$

where N_0 is the one-sided PSD of the AWGN.[4] The average values of γ_0, γ_1, and γ_2 with respect to channel fading are denoted μ_0, μ_1, and μ_2.

The capacities of the SD, SR, and RD links are denoted C_0, C_1, and C_2, respectively. Also, the sum-rate capacity of the multiaccess channel from the source and relay to the destination is denoted $C_{\rm m}$. In the case of Gaussian-input or average-power-constrained-input channels, one has [79, Chapter 15]

$$C_0 = \mathcal{C}(\gamma_0) \tag{5.7a}$$

$$C_1 = \mathcal{C}(\gamma_1) \tag{5.7b}$$

$$C_2 = \mathcal{C}(\gamma_2) \tag{5.7c}$$

and

$$C_{\rm m} = \mathcal{C}(\gamma_0 + \gamma_2) \tag{5.7d}$$

in nats, where

$$\mathcal{C}(x) \triangleq \ln(1+x). \tag{5.7e}$$

In Sections 5.3 and 5.6, general-input channels are considered, except for Subsection 5.6.2 where only Gaussian-input channels are studied. Also, the numerical examples in Section 5.8 are given for Rayleigh fading, Gaussian-input channels

Note that in general-input channels, we naturally assume that C_0, C_1, C_2, and $C_{\rm m}$ are increasing functions of the corresponding SNRs. Also, we have [79, Section 15.3]

$$\max\{C_0, C_2\} < C_{\rm m} < C_0 + C_2. \tag{5.8}$$

Throughout, we make use of the following terminology:

- The *short-term average rate*, R, refers to the MI communicated to the destination per 2-D DoF in a given CR. The maximum possible R in a CR is denoted $R_{\max}$.
- The *long-term average rate*, $R_{\rm avg}$, refers to the maximum MI communicated to the destination per 2-D DoF averaged over infinitely many CRs.
- The *short-term average energy per symbol*, E, refers to the average total energy expended by the whole system for wireless transmission per 2-D DoF in a given CR.

[4] We assume without loss of generality that AWGN has the same PSD in all channels.

For example, if in a CR, lasting n 2-D symbols, the source and relay respectively transmit $n_{\rm S}$ and $n_{\rm R}$ symbols with energies $\mathcal{E}_{\rm S}$ and $\mathcal{E}_{\rm R}$ per symbol, then

$$E = \frac{n_{\rm S}\,\mathcal{E}_{\rm S} + n_{\rm R}\,\mathcal{E}_{\rm R}}{n}. \tag{5.9}$$

Note that

$$n_{\rm S} + n_{\rm R} \geq n \tag{5.10}$$

considering the possibility of an overlap between the source and relay transmissions in some protocols.

- The *short-term average energy per bit*, EB, in a CR refers to the ratio E/R when R is expressed in bits. The minimum possible EB in a CR is denoted $\mathrm{EB}_{\min}$.

- The *long-term average energy per bit*, $\mathrm{EB}_{\rm avg}$ refers to the minimum ratio of the total energy expended by the whole system for wireless transmission to the total MI in bits communicated to the destination in duration t, when t approaches infinity.

- The *PPC* refers to the constraint that the source and relay operate at their peak power P or peak energy per 2-D DoF $\mathcal{E}$.

- The *APC* refers to the constraint that the source and relay virtually scale their powers (respectively, energies per 2-D DoF) such that the average total power in a CR is P, or equivalently, $E = \mathcal{E}$.

In the next section, the protocols are introduced and their $R_{\max}$'s and E's under the PPC, are derived. Then in Section 5.6, to draw a fair comparison on a power basis between the achievable rates of the protocols, first we study and compare the $\mathrm{EB}_{\min}$'s of the protocols under the PPC. Second, we examine the $R_{\max}$'s of the protocols under the APC.

In the following, the rates and energies in the different protocols are distinguished by superscripts "(DT)", "(P-1)", "(P-2)", and "(P-3)". For example, $R^{\text{(P-1)}}$ and $E^{\text{(P-1)}}$ represent the short-term average rate and energy per symbol in P-1.

5.3 Rateless Coded Protocols

All the schemes in this section with their rates, and energies under the PPC, are summarized in Table 5.1. In this table, B_i refers to both the source's ith message and the rateless encoded

TABLE 5.1
DIFFERENT TRANSMISSION SCHEMES WITH THEIR MAXIMUM SHORT-TERM AVERAGE RATES AND CORRESPONDING SHORT-TERM AVERAGE ENERGIES PER SYMBOL

DT

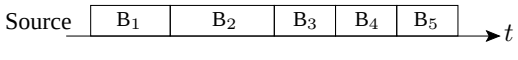

$$R_{\max} = C_0$$

$$E = \mathcal{E}$$

P-1

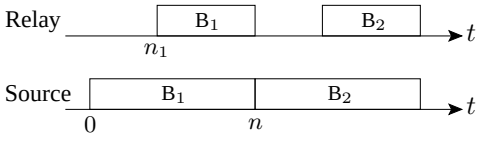

$C_0 < C_1$

$$R_{\max} = \begin{cases} C_0, & C_1 \le C_0 \\ \frac{C_{\mathrm{m}} C_1}{C_{\mathrm{m}} + C_1 - C_0}, & C_1 > C_0 \end{cases}$$

$$E = \begin{cases} \mathcal{E}, & C_1 \le C_0 \\ \mathcal{E}\left(1 + \frac{C_1 - C_0}{C_{\mathrm{m}} + C_1 - C_0}\right), & C_1 > C_0 \end{cases}$$

P-2

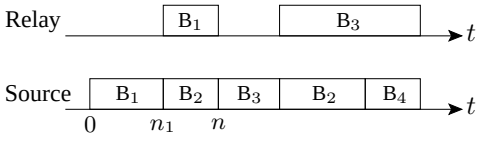

$C_0 < C_1$

$$R_{\max} = \begin{cases} C_0, & C_1 \le C_0 \\ \frac{C_{\mathrm{m}} C_1 - C_0^2}{C_{\mathrm{m}} + C_1 - 2C_0}, & C_1 > C_0 \end{cases}$$

$$E = \begin{cases} \mathcal{E}, & C_1 \le C_0 \\ \mathcal{E}\left(1 + \frac{C_1 - C_0}{C_{\mathrm{m}} + C_1 - 2C_0}\right), & C_1 > C_0 \end{cases}$$

P-3

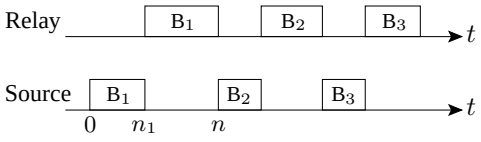

$C_0 < \min\{C_1, C_2\}$

$$R_{\max} = \begin{cases} C_0, & \min\{C_1, C_2\} \le C_0 \\ \frac{C_1 C_2}{C_1 + C_2 - C_0}, & \min\{C_1, C_2\} > C_0 \end{cases}$$

$$E = \mathcal{E}$$

block for the ith message. Also, Table 5.2 presents a summary of the requirements and/or favorable situations of each protocol. We commence with DT as the baseline and introduce the other protocols in sequence.

5.3.1 The DT Scheme

In this case, no relay is used and the source is the only transmitter in the available bandwidth, W. In a fixed-rate coded system, the Shannon capacity of DT for a flat fading channel with no CSI at the transmitter is the ergodic capacity $\mathrm{E}\{C_0\}$ [87, Section 4.2.3], which is bounded above zero. The rate $\mathrm{E}\{C_0\}$ is approached if the codeword of the trans-

TABLE 5.2
FEATURES OF THE DIFFERENT TRANSMISSION SCHEMES
(ACK = acknowledgment signal, MUD = multiuser detection)

DT	• Best when $\gamma_1 \leq \gamma_0$.
P-1	• Requires $\gamma_1 > \gamma_0$. • Stringent synchronization at the relay. • No ACK between the source and relay. • No MUD at the destination.
P-2	• Requires $\gamma_1 > \gamma_0$. • No stringent synchronization between the source and relay. • Requires ACKs from the relay or destination to the source. • Requires MUD at the destination.
P-3	• Requires $\min\{\gamma_1, \gamma_2\} > \gamma_0$. • No stringent synchronization between the source and relay. • Requires ACKs from the relay or destination to the source. • No MUD at the destination.

mitter is long enough that is affected by all fading channel states. In a rateless system, the same rate can be achieved, as the indefinitely long, ratelessly encoded stream of symbols is capacity-approaching and can experience virtually all fading channel states. Therefore, the long-term average rate for DT, $R_{\text{avg}}^{(\text{DT})}$, is

$$R_{\text{avg}}^{(\text{DT})} = \text{E}\{C_0\} \tag{5.11}$$

which, in the case of a Rayleigh fading, Gaussian-input channel, becomes, like (4.76),

$$R_{\text{avg}}^{(\text{DT})} = \frac{1}{\mu_0} \int_0^\infty \text{e}^{-\gamma/\mu_0} \ln(1+\gamma)\, \text{d}\gamma = \mathcal{S}\left(\frac{1}{\mu_0}\right) \tag{5.12}$$

where $\mathcal{S}(\cdot)$ is given by (4.69). We can also derive the long-term average energy per bit, introduced in Section 5.2, for DT as follows. We know that the energy per symbol is constant for DT at $\mathcal{E}$, where $\mathcal{E}$ is defined in (5.2). Therefore, assuming that the value of C_0 in bits at Symbol i is denoted $C_0[i]$, we obtain

$$\text{EB}_{\text{avg}}^{(\text{DT})} = \lim_{m\to\infty} \frac{m\,\mathcal{E}}{C_0[1] + \cdots + C_0[m]} = \frac{\mathcal{E}}{\text{E}\{C_0\}} = \frac{\mathcal{E}}{R_{\text{avg}}^{(\text{DT})}}. \tag{5.13}$$

5.3.2 The P-1 Scheme

The P-1 protocol is taken from the rateless DF relaying protocol suggested in [91], which itself was built upon a commensurate block-coded fixed-rate system in [103]. In P-1, the source broadcasts rateless encoding symbols to the relay and destination in Phase I. When the relay is capable of decoding the source message, Phase II begins where the relay forms an Alamouti transmission scheme [104] with the source, to send new rateless symbols to the destination until the destination decodes. An advantage of P-1 is that the source does not need to be aware of the relay or when the relay decodes. However, a drawback is the greater complexity in the relay for synchronization with the source at the symbol level.

To derive $R_{\max}^{(\text{P-1})}$, we first note that if the SR link is not stronger than the SD link, i.e. if $C_0 \geq C_1$, the relay is not used and the system reverts to DT. Now, assume that $C_0 < C_1$ and that the relay and destination decode the message after receiving n_1 and n symbols in total, respectively, as depicted in Table 5.1. On the one hand, we can write

$$H = n_1 C_1 \tag{5.14}$$

where H is the entropy of the message. On the other, the source communicates $n_1 C_0$ units of MI to the destination during Phase I, and the source and relay together communicate $(n - n_1)C_{\text{m}}$ units of MI to the destination during Phase II. Therefore, we have

$$H = n_1 C_0 + (n - n_1)C_{\text{m}}. \tag{5.15}$$

Based on the definition of $R_{\max}$ and from (5.14) and (5.15), one obtains

$$R_{\max}^{(\text{P-1})} = \frac{H}{n} = \frac{C_{\text{m}}\, C_1}{C_{\text{m}} + C_1 - C_0} \tag{5.16}$$

consistent with the result [21, Corollary 1].

To derive $E^{(\text{P-1})}$ under the PPC assuming that $C_0 < C_1$, we note that the total energy expended per DoF equals $\mathcal{E}$ when only the source transmits, and equals $2\mathcal{E}$ when both the source and relay transmit. Therefore, we have

$$E^{(\text{P-1})} = \frac{n_1 \mathcal{E} + 2(n - n_1)\mathcal{E}}{n} = \left(1 + \frac{C_1 - C_0}{C_{\text{m}} + C_1 - C_0}\right)\mathcal{E} \tag{5.17}$$

where the second equality is obtained by applying (5.14) and (5.15).

5.3.3 The P-2 Scheme

The P-2 protocol is based on the rateless DF relaying protocol proposed in [95]. The difference between P-1 and P-2 lies in the second phase of a CR. In P-1 during Phase II, the source, unaware of the relay cooperation, continues to transmit the same message to the destination. However in P-2, the source transmits a new message in Phase II, where the destination attempts to jointly decode the source and relay transmissions. As the relay is half-duplex, it cannot monitor the new message. For example, in the P-2 scheme depicted in Table 5.1, the source is not assisted by the relay in the transmission of B_2 and B_4.

The method of coordination between the source and relay transmissions in P-2 has been explained in [95], and is based on ACKs. An achievable rate under P-2 has been given in [95] in terms of MI functions without derivation details. Here, we derive the result in [95], and find the maximum rate under P-2 by obtaining the optimal operating rates in the multiaccess channel from the source and relay to the destination (i.e. the rates realized in Phase II). If we assume that the destination uses serial interference cancellation which is an optimal MUD in multiaccess channels [80, Section 6.1.1], then the rate is shown to be maximized when the destination first decodes and cancels the relay message and then decodes the source message.

Here again, if $C_0 \geq C_1$, the relay is not used and one has $R_{\max}^{(\text{P-2})} = C_0$ and $E^{(\text{P-2})} = \mathcal{E}$. Therefore, assume that $C_0 < C_1$, and consider the example shown in Table 5.1 where the relay and destination decode B_1 after n_1 and n 2-D DoFs are exhausted, respectively.

To derive $R_{\max}^{(\text{P-2})}$ in P-2, first, note that as the relay decodes B_1 at n_1, (5.14) holds. Second, assume that X_{S} and X_{R} are the source and relay rates when the source and relay simultaneously transmit B_2 and B_1, respectively. The shaded area in Fig. 5.1 represents all achievable rates $(X_{\mathrm{S}}, X_{\mathrm{R}})$.[5] Now, as the destination decodes B_1 by receiving n_1 symbols from the source at rate C_0 and $n - n_1$ symbols from the relay at rate X_{R}, we can write

$$H = n_1 C_0 + (n - n_1) X_{\mathrm{R}}. \tag{5.18}$$

Meanwhile, during the period when the destination is receiving for B_1, it also receives $n - n_1$ symbols for B_2 from the source at rate X_{S}. Therefore, an achievable short-term average rate can be written as

[5] The reader is referred to [79, Section 15.3.6] or [50, Section 16.2] for the capacity of Gaussian multiaccess channels.

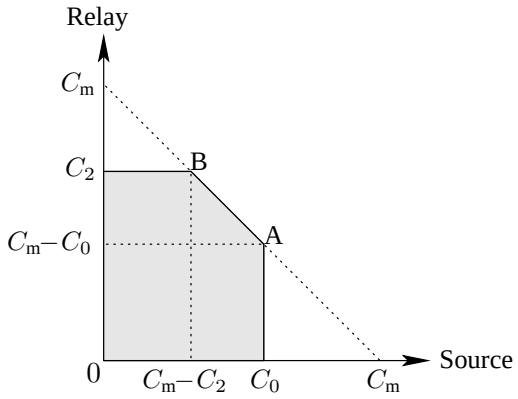

Fig. 5.1. The rate region for the multiaccess channel from the source and relay to the destination.

$$R^{(\text{P-2})} = \frac{H + (n - n_1)X_{\rm S}}{n} = \frac{(C_1 - C_0)X_{\rm S} + C_1 X_{\rm R}}{C_1 - C_0 + X_{\rm R}} \tag{5.19}$$

where the second equality comes from (5.14) and (5.18). Note that (5.19) is in agreement with the result [95, eq. (4)].

As the energy per DoF during Phase I is $\mathcal{E}$, and during phase II is $2\mathcal{E}$, the short-term average energy per DoF corresponding to the rate (5.19) is obtained as,

$$\frac{n_1\mathcal{E} + 2(n - n_1)\mathcal{E}}{n} = \frac{X_{\rm R} + 2\,C_1 - 2\,C_0}{X_{\rm R} + C_1 - C_0}\,\mathcal{E} \tag{5.20}$$

where the equality again results from (5.14) and (5.18).

The maximum rate $R_{\max}^{(\text{P-2})}$ is obtained by maximizing the rate (5.19) over all achievable $(X_{\rm S}, X_{\rm R})$. It can be verified that $X_{\rm S} = C_0$ and $X_{\rm R} = C_{\rm m} - C_0$, corresponding to point A in Fig. 5.1, lead to the maximum rate which is

$$R_{\max}^{(\text{P-2})} = \frac{C_{\rm m}\,C_1 - C_0^2}{C_{\rm m} + C_1 - 2\,C_0}. \tag{5.21}$$

If we assume that the destination performs serial interference cancellation in Phase II, point A is achieved if the destination first decodes the relay signal treating the source signal as interference, and then, eliminates the relay signal and decodes the source message. The PPC short-term average energy per symbol corresponding to (5.21) is obtained from (5.20) after replacing $X_{\rm R}$ with $C_{\rm m} - C_0$, as

$$E^{(\text{P-2})} = \left(1 + \frac{C_1 - C_0}{C_{\rm m} + C_1 - 2\,C_0}\right)\mathcal{E}. \tag{5.22}$$

5.3.4 The P-3 Scheme

Protocol P-3 is the scheme proposed here. It is built upon P-1 and P-2 and opportunistic communication. The general idea is that after the relay decodes the message, the system imitates a two-transmitting, one-receiving antenna scheme. In such a scheme, if the qualities of the channels are known at the transmitters, the OPA between the source and relay, based on opportunistic communication [80, Chapter 6], is to devote all power to the antenna observing the stronger channel. This translates to the idea, depicted in Table 5.1, that if $\gamma_2 \leq \gamma_0$ or $C_2 \leq C_0$, the relay must not be used. Otherwise, the source must back off, clearing the channel for the relay transmission. This reasoning suggests that P-3 offers a larger rate than P-1 and P-2 for the same energy expenditure. The numerical results in Section 5.8 confirm this intuition in most cases.

Note that in P-3, relaying is not used when the SD link is stronger than either of the SR or RD links, i.e. if $C_0 \geq \min\{C_1, C_2\}$. This is in contrast to P-1 and P-2 where the relay is (automatically) utilized whenever $C_0 < C_1$. The method of coordinating the source and relay transmissions in P-3 is similar to, yet simpler than, that used in [95] based on ACKs. In fact and in contrast to P-2, in P-3 the destination does not monitor any ACK from the relay, and can also decode the source's messages in order of transmission. Also, note that in P-3 the destination is relieved of MUD needed in P-2.

Now to derive $R_{\max}^{(\text{P-3})}$ when $C_0 < \min\{C_1, C_2\}$, consider the example shown in Table 5.1 and note that (5.14) still holds. Also, as the destination decodes the message by receiving n_1 and $n - n_1$ symbols from the source and relay, respectively, we can write

$$H = n_1 C_0 + (n - n_1) C_2. \tag{5.23}$$

Combining (5.14) and (5.23), one obtains

$$R_{\max}^{(\text{P-3})} = \frac{H}{n} = \frac{C_1\, C_2}{C_1 + C_2 - C_0}. \tag{5.24}$$

Also, it is clear from the description of P-3 that similar to DT, we have

$$E^{(\text{P-3})} = \mathcal{E} \tag{5.25}$$

under the PPC.

5.4 Feedback Requirements and Effects

The rateless coded schemes have different feedback requirements as follows. These requirements are based on the ACKs needed for each protocol as indicated in Table 5.2.

The conventional DT scheme needs only a single feedback bit per CR from the destination to inform the source of the successful decoding. This one-bit feedback from the destination, referred to as the *STOP feedback* here, is needed in any rateless coded system.

The feedback requirement in P-1 is similar to that in DT, i.e. only the STOP feedback is needed. In fact, in P-1 the source can be unaware of the existence of the relay [105].

In P-2, other than the STOP feedback, a one-bit feedback from the relay broadcast to the source and destination is needed when the relay decodes. This feedback has the source resume the transmission of an unfinished message from the previous CR if there is any, or start the transmission of a new message. It also has the destination switch from single user detection to MUD and detect the source and relay messages (see Section 5.3.3).

The P-3 scheme needs 3 one-bit feedbacks per CR, and, therefore, its feedback requirement is more than that of DT, P-1, and P-2. In addition to the STOP feedback and a one-bit decoding-success feedback from the relay, P-3 needs a one-bit feedback from the destination to indicate which node, the source or relay, shall transmit after the relay decodes.

It is also worth considering feedback implications in the protocols. First, any feedback is possibly included in a packet containing header and other signaling information as well. If the packet carrying a one-bit feedback contains f bits data, then a scheme needing m separate one-bit feedbacks in a CR needs transmission of m f bits per CR for feedback.

Second, assume that a low-rate, narrowband channel is dedicated to feedback. Then, on the one hand, feedback transmission can take a non-negligible duration compared to the duration of a CR, and on the other, the nodes need to receive feedback data before setting their subsequent transmission strategies. This delay in receiving feedback has a negative impact on the rate performance. Even if we increase the feedback bandwidth to hasten feedback communication, we lose spectrum, and the spectral efficiency diminishes again.

Here, we do not consider the effects of feedback in the protocols considered and assume that the feedback is instantaneous for simplicity [22].

5.5 Power Fairness

All the protocols revert to DT with $R_{\max} = C_0$ and $E = \mathcal{E}$ when $C_0 \geq C_1$. However when $C_0 < C_1$, inspection of the achievable rates in DT, P-1, P-2, and P-3 reveals that

$$R_{\max}^{(\text{P-2})} - R_{\max}^{(\text{P-1})} = \frac{C_0(C_1 - C_0)(C_{\text{m}} - C_0)}{(C_1 + C_{\text{m}} - 2\,C_0)(C_1 + C_{\text{m}} - C_0)} \tag{5.26}$$

$$R_{\max}^{(\text{P-1})} - R_{\max}^{(\text{P-3})} = \frac{C_1(C_1 - C_0)(C_{\text{m}} - \max\{C_2, C_0\})}{(C_1 + \max\{C_2, C_0\} - C_0)(C_1 + C_{\text{m}} - C_0)} \tag{5.27}$$

and

$$R_{\max}^{(\text{P-3})} - R_{\max}^{(\text{DT})} = \frac{(C_1 - C_0)(\max\{C_2, C_0\} - C_0)}{C_1 + \max\{C_2, C_0\} - C_0} \tag{5.28}$$

and therefore, one has

$$R_{\max}^{(\text{P-2})} > R_{\max}^{(\text{P-1})} > R_{\max}^{(\text{P-3})} \geq R_{\max}^{(\text{DT})}. \tag{5.29}$$

Moreover, inspecting the average energies under the PPC when $C_0 < C_1$ gives

$$E^{(\text{P-2})} - E^{(\text{P-1})} = \frac{C_0(C_1 - C_0)}{(C_1 + C_{\text{m}} - 2\,C_0)(C_1 + C_{\text{m}} - C_0)}\,\mathcal{E} \tag{5.30}$$

and

$$E^{(\text{P-1})} - E^{(\text{P-3})} = \frac{C_1 - C_0}{C_1 + C_{\text{m}} - C_0}\,\mathcal{E} \tag{5.31}$$

which show that

$$E^{(\text{P-2})} > E^{(\text{P-1})} > E^{(\text{P-3})} = E^{(\text{DT})}. \tag{5.32}$$

Therefore, although P-2 surpasses P-1, and P-1 outperforms P-3 in terms of the achievable rates, these superiorities come at the expense of expending more energy. In other words, achieving larger rates does not necessarily translate into larger energy efficiency.

5.6 Energy Efficiency

As observed in Section 5.5, the different schemes, in general, use different amounts of energy in a CR to achieve different rates, making it difficult to evaluate the merit of the protocols in terms of energy efficiency. To address this issue and to draw a fair comparison between the protocols on a power basis, we propose the following two methods.

5.6.1 Minimum Energy per Bit Under the PPC

The study of EB, defined in Section 5.2, allows us to determine how much energy on average a relaying strategy requires to communicate 1 bit of information to the destination in a CR. Obviously, a smaller EB translates into larger energy efficiency. In the following, we derive the minimum EBs of the P-1, P-2, and P-3 protocols under the PPC, assuming that all rates are expressed in bits. Note that when $C_0 \geq C_1$, we have

$$\mathrm{EB}_{\min} = \frac{\mathcal{E}}{C_0} \tag{5.33}$$

for all the protocols. Therefore, we only consider the case $C_0 < C_1$.

In P-1, it can be observed from (5.16) and (5.17) that

$$\mathrm{EB}_{\min}^{(\text{P-1})} = \frac{C_{\mathrm{m}} + 2(C_1 - C_0)}{C_{\mathrm{m}}\, C_1}\, \mathcal{E}. \tag{5.34}$$

In P-2, from (5.19) and (5.20), a general expression for the EB in terms of the source and relay rates in Phase II, X_{S} and X_{R}, is obtained as

$$\mathrm{EB}^{(\text{P-2})} = \frac{2(C_1 - C_0) + X_{\mathrm{R}}}{(C_1 - C_0)X_{\mathrm{S}} + C_1 X_{\mathrm{R}}}\, \mathcal{E}. \tag{5.35}$$

Note that the shaded area in Fig. 5.1 designate all achievable $(X_{\mathrm{S}}, X_{\mathrm{R}})$. It can be verified that (5.35) is minimized with $(X_{\mathrm{S}}, X_{\mathrm{R}}) = (C_0, C_{\mathrm{m}} - C_0)$ (point A in Fig. 5.1) when $2\,C_0 \leq C_{\mathrm{m}}$, and with $(X_{\mathrm{S}}, X_{\mathrm{R}}) = (C_{\mathrm{m}} - C_2, C_2)$ (point B in Fig. 5.1) when $2\,C_0 > C_{\mathrm{m}}$. Therefore, we obtain

$$\mathrm{EB}_{\min}^{(\text{P-2})} = \begin{cases} \frac{C_{\mathrm{m}} + 2\,C_1 - 3\,C_0}{C_{\mathrm{m}}\,C_1 - C_0^2}\, \mathcal{E}, & 2\,C_0 \leq C_{\mathrm{m}} \\ \frac{C_2 + 2(C_1 - C_0)}{C_0\,C_2 + C_{\mathrm{m}}(C_1 - C_0)}\, \mathcal{E}, & 2\,C_0 > C_{\mathrm{m}} \end{cases}. \tag{5.36}$$

Note that although the maximum rate (5.21) always corresponds to point A in Fig. 5.1, the minimum EB corresponds to point A or point B depending on C_0 and C_{m}. In other words, while to achieve the maximum rate the destination always needs to decode the relay message first, to achieve the minimum EB, sometimes the source message has to be decoded first. It can be observed that the condition $2\,C_0 \leq C_{\mathrm{m}}$ or $2\,C_0 > C_{\mathrm{m}}$ is satisfied in Gaussian-input channels (where we have (5.7)) when γ_0 in dB is smaller or greater than almost half γ_2 in dB, respectively.

Finally, the minimum EB in P-3 when $C_0 < C_1$ is obtained from (5.24) and (5.25) as

$$\mathrm{EB}_{\min}^{(\text{P-3})} = \begin{cases} \frac{C_1+C_2-C_0}{C_1 C_2}\,\mathcal{E}, & C_0 < C_2 \\ \frac{\mathcal{E}}{C_0}, & C_0 \geq C_2 \end{cases}. \tag{5.37}$$

Theorem 5.1 provides a comparison between the $\mathrm{EB}_{\min}$'s under the PPC.

Theorem 5.1 (Comparison of the $\mathrm{EB}_{\min}$'s in P-1, P-2, and P-3). Considering P-1, P-2, and P-3 under the PPC in a given CR where $C_0 < C_1$, one of the following three cases with the corresponding relationships between the $\mathrm{EB}_{\min}$'s given in each case, can happen:

i) $2\,C_0 > C_{\mathrm{m}}$: $\mathrm{EB}_{\min}^{(\text{P-3})} < \mathrm{EB}_{\min}^{(\text{P-1})} < \mathrm{EB}_{\min}^{(\text{P-2})}$.

ii) $2\,C_0 \leq C_{\mathrm{m}}$ and $C_0(C_2 - C_0) < C_1(2\,C_2 - C_{\mathrm{m}})$: $\mathrm{EB}_{\min}^{(\text{P-3})} < \mathrm{EB}_{\min}^{(\text{P-2})} \leq \mathrm{EB}_{\min}^{(\text{P-1})}$.

iii) $2\,C_0 < C_{\mathrm{m}}$ and $C_0(C_2 - C_0) \geq C_1(2\,C_2 - C_{\mathrm{m}})$: $\mathrm{EB}_{\min}^{(\text{P-2})} \leq \mathrm{EB}_{\min}^{(\text{P-3})} < \mathrm{EB}_{\min}^{(\text{P-1})}$.

Proof. The theorem can be proved by comparing the $\mathrm{EB}_{\min}$'s of the different protocols given in (5.34), (5.36), and (5.37), and performing algebraic manipulations. It should only be noted that when considering the different possible cases, the case $C_{\mathrm{m}} \geq 2\max\{C_0, C_2\}$ never happens as from (5.8) we always have

$$C_{\mathrm{m}} < 2\max\{C_0, C_2\}. \tag{5.38}$$

Also, to derive $\mathrm{EB}_{\min}^{(\text{P-1})} < \mathrm{EB}_{\min}^{(\text{P-2})}$ in Case i, we use the fact that $C_2 < C_{\mathrm{m}}$ from (5.8). ■

Note that based on Theorem 5.1, P-3, the proposed protocol, has the best situation among all the protocols in terms of $\mathrm{EB}_{\min}$; it is never the worst protocol; and, it is the best protocol in the two of the three cases. This is in sharp contrast with the result obtained for the maximum achievable rates under the PPC that P-3 is the poorest. In fact, although P-3 leads to smaller rates in PPC regimes, it consumes less energy such that it often offers the best energy efficiency among all the protocols.

5.6.2 Maximum Rate Under the APC

Another technique proposed here to make a fair comparison of the protocols based on energy expenditure, is to calculate the maximum rate per 2-D DoF of each protocol under the APC, defined as the constraint that the short-term average energy per symbol is fixed. Rigorously speaking, we assume that the source and relay transmit with powers $P_{\mathrm{S}} = p\,P$ and

$P_{\mathrm{R}} = q\,P$, or with energies per 2-D symbol equal to $\mathcal{E}_{\mathrm{S}} = p\,\mathcal{E}$ and $\mathcal{E}_{\mathrm{R}} = q\,\mathcal{E}$, respectively, for some $p > 0$ and $q \geq 0$, such that $E = \mathcal{E}$. [6]

As the APC analysis needs explicit formulas of the capacity in terms of SNR, and as the Gaussian-input channel has the simple capacity expression (5.7e), we restrict our investigation here to Gaussian-input channels and use (5.7e) as the capacity formula. Gaussian-input channels are suitable for this study also because they have the largest capacity among AWGN channels with average-power-constrained input [79, Chapter 9], thus providing upper bounds on achievable APC rates.

It is not trivial that how many pairs (p, q), in general, can satisfy the APC. It is observed in Appendix F that for any $\mathcal{E}$ and instantaneous channel conditions provided that $\gamma_0 < \gamma_1$, infinitely many pairs (p, q) exist that satisfy the APC, and one has to find the optimal (p, q) resulting in the maximum rate in each case. Also, when $\gamma_0 \geq \gamma_1$, the systems revert to DT and become independent of q such that the APC is trivially satisfied by $p = 1$ and any q.

The maximum rates under the APC for the different protocols when $\gamma_0 < \gamma_1$ are derived in Appendix F with the following results. In P-1, we have

$$R_{\max}^{(\text{P-1})} = \max_{0<p\leq 1} \frac{\mathcal{C}(p\,\gamma_0 + q\,\gamma_2)\,\mathcal{C}(p\,\gamma_1)}{\mathcal{C}(p\,\gamma_0 + q\,\gamma_2) + \mathcal{C}(p\,\gamma_1) - \mathcal{C}(p\,\gamma_0)} \tag{5.39a}$$

where

$$q = \begin{cases} -\frac{1}{\gamma_2}\left\{\frac{1}{\xi}\mathrm{W}_{-1}\left(-\xi\,\mathrm{e}^{-[1+p\,\gamma_0+(1-p)\gamma_2]\,\xi}\right) + 1 + p\,\gamma_0\right\}, & 0 < p < 1 \\ 0, & p = 1 \end{cases} \tag{5.39b}$$

where $\mathrm{W}_k(\cdot)$ is the kth branch of the Lambert W-function [106], and where

$$\xi \triangleq \frac{\mathcal{C}(p\,\gamma_1) - \mathcal{C}(p\,\gamma_0)}{(1-p)\gamma_2}. \tag{5.39c}$$

We obtain, for P-2,

$$R_{\max}^{(\text{P-2})} = \max_{0<p\leq 1} \frac{\mathcal{C}\left(p\,\gamma_0 + q\,\gamma_2\right)\,\mathcal{C}(p\,\gamma_1) - \mathcal{C}^2(p\,\gamma_0)}{\mathcal{C}\left(p\,\gamma_0 + q\,\gamma_2\right) + \mathcal{C}(p\,\gamma_1) - 2\,\mathcal{C}(p\,\gamma_0)} \tag{5.40a}$$

where

$$q = \begin{cases} -\frac{1}{\gamma_2}\left\{\frac{1}{\xi}\mathrm{W}_{-1}\left(-(1+p\,\gamma_0)\,\xi\,\mathrm{e}^{-[1+p\,\gamma_0+(1-p)\gamma_2]\,\xi}\right) + 1 + p\,\gamma_0\right\}, & 0 < p < 1 \\ 0, & p = 1 \end{cases}. \tag{5.40b}$$

[6] Note that scaling the powers of the source and relay is conceptual and not generally followed in practice, as the transmitters are assumed to be oblivious to CSI. The power scaling is performed here only for analytical purposes and for making the schemes comparable on a power basis.

Finally, the result for P-3 is

$$R_{\max}^{\text{(P-3)}} = \begin{cases} \max_{0<p<p_0} \frac{\mathcal{C}(p\,\gamma_1)\,\mathcal{C}(q\,\gamma_2)}{\mathcal{C}(p\,\gamma_1)+\mathcal{C}(q\,\gamma_2)-\mathcal{C}(p\,\gamma_0)}, & \gamma_0 < \gamma_2 \\ \mathcal{C}(\gamma_0), & \gamma_0 \geq \gamma_2 \end{cases} \tag{5.41a}$$

where p_0 is the only root of,

$$p\left[\left(1-\frac{\gamma_0}{\gamma_2}\right)\frac{\mathcal{C}(p\,\gamma_0)}{\mathcal{C}(p\,\gamma_1)}+\frac{\gamma_0}{\gamma_2}\right]-1 \tag{5.41b}$$

as a function of p, and where

$$q = \begin{cases} -\frac{1}{\gamma_2}\left\{\frac{1}{\xi}\mathrm{W}_k\left(-\xi\,\mathrm{e}^{-(1+\gamma_2)\,\xi}\right)+1\right\}, & p \neq 1 \\ 1, & p = 1 \end{cases} \tag{5.41c}$$

where $k=-1$ if $p<1$ and $k=0$ if $p>1$. Section F.3 provides insight into the value of, and the method of calculating, p_0.

5.7 Long-Term Average Behavior

The short-term average performance measures, $R_{\max}$, E, and $\mathrm{EB}_{\min}$, studied in Sections 5.3 and 5.6 are not suitable to judge the merit of the protocols, as the figures represent instantaneous behaviors which are functions of fading gains. Instead, we can compare the performances when averaged over a period long enough to let the system experience virtually all fading channel states. The long-term average rate, R_{avg}, and the long-term average energy per bit, EB_{avg}, introduced in Section 5.2, are appropriate performance measures for this purpose.

In addition to the long-term average rate and energy per bit, we introduce and study the relay-to-source usage ratio (RSUR), as an indicator of the average amount of relay usage relative to source usage in a protocol. In some applications, it may be desirable that a larger transmission burden be imposed on the source or relay. The RSUR is defined as the ratio of the total relay transmission time to the total source transmission time, over a long observation period. Rigorously speaking, assume that the durations of the source and relay transmissions in the ith CR are denoted $T_{\mathrm{S}}[i]$ and $T_{\mathrm{R}}[i]$, respectively. Note that in P-1 and P-2, we have $T_{\mathrm{S}}[i]=T[i]$ and $T_{\mathrm{R}}[i]<T[i]$, where $T[i]$ is the duration of the ith CR, while in P-3, we have $T_{\mathrm{S}}[i]+T_{\mathrm{R}}[i]=T[i]$. Now, the RSUR is defined as

$$\mathrm{RSUR} = \lim_{m\to\infty}\frac{\sum_{i=1}^{m} T_{\mathrm{R}}[i]}{\sum_{i=1}^{m} T_{\mathrm{S}}[i]} = \frac{\mathrm{E}\{T_{\mathrm{R}}\}}{\mathrm{E}\{T_{\mathrm{S}}\}}. \tag{5.42}$$

The RSUR is obviously zero in DT. Note that if the source and relay transmit with energies per symbol $\mathcal{E}_{\rm S}$ and $\mathcal{E}_{\rm R}$, respectively, the amount of energy expended by the relay to that expended by the source in the long term is obtained as the RSUR multiplied by $\mathcal{E}_{\rm R}/\mathcal{E}_{\rm S}$.

In the following, we derive general formulas for evaluating $R_{\rm avg}$ under the PPC or APC, and $\mathrm{EB}_{\rm avg}$ and the RSUR under the PPC in P-1, P-2, and P-3. Note that $R_{\rm avg}$ and $\mathrm{EB}_{\rm avg}$ for DT have been derived in (5.11)–(5.13). In DT, the PPC and APC coincide as the only transmitter has a constant energy per symbol $\mathcal{E}$.

We do not consider $\mathrm{EB}_{\rm avg}$ and the RSUR under the APC for the following reasons. The energy per bit defined and studied in Sections 5.2 and 5.6.1 in the PPC case, can be identically defined in the APC case. However, $\mathrm{EB}_{\rm min}$ and $\mathrm{EB}_{\rm avg}$ under the APC simply equal $\mathcal{E}/R_{\rm max}$ and $\mathcal{E}/R_{\rm avg}$ for all protocols, respectively, where $R_{\rm max}$ and $R_{\rm avg}$ are the APC rates. This is because the energy per symbol in the APC case is always constant at $\mathcal{E}$. This argument shows that $\mathrm{EB}_{\rm avg}$ in the APC case is uninteresting, and does not convey any more information on the energy efficiency of the protocols than that provided by $R_{\rm avg}$. Regarding the RSUR, it is only considered under the PPC, as the APC is conceptual, not necessarily imposed in practice, and is only proposed here to make a fair comparison of the energy efficiencies of the protocols.

5.7.1 Long-Term Average Rate

Assume that $T[i]$ represents the duration of the ith CR. Also, let $R_{\rm max}$ in the ith CR be denoted $R_{\rm max}[i]$. Then, we can write, from (5.1) for the PPC or APC,

$$\begin{aligned} R_{\rm avg} &= \lim_{m\to\infty} \frac{m\,H}{W(T[1]+\cdots+T[m])} \\ &= \lim_{m\to\infty} \frac{m\,H}{W\left(\frac{H}{W\,R_{\rm max}[1]}+\cdots+\frac{H}{W\,R_{\rm max}[m]}\right)} \\ &= \left(\mathrm{E}\left\{\frac{1}{R_{\rm max}}\right\}\right)^{-1}. \end{aligned} \tag{5.43}$$

The expressions of $R_{\rm max}$ needed for evaluating (5.43) in the PPC case have been given in Table 5.1, which reduce to the case of Gaussian-input channels under the substitutions given in (5.7). The expressions of $R_{\rm max}$ in the APC case for Gaussian-input channels are obtained from (5.39)–(5.41).

5.7.2 Long-Term Average Energy per Bit

To derive $\mathrm{EB}_{\mathrm{avg}}$, consider the PPC and assume that the $\mathrm{EB}_{\min}$ realized in the ith CR is denoted $\mathrm{EB}_{\min}[i]$. Therefore, the total energy expended by the system in the ith CR equals $H\ \mathrm{EB}_{\min}[i]$ as the amount of MI communicated to the destination during any CR is H. Now, we can write

$$\mathrm{EB}_{\mathrm{avg}} = \lim_{m\to\infty} \frac{H\,\mathrm{EB}_{\min}[1] + \cdots + H\,\mathrm{EB}_{\min}[m]}{m\,H} = \mathrm{E}\{\mathrm{EB}_{\min}\}. \tag{5.44}$$

The RV $\mathrm{EB}_{\min}$ in (5.44) is given by (5.33) for all the protocols when $C_0 \geq C_1$, and by (5.34), (5.36), and (5.37), when $C_0 < C_1$. Again, the substitutions given in (5.7) lead to the corresponding results for Gaussian-input channels.

5.7.3 The RSUR

Assume that T_{S}, T_{R}, and T in the relaying protocols respectively denote the durations of the source transmission, relay transmission and CR, and that n_{S}, n_{R}, and n represent the corresponding numbers of the DoFs. Note that we can write $n_{\mathrm{S}} = W\,T_{\mathrm{S}}$, $n_{\mathrm{R}} = W\,T_{\mathrm{R}}$, and $n = W\,T$. Also note from (5.1) that $T = H/(W\,R)$, where R denotes the realized short-term average rate. Now, we have, from (5.42),

$$\mathrm{RSUR} = \frac{\mathrm{E}\left\{\frac{T_{\mathrm{R}}}{T}\,T\right\}}{\mathrm{E}\left\{\frac{T_{\mathrm{S}}}{T}\,T\right\}} = \frac{\mathrm{E}\left\{\frac{n_{\mathrm{R}}}{n}\,\frac{H}{W\,R}\right\}}{\mathrm{E}\left\{\frac{n_{\mathrm{S}}}{n}\,\frac{H}{W\,R}\right\}} = \frac{\mathrm{E}\left\{\frac{n_{\mathrm{R}}}{n}\,\frac{1}{R}\right\}}{\mathrm{E}\left\{\frac{n_{\mathrm{S}}}{n}\,\frac{1}{R}\right\}}. \tag{5.45}$$

Let n_1, as used in Table 5.1 and Sections 5.3.2–5.3.4, denote the number of symbols required by the relay to decode the message. Then, assuming that reversion to DT does not occur in a given CR, we have $n_{\mathrm{S}} = n$ and $n_{\mathrm{R}} = n - n_1$ for P-1 and P-2, whereas we have $n_{\mathrm{S}} = n_1$ and $n_{\mathrm{R}} = n - n_1$ for P-3. We define n_1 as being equal to n in a CR where the system reduces to DT. Using these definitions and relations, we obtain, from (5.45),

$$\mathrm{RSUR} = \begin{cases} 1 - \left(\mathrm{E}\{\frac{1}{R}\}\right)^{-1} \mathrm{E}\left\{\frac{n_1}{n\,R}\right\}, & \text{P-1 and P-2} \\ \mathrm{E}\{\frac{1}{R}\}\left(\mathrm{E}\left\{\frac{n_1}{n\,R}\right\}\right)^{-1} - 1, & \text{P-3} \end{cases}. \tag{5.46}$$

The result (5.46) is general, and gives the RSUR for any realized rate R and the corresponding values of n_1 and n as RVs. However, we are normally interested in the cases where the maximum value of R is achieved, i.e. when $R = R_{\max}$, or the cases where the minimum energy per bit is reached. Recall from Section 5.6.1 that in P-1 and P-3 the maximum rate corresponds to the minimum energy per bit. However in P-2, while the maximum rate is

achieved by operating at point A of the multiaccess rate region depicted in Fig. 5.1, the minimum energy per bit is obtained by operating at point A or B depending on the values of the SD and RD SNRs. Next, we derive expressions for $1/R$ and $n_1/(n\,R)$ in (5.46) in terms of the capacities C_0, C_1, C_2, and $C_{\rm m}$ for P-1 and P-3 when $R = R_{\max}$, and for P-2 when the rate is maximized and when the energy per bit is minimized. In the derivations, we use the fact that in a CR, the system reduces to DT in P-1 and P-2 when $C_0 \geq C_1$, and in P-3 when $C_0 \geq \min\{C_1, C_2\}$.

In P-1, using (5.14)–(5.16) we obtain

$$\frac{1}{R} = \begin{cases} \frac{1}{C_{\rm m}} + \frac{1}{C_1} - \frac{C_0}{C_{\rm m}\,C_1}, & C_0 < C_1 \\ \frac{1}{C_0}, & C_0 \geq C_1 \end{cases} \tag{5.47}$$

and

$$\frac{n_1}{n\,R} = \frac{1}{\max\{C_0, C_1\}} \tag{5.48}$$

for the case where R is maximized or the energy per bit is minimized.

In P-2, assuming that $X_{\rm S}$ and $X_{\rm R}$ are the source and relay rates in Phase II, respectively, we obtain, from (5.14), (5.18), and (5.19),

$$\frac{1}{R} = \begin{cases} \frac{C_1 - C_0 + X_{\rm R}}{(C_1 - C_0)X_{\rm S} + C_1 X_{\rm R}}, & C_0 < C_1 \\ \frac{1}{C_0}, & C_0 \geq C_1 \end{cases} \tag{5.49}$$

and

$$\frac{n_1}{n\,R} = \begin{cases} \frac{X_{\rm R}}{(C_1 - C_0)X_{\rm S} + C_1 X_{\rm R}}, & C_0 < C_1 \\ \frac{1}{C_0}, & C_0 \geq C_1 \end{cases}. \tag{5.50}$$

Now, the substitution $(X_{\rm S}, X_{\rm R}) = (C_0, C_{\rm m} - C_0)$ in (5.49) and (5.50) leads to the results related to the rate maximization case (see Section 5.3.3). Also, based on the results derived in Section 5.6.1, $(X_{\rm S}, X_{\rm R}) = (C_0, C_{\rm m} - C_0)$ when $2\,C_0 \leq C_{\rm m}$ and $(X_{\rm S}, X_{\rm R}) = (C_{\rm m} - C_2, C_2)$ when $2\,C_0 > C_{\rm m}$ convert (5.49) and (5.50) to the relations corresponding to the energy-per-bit minimization case. Combining these facts, we obtain

$$\frac{1}{R} = \begin{cases} \frac{C_{\rm m} + C_1 - 2C_0}{C_{\rm m}\,C_1 - C_0^2}, & C_0 < C_1 \\ \frac{1}{C_0}, & C_0 \geq C_1 \end{cases} \tag{5.51}$$

and

$$\frac{n_1}{n\,R} = \begin{cases} \frac{C_{\rm m}-C_0}{C_{\rm m}\,C_1-C_0^2}, & C_0 < C_1 \\ \frac{1}{C_0}, & C_0 \geq C_1 \end{cases} \tag{5.52}$$

corresponding to the case where the rate maximization is desired. Also, we obtain

$$\frac{1}{R} = \begin{cases} \frac{C_{\rm m}+C_1-2C_0}{C_{\rm m}\,C_1-C_0^2}, & C_0 < C_1,\ 2\,C_0 \leq C_{\rm m} \\ \frac{C_1+C_2-C_0}{C_0\,C_2+C_{\rm m}(C_1-C_0)}, & C_{\rm m}/2 < C_0 < C_1 \\ \frac{1}{C_0}, & C_0 \geq C_1 \end{cases} \tag{5.53}$$

and

$$\frac{n_1}{n\,R} = \begin{cases} \frac{C_{\rm m}-C_0}{C_{\rm m}\,C_1-C_0^2}, & C_0 < C_1,\ 2\,C_0 \leq C_{\rm m} \\ \frac{C_2}{C_0\,C_2+C_{\rm m}(C_1-C_0)}, & C_{\rm m}/2 < C_0 < C_1 \\ \frac{1}{C_0}, & C_0 \geq C_1 \end{cases} \tag{5.54}$$

corresponding to the case where the energy per bit is minimized.

In P-3, using (5.14), (5.23), and (5.24) one obtains

$$\frac{1}{R} = \begin{cases} \frac{1}{C_1} + \frac{1}{C_2} - \frac{C_0}{C_1\,C_2}, & C_0 < \min\{C_1, C_2\} \\ \frac{1}{C_0}, & C_0 \geq \min\{C_1, C_2\} \end{cases} \tag{5.55}$$

and

$$\frac{n_1}{n\,R} = \begin{cases} \frac{1}{C_1}, & C_0 < \min\{C_1, C_2\} \\ \frac{1}{C_0}, & C_0 \geq \min\{C_1, C_2\} \end{cases}. \tag{5.56}$$

corresponding to the rate maximization or energy-per-bit minimization case. Now, applying (5.47), (5.48), and (5.51)–(5.56) to (5.46) gives the corresponding expressions for the RSURs.

5.8 Numerical Examples

In this section, we consider Gaussian-input channels and study $R_{\rm avg}$ under the PPC, ${\rm EB}_{\rm avg}$ under the PPC, the RSUR under the PPC, and $R_{\rm avg}$ under the APC for the different schemes. It is assumed that γ_0, γ_1, and γ_2 are exponentially distributed (corresponding to Rayleigh fading) with mean values μ_0, μ_1, and μ_2. To obtain the long-term average performances, we use (5.12) and (5.13) for DT, and Monte Carlo simulation of (5.43), (5.44), (5.46)–

(5.48), and (5.51)–(5.56) with 10^5 iterations for the relaying systems.[7] Note that the long-term average rate under the PPC does not lead to a fair comparison in terms of energy expenditure, as explained in Section 5.5. However, it serves as a figure of merit for the rate performances of the protocols in energy unconstrained scenarios.

Figs. 5.2–5.5 respectively show the PPC long-term average rate in bits, the PPC normalized long-term average energy per bit, the APC long-term average rate in bits, and the RSUR under the PPC versus μ_0, for the different protocols. In these figures, it is assumed that the average channel gains are constant, but P, and hence γ (see (5.2)–(5.6)), changes such that we have $\mu_1 = \mu_0 + 25$ dB and $\mu_2 = \mu_0 + 10$ dB. This scenario normally corresponds to the case where the relay is closer to the source than to the destination.

Fig. 5.2 shows that P-1, P-2, and P-3 outperform DT with a difference in performance on the order of 1 to 1.5 bits. Also, P-1 and P-3 have a similar PPC rate performance, which is inferior to that of P-2. The superiority of P-2 over P-1 and P-3 increases with μ_0.

Fig. 5.3 indicates that P-3 has the best $\mathrm{EB}_{\mathrm{avg}}$ performance. In fact, under the PPC, although P-3 leads to smaller rates, it uses less energy per bit compared to the other schemes.

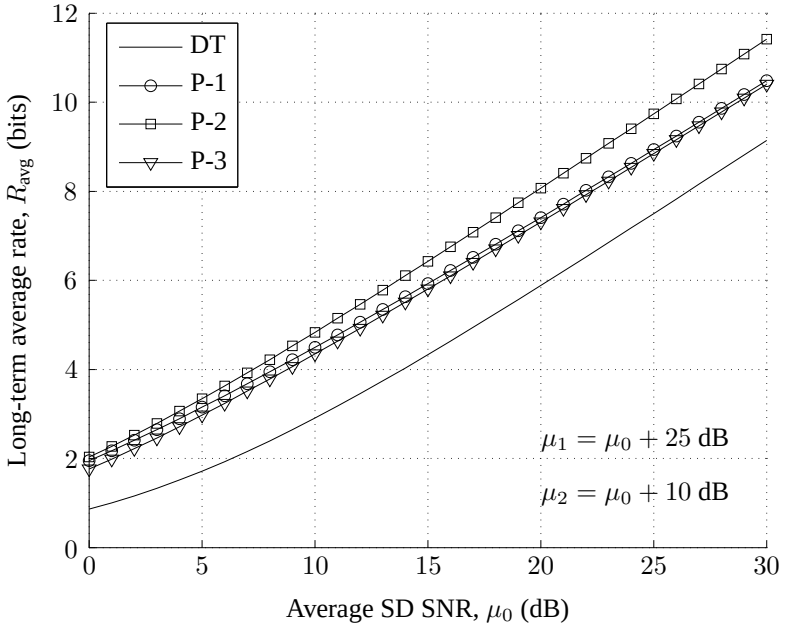

Fig. 5.2. The long-term average rate under the PPC versus the average SD SNR for the different schemes.

[7] In the case of Gaussian-input channels (where (5.7) holds) under the PPC, it is possible to calculate the expectations and derive more explicit analytical expressions for the long-term performance measures. However, we postpone such analyses to Chapter 6, where only generalizations of P-3 are investigated. In fact, we observe in Section 5.8 that P-3 is the most appealing relaying protocol of the three relaying strategies considering combination of performance and complexity.

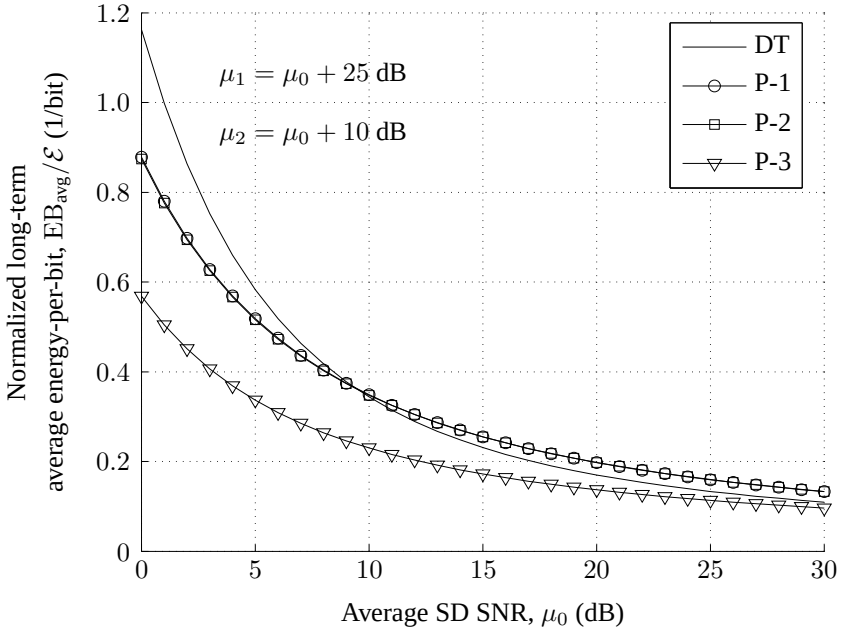

Fig. 5.3. The long-term average energy per bit, normalized by $\mathcal{E}$, under the PPC versus the average SD SNR for the different schemes.

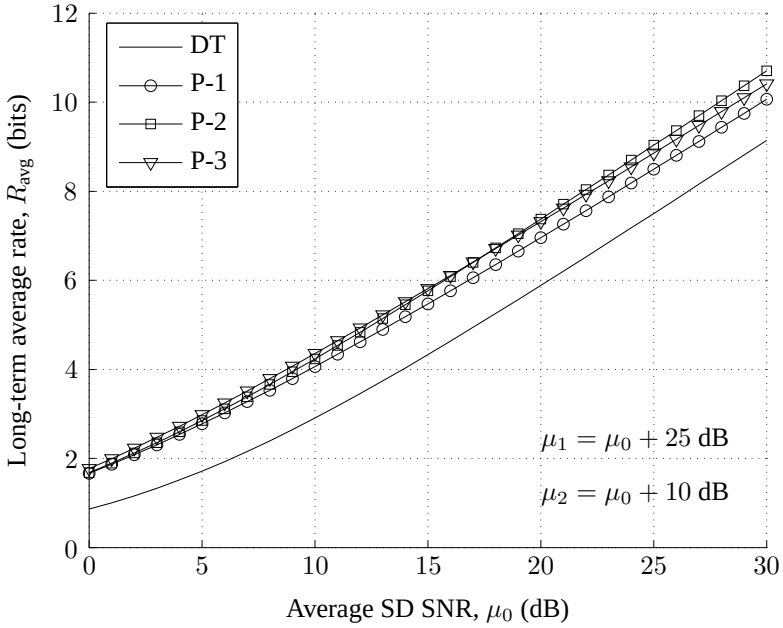

Fig. 5.4. The long-term average rate under the APC versus the average SD SNR for the different schemes.

The superiority of P-3 diminishes as the SD link improves. This figure also shows that the energy per bit in DT becomes smaller than that in P-1 and P-2 as μ_0 becomes greater than a certain value.

The other measure of energy efficiency, the APC rate, is studied in Fig. 5.4. It is ob-

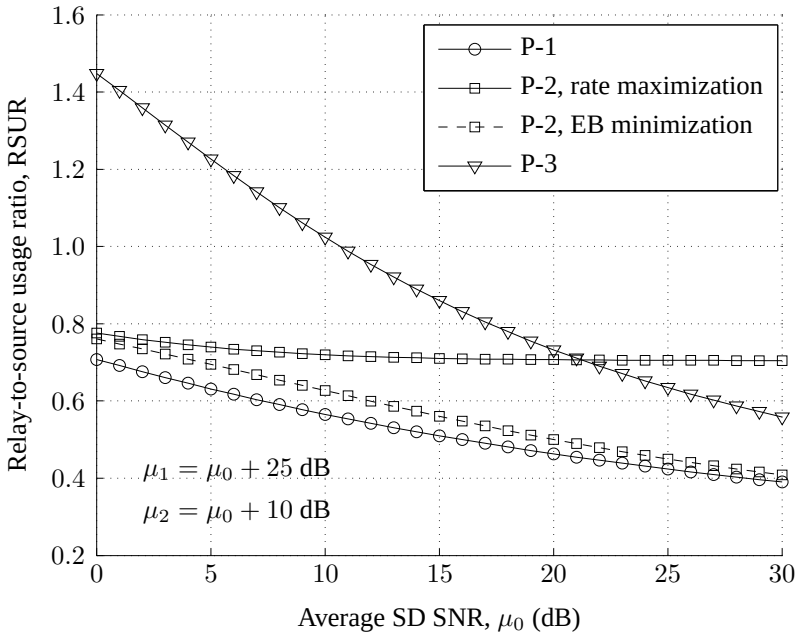

Fig. 5.5. The RSUR versus the average SD SNR for the different relaying schemes.

served that all the relaying schemes have larger APC rates on the order of one bit compared to DT. Also, the relaying schemes exhibit close performances. The P-1 scheme has the poorest performance. The P-3 scheme surpasses P-2 at small to medium values of μ_0, but becomes inferior to P-2 in a large SNR regime.

Fig. 5.5 depicts the RSUR versus μ_0 for P-1, P-2 in the rate maximization and energy per bit minimization cases (see Section 5.7.3), and P-3. Observe from this figure that while P-1 has the smallest RSUR for all the SNR range shown, P-3 has the largest RSUR for small to medium SNR values. One reason why the relay usage ratio is normally larger in P-3 than the other protocols is that in P-3 the source does not transmit in the second phase. Fig. 5.5 also shows that as μ_0 increases the RSUR in the schemes decreases, which is roughly because reversion to DT (and hence, not using the relay) happens more frequently as the SD link improves. Additionally note that there is a significant difference in the RSURs of the rate maximizing and energy per bit minimizing P-2 schemes; the former utilizes the relay much more than the latter does for medium to large values of μ_0.

The numerical results in the remaining figures are given for a linear network topology, similar to that used in Section 4.5, for which (4.71)–(4.73) hold. Recall that d_{SD}, d_{SR}, and d_{RD} are the SD, SR, and RD distances in the model. Here, we assume for the network topology that $\mu_0 = 5$ dB and the path loss exponent α is 3.

Figs. 5.6–5.9 respectively show $R_{\rm avg}$ under the PPC, $\mathrm{EB}_{\rm avg}$ under the PPC, $R_{\rm avg}$ under the APC, and the RSUR under the PPC versus $d_{\rm SR}/d_{\rm SD}$, for the different schemes. The ratio $d_{\rm SR}/d_{\rm SD}$ ranges from 0.1 to 0.9, representing the situation where starting from the vicinity of the source, the relay approaches the destination. The performance of DT is obviously unchanging with $d_{\rm SR}/d_{\rm SD}$.

Fig. 5.6 clearly shows that

$$R_{\rm avg}^{\rm (P\text{-}2)} > R_{\rm avg}^{\rm (P\text{-}1)} > R_{\rm avg}^{\rm (P\text{-}3)} > R_{\rm avg}^{\rm (DT)} \tag{5.57}$$

under the PPC, as expected (see Section 5.5). Fig. 5.6 also shows that the favorable position of the relay for achieving larger PPC rates in P-1 and P-2 is closer to the source, while in P-3 it is around the middle of the line connecting the source and destination.

Figs. 5.7 and 5.8 verify the superiority of P-3 compared to the other schemes in terms of energy efficiency. The performance superiority ranges approximately from 0.03 to 0.45 and from 0.008 bits to 0.49 bits in terms of $\mathrm{EB}_{\rm avg}/\mathcal{E}$ and $R_{\rm avg}$, respectively. The figures also show that the favorable position of the relay in P-3 for achieving larger energy efficiency is always around the midpoint between the source and destination. However, in P-1 and P-2, this position is closer to the destination for $\mathrm{EB}_{\rm avg}$, but around the midpoint for $R_{\rm avg}$.

Fig. 5.9 shows that all the RSURs decrease as $d_{\rm SR}/d_{\rm SD}$ increases. In fact, as the relay

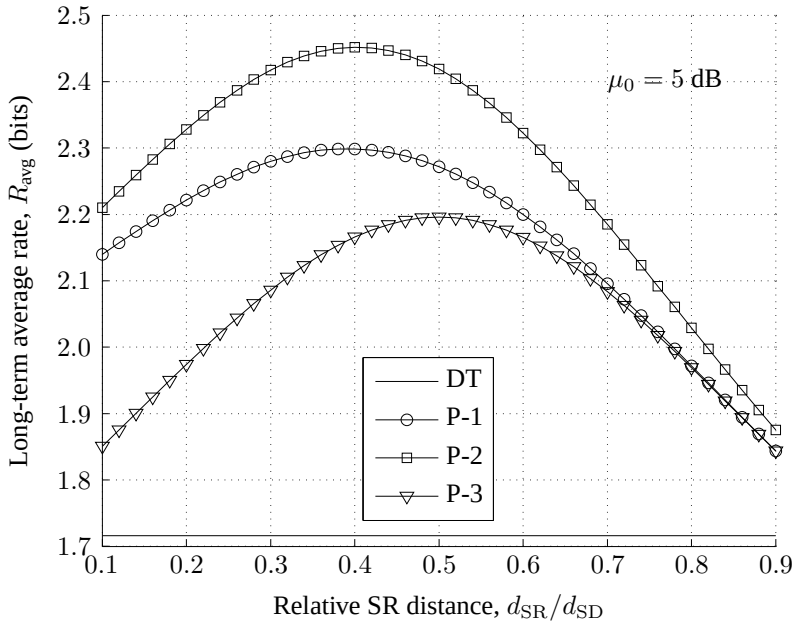

Fig. 5.6. The long-term average rate under the PPC versus the SR distance normalized by the SD distance, for the different schemes and a linear network topology.

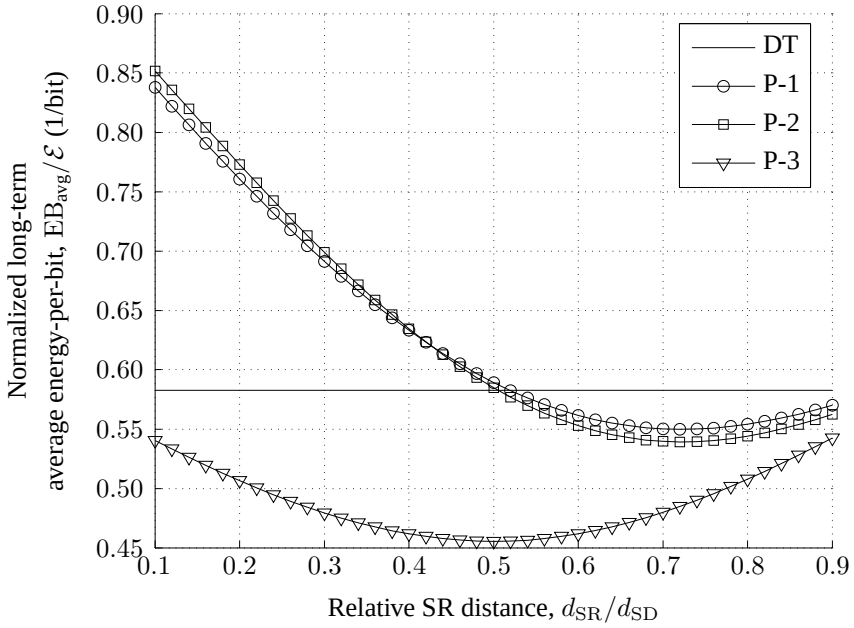

Fig. 5.7. The long-term average energy per bit, normalized by $\mathcal{E}$, under the PPC versus the SR distance normalized by the SD distance, for the different schemes and a linear network topology.

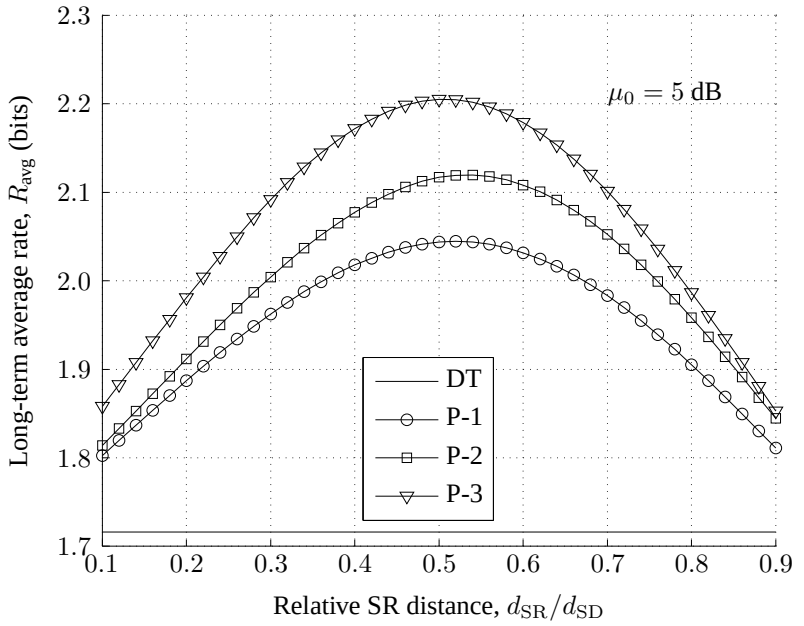

Fig. 5.8. The long-term average rate under the APC versus the SR distance normalized by the SD distance, for the different schemes and a linear network topology.

moves farther from the source, the SR link weakens and the relay usage ratio decreases. Another result obtained is that here again, like what observed in Fig. 5.5, P-1 achieves the least use of the relay among the protocols, and P-3 in almost all cases benefits from the

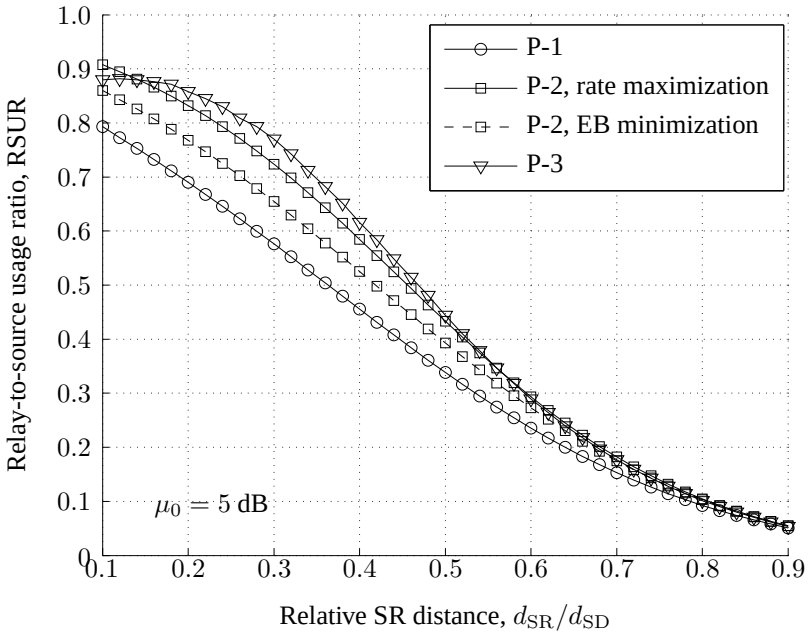

Fig. 5.9. The RSUR versus the SR distance normalized by the SD distance, for the different relaying schemes and a linear network topology.

relay most. Also, the rate maximization in P-2 demands the relaying operation more than the energy per bit minimization does.

5.8.1 Discussion on Rate and Energy Efficiency

As shown in Section 5.5 and confirmed by numerical examples in Section 5.8, P-2, P-1, and P-3 rank first to third in rate efficiency under the PPC. However, as suggested by the results in Sections 5.6.1 and 5.8, P-3, P-2, and P-1 rank first to third in energy efficiency in most cases. Here, we show that it is possible to roughly explain these relationships by intuition.

In a PPC regime, P-2 outperforms P-1 as it opportunistically uses the SD link to transmit some of the messages without using the relay. In P-1, all messages are transmitted cooperatively. Also, P-1 and P-2 achieve larger rates than P-3 as they benefit from simultaneous source and relay transmissions. The larger rates are achieved at the cost of more energy per bit and higher complexity.

However in a fair comparison on a power basis, e.g. in an APC regime, P-3 excels in the achievable rate, as at any given time, only a single best node transmits. This paradigm can use energy more efficiently compared to the multinode transmission paradigms of P-1 and P-2, as explained in Section 5.3.4. Also, P-2 performs better than P-1 for reasons similar to those in the PPC case.

Chapter 6

Rateless Coded Relaying: Multirelay Case[1]

6.1 Introduction

Rateless codes were introduced and their application to single-relay cooperative networks was examined in Chapter 5. As mentioned in Chapter 5, in rateless coding, the transmitter produces an indefinitely long stream of encoding packets/symbols. The receiver accumulates information from the packets/symbols already received, and periodically attempts to decode the message. The receiver can decode successfully as soon as the received MI marginally exceeds the entropy of the message [99, Chapter 50], [21], [22]. The main benefits of rateless codes are summarized as adapting to the channel condition and approaching the capacity with a transmitter oblivious to instantaneous CSI [99, Chapter 50], [21]. In addition, fountain codes, an important category of rateless codes, have simple, almost linear time encoding/decoding algorithms [99, Chapter 50].

The applicability and excellent fit of rateless coding to DF relaying networks were first noted and demonstrated in [91]. A protocol in which a decoding relay forms a DSTC scheme with the source was introduced in [21], [91]. In [94], several rateless coded cooperation methods which yield large outage capacity gains in low power regimes were proposed. In [95], different single-relay schemes based on ACKs were introduced, and

[1] *A version of this chapter has been published in part in the Proceedings of the IEEE Global Telecommunications Conference (GLOBECOM), 2008, and has been submitted to the IEEE Transactions on Wireless Communications.*

their achievable rates were obtained. Moreover, several novel multirelay, quasisynchronous and asynchronous, rateless coded schemes were proposed in [22]. In the quasisynchronous case, when the number of decoding relays reaches a preset value, all decoding relays collaborate to communicate the message to the destination. In the asynchronous case, as soon as a relay decodes, it starts broadcasting the message for the other relays and destination. Note that such schemes need either CDMA, interrelay synchronizations at the symbol level, or MUD at the destination and/or relays, entailing complexity and/or performance loss. In addition, knowledge of the qualities of the SD and RD links is not used in the cooperation. Three protocols, analogous to those proposed in [21], [22], were also investigated in [96] for single-relay cases. Achievable rates using practical rateless codes and modulation were examined, considering deeply interleaved data streaming and block fading, respectively for delay unlimited and delay constrained scenarios.

In Chapter 5, we studied several rateless coded protocols, namely P-1, P-2, and P-3, for single-relay collaborative networks. We observed that P-3 is very efficient in terms of implementation complexity and energy consumption as compared to P-1 and P-2. In this chapter, we propose and investigate the application of rateless codes to multirelay, dual-hop networks by developing and analyzing three novel, low-complexity protocols, which can be viewed as generalizations of P-3 to the multirelay case.

The proposed protocols have simple single-parameter strategies that employ two-phase selection cooperation, previously proposed and investigated for fixed-rate systems [58], [68], [107]. In contrast to fixed-rate schemes, where the duration of the source broadcasting is fixed, in rateless schemes, this duration can last until the destination decodes successfully or a system timeout occurs. Here, we assume for simplicity of illustration that the a CR does not have a timeout. In the proposed protocols, different stopping criteria for the first phase are introduced. As soon as the criteria are met, the second phase starts in which only the best of the source and decoding relays transmits to the destination until it decodes. All the protocols amount to P-3 in the single-relay case when their parameters are optimally chosen. Recall from Section 5.3.4 that P-3 is also based on selection cooperation. The selection techniques in the proposed protocols, much like the selection method in P-3, obviate the need for CDMA, stringent synchronization, and MUD, and make all SD, SR, and RD channel gains matter in the selection process. Also, they can be readily implemented in a distributed fashion [68], [107].

The remainder of the chapter is organized as follows. Section 6.2 describes the system model and assumptions. The rateless coded protocols are introduced and analyzed in Sections 6.3 and 6.4, respectively. Finally, Sections 6.5 and 6.6 provide some numerical examples and results, and discusses the design and performance implications of the proposed protocols, respectively.

6.2 System Model

We use a system model similar to that in [22]. Consider the dual-hop relaying network depicted in Fig. 4.1, consisting of a source, a destination, and M relays. All nodes are single-antenna and share the same frequency band of baseband width W. The source and relays are assumed to use rateless coding for transmitting data. The rateless coded protocols introduced in Section 6.3 allow half-duplex operation for the relays [9] by not having them simultaneously transmit and receive.

As in Chapter 5, a CR refers to the period over which a message of the source is fully communicated to the destination. Every message of the source has a constant entropy H. Hence, given a CR, if R and T are the average rate per channel use in the CR and the duration of the CR, respectively, we have, in the same manner as (5.1),

$$R = \frac{H}{WT}. \tag{6.1}$$

The channel model and assumptions are similar to those in Chapter 5. We assume that the SD, SR$_m$, and R$_m$D links undergo independent flat fading, and suffer AWGN. Channel state information is assumed to be estimated by, and only available to the receivers for coherent reception. The instantaneous SNRs associated with the SD, SR$_m$, and R$_m$D links are denoted γ_{SD}, $\gamma_{\mathrm{S}m}$, and $\gamma_{m\mathrm{D}}$.

As CSI is not available at the transmitters, no power optimization is assumed to be executed. We additionally assume that the source and relays transmit with the same power P, or energy per symbol $\mathcal{E}$ (note that in this case (5.2) holds). In other words, we consider the PPC introduced and used in Chapter 5. This assumption is for analytical simplicity and also for making the schemes easy to compare in terms of energy efficiency, as will be observed in Section 6.4. We explain in Section 6.4 that the PPC suffices to provide a fair comparison between the protocols on a power basis and that the APC, introduced in Chapter

5 for fairly comparing the achievable rates of P-1, P-2, and P-3, is not needed here.

Assume that $C(\gamma_{\rm sub})$ is the capacity per 2-D DoF of a single-hop AWGN link with SNR $\gamma_{\rm sub}$, where "sub" is any descriptive string, such as "SD", "th", "Sm", "mD". For example,

$$C(x) = \ln(1+x) \tag{6.2}$$

nats for Gaussian-input or average-power-constrained-input AWGN channels, and

$$C(x) = 2\,\ln 2 - \sqrt{\frac{2}{\pi}} \int_{-\infty}^{\infty} {\rm d}t\; {\rm e}^{-t^2/2}\; \ln\left(1+{\rm e}^{-2\sqrt{x}\,t-2\,x}\right) \tag{6.3}$$

nats for binary-input AWGN channels [108]. Now, we define the convenient notation

$$\tau_{\rm sub} \triangleq \frac{H}{W\,C(\gamma_{\rm sub})} \tag{6.4}$$

utilized throughout. The value $\tau_{\rm sub}$ is the time required for transmitting a message of entropy H using a capacity-approaching code over an AWGN channel with baseband bandwidth W and the received value of SNR $\gamma_{\rm sub}$. We assume here that as in Chapter 5, the rateless codes considered are capacity-approaching [21], [22], [95]. Therefore, we can exploit (6.4) to obtain the transmission time using the rateless coding.[2] It is assumed that in general, $C(x)$ is a strictly increasing function of x, such that based on (6.4), there is a one-to-one correspondence between $\tau_{\rm sub}$ and $\gamma_{\rm sub}$. Employing $\tau_{\rm sub}$ instead of $\gamma_{\rm sub}$ simplifies the description and analysis of the protocols in Sections 6.3 and 6.4.

6.3 Rateless Coded Selection Strategies

6.3.1 General Description

Three rateless coded selection protocols, called P-n, P-γ, and P-t, are introduced in this section, each being a generalization of the P-3 protocol proposed in Chapter 5. A summary of the three schemes is enumerated as follows:

1. The source splits its message into a number of packets, and performs rateless coding to generate an indefinitely long stream of encoded packets.

2. A CR consists of uplink and downlink phases. In the uplink, the source broadcasts its message.

[2] More precisely, we can omit the assumption of being capacity-approaching by replacing H in (6.4) with $(1+\varepsilon)H$, where ε is the code inefficiency, independent of $\gamma_{\rm sub}$ [21], [99]. Setting $\varepsilon = 0$ is for simplicity and does not incur loss of generality in subsequent analysis.

3. The relays and destination accumulate information and periodically attempt to decode the message.

4. If the destination can decode in the uplink, the CR ends without the downlink phase.

5. In P-n, the uplink continues until a preset number of relays decode the message. In P-γ, the uplink stopping criterion is the source or a decoding relay has a link to the destination with SNR greater than a threshold. In P-t, the uplink ends whenever the destination can decode in less than a preset time using the best of the source and already decoding relays.

6. In P-γ and P-t, the uplink ends also if all relays decode.

7. In the downlink, the best of the source and decoding relays transmits to the destination until it decodes.

Note that the scheme P-n can also be viewed as the selection version of the quasisynchronous protocols in [22]. In Section 6.6, we expound more on the rationales behind our ad hoc schemes and their design and performance implications.

6.3.2 Mathematical Description

Let the set of the indices of all decoding relays at time t be denoted $\mathcal{D}(t)$. Note that $\mathcal{D}(t)$ is time varying and grows as time elapses. It is assumed that when R_m decodes, for any m, it broadcasts an ACK, which is received and used to estimate $\gamma_{m\mathrm{D}}$ by the destination. Also, the destination is capable of estimating γ_{SD} using direct reception from the source.

6.3.2.1 The P-n Scheme

In P-n, the uplink lasts until the destination decodes or L relays decode, where L is a parameter ranging from 1 to M. In the latter case, the downlink starts where the node corresponding to SNR,

$$\max_{X \in \{\mathrm{S}\} \cup \mathcal{D}(T_{\mathrm{UL}})} \gamma_{X\mathrm{D}} \tag{6.5}$$

where T_{UL} is the uplink duration, is signaled by the destination and transmits rateless encoded packets until the destination decodes. Note that based on the description, T_{UL} in this protocol can be written as

$$T_{\mathrm{UL}} = \min\{\tau_{\mathrm{S}(L)}, \tau_{\mathrm{SD}}\} \tag{6.6}$$

where $\tau_{\mathrm{S}(m)}$ for any m is defined as the time at which the mth relay can decode, and where τ_{SD}, defined by (6.4), is the DT time.

6.3.2.2 The P-γ Scheme

In P-γ, the downlink starts when an *above-threshold (AT) node* is found or all relays decode before the destination decodes. An AT node is the source or a decoding relay which has a link to the destination with SNR greater than a parametric threshold SNR, γ_{th}. The AT node found becomes the solitary downlink transmitter of fountain packets until the destination decodes. If all relays decode before an AT node is found, the node corresponding to SNR,

$$\max_{X \in \{\mathrm{S}\} \cup \{1, \cdots, M\}} \gamma_{X\mathrm{D}} \tag{6.7}$$

is selected to transmit in the downlink. Note that if $\gamma_{\mathrm{SD}} > \gamma_{\mathrm{th}}$ in a CR, the source becomes the AT node such that the system amounts to DT in the CR. It can be observed that T_{UL}, the uplink time, in P-γ can be written as

$$T_{\mathrm{UL}} = \min\left\{\Theta^{(\gamma)}, \tau_{\mathrm{S}(M)}\right\} \tag{6.8a}$$

where

$$\Theta^{(\gamma)} \triangleq \min\ t \tag{6.8b}$$

subject to

$$\max_{X \in \{\mathrm{S}\} \cup \mathcal{D}(t)} \gamma_{X\mathrm{D}} \geq \gamma_{\mathrm{th}} \tag{6.8c}$$

and where $\tau_{\mathrm{S}(M)}$ is the time that the last relay decodes.

6.3.2.3 The P-t Scheme

In P-t, the uplink continues until time T_{UL} at which one of the following cases occurs. 1) The destination decodes, in which case the CR ends. 2) All relays decode, in which case X_{DL}, defined as the node corresponding to the SNR given in (6.5), transmits in the downlink until the destination decodes. 3) The destination calculates that it is capable of decoding by the next t_0 seconds provided that X_{DL} transmits in the downlink, where t_0 is a system parameter. In this case, X_{DL} is signaled by the destination to be the downlink transmitter.

Protocol P-t essentially relies on the fact that at any given time t during the source broadcasting, the destination can determine how much more information it requires to accumulate by receiving rateless encoded packets for successful decoding. In fact, the destination receives $t\,W\,C(\gamma_{\rm SD})$ units of MI from the source's transmission up to time t, where the capacity function $C(\cdot)$ has been defined in Section 6.2. The destination needs additional,

$$H - t\,W\,C(\gamma_{\rm SD}) \tag{6.9}$$

units of MI to decode the message. Given that the destination knows the constants H and W, and can measure $\gamma_{\rm SD}$, it can calculate (6.9).

Lemma 6.1. The uplink time in P-t is given by

$$T_{\rm UL} = \min\left\{\Theta, \tau_{{\rm S}(M)}\right\} \tag{6.10a}$$

where

$$\Theta \triangleq \min\ t \tag{6.10b}$$

subject to

$$\left(1 - \frac{t}{\tau_{\rm SD}}\right) \min_{X \in \{\rm S\} \cup \mathcal{D}(t)} \tau_{X\rm D} \leq t_0 \tag{6.10c}$$

where $\tau_{\rm SD}$ and $\tau_{X\rm D}$ are defined by (6.4).

Proof. First, if $\tau_{\rm SD} \leq t_0$, the Lemma results in $T_{\rm UL} = 0$ (note that $\mathcal{D}(0) = \varnothing$), which is correct because, utilizing only the source, the destination can decode in $\tau_{\rm SD}$ seconds, i.e. by the next t_0 seconds. Therefore, based on the protocol description, $T_{\rm UL} = 0$ and the system behaves as DT.

Next, assume that $\tau_{\rm SD} > t_0$. If the source broadcasts for t seconds, where $t < \tau_{\rm SD}$, the destination accumulates $t\,W\,C(\gamma_{\rm SD})$ units of information, and requires $H - t\,W\,C(\gamma_{\rm SD})$ units more information to decode. If the remaining amount is provided by Node X, where $X \in \{\rm S\} \cup \mathcal{D}(t)$, it takes time

$$\Theta_X(t) \triangleq \frac{H - t\,W\,C(\gamma_{\rm SD})}{W\,C(\gamma_{\rm XD})} = \left(1 - \frac{t}{\tau_{\rm SD}}\right)\tau_{X\rm D} \tag{6.11}$$

until the destination decodes, where the second equality is obtained by invoking (6.4). Therefore, the smallest possible decoding time is given as

$$\Theta_b(t) \triangleq \min_{X \in \{\rm S\} \cup \mathcal{D}(t)} \Theta_X(t) = \left(1 - \frac{t}{\tau_{\rm SD}}\right) \min_{X \in \{\rm S\} \cup \mathcal{D}(t)} \tau_{X\rm D} \tag{6.12}$$

and the first instant t at which $\Theta_b(t)$ is exceeded by t_0 is given by Θ (6.10b), (6.10c). The time Θ gives the uplink time if not all relays decode within Θ seconds. Otherwise, T_{UL} is the time at which the last relay decodes, i.e. $T_{\mathrm{UL}} = \tau_{\mathrm{S}(M)}$. This concludes the proof. ■

In Lemma 6.1, $\Theta_b(t)$ is a decreasing function of t. This lemma states that in P-t, the uplink continues until either all relays decode or $\Theta_b(t)$ falls below t_0.

Observe that in all the protocols, the downlink transmitter is always X_{DL}, the node corresponding to the SNR given in (6.5). It is the uplink stopping criterion that differentiates the protocols. In the downlink, the optimal strategy is rather clear, i.e. having the best node knowing the message transmit to the destination. In fact, in a fashion similar to (6.12), the downlink duration, T_{DL}, can be obtained for all protocols as

$$T_{\mathrm{DL}} = \left(1 - \frac{T_{\mathrm{UL}}}{\tau_{\mathrm{SD}}}\right) \min_{X \in \{\mathrm{S}\} \cup \mathcal{D}(T_{\mathrm{UL}})} \tau_{X\mathrm{D}} \tag{6.13}$$

where T_{UL} is the uplink time in the different protocols given by (6.6), (6.8), and (6.10).

6.4 Performance Analysis

In this section, the long-term average performances of P-n, P-γ, and P-t are analyzed. We also propose and examine a rate optimal selection protocol, denoted P-o, as a baseline for performance comparison.

Recall from Section 6.2 that we impose the PPC, i.e. the energy per symbol is considered to be constant at $\mathcal{E}$ for all nodes. Since in all schemes, there is only one transmitter at any time, the short-term average energy per symbol (see Section 5.2) is $\mathcal{E}$ in all the protocols, analogous to DT and P-3 (see Sections 5.3.1 and 5.3.4). This obviates the need for examining the energy per bit or imposing the APC, as in Chapter 5, to compare the schemes fairly on a power basis; the schemes are already comparable as all of them use the same amount of energy per symbol. Therefore, here we only consider the PPC long-term average rate and RSUR, studied in Section 5.7, to evaluate the long-term performances.

In contrast to the single-relay case studied in Chapter 5, where the only relay in the system cooperates with the source, in the multirelay case, there are more than one candidate relay for the downlink transmission. This makes it difficult to use the approaches taken in Chapter 5 for the performance evaluation here, i.e. to derive expressions for the short-term average rates and use (5.43) and (5.45) to calculate the long-term average rate and RSUR.

In the sequel, we explain how these long-term average quantities can be obtained in the case of P-n, P-γ, and P-t.

Assuming that the duration of the mth CR is denoted $T[m]$, we obtain, in a manner similar to (5.43),

$$R_{\text{avg}} = \lim_{m\to\infty} \frac{m\,H}{W(T[1]+\cdots+T[m])} = \frac{H}{W\,\mathrm{E}\{T\}}. \tag{6.14}$$

Also, regarding the RSUR, assume that T_{S} and T_{R_m} are the durations of the source and R_m transmissions. Note that in any CR for each of the protocols, $T_{\mathrm{S}} > 0$ and at most one of $T_{\mathrm{R}_1}, \ldots, T_{\mathrm{R}_M}$ is nonzero. Also, we have

$$T = T_{\mathrm{S}} + T_{\mathrm{R}_1} + \cdots + T_{\mathrm{R}_M} = T_{\mathrm{UL}} + T_{\mathrm{DL}} \tag{6.15}$$

where T_{UL} and T_{DL} are the uplink and downlink times. Now, using the definition of the RSUR in Section 5.7, one obtains, much like (5.42),

$$\mathrm{RSUR} = \frac{\mathrm{E}\{T_{\mathrm{R}_1}\} + \cdots + \mathrm{E}\{T_{\mathrm{R}_M}\}}{\mathrm{E}\{T_{\mathrm{S}}\}}. \tag{6.16}$$

Note that $\mathrm{E}\{T_X\}$ shows how active on average Node X is.

Based on (6.14) and (6.16), we need to calculate $\mathrm{E}\{T\}$, $\mathrm{E}\{T_{\mathrm{S}}\}$, $\mathrm{E}\{T_{\mathrm{R}_1}\}$, $\cdots$, and $\mathrm{E}\{T_{\mathrm{R}_M}\}$ for evaluating R_{avg} and the RSUR. We know that if Z is a nonnegative RV, we have [81, eq. (5-53)] (cf. (4.2))

$$\mathrm{E}\{Z\} = \int_0^\infty \Pr\{Z > t\}\,\mathrm{d}t \tag{6.17}$$

when Z has finite mean and variance. We utilize (6.17) to calculate $\mathrm{E}\{T_{\mathrm{S}}\}$, $\mathrm{E}\{T_{\mathrm{R}_1}\}$, $\cdots$, and $\mathrm{E}\{T_{\mathrm{R}_M}\}$; then, we use (6.15) to obtain $\mathrm{E}\{T\}$. This approach to deriving $\mathrm{E}\{T\}$ for the protocols is less intricate than a direct derivation approach, e.g. directly based on (6.17).

Next, we provide the results for each protocol and relegate the derivation details to Appendix G. We consider a general fading model for the SNRs. However, only Rayleigh fading is considered for the examples in Section 6.5. The integrals involved in the results are computable efficiently for Rayleigh fading using standard numerical integration techniques.

6.4.1 The P-n Scheme

Let $u_{\mathrm{SD}}(\cdot)$, $u_{\mathrm{S}m}(\cdot)$, $u_{m\mathrm{D}}(\cdot)$, $U_{\mathrm{SD}}(\cdot)$, $U_{\mathrm{S}m}(\cdot)$, and $U_{m\mathrm{D}}(\cdot)$ denote the PDF of τ_{SD}, PDF of $\tau_{\mathrm{S}m}$, PDF of $\tau_{m\mathrm{D}}$, CDF of τ_{SD}, CDF of $\tau_{\mathrm{S}m}$, and CDF of $\tau_{m\mathrm{D}}$, respectively, where τ_{SD}, $\tau_{\mathrm{S}m}$, and $\tau_{m\mathrm{D}}$ are defined by (6.4). Recall that M is the number of relays and L is the

system parameter. Then, we can show that

$$\begin{aligned}\mathrm{E}\{T_{\mathrm{S}}\} = &\sum_{\substack{\mathcal{A}\subset\{1,\cdots,M\}\\ |\mathcal{A}|\le L-1}} \int_0^\infty \mathrm{d}t\,[1-U_{\mathrm{SD}}(t)] \prod_{m\in\mathcal{A}} U_{\mathrm{S}m}(t) \prod_{m\in\mathcal{A}^{\mathrm{c}}} [1-U_{\mathrm{S}m}(t)] \\ &+ \sum_{\substack{\mathcal{A}\subset\{1,\cdots,M\}\\ |\mathcal{A}|=L}} \sum_{k\in\mathcal{A}} \int_0^\infty \mathrm{d}x \int_0^x \mathrm{d}y\,(x-y)\,u_{\mathrm{SD}}(x)\,u_{\mathrm{S}k}(y) \\ &\times \prod_{m\in\mathcal{A}} [1-U_{m\mathrm{D}}(x)] \prod_{\substack{m\in\mathcal{A}\\ m\ne k}} U_{\mathrm{S}m}(y) \prod_{m\in\mathcal{A}^{\mathrm{c}}} [1-U_{\mathrm{S}m}(y)] \end{aligned} \tag{6.18}$$

and that

$$\begin{aligned}\mathrm{E}\{T_{\mathrm{R}_m}\} = &\sum_{\substack{\mathcal{A}\subset\{1,\cdots,M\}-\{m\}\\ |\mathcal{A}|=L-1}} \sum_{k\in\mathcal{A}\cup\{m\}} \int_0^\infty \mathrm{d}x \int_0^\infty \mathrm{d}y \int_0^x \mathrm{d}t\; u_{m\mathrm{D}}(x)\,u_{\mathrm{S}k}(y) \\ &\times \left[1-U_{\mathrm{SD}}\left(\max\left\{x, \frac{x\,y}{x-t}\right\}\right)\right] \prod_{i\in\mathcal{A}} [1-U_{i\mathrm{D}}(x)] \\ &\times \prod_{\substack{i\in\mathcal{A}\cup\{m\}\\ i\ne k}} U_{\mathrm{S}i}(y) \prod_{\substack{i\in\mathcal{A}^{\mathrm{c}}\\ i\ne m}} [1-U_{\mathrm{S}i}(y)] \end{aligned} \tag{6.19}$$

for $m = 1, \ldots, M$.

6.4.2 The P-γ Scheme

Recall that γ_{th}, a threshold SNR, is the P-γ parameter. Let τ_{th} be defined by (6.4) using γ_{th}. Then, it can be shown that

$$\begin{aligned}\mathrm{E}\{T_{\mathrm{S}}\} = &\int_0^{\tau_{\mathrm{th}}} \mathrm{d}t\; t\,u_{\mathrm{SD}}(t) + \int_0^\infty \mathrm{d}t\,[1-U_{\mathrm{SD}}(\max\{t,\tau_{\mathrm{th}}\})] \\ &\times \left\{ \prod_{m=1}^M [1-U_{\mathrm{S}m}(t)\,U_{m\mathrm{D}}(\tau_{\mathrm{th}})] - \prod_{m=1}^M U_{\mathrm{S}m}(t)[1-U_{m\mathrm{D}}(\tau_{\mathrm{th}})] \right\} \\ &+ \int_{\tau_{\mathrm{th}}}^\infty \mathrm{d}x \int_0^x \mathrm{d}t\; u_{\mathrm{SD}}(x) \prod_{m=1}^M U_{\mathrm{S}m}(t)[1-U_{m\mathrm{D}}(x)] \end{aligned} \tag{6.20}$$

and that

$$\begin{aligned}\mathrm{E}\{T_{\mathrm{R}_m}\} = &\int_0^\infty \mathrm{d}x \int_0^{\tau_{\mathrm{th}}} \mathrm{d}y \int_0^1 \mathrm{d}t\; y\,u_{\mathrm{S}m}(x)\,u_{m\mathrm{D}}(y) \left[1-U_{\mathrm{SD}}\left(\max\left\{\frac{x}{t}, \tau_{\mathrm{th}}\right\}\right)\right] \\ &\times \prod_{\substack{k=1\\ k\ne m}}^M [1-U_{\mathrm{S}k}(x)\,U_{k\mathrm{D}}(\tau_{\mathrm{th}})] + \int_{\tau_{\mathrm{th}}}^\infty \mathrm{d}x \int_{\tau_{\mathrm{th}}}^x \mathrm{d}y \int_0^1 \mathrm{d}t\; y\,u_{\mathrm{SD}}(x)\,u_{m\mathrm{D}}(y) \\ &\times \prod_{k=1}^M U_{\mathrm{S}k}(x\,t) \prod_{\substack{k=1\\ k\ne m}}^M [1-U_{k\mathrm{D}}(y)] \end{aligned} \tag{6.21}$$

for $m = 1, \ldots, M$.

6.4.3 The P-t Scheme

Recall that t_0 is the P-γ parameter. We obtain for this protocol

$$\begin{aligned}
\mathrm{E}\{T_{\mathrm{S}}\} = &\int_0^{t_0} \mathrm{d}t\, t\, u_{\mathrm{SD}}(t) + t_0 \int_{t_0}^{\infty} \mathrm{d}x\, u_{\mathrm{SD}}(x) \prod_{m=1}^{M} \left[1 - U_{\mathrm{S}m}(x - t_0)\, U_{m\mathrm{D}}(x)\right] \\
&+ \int_{t_0}^{\infty} \mathrm{d}x \int_0^{x-t_0} \mathrm{d}t\, u_{\mathrm{SD}}(x) \Bigg\{ \prod_{m=1}^{M} \left[1 - U_{\mathrm{S}m}(t)\, U_{m\mathrm{D}}\left(\frac{t_0\, x}{x-t}\right)\right] \\
&- \prod_{m=1}^{M} U_{\mathrm{S}m}(t) \left[U_{m\mathrm{D}}(x) - U_{m\mathrm{D}}\left(\frac{t_0\, x}{x-t}\right)\right] \Bigg\} \qquad (6.22)
\end{aligned}$$

and

$$\begin{aligned}
\mathrm{E}\{T_{\mathrm{R}_m}\} = &\int_{t_0}^{\infty} \mathrm{d}x \int_0^{x-t_0} \mathrm{d}y \int_0^{t_0} \mathrm{d}t\, \frac{x\, t}{x-y}\, u_{\mathrm{SD}}(x)\, u_{\mathrm{S}m}(y)\, u_{m\mathrm{D}}\left(\frac{x\, t}{x-y}\right) \\
&\times \prod_{\substack{k=1 \\ k \neq m}}^{M} \left[1 - U_{\mathrm{S}k}(y)\, U_{k\mathrm{D}}\left(\frac{x\, t_0}{x-y}\right)\right] \\
&+ t_0 \int_{t_0}^{\infty} \mathrm{d}x \int_{t_0}^{x} \mathrm{d}y\, u_{\mathrm{SD}}(x)\, u_{m\mathrm{D}}(y)\, U_{\mathrm{S}m}\left(x\left(1 - \frac{t_0}{y}\right)\right) \\
&\times \prod_{\substack{k=1 \\ k \neq m}}^{M} \left[1 - U_{\mathrm{S}k}\left(x\left(1 - \frac{t_0}{y}\right)\right) U_{k\mathrm{D}}(y)\right] \\
&+ \int_{t_0}^{\infty} \mathrm{d}x \int_{t_0}^{x} \mathrm{d}y \int_0^{1-t_0/y} \mathrm{d}t\, y\, u_{\mathrm{SD}}(x)\, u_{m\mathrm{D}}(y) \\
&\times U_{\mathrm{S}m}(x\, t) \prod_{\substack{k=1 \\ k \neq m}}^{M} U_{\mathrm{S}k}(x\, t)[1 - U_{k\mathrm{D}}(y)] \qquad (6.23)
\end{aligned}$$

for $m = 1, \ldots, M$.

6.4.4 The P-o Scheme

This protocol is optimal in the sense that it minimizes the instantaneous CR duration, T, as follows. First, assume that only one relay R monitors, and cooperates with, the source. We show that in this case the optimal protocol is the same as P-3 proposed in Chapter 5. The time that relay R requires to decode the message is τ_{SR} (see (6.4)). If $\tau_{\mathrm{SR}} \geq \tau_{\mathrm{SD}}$, the destination decodes no later than relay R, and we have $T = \tau_{\mathrm{SD}}$. Otherwise, relay R can decode sooner, and provide the destination with encoding packets in the downlink until it decodes. Following steps similar to those leading to (6.11) and using the definition of $\Theta_{\cdot}(\cdot)$

given in (6.11) , we obtain

$$T = \tau_{\mathrm{SR}} + \Theta_{\mathrm{R}}(\tau_{\mathrm{SR}}) = \tau_{\mathrm{SR}} + \left(1 - \frac{\tau_{\mathrm{SR}}}{\tau_{\mathrm{SD}}}\right)\tau_{\mathrm{RD}} = \tau_{\mathrm{SR}} + \tau_{\mathrm{RD}} - \frac{\tau_{\mathrm{SR}}\,\tau_{\mathrm{RD}}}{\tau_{\mathrm{SD}}}. \tag{6.24}$$

Note that (6.24) is obtained given that $\tau_{\mathrm{SR}} < \tau_{\mathrm{SD}}$. Meanwhile, it can be shown that if $\tau_{\mathrm{RD}} \geq \tau_{\mathrm{SD}}$ in (6.24), then $T \geq \tau_{\mathrm{SD}}$ such that the system should not use the relay, as it can perform better without it. In summary, R cannot be or is not utilized if and only if $\max\{\tau_{\mathrm{SR}}, \tau_{\mathrm{RD}}\} \geq \tau_{\mathrm{SD}}$. Thus, the protocol obtained is the same as P-3.

Now, combining all the facts, we can propose P-o as a generalization of P-3 as follows. If in a CR for any m, $\max\{\tau_{\mathrm{S}m}, \tau_{m\mathrm{D}}\} \geq \tau_{\mathrm{SD}}$, no relay is used in that CR and DT is employed. Otherwise, at the beginning of the CR, Relay R_k, where

$$k = \underset{\substack{m\in\{1,\ldots,M\}\\ \max\{\tau_{\mathrm{S}m},\tau_{m\mathrm{D}}\}<\tau_{\mathrm{SD}}}}{\operatorname{argmin}} \quad \tau_{\mathrm{S}m} + \tau_{m\mathrm{D}} - \frac{\tau_{\mathrm{S}m}\,\tau_{m\mathrm{D}}}{\tau_{\mathrm{SD}}} \tag{6.25}$$

is signaled by the destination to be the only relay that monitors the source and decodes its message, and then transmits in the downlink. It can be verified that in P-o, we always have

$$T = \min_{m\in\{1,\ldots,M\}} \Bigg\{ \min\{\tau_{\mathrm{S}m}, \tau_{\mathrm{SD}}\} + \min\{\tau_{m\mathrm{D}}, \tau_{\mathrm{SD}}\} - \frac{\min\{\tau_{\mathrm{S}m}, \tau_{\mathrm{SD}}\}\,\min\{\tau_{m\mathrm{D}}, \tau_{\mathrm{SD}}\}}{\tau_{\mathrm{SD}}} \Bigg\}. \tag{6.26}$$

Compared to the other protocols, P-o needs global channel power gain information (only when $M > 1$, as explained in Section 6.4.5), and, the cooperating relay is chosen at the outset of the CR, rather than at the end of the uplink phase. Although the P-o performance analysis is mathematically solvable, we do not present the analytical results due to large computational complexity, and only provide simulation results as a comparison baseline in Section 6.5.

6.4.5 Single-Relay Case

In the important single-relay case (i.e. when $M = 1$), it can be verified that all the protocols P-n, P-γ, and P-t coincide with the optimal protocol, P-3 (i.e. P-o in the single-relay case), if their parameters are chosen to be $L = 1$, $\gamma_{\mathrm{th}} = \infty$, and $t_0 = 0$. Note that in P-n, L can only be 1 when $M = 1$.

The P-3 protocol was proposed in Chapter 5, but its long-term average behavior was not analytically investigated. As in P-1 and P-2 from Chapter 5 and P-n, P-γ, and P-t, no global channel information is required for the P-3 implementation.

It can be observed from (6.6) and (6.13) that the uplink and downlink times in P-3 are given as

$$T_{\mathrm{UL}} = \min\{\tau_{\mathrm{SD}}, \tau_{\mathrm{S1}}\} \tag{6.27}$$

and

$$T_{\mathrm{DL}} = \left(1 - \frac{\min\{\tau_{\mathrm{SD}}, \tau_{\mathrm{S1}}\}}{\tau_{\mathrm{SD}}}\right) \min\{\tau_{\mathrm{SD}}, \tau_{\mathrm{1D}}\}. \tag{6.28}$$

Also, $\mathrm{E}\{T_{\mathrm{S}}\}$ and $\mathrm{E}\{T_{\mathrm{R_1}}\}$ can be derived from (6.22) and (6.23) with $t_0 = 0$ as

$$\mathrm{E}\{T_{\mathrm{S}}\} = \int_0^{\infty} \mathrm{d}x \int_0^{x} \mathrm{d}t \; u_{\mathrm{SD}}(x) \left\{1 - U_{\mathrm{S1}}(t)\, U_{\mathrm{1D}}(x)\right\} \tag{6.29}$$

and

$$\mathrm{E}\{T_{\mathrm{R_1}}\} = \int_0^{\infty} \mathrm{d}x \int_0^{x} \mathrm{d}y \int_0^{1} \mathrm{d}t \; y\, u_{\mathrm{SD}}(x)\, u_{\mathrm{1D}}(y)\, U_{\mathrm{S1}}(x\, t). \tag{6.30}$$

6.4.6 Optimal Parameters

To obtain the optimal or near-optimal values of the P-n, P-γ, and P-t parameters that lead to the greatest R_{avg} or smallest $\mathrm{E}\{T\}$ (see (6.14)), we can exploit numerical integration and optimization of (6.18)–(6.23), or employ experimental optimization based on steepest descent or analytical optimization, as explained in the subsequent sections. While the experimental method obviates the need for global channel information, the numerical and analytical methods require that the channel gain statistics of all links be estimated at the destination, i.e. by acquiring SR channel gain information (note that SD and RD channel information is locally estimated at the destination).[3]

6.4.6.1 Experimental Steepest-Descent Optimization

An experimental steepest-descent method can be executed by starting at an appropriate initial value for the parameter and adding adaptively changing positive or negative increments until the best rate performance is obtained.[4] The destination evaluates the rate performance for any given value of the parameter, by averaging the realized rate over a limited number

[3]Such statistics can also be acquired at a central controller, which calculates the optimal value and feedbacks it to the destination.

[4]The symmetry of the problem suggests that R_{avg} in P-n, P-γ, and P-t is concave in L, γ_{th}, and t_0, respectively. No proof is provided here. The concavity assures that the optimal point obtained by the method of steepest descent is globally optimal as well. Note that standard convex optimization methods are not used in the experimental method, as all of them need access to global power gain information at the destination.

of CRs. Note that this method can be used only when the system has no more than one parameter to optimize, as is the case for the suboptimal protocols; the effort required increases exponentially with the number of parameters.

6.4.6.2 Analytical Optimization: Large SNR Approximations

Exact analytical derivation of the optimal parameters is in general mathematically intractable. Here, we develop large SNR approximations to the optimal values, which are also satisfactory for other SNR regimes. We consider Rayleigh fading where the SNRs are exponentially distributed. Assuming that all T, τ, and t variables are normalized by H/W, we obtain, from (6.4), the CDF of $\tau_{\rm sub}$, denoted $U_{\rm sub}(\cdot)$, as

$$U_{\rm sub}(t) = \mathrm{e}^{(1-\mathrm{e}^{1/t})/\mu_{\rm sub}} \tag{6.31}$$

where $\mu_{\rm sub}$ is the average value of $\gamma_{\rm sub}$. Recall that "sub" can be "SD", "th", "Sm", "mD", etc. When $\mu_{\rm sub}$ is large enough, $U_{\rm sub}(t)$ can be well approximated as

$$U_{\rm sub}(t) \approx \mathrm{H}(t - \epsilon_{\rm sub}) \tag{6.32}$$

where $\mathrm{H}(\cdot)$ is the Heaviside step function, and where $\epsilon_{\rm sub}$ is the point x at which $u_{\rm sub}(x)$, the PDF of $\gamma_{\rm sub}$, reaches its maximum. We obtain, from (6.31), that $\epsilon_{\rm sub}$ is the unique positive root of

$$\frac{\mathrm{e}^{1/x}}{2x+1} = \mu_{\rm sub} \tag{6.33}$$

which can be accurately obtained by the fixed point iteration $x_{n+1} = 1/\ln[\mu_{\rm sub}\,(2x_n+1)]$ for $n = 0, 1, \cdots$ and $x_0 = 1$, and $\mu_{\rm sub} > 0.6$. The approximation (6.32) shows that

$$u_{\rm sub}(x) \approx \delta(x - \epsilon_{\rm sub}) \tag{6.34}$$

for large SNR, where $\delta(\cdot)$ is the Dirac delta function.

Applying approximations (6.32) and (6.34) to (6.18)–(6.23), and after simplification, we obtain the following algorithm for calculating $L_{\rm opt}$, $\gamma_{\rm th,opt}$ or $\tau_{\rm th,opt}$ (see (6.4)), and $t_{0,\rm opt}$, the optimal values of the P-n, P-γ, and P-t parameters. Assume that $\epsilon_{\rm SD}$, $\epsilon_{{\rm S}m}$, and $\epsilon_{m\rm D}$ are obtained by solving (6.33) for $\mu_{\rm sub} = \mu_{\rm SD}$, $\mu_{{\rm S}m}$, $\mu_{m\rm D}$. Also, we sort $\epsilon_{{\rm S}m}$ in increasing order as $\epsilon_{{\rm S}(1)}, \ldots, \epsilon_{{\rm S}(M)}$, and represent the corresponding $\epsilon_{m\rm D}$'s (which are out of order in general) as $\epsilon_{(1)\rm D}, \ldots, \epsilon_{(M)\rm D}$. Now, if $\epsilon_{\rm SD} < \epsilon_{{\rm S}(1)}$, then $L_{\rm opt} = 1$, $\gamma_{\rm th,opt} = 0$, and $t_{0,\rm opt} = \epsilon_{\rm SD}/2$. However, if $\epsilon_{\rm SD} > \epsilon_{{\rm S}(1)}$, assume that K is the largest k for which

$\epsilon_{\mathrm{SD}} > \epsilon_{\mathrm{S}(k)}$. Obviously, K can range from 1 to M.

If $\epsilon_{\mathrm{SD}} < \min\{\epsilon_{(1)\mathrm{D}}, \ldots, \epsilon_{(K)\mathrm{D}}\}$, then again $L_{\mathrm{opt}} = 1$, $\gamma_{\mathrm{th,opt}} = 0$, and $t_{0,\mathrm{opt}} = \epsilon_{\mathrm{SD}}/2$. Otherwise, assume that N of $\epsilon_{(1)\mathrm{D}}, \ldots, \epsilon_{(K)\mathrm{D}}$ are less than ϵ_{SD}, and ordered as $\epsilon_{(i_1)\mathrm{D}} < \cdots < \epsilon_{(i_N)\mathrm{D}} < \epsilon_{\mathrm{SD}}$. Also, assume that the sequence $m_1, \ldots, m_P$ is recursively obtained from $i_1, \ldots, i_N$ as follows. We have $m_1 = i_1$, and for $\ell > 1$, if $m_{\ell-1} = i_j$ for some j, m_ℓ is the first term in the sequence $i_{j+1}, \ldots, i_N$ less than i_j. For example, if $i_1, \ldots, i_N = 4, 2, 6, 1, 3$ (i.e. $N = 5$), then $m_1, \ldots, m_P = 4, 2, 1$ (i.e. $P = 3$). Now, we have

$$L_{\mathrm{opt}} = \underset{L=m_1,\ldots,m_P}{\operatorname{argmin}} \epsilon_{\mathrm{S}(L)} + \left(1 - \frac{\epsilon_{\mathrm{S}(L)}}{\epsilon_{\mathrm{SD}}}\right)\epsilon_{(L)\mathrm{D}} \tag{6.35}$$

and, if c is such that $L_{\mathrm{opt}} = m_c$,

$$\tau_{\mathrm{th,opt}} = \frac{1}{2}\begin{cases}\epsilon_{(m_c)\mathrm{D}} + \epsilon_{(m_{c+1})\mathrm{D}}, & c < P \\ \epsilon_{(m_P)\mathrm{D}} + \epsilon_{\mathrm{SD}}, & c = P\end{cases} \tag{6.36}$$

and

$$t_{0,\mathrm{opt}} = \left(1 - \frac{\epsilon_{\mathrm{S}(m_c)}}{\epsilon_{\mathrm{SD}}}\right)\tau_{\mathrm{th,opt}}. \tag{6.37}$$

Figs. 6.1a and 6.1b show the exact and approximate values of $\gamma_{\mathrm{th,opt}}$ and $t_{0,\mathrm{opt}}$ for two relays and different average SR and RD SNRs. The exact values have been obtained by numerical optimization. As expected, and also suggested by both figures, the approximations for any single scenario become more accurate as the SD, SR, and RD SNRs increase. The approximate values in the case of P-γ differ from the exact values by about 1 dB to about 3 dB. In the case of P-t, the difference ranges from $0.007\,H/W$ to $0.062\,H/W$. Also, both the exact and approximate values of L_{opt}, the optimal P-n parameter, are always 1 for the scenarios in Fig. 6.1.

6.5 Numerical Examples

In this section, we assume for simplicity that all time variables, including the τ's and T's, are normalized by H/W. Also, we consider Gaussian-input, Rayleigh fading channels where the different SNRs are exponentially distributed and where (6.2) is used as the capacity function. Moreover, for ease of illustration, symmetric cases are considered where all SR SNRs are identically distributed, as are also all RD SNRs. We denote the average SD, SR, and RD SNRs by μ_{SD}, μ_{SR}, and μ_{RD}.

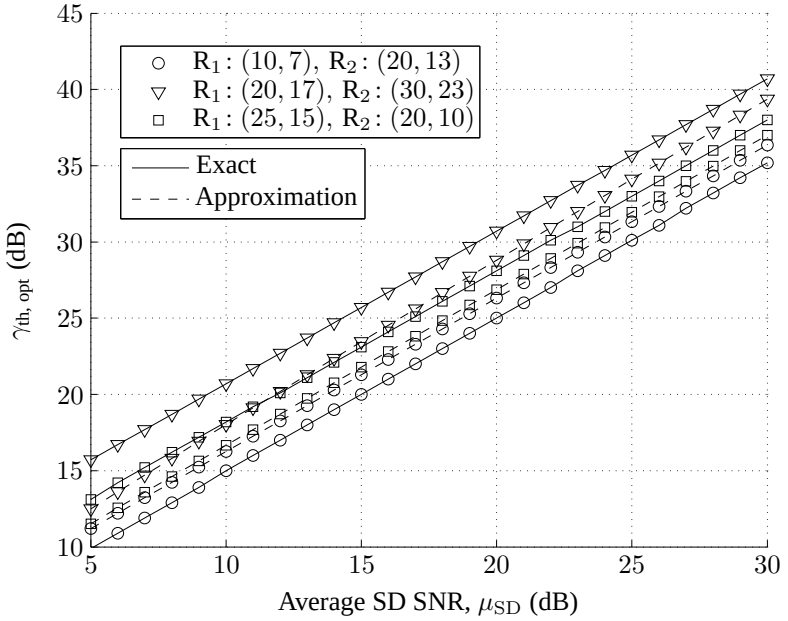

(a) The optimal value of γ_{th} versus μ_{SD}.

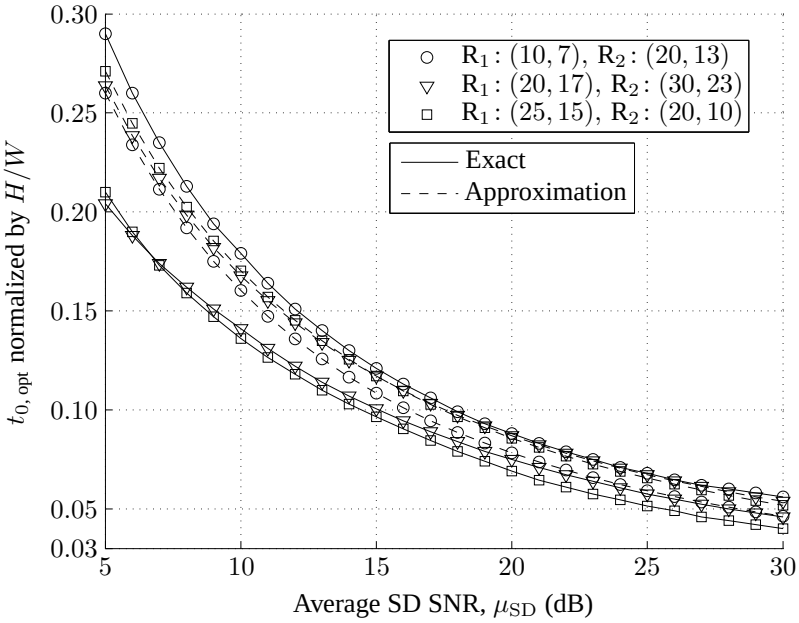

(b) The optimal value of t_0 versus μ_{SD}.

Fig. 6.1. The optimal parameters of P-γ and P-t versus the average SD SNR for $M = 2$. In the figure, "$\text{R}_m : (a, b)$" denotes that for Relay R_m, we have $(\mu_{\text{S}m}, \mu_{m\text{D}}) = \mu_{\text{SD}} + (a, b)$ dB.

In Section 6.5.1, the tradeoffs between the optimal parameters of the rate suboptimal schemes, obtained numerically, and the link qualities and number of relays are studied. In Section 6.5.2, the different optimal and suboptimal schemes are compared in terms of R_{avg} and the RSUR (see Section 6.4). The suboptimal schemes are considered to operate with

their optimal parameters.

6.5.1 Numerical Optimization of the Parameters

Figs. 6.2–6.7 show the optimal parameters of the suboptimal schemes for a wide range of scenarios. The optimal values in these figures have been obtained numerically using the analytical results (6.18)–(6.23), which are verified via simulation in Section 6.5.2.

Figs. 6.2 and 6.3 depict $L_{\rm opt}$, the optimal value of L, in a P-n scheme versus $\mu_{\rm SR}$ and $\mu_{\rm RD}$ and versus $\mu_{\rm SD}$ and M, respectively. Fig. 6.2 suggests that $L_{\rm opt}$ increases as $\mu_{\rm SR}$ increases and $\mu_{\rm RD}$ decreases. In fact, larger $\mu_{\rm SR}$ allows for increasing L without appreciably increasing the uplink time, while smaller $\mu_{\rm RD}$ warrants having a larger L to partially compensate for the poor RD links that may lengthen the downlink time.

Fig. 6.3 shows that for a given $\mu_{\rm SR}$ and $\mu_{\rm RD}$, $L_{\rm opt}$ decreases with $\mu_{\rm SD}$, but increases with M. The former is because the destination needs a smaller number of cooperative decoding relays when the SD link itself improves. In fact, a large L in the presence of a sufficiently large $\mu_{\rm SD}$ or small $\tau_{\rm SD}$ can almost block the use of relays. The latter (the increase with M) is natural as when M increases, the number of candidate relays increases, allowing the system to take advantage of more decoding relays for the downlink.

Figs. 6.4 and 6.5 show results for $\gamma_{\rm th,opt}$, the optimal value of $\gamma_{\rm th}$, in P-γ schemes. These figures show that $\gamma_{\rm th,opt}$ increases with an increase in M, $\mu_{\rm SD}$, $\mu_{\rm SR}$, or $\mu_{\rm RD}$. In fact, increasing M, $\mu_{\rm SR}$, or $\mu_{\rm RD}$ improves the quality of the downlink for a given $\gamma_{\rm th}$. In this case, the downlink time can be decreased further by toughening the qualification criterion, i.e. by increasing $\gamma_{\rm th}$. Also, $\gamma_{\rm th,opt}$ is an increasing function of $\mu_{\rm SD}$ because increasing $\mu_{\rm SD}$ while $\gamma_{\rm th}$ is fixed, makes it more likely that the source becomes AT, i.e. DT occurs. To avoid this and to better utilize relaying, one should increase $\gamma_{\rm th}$.

Fig. 6.4 shows that for a given $\mu_{\rm SD}$ and M, $\gamma_{\rm th,opt}$ can change broadly with, and is almost planar in, $\mu_{\rm SR}$ and $\mu_{\rm RD}$. In contrast, Fig. 6.5 suggests that for a given $\mu_{\rm SR}$ and $\mu_{\rm RD}$, $\gamma_{\rm th,opt}$ does not change as widely with $\mu_{\rm SD}$, particularly as M increases. Also, $\gamma_{\rm th,opt}$ exhibits a gentler increase with M at larger values of $\mu_{\rm SD}$.

Similarly, Figs. 6.6 and 6.7 depict the behavior of $t_{0,\rm opt}$, the optimal value of t_0, in P-t, with respect to $\mu_{\rm SR}$, $\mu_{\rm RD}$, $\mu_{\rm SD}$, and M. Recall that $t_{0,\rm opt}$ is considered normalized by H/W. These figures suggest that $t_{0,\rm opt}$ is a decreasing function of $\mu_{\rm SD}$, $\mu_{\rm SR}$, or $\mu_{\rm RD}$, but a decreasing or increasing function of M, which can be justified by the uplink-downlink

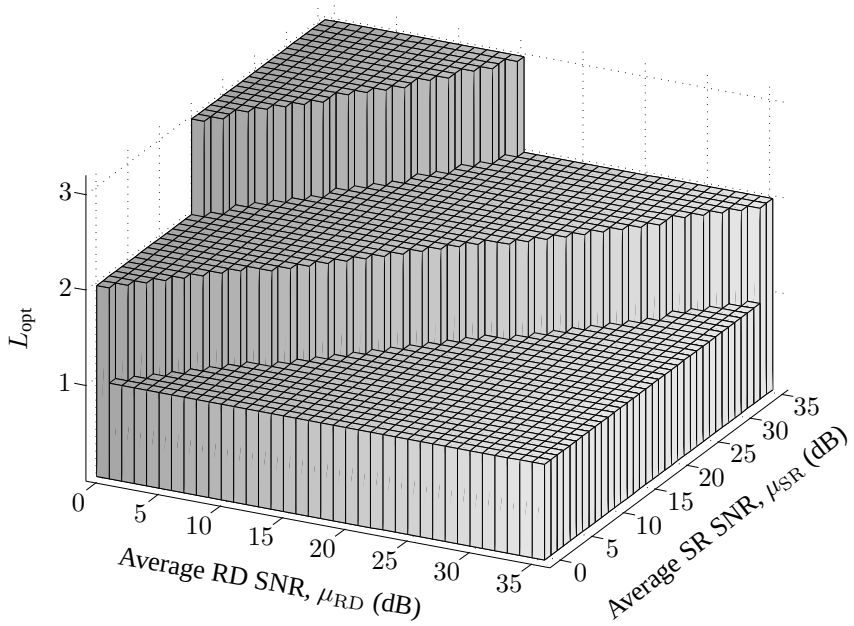

Fig. 6.2. The optimal parameter L in a P-n scheme versus the average SR and RD SNRs, when $M = 3$ and $\mu_{\text{SD}} = 7$ dB.

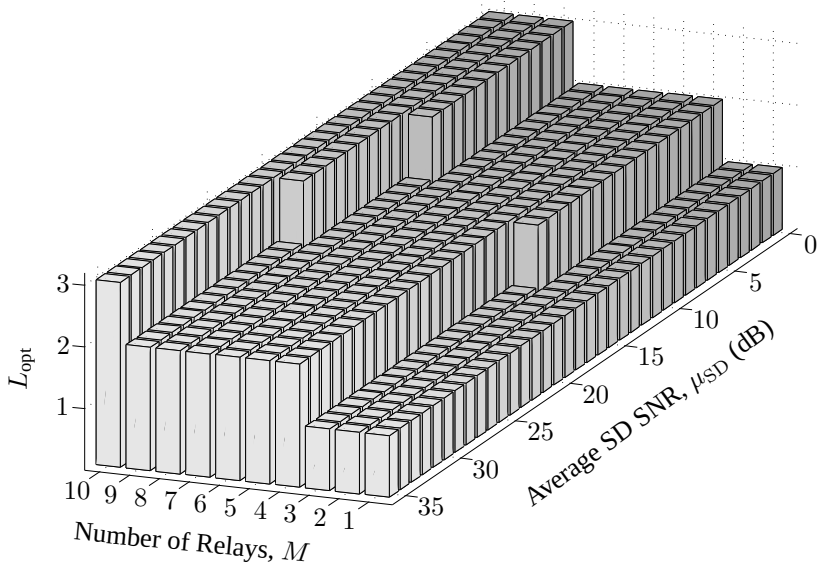

Fig. 6.3. The optimal parameter L in a P-n scheme versus the number of relays and average SD SNR, when $\mu_{\text{SR}} = \mu_{\text{RD}} = 20$ dB.

tradeoff when t_0 changes, as follows. Recall from Section 6.3 that the downlink time in P-t is bounded by t_0. Decreasing t_0 diminishes T_{DL} on average, but at the possible expense of increasing T_{UL}. This is because at a smaller t_0, more time on average is needed until a qualifying downlink node can be found, i.e. one with a RD link strong enough to help

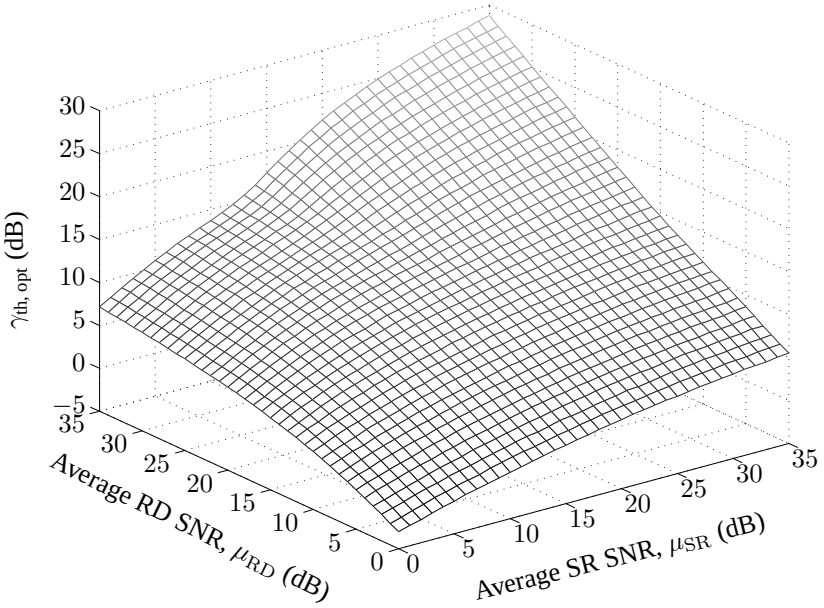

Fig. 6.4. The optimal parameter γ_{th} in a P-γ scheme versus the average SR and RD SNRs, when $M = 3$ and $\mu_{\text{SD}} = 7$ dB.

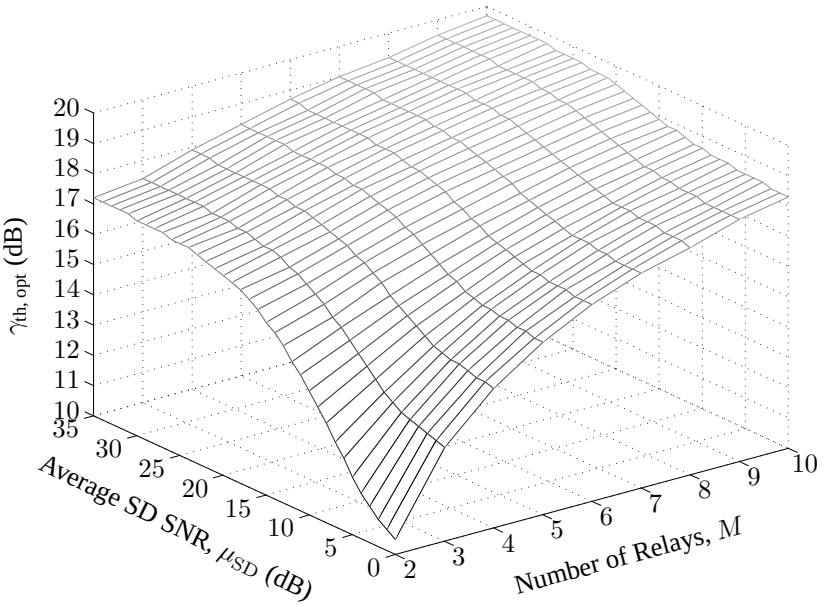

Fig. 6.5. The optimal parameter γ_{th} in a P-γ scheme versus the number of relays and average SD SNR, when $\mu_{\text{SR}} = \mu_{\text{RD}} = 20$ dB. The optimal γ_{th} is ∞ when $M = 1$.

the destination decode within time t_0. Increasing t_0 causes the opposite behavior to occur. Now, increasing the average system SNRs or M helps the qualifying downlink node emerge sooner on average, thus decreasing $\mathrm{E}\{T_{\text{UL}}\}$. However, it appears from the figures that it is only in the former case (increasing μ_{SD}, μ_{SR}, or μ_{RD}) that decreasing t_0 to some extent,

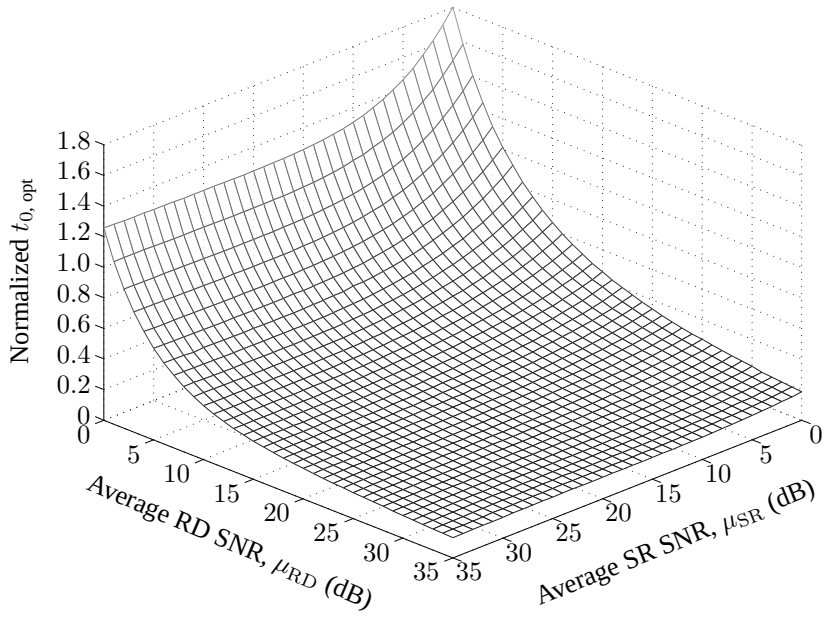

Fig. 6.6. The optimal parameter t_0, normalized by H/W, in a P-t scheme versus the average SR and RD SNRs, when $M = 3$ and $\mu_{\text{SD}} = 7$ dB.

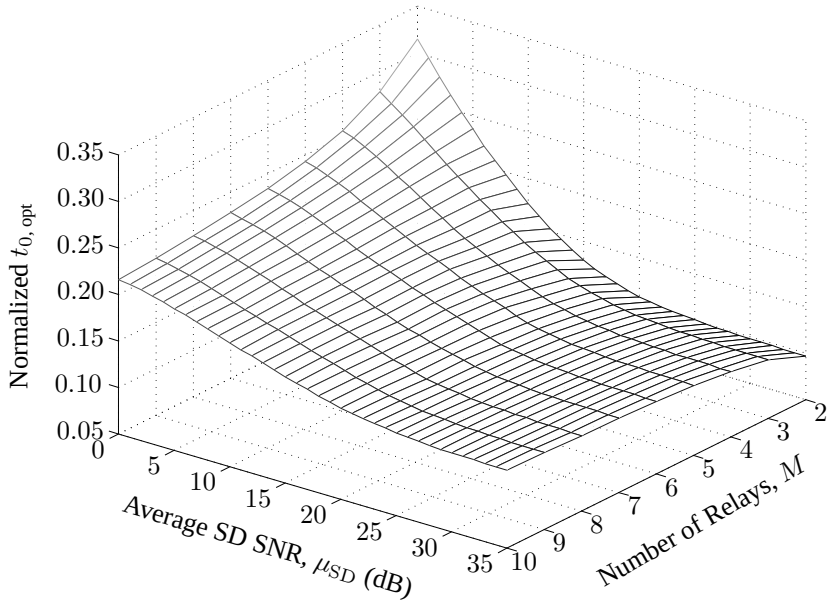

Fig. 6.7. The optimal parameter t_0, normalized by H/W, in a P-t scheme versus the number of relays and average SD SNR, when $\mu_{\text{SR}} = \mu_{\text{RD}} = 20$ dB. The optimal t_0 is 0 when $M = 1$.

which adds to $\mathrm{E}\{T_{\text{UL}}\}$ but takes from $\mathrm{E}\{T_{\text{DL}}\}$, can shrink the whole transmission time. In the latter case (increasing M) for some scenarios, the decrease of $\mathrm{E}\{T_{\text{UL}}\}$ is not great such that increasing t_0, which additionally reduces $\mathrm{E}\{T_{\text{UL}}\}$, can diminish the whole transmission time despite an increase in $\mathrm{E}\{T_{\text{DL}}\}$.

6.5.2 Performance Comparison

Figs. 6.8 and 6.9 show the R_{avg} and RSUR (see (6.14) and (6.16)) of the optimal and suboptimal schemes versus μ_{SD}, for $M = 1$ and $M = 5$, when there is a fixed difference in dB among μ_{SD}, μ_{SR}, and μ_{RD}. The DT average rate, obtained from (5.12), is also depicted as a baseline for performance comparison. Both analytical and simulation results are shown, except for DT where no simulation for (5.12) is required, and for P-o with $M = 5$ where only simulation results are available. In all cases, the simulation and analytical results are in good agreement. Recall that when $M = 1$, all the suboptimal protocols coincide with P-o when their parameters are chosen to be optimal (see Section 6.4.5).

It is observed from Fig. 6.8 that there is not much difference between the average rate performances of the schemes when $M = 5$, with P-t exhibiting a slightly inferior performance for larger values of μ_{SD}. In other words, P-n and P-γ perform near-optimally. The difference in performance between $M = 1$ and $M = 5$ is not significant and diminishes from around 1 bit to around 0.5 bits as the SD link improves. This suggests that adding more relays is not necessarily efficient in terms of the achievable rate. Note that in the single-relay case, the schemes outperform DT by an amount ranging from around 0.5 bits for small SNR values to a steady-state difference of around 1.34 bits for large SNR values.

Fig. 6.9 shows that the schemes are largely different in terms of the transmission burden imposed on relays, in contrast to Fig. 6.8 where the schemes are similar in the rate performance. Recall that the RSUR shows how much on average relays are used compared to the source. The optimal scheme, P-o, and the scheme P-n respectively make the least and most use of relays in transmission. Also, there is a peak in the RSUR for all the schemes. This peak can be explained by noting that all the systems utilize the relays less frequently if the SNR values are small or large enough. In a small SNR regime, relays are less likely to decode soon and to be used on a longer period. In a large SNR regime, the destination is more likely to decode soon, decreasing relay usage. Hence, the maximum relay usage occurs in a medium SNR regime.

Figs. 6.10 and 6.11 depict R_{avg} and the RSUR versus M for a fixed average SNR scenario. Again, simulation and analytical results are in excellent agreement. Fig. 6.10 shows that P-t and P-γ have the worst and best performances among the suboptimal schemes, respectively. Nevertheless, the difference in the rate performances of the schemes is not

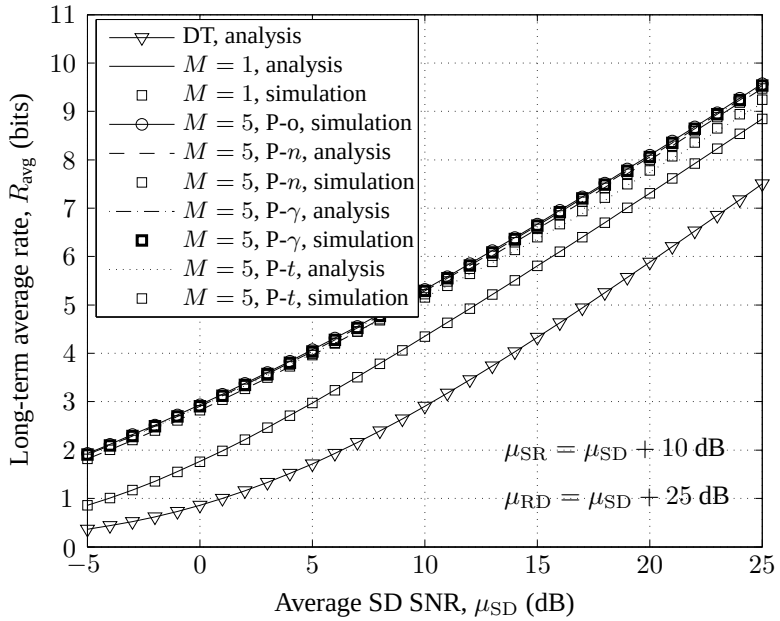

Fig. 6.8. The average transmission rate in bits versus the average SD SNR in dB, for $M = 1$ and $M = 5$ and the different optimal and suboptimal schemes.

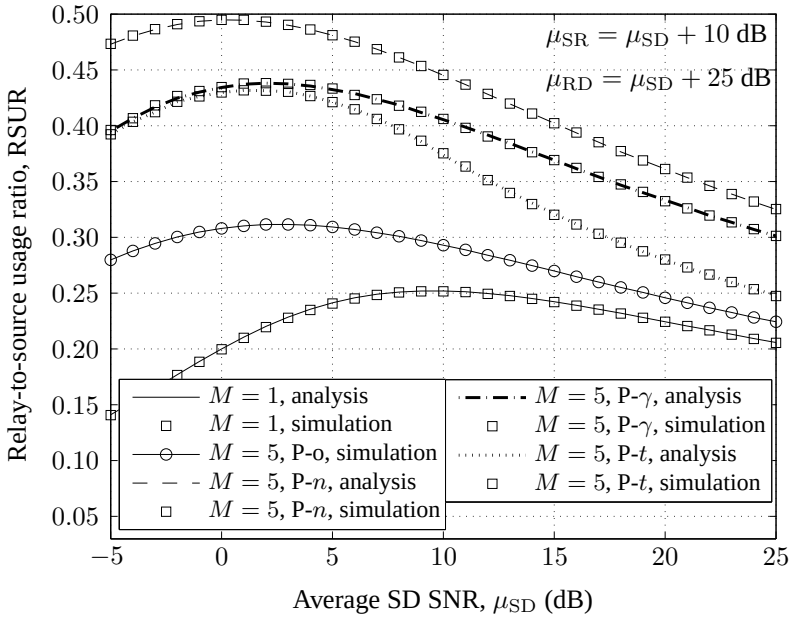

Fig. 6.9. The RSUR versus the average SD SNR in dB, for $M = 1$ and $M = 5$ and the different optimal and suboptimal schemes.

significant and does not exceed 0.25 bits. Also, this figure suggests that the schemes exhibit quickly diminishing returns as M increases. Note that in Fig. 6.10, the long-term average DT rate, obtainable from (5.12), is almost 2.91 bits (obviously independent of M), appreciably smaller than the rates achieved by the relaying schemes.

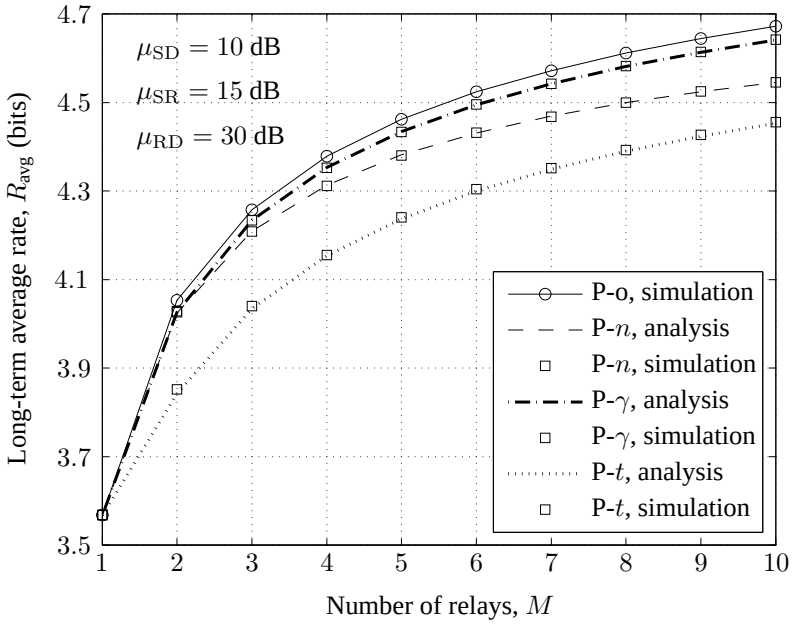

Fig. 6.10. The average transmission rate in bits versus the number of relays for the different optimal and suboptimal schemes.

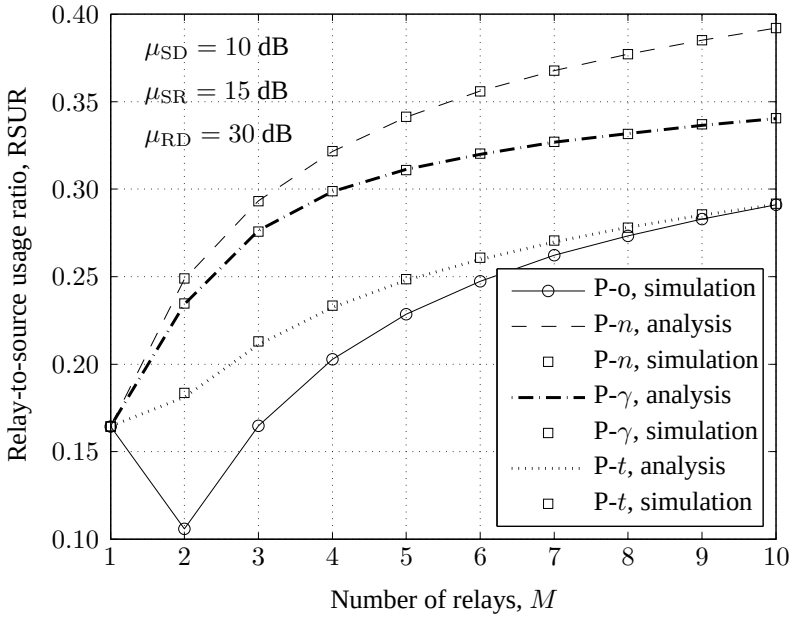

Fig. 6.11. The RSUR versus the number of relays for the different optimal and suboptimal schemes.

Fig. 6.11 indicates, much like Fig. 6.9, that the schemes largely differ in the RSUR performance, with P-o and P-n having the smallest and largest RSUR. Also, increasing the number of relays generally increases the chance that the relays are utilized, hence the increase in the RSUR with the number of relays. However, there is a seeming irregularity observed in the case of P-o when M increases from 1 to 2. This irregularity is explained

by the fact that adding more relays can also strengthen the average quality of the RD links. Then, a stronger relay may help the destination decode more quickly, reducing the amount of the time that the relay is employed. This effect appears to be dominant in P-o when raising M from 1 to 2, leading to a reduction in the RSUR.

6.6 Design and Performance Implications

The rate suboptimal selection protocols proposed are natural selection strategies for dual-hop relaying based on rateless coding. In fact, the optimal downlink strategy for rateless dual-hop relaying based on reactive selection (i.e. when the cooperative relay is selected *after* the source broadcasting) is rather clear, and is the same for all the proposed schemes as mentioned in Section 6.3.1. It is the uplink stopping criteria that differentiate these schemes.

There can be many other alternatives, not necessarily as efficient and simple as the schemes proposed. For example, it is generally possible for rateless selection techniques that the expected transmission time of a message approaches infinity in Rayleigh fading. The protocols proposed avoid this problem. Also, although suboptimal selection techniques may involve the use of multiple parameters, each of the protocols proposed here is characterized by a single parameter, yet exhibiting near-optimal rate performances. Additionally, the system complexity is independent of the system parameter.[5]

The protocols have low complexity also in terms of feedback. The only feedbacks required are limited to those from the decoding relays to the destination for declaring successful decoding, and the two feedbacks broadcast by the destination, a message of $\log_2(M+1)$ bits to indicate which node shall transmit next, and a one-bit message to declare successful decoding.

It is not obvious which one of the P-n, P-γ, and P-t protocols is worse or better in terms of the average rate. However, the numerical results in Section 6.5 suggest that P-γ is always the best, and that the P-n rate is larger than the P-t rate; the differences are small though.

[5]However, a restriction is that the destination should be able to find or estimate the optimal or near-optimal values of the parameters, as examined in Section 6.4.6.

Chapter 7

Conclusions and Future Research Directions

In this chapter, first we present a summary of the contributions in the thesis and the conclusions obtained. Then, we proceed to suggest avenues and directions for future research.

7.1 Conclusions

The thesis essentially focused on the performance evaluation and comparison in fixed-rate and rateless coded dual-hop relaying networks, and on creating new concepts and protocols for these networks.

We commenced by analyzing a three-node (the simplest) relay channel in Chapter 2 with static links and basic AF and DF operations. The exact OPA ratio for maximizing the end-to-end SNR in the AF case, and the MRC and ML detection rules and BERs in the DF case were derived. The cause of the error floor in the performance of DF relaying was shown to be suboptimal MRC detection at the destination. Power optimization between the source and relay, and successful decoding at the relay were shown to be required to assure the superiority of DF relaying over AF relaying. The best relaying strategy and OPA ratio was determined under a total power constraint assuming that the transmission options are DT, AF relaying, and DF relaying. Additionally, the maximum CG was derived for each case. It was found that the CG has an inverse relationship with the quality of the SD link, but a direct relationship with the qualities of SR and RD links. Furthermore, while stronger SR links favor DF relaying, AF relaying yields larger CG as compared to DF relaying for

stronger SD and RD links. The value CG can be used as a criterion for relay selection among a set of candidate relays.

In Chapter 3, a multirelay, dual-hop AF relaying network was considered. Three common AF schemes include superimposed, selection, and orthogonal AF relaying, out of which we only considered superimposed and selection relaying. In fact, orthogonal AF relaying has been well investigated in the literature, and shown to be inferior to selection AF relaying. We viewed selection AF relaying as a special power allocation scheme for superimposed AF relaying, in which the whole relaying power is given to a single relay in every CR. This relay is selected such that it maximizes the largest instantaneous equivalent SNR from the source to the destination, or minimizes the outage probability at any rate.

The problem of OPA in superimposed AF relaying under an aggregate relay power was formulated as a nonconcave fractional global optimization program, which generally lacks a closed-form solution. The selection power allocation scheme can be optimal or suboptimal for superimposed relaying, depending on the instantaneous link coefficients. A necessary condition for the selection AF optimality in terms of the instantaneous link coefficients was derived. It was shown that the selection AF power allocation is asymptotically strictly suboptimal in the sense that the selection AF outage optimality approaches zero exponentially as the number of relays increases. This result was obtained independently of the individual link fading model provided only that different links suffer independent fading and that the phase distortion is uniformly distributed. For example, the selection AF suboptimality is almost certain for more than 11 available relays. It was also observed that the selection AF protocol deviates noticeably more from optimality as the fading moderates.

A closed-form, suboptimal relay power allocation solution was also developed for superimposed AF relaying, which performs almost as well as the optimal scheme for different numbers of relays. The proposed suboptimal scheme does not contend with indefinite search and convergence issues, which generally arise in global optimization algorithms. However, while the selection AF protocol can be implemented in centralized [48] or distributed [107] manners with comparable advantages and drawbacks, the proposed suboptimal scheme is only amenable to centralized implementation in which the destination needs to calculate the power allocation ratios and feeds them back to the relays. Nonetheless, the complexity requirements of the proposed scheme can be shown not to exceed those needed for a centralized selection AF scheme.

In Chapter 4, we considered multirelay, dual-hop DF relaying networks with three common, fixed-rate DF relaying operations, called superimposed, selection, and orthogonal DF relaying, each with PCC or RC. The PCC and RC techniques are two extreme cooperation methods, allowing to study the limiting behavior of the relaying systems. We discussed the complexity issues related to CSI acquisition, feedback, and overhead, in the different protocols. Next, the maximum instantaneous achievable rates of the schemes were determined. A general methodology to derive the rate-adaptive, power-nonadaptive average capacity of the schemes via the calculation of their outage probabilities was presented, and the outage probabilities were derived for a general fading model. The results were specialized to Rayleigh fading, and the outage probabilities and average capacities of all the schemes in the different cases of asymmetric and symmetric links, each with and without the effect of the SD link, were calculated. All the results were exact, except for orthogonal relaying with PCC, where only lower and upper bounds were derived. It was observed that the lower bound on the outage probability and the upper bound on the average capacity are very tight, but the other two bounds are not. The analytical results obtained were verified for two asymmetric and symmetric scenarios by Monte Carlo simulation. Full diversity in the size of the network was observed from the outage probability graphs for all the schemes. Also, the PCC over RC gain was observed to be about $2 \sim 4$ dB for the outage probabilities and $8 \sim 8.5$ dB for the average capacities, for the different relaying systems.

The outage and capacity performances of the schemes were compared to each other and to those of DT by two numerical examples. In one example, we considered a symmetric case with a linear network topology and a simplified path loss model, and showed the performances versus the normalized distance of the relays from the source. It was observed that superimposed relaying has the best and orthogonal relaying has the worst performance for the same cooperation strategy (PCC or RC), and that all the relaying schemes, except for orthogonal relaying in some cases, outperform DT significantly. Also, the schemes benefit from the best performance for an optimal distance of the relays from the source. This optimal distance is different for the different schemes.

In another example, the changes in the outage and capacity performances with an increase in the number of relays were studied for a symmetric case. It was observed that the outage performance of orthogonal relaying improve up to 3 relays, and then deteriorate. Also, the capacity performance of orthogonal relaying deteriorates with the number

of relays, and become worse than the DT performance for more than 3 or 4 relays. The deteriorations are generally attributed to orthogonalization loss. The performances of the other relaying schemes improve with an increase in the number of relays. The improvement rate is continuous and almost constant for the outage performance, but exhibits diminishing returns for the capacity performance. Also, the improvement rate is larger for superimposed relaying than selection relaying for the outage performance, but is similar for superimposed and selection relaying for the capacity performance.

Chapters 5 and 6 were devoted to examining rateless coded dual-hop relaying networks. Rateless codes are an excellent match for DF relaying schemes, making possible less complex, more energy efficient implementation of collaborative systems. In Chapter 5, single-relay systems were considered and the performances of three rateless coded DF schemes, called P-1, P-2, and P-3, were investigated. The P-1 and P-2 schemes were taken from previous research, whereas P-3 was proposed here. It was built upon P-1 and P-2 and opportunistic communication, aiming at larger energy efficiency and less complexity compared to P-1 and P-2. The salient implementation and complexity features of the protocols were also addressed.

The maximum achievable rate and minimum energy per symbol and per bit of the protocols were derived under two power constraints, called the PPC and APC. The PPC is suitable for energy unconstrained scenarios, while the APC was considered to draw a fair comparison of the protocols on a power basis. In fact, it was observed that the relaying systems consume different amounts of energy and achieve different rates in different CRs, making it almost impossible to compare their energy efficiency directly based on their achievable rates in a PPC regime. More specifically, P-1, P-2, and P-3 rank second, first, and third either in order of achieving larger rates or in order of expending more energy per symbol. This means, inter alia, that larger rates may be the result of more energy expenditure. Indeed, this is a general issue in analyzing rateless coded systems. In Chapter 5, two methods were proposed and investigated for comparing the protocols fairly in terms of power, the minimum energy per bit under the PPC and the maximum rate under the APC.

To characterize and study the long-term behavior of the protocols, we considered the long-term average rate and energy per bit, and also introduced the RSUR which indicates how much the relay is utilized compared to the source in the long term. We derived general expressions for these quantities, and utilized the results obtained to compare the protocols

in several numerical examples. The numerical results attested the superiority of P-3 over the other schemes in energy efficiency in most cases. Also, the optimal position of the relay in P-3 leading to the largest rate or energy efficiency was almost the midpoint between the source and destination for a linear network topology. The corresponding position in P-1 and P-2 was closer to the source, around the midpoint, or closer to the destination, depending on the desired figure of merit.

Regarding the relay usage, it was observed that in all schemes the RSUR decreases as the SD link improves or the SR link deteriorates, as expected. Also, P-1 realizes the least use of relaying, while P-3 in almost all cases is the most relay utilizing protocol. Therefore, P-3 may not be attractive in the situations where it is not desirable, due to energy considerations, that a significant portion of the entire transmission burden in the system be placed on the relay. It was also observed that the rate maximizing version of P-2 uses the relay appreciably more compared to the EB minimizing version of P-2.

Overall, we observe that the P-3 protocol proposed is a promising, easy-to-implement, and energy efficient relaying strategy for rateless coded, single-relay networks. Although it is inferior to P-1 and P-2 in energy unconstrained regimes, and slightly inferior to P-2 in certain energy constrained scenarios, P-3 can be most appealing owing to its lowest complexity and implementation costs. It can also be extended with minimum complexity to the case of multiple parallel relays, as executed in Chapter 6.

In Chapter 6, three protocols, denoted P-n, P-γ, and P-t, based on rateless coding and selection cooperation for multirelay, dual-hop relaying networks were introduced. Each protocol has only one design parameter and does not rely on global channel gain information at any node. The protocols are distinguished via their uplink stopping criteria, but are essentially the same in the downlink phase, where the uplink and downlink respectively refer to the source broadcasting, and relaying transmission phases. The design of the protocols focuses on simplicity and avoidance of unbounded average transmission time for block Rayleigh fading. All the protocols in the single-relay case, if used with their optimal parameters, convert to the P-3 scheme introduced in Chapter 5.

An analysis of the long-term average rate and RSUR of the protocols was presented. The protocols are not generally rate optimal, but become rate optimal in the single-relay case ($M = 1$) with their parameters optimally chosen, i.e. when they become equivalent to P-3. The optimal values of the parameters were trivially determined for $M = 1$, and

numerically investigated for $M > 1$ for different average SNR scenarios and a Rayleigh fading environment. A large SNR approximation to the optimal parameters for $M > 1$ was also obtained, which is satisfactory for a wide range of SNR values. A comparison of the average rates achieved by DT and the proposed protocols showed that the proposed schemes are capable of outperforming DT significantly.

As in Chapter 5, we used the RSUR to study how energy consuming the relays are, compared to the source, in the different protocols. The average rate and RSUR performances were compared against those of the rate optimal protocol, P-o. It was observed that all the suboptimal protocols, especially P-γ, exhibit near-optimal rate performances if their parameters are optimized. However, they exhibit diverse RSUR performances, with P-n making the most, and P-o making the least, use of relay energy. Also, the systems utilize more relay energy when the average SNRs are middle ranged.

7.2 Possibilities for Future Research

In the following, several directions for future research are suggested, including multisource cooperation, small and large SNR characterization of the behavior of relaying networks, opportunistic rateless coded relaying, comparison between fixed-rate and rateless coded cooperation, optimal power allocation, and protocol design and an analysis of the capacity and resource allocation for rateless coded multihop relaying networks.

7.2.1 Multisource Cooperation

In the multirelay systems investigated in the thesis, several relays, not having or transmitting messages of their own, assist a source to communicate its messages. In practice, there are situations where a group of independent sources cooperate to send their data to their respective destinations. We refer to this type of cooperation, where more than one node have independent messages to send, as *multisource cooperation*.

One possible direction for research is to explore multisource versions of the protocols examined in Chapters 3, 4, and 6. For example, consider a scenario in which N nodes, $\mathrm{S}_0, \ldots, \mathrm{S}_{N-1}$, cooperate to pass their messages. Such a scenario can happen in a clustered sensor network, where each cluster of sensors has a cluster head that receives data from any other sensor in the cluster. Assume that the transmitting nodes have orthogonal

channels facilitating half-duplex operation, and that in a CR, S_n monitors, and is monitored by, exactly J other nodes, for $n = 0, \cdots, N-1$, where J is a design parameter. Such a partner assignment policy is viable in different ways. For example, let π be an arbitrary permutation of $\{0, \cdots, N-1\}$. It can be shown that if for any n, S_n monitors $\mathrm{S}_{\pi(\mathrm{mod}(\pi^{-1}(n)+1,N))}$, $\ldots$, $\mathrm{S}_{\pi(\mathrm{mod}(\pi^{-1}(n)+J,N))}$, where $\mathrm{mod}(\cdot,\cdot)$ is the modulus operator, then for any n, S_n is monitored by $\mathrm{S}_{\pi(\mathrm{mod}(\pi^{-1}(n)-1,N))}$, $\ldots$, $\mathrm{S}_{\pi(\mathrm{mod}(\pi^{-1}(n)-J,N))}$. Also, assume that each node transmits its own data with power $(1-\alpha)P$, and if selected to assist any other node, transmits the data of the other node with power $\alpha P/J$, where P is the maximum sustainable power of any node, and where α is a design parameter representing the level of cooperation. Altogether, the analysis of the whole system is decomposed into the analyses of N *independent* models of the type depicted in Fig. 4.1, where the power of Node S is $(1-\alpha)P$, but the power of each relay is $\alpha P/J$.

It is interesting to determine optimal or near-optimal values of J and α for optimizing different rate or energy performances in the setup just described. Note that as J is increased, the number of cooperative relays for a node increases, but the relay power diminishes. A similar tradeoff exists for α. When α is decreased, the source power increases, but the relay power decreases.

7.2.2 Small and Large SNR Characterization

The limiting behavior of relaying systems in terms of small or large values of SNR is worth analyzing for two main reasons. First, such an analysis usually leads to simpler, tractable, and closed-form results which give insight on how the system generally operates. Second, there are many practical scenarios that fit into small or large SNR regimes. A large body of research on the diversity order and diversity-multiplexing tradeoff in relaying networks is an example of such studies on limiting behaviors.

It is suggested that research is made to characterize the long-term average rate of the fixed-rate and rateless coded networks of Chapters 4 and 6 in small and large SNR regimes. If the capacity can roughly be written as $m\log(p\,\mathrm{SNR}+1)$ or $m\log(p\,\mathrm{SNR})$ for small or large SNR scenarios, respectively, then m and p can be respectively regarded as the multiplexing order and coding power gain of the system.

7.2.3 Opportunistic Rateless Coded Relaying

Recent research has proposed selecting the best available relay among a set of candidates *proactively*, i.e. before cooperation takes place. This scheme, referred to as opportunistic relaying [107], [109], contrasts with *reactive* selection, where the cooperative relay is determined after a source broadcasting phase. Opportunistic relaying has benefits over and above reactive selection relaying, such as saving processing energy at the relays and minimizing overhead information for CSI acquisition [107], [109]. In dual-hop opportunistic relaying, the merit of a relay is assessed by a metric which is only a function of the instantaneous local SNRs at the relay, γ_{SR} and γ_{RD}. For example, $\min\{\gamma_{\mathrm{SR}}, \gamma_{\mathrm{RD}}\}$ is a metric proposed for fixed-rate DF relaying networks.

Opportunistic relaying has been only utilized and investigated for fixed-rate relaying schemes to date, where outage is the major concern. We suggest to apply this type of relaying to fountain-based dual-hop relaying networks. In fact, retaining its benefits, opportunistic relaying can be easily integrated with rateless coded relaying systems. Then, the long-term average rate and RSUR performances of opportunistic rateless coded relaying can be evaluated, and compared to those of the schemes proposed in Chapter 6. Also, an interesting research problem arises here that what metric function is more appropriate for rateless coded relaying.

7.2.4 Comparing Fixed-Rate and Rateless Coded Relaying Networks

The focus of attention in the realms of cooperative communication has been devoted mostly to the system design and performance analysis of fixed-rate or rateless schemes to date, without any comparison made between these schemes. As explained earlier, rateless coded schemes provide great potential for relaying systems and avoid some drawbacks of fixed-rate schemes [105]. Therefore, it is informative and insightful to draw a fair comparison between the achievable rates in fixed-rate and rateless relaying systems, and to quantify the energy efficiencies of these systems.

To draw the comparisons, we propose to use the *throughput* and RSUR as suitable performance measures, where the throughput, in the case of fixed-rate systems, can refer to the average capacity considered in Chapter 4, or to the rate r for which r multiplied by the nonoutage probability at rate r is maximized. In rateless systems, the throughput is taken

to equal the long-term average rate, as used in Chapters 5 and 6.

We also need two general commensurate fixed-rate and rateless relaying schemes to compare their achievable expected throughputs. To retain both generality and simplicity and to achieve large energy efficiency, we consider any of the schemes proposed in Chapter 6 as the rateless scheme required. The fixed-rate relaying system selected for comparison should be commensurate with the rateless scheme in terms of bandwidth and energy expenditure, as well as complexity. A novel fixed-rate scheme, called fixed-rate coded selection cooperation (FISC), is proposed for this purpose, which is essentially taken from the coded cooperation scheme of [16], but avoids some of its drawbacks in multiuser cases. The FISC protocol from fixed-rate systems has a duality relationship with the rateless protocols from Chapter 6. Next, we introduce the FISC protocol.

Consider the multirelay system in Fig. 4. All nodes transmit with the same power and on the same frequency band. Node S splits its codeword of length N symbols to two parts; the first is a codeword of length $N_1 = (1-\beta)N$ which can be decoded on its own, and the second contains parities and is of length $N_2 = \beta N$ symbols. The parameter β represents the level of cooperation [16], and we have $0 \leq \beta < 1$. Node S broadcasts the first part of its codeword in the first phase. The relays monitor Node S's transmissions and attempt to decode its message. At the end of the first phase, each decoding relay declares its decoding success to Node D via feedback. Subsequently, Node D signals Node $\mathrm{argmax}_{\mathrm{X}\in\{\mathrm{S}\}\cup\mathcal{D}}\{\gamma_{\mathrm{XD}}\}$ to be the transmitter of the N_2-symbol part of the codeword in the second phase, where $\mathcal{D}$ denotes the set of the decoding relays and where γ_{XD} is the SNR associated with the link from Node X to Node D. The multisource version of FISC can also be obtained via the same technique introduced in Section 7.2.1. It can be shown that FISC avoids the DSTC or MUD needed in the multiuser coded cooperation of [17], [42], and has a tractable outage analysis.

7.2.5 Optimal Power Allocation

The use of optimal or near-optimal power allocation, instead of equal power allocation, has been shown to significantly improve the performance of cooperative systems, especially when the number of nodes in the system and/or imbalances between the strengths of the different links increase. However, one major challenge is to find low complexity centralized or distributed solutions that do not entail much signaling overhead or a heavy use of feedback,

and that do not cause intolerable delays. The investigation in Chapter 2 considered power allocation in multirelay, dual-hop AF relaying networks, and led to a near-optimal solution. Similar studies can be performed for the DF relaying networks considered in Chapters 4–6.

7.2.6 Rateless Coded Multihop Relaying Networks

Multihop relaying networks become important when it is needed to inexpensively extend the coverage area or nodes' battery lives. Although much progress has been made in the performance evaluation and protocol design of fixed-rate coded multihop networks to date, rateless coded multihop networks remain to be sufficiently explored. The rateless coded multihop protocol, proposed in [22] based on asynchronous transmissions from the decoding relays, and the low complexity routing algorithms introduced in [110] for rateless coded multirelay networks, are examples of research in this area.

As a future research direction, the possibility of extending the rateless coded schemes of Chapter 6 to the multihop case can be examined. Also, in a multirelay network, assuming that a multihop route has been found (e.g. by the methods proposed in [110]) from the source to the destination, one interesting research problem is to find the maximum long-term average rate between the source and destination, given that the power, time, and bandwidth allocated to each relay in the route are known. Importantly, note that when a relay is forwarding information, the preceding relays are allowed to receive and pass new data from the source. Another similar problem is to find optimal resource allocation for the relays in a given route such that the achievable long-term average rate using the route is maximized.

References

[1] E. C. van der Meulen, "Three-terminal communication channels," *Adv. Appl. Prob.*, vol. 3, pp. 120–154, 1971.

[2] E. C. van der Meulen, "A survey of multi-way channels in information theory: 1961–1976," *IEEE Trans. Inf. Theory*, vol. 23, no. 1, pp. 1–37, Jan. 1977.

[3] T. M. Cover and A. A. El Gamal, "Capacity theorems for the relay channel," *IEEE Trans. Inf. Theory*, vol. 25, no. 5, pp. 572–584, Sep. 1979.

[4] G. Kramer, M. Gastpar, and P. Gupta, "Cooperative strategies and capacity theorems for relay networks," *IEEE Trans. Inf. Theory*, vol. 51, no. 9, pp. 3037–3063, Sep. 2005.

[5] A. Høst-Madsen and J. Zhang, "Capacity bounds and power allocation for wireless relay channels," *IEEE Trans. Inf. Theory*, vol. 51, no. 6, pp. 2020–2040, Jun. 2005.

[6] A. Sendonaris, E. Erkip, and B. Aazhang, "User cooperation diversity—part I: System description," *IEEE Trans. Commun.*, vol. 51, no. 11, pp. 1927–1938, Nov. 2003.

[7] A. Sendonaris, E. Erkip, and B. Aazhang, "User cooperation diversity—part II: Implementation aspects and performance analysis," *IEEE Trans. Commun.*, vol. 51, no. 11, pp. 1939–1948, Nov. 2003.

[8] F. M. J. Willems, E. C. van der Meulen, and J. P. M. Schalkwijk, "An achievable rate region for the multiple access channel with generalized feedback," in *Proc. Allerton Conf. Commun., Contr., Comput.*, Monticello, IL, Oct. 5–7, 1983, pp. 284–292.

[9] J. N. Laneman and G. W. Wornell, "Distributed space-time-coded protocols for exploiting cooperative diversity in wireless networks," *IEEE Trans. Inf. Theory*, vol. 49, no. 10, pp. 2415–2425, Oct. 2003.

[10] J. N. Laneman, D. N. C. Tse, and G. W. Wornell, "Cooperative diversity in wireless networks: Efficient protocols and outage behavior," *IEEE Trans. Inf. Theory*, vol. 50, no. 12, pp. 3062–3080, Dec. 2004.

[11] R. U. Nabar, H. Bölcskei, and F. W. Kneubühler, "Fading relay channels: Performance limits and space-time signal design," *IEEE J. Sel. Areas Commun.*, vol. 22, no. 6, pp. 1099–1109, Aug. 2004.

[12] A. Stefanov and E. Erkip, "Cooperative space-time coding for wireless networks," *IEEE Trans. Commun.*, vol. 53, no. 11, pp. 1804–1809, Nov. 2005.

[13] P. A. Anghel and M. Kaveh, "On the performance of distributed space-time coding systems with one and two non-regenerative relays," *IEEE Trans. Wireless Commun.*, vol. 5, no. 3, pp. 682–692, Mar. 2006.

[14] Y. Jing and B. Hassibi, "Distributed space-time coding in wireless relay networks," *IEEE Trans. Wireless Commun.*, vol. 5, no. 12, pp. 3524–3536, Dec. 2006.

[15] K. Azarian, H. El Gamal, and P. Schniter, "On the achievable diversity-multiplexing tradeoff in half-duplex cooperative channels," *IEEE Trans. Inf. Theory*, vol. 51, no. 12, pp. 4152–4172, Dec. 2005.

[16] T. E. Hunter and A. Nosratinia, "Diversity through coded cooperation," *IEEE Trans. Wireless Commun.*, vol. 5, no. 2, pp. 283–289, Feb. 2006.

[17] T. E. Hunter, S. Sanayei, and A. Nosratinia, "Outage analysis of coded cooperation," *IEEE Trans. Inf. Theory*, vol. 52, no. 2, pp. 375–391, Feb. 2006.

[18] M. Janani, A. Hedayat, T. E. Hunter, and A. Nosratinia, "Coded cooperation in wireless communications: Space-time transmission and iterative decoding," *IEEE Trans. Signal Process.*, vol. 52, no. 2, pp. 362–371, Feb. 2004.

[19] A. Stefanov and E. Erkip, "Cooperative coding for wireless networks," *IEEE Trans. Commun.*, vol. 52, no. 9, pp. 1470–1476, Sep. 2004.

[20] P. Razaghi and W. Yu, "Parity forwarding for multiple-relay networks," *IEEE Trans. Inf. Theory*, vol. 55, no. 1, pp. 158–173, Jan. 2009.

[21] J. Castura and Y. Mao, "Rateless coding for wireless relay channels," *IEEE Trans. Wireless Commun.*, vol. 6, no. 5, pp. 1638–1642, May 2007.

[22] A. F. Molisch, N. B. Mehta, J. S. Yedidia, and J. Zhang, "Performance of fountain codes in collaborative relay networks," *IEEE Trans. Wireless Commun.*, vol. 6, no. 11, pp. 4108–4119, Nov. 2007.

[23] A. Chakrabarti, A. Sabharwal, and B. Aazhang, "Cooperative communications: Fundamental limits and practical implementation," in *Cooperation in Wireless Networks: Principles and Applications*, F. H. P. Fitzek and M. D. Katz, Eds. Springer, 2006, ch. 2, pp. 29–68.

[24] J. N. Laneman and G. W. Wornell, "Energy-efficient antenna sharing and relaying for wireless networks," in *Proc. IEEE Wireless Commun. Netw. Conf. (WCNC)*, vol. 1, Chicago, IL, Sep. 23–28, 2000, pp. 7–12.

[25] J. N. Laneman and G. W. Wornell, "Exploiting distributed spatial diversity in wireless networks," in *Proc. Allerton Conf. Commun., Contr., Comput.*, Monticello, IL, Oct. 3–6, 2000, pp. 1–10.

[26] B. Zhao and M. C. Valenti, "Some new adaptive protocols for the wireless relay channel," in *Proc. Allerton Conf. Commun., Contr., Comput.*, vol. 41, part 3, Monticello, IL, Oct. 1–3, 2003, pp. 1588–1589.

[27] J. Boyer, D. D. Falconer, and H. Yanikomeroglu, "Multihop diversity in wireless relaying channels," *IEEE Trans. Commun.*, vol. 52, no. 10, pp. 1820–1830, Oct. 2004.

[28] A. Nosratinia, T. E. Hunter, and A. Hedayat, "Cooperative communication in wireless networks," *IEEE Commun. Mag.*, vol. 42, no. 10, pp. 74–80, Oct. 2004.

[29] X. Bao and J. Li, "Efficient message relaying for wireless user cooperation: Decode-amplify-forward (DAF) and hybrid DAF and coded-cooperation," *IEEE Trans. Wireless Commun.*, vol. 6, no. 11, pp. 3975–3984, Nov. 2007.

[30] M. O. Hasna and M.-S. Alouini, "Optimal power allocation for relayed transmissions over Rayleigh-fading channels," *IEEE Trans. Wireless Commun.*, vol. 3, no. 6, pp. 1999–2004, Nov. 2004.

[31] M. O. Hasna and M.-S. Alouini, "Harmonic mean and end-to-end performance of transmission systems with relays," *IEEE Trans. Commun.*, vol. 52, no. 1, pp. 130–135, Jan. 2004.

[32] J. N. Laneman, "Network coding gain of cooperative diversity," in *Proc. IEEE Military Commun. Conf. (MILCOM)*, Monterey, CA, Oct. 31–Nov. 3, 2004, pp. 106–112.

[33] M. Yu and J. Li, "Is amplify-and-forward practically better than decode-and-forward or vice versa?" in *Proc. IEEE Int. Conf. Acoust., Speech, Signal Process. (ICASSP)*, vol. 3, Philadelphia, PA, Mar. 18–23, 2005, pp. 365–368.

[34] M. Yu, J. Li, and H. Sadjadpour, "Amplify-forward and decode-forward: The impact of location and capacity contour," in *Proc. IEEE Military Commun. Conf. (MILCOM)*, vol. 3, Atlantic City, NJ, Oct. 17–20, 2005, pp. 1609–1615.

[35] Y.-W. Hong, W.-J. Huang, F.-H. Chiu, and C.-C. J. Kuo, "Cooperative communications in resource-constrained wireless networks," *IEEE Signal Process. Mag.*, vol. 24, no. 3, pp. 47–57, May 2007.

[36] R. Annavajjala, P. C. Cosman, and L. B. Milstein, "Statistical channel knowledge-based optimum power allocation for relaying protocols in the high SNR regime," *IEEE J. Sel. Areas Commun.*, vol. 25, no. 2, pp. 292–305, Feb. 2007.

[37] Y. Li, B. Vucetic, Z. Zhou, and M. Dohler, "Distributed adaptive power allocation for wireless relay networks," *IEEE Trans. Wireless Commun.*, vol. 6, no. 3, pp. 948–958, Mar. 2007.

[38] T. C.-Y. Ng and W. Yu, "Joint optimization of relay strategies and resource allocations in cooperative cellular networks," *IEEE J. Sel. Areas Commun.*, vol. 25, no. 2, pp. 328–339, Feb. 2007.

[39] S. D. Gupta and D. Reynolds, "Position dependent power allocation strategies in cooperative relay networks," in *Proc. IEEE Military Commun. Conf. (MILCOM)*, Washington, D.C., Oct. 23–25, 2006, pp. 1–7.

[40] I. Marić and R. D. Yates, "Bandwidth and power allocation for cooperative strategies in Gaussian relay networks," *IEEE Trans. Inf. Theory*, vol. 56, no. 4, pp. 1880–1889, Apr. 2010.

[41] D. Chen and J. N. Laneman, "Modulation and demodulation for cooperative diversity in wireless systems," *IEEE Trans. Wireless Commun.*, vol. 5, no. 7, pp. 1785–1794, Jul. 2006.

[42] T. E. Hunter and A. Nosratinia, "Distributed protocols for user cooperation in multi-user wireless networks," in *Proc. IEEE Global Telecommun. Conf. (GLOBECOM)*, vol. 6, Dallas, TX, Nov. 29–Dec. 3, 2004, pp. 3788–3792.

[43] A. Høst-Madsen, "On the achievable rate for receiver cooperation in ad-hoc networks," in *Proc. IEEE Int. Symp. Inf. Theory (ISIT)*, Chicago, IL, Jun. 27–Jul. 2, 2004, p. 268.

[44] H. Ochiai, P. Mitran, and V. Tarokh, "Design and analysis of collaborative diversity protocols for wireless sensor networks," in *Proc. IEEE Veh. Technol. Conf. (VTC)*, vol. 7, Sep. 26–29, 2004, pp. 4645–4649.

[45] A. del Coso, U. Spagnolini, and C. Ibars, "Cooperative distributed MIMO channels in wireless sensor networks," *IEEE J. Sel. Areas Commun.*, vol. 25, no. 2, pp. 402–414, Feb. 2007.

[46] N. Shastry, J. Bhatia, and R. S. Adve, "A theoretical analysis of cooperative diversity in wireless sensor networks," in *Proc. IEEE Global Telecommun. Conf. (GLOBECOM)*, vol. 6, St. Louis, MO, Nov. 28–Dec. 2, 2005, pp. 3269–3273.

[47] N. C. Beaulieu and J. Hu, "A noise reduction amplify-and-forward relay protocol for distributed spatial diversity," *IEEE Commun. Lett.*, vol. 10, no. 11, pp. 787–789, Nov. 2006.

[48] Y. Zhao, R. S. Adve, and T. J. Lim, "Improving amplify-and-forward relay networks: Optimum power allocation versus selection," *IEEE Trans. Wireless Commun.*, vol. 6, no. 8, pp. 3114–3123, Aug. 2007.

[49] B. Can, H. Yomo, and E. De Carvalho, "Hybrid forwarding scheme for cooperative relaying in OFDM based networks," in *Proc. IEEE Int. Conf. Commun. (ICC)*, vol. 10, Istanbul, Turkey, Jun. 11–15, 2006, pp. 4520–4525.

[50] J. G. Proakis and M. Salehi, *Digital Communications*, 5th ed. McGraw-Hill, 2008.

[51] Q. Zhao and H. Li, "Distributed modulation for cooperative wireless communications," in *Proc. IEEE Conf. Inf. Sci. Syst. (CISS)*, Princeton, NJ, Mar. 22–24, 2006, pp. 1068–1072.

[52] T. J. Richardson and R. L. Urbanke, "The capacity of low-density parity-check codes under message-passing decoding," *IEEE Trans. Inf. Theory*, vol. 47, no. 2, pp. 599–618, Feb. 2001.

[53] D. S. Michalopoulos, G. K. Karagiannidis, T. A. Tsiftsis, and R. K. Mallik, "An optimized user selection method for cooperative diversity systems," in *Proc. IEEE Global Telecommun. Conf. (GLOBECOM)*, San Francisco, CA, Nov. 27–Dec. 1 2006.

[54] A. Bletsas, H. Shin, and M. Z. Win, "Outage optimality of opportunistic amplify-and-forward relaying," *IEEE Commun. Lett.*, vol. 11, no. 3, pp. 261–263, Mar. 2007.

[55] Y. Jing and H. Jafarkhani, "Network beamforming using relays with perfect channel information," *IEEE Trans. Inf. Theory*, vol. 55, no. 6, pp. 2499–2517, Jun. 2009.

[56] Y. Jing and H. Jafarkhani, "Single and multiple relay selection schemes and their achievable diversity orders," *IEEE Trans. Wireless Commun.*, vol. 8, no. 3, pp. 1414–1423, Mar. 2009.

[57] G. Farhadi and N. C. Beaulieu, "On the ergodic capacity of multi-hop wireless relaying systems," *IEEE Trans. Wireless Commun.*, vol. 8, no. 5, pp. 2286–2291, May 2009.

[58] R. Madan, N. B. Mehta, A. F. Molisch, and J. Zhang, "Energy-efficient cooperative relaying over fading channels with simple relay selection," *IEEE Trans. Wireless Commun.*, vol. 7, no. 8, pp. 3013–3025, Aug. 2008.

[59] S. Lee, M. Han, and D. Hong, "Average SNR and ergodic capacity analysis for opportunistic DF relaying with outage over Rayleigh fading channels," *IEEE Trans. Wireless Commun.*, vol. 8, no. 6, pp. 2807–2812, Jun. 2009.

[60] A. W. Lo and A. C. MacKinlay, "Maximizing predictability in the stock and bond markets," *Macroecon. Dynam.*, vol. 1, no. 01, pp. 102–134, Jan. 1997.

[61] J.-Y. Gotoh and H. Konno, "Maximization of the ratio of two convex quadratic functions over a polytope," *Comput. Optim. Appl.*, vol. 20, no. 1, pp. 43–60, Oct. 2001.

[62] H. P. Benson, "Maximizing the ratio of two convex functions over a convex set," *Nav. Res. Logist.*, vol. 53, no. 4, pp. 309–317, 2006.

[63] R. A. Horn and C. R. Johnson, *Matrix Analysis*. Cambridge University Press, 1990.

[64] M. Gastpar and M. Vetterli, "On the capacity of large Gaussian relay networks," *IEEE Trans. Inf. Theory*, vol. 51, no. 3, pp. 765–779, Mar. 2005.

[65] A. Høst-Madsen, "Capacity bounds for cooperative diversity," *IEEE Trans. Inf. Theory*, vol. 52, no. 4, pp. 1522–1544, Apr. 2006.

[66] A. del Coso and C. Ibars, "Capacity of decode-and-forward cooperative links with full channel state information," in *Proc. Asilomar Conf. Signals, Syst., Comput.*, Pacific Grove, CA, Oct. 30–Nov. 2, 2005, pp. 1514–1518.

[67] A. del Coso and C. Ibars, "Bounds on ergodic capacity of multirelay cooperative links with channel state information," in *Proc. IEEE Wireless Commun. Netw. Conf. (WCNC)*, Las Vegas, NV, Apr. 3–6, 2006, pp. 902–907.

[68] E. Beres and R. S. Adve, "Selection cooperation in multi-source cooperative networks," *IEEE Trans. Wireless Commun.*, vol. 1, no. 7, pp. 118–127, Jan. 2008.

[69] M. Chen, S. Serbetli, and A. Yener, "Distributed power allocation strategies for parallel relay networks," *IEEE Trans. Wireless Commun.*, vol. 7, no. 2, pp. 552–561, Feb. 2008.

[70] M. O. Hasna, "On the capacity of cooperative diversity systems with adaptive modulation," in *Proc. IEEE Wireless Optical Commun. Networks Conf. (WOCN)*, Dubai, United Arab Emirates, Mar. 6–9, 2005, pp. 432–436.

[71] S. S. Ikki and M. H. Ahmed, "Exact error probability and channel capacity of the best-relay cooperative-diversity networks," *IEEE Signal Process. Lett.*, vol. 16, no. 12, pp. 1051–1054, Dec. 2009.

[72] S. S. Ikki and M. H. Ahmed, "Performance analysis of adaptive decode-and-forward cooperative diversity networks with best-relay selection," *IEEE Trans. Commun.*, vol. 58, no. 1, pp. 68–72, Jan. 2010.

[73] T. Q. Duong and V. N. Q. Bao, "Performance analysis of selection decode-and-forward relay networks," *Electron. Lett.*, vol. 44, no. 20, pp. 1206–1207, Sep. 2008.

[74] D. S. Michalopoulos and G. K. Karagiannidis, "Performance analysis of single relay selection in Rayleigh fading," *IEEE Trans. Wireless Commun.*, vol. 7, no. 10, pp. 3718–3724, Oct. 2008.

[75] M. Nasiri Khormuji and E. G. Larsson, "Cooperative transmission based on decode-and-forward relaying with partial repetition coding," *IEEE Trans. Wireless Commun.*, vol. 8, no. 4, pp. 1716–1725, Apr. 2009.

[76] N. C. Beaulieu and J. Hu, "A closed-form expression for the outage probability of decode-and-forward relaying in dissimilar Rayleigh fading channels," *IEEE Commun. Lett.*, vol. 10, no. 12, pp. 813–815, Dec. 2006.

[77] P. A. Anghel, M. Kaveh, and Z.-Q. Luo, "Optimum power allocation for cooperative systems with orthogonal space-time transmissions," in *Proc. IEEE Int. Symp. Inf. Theory (ISIT)*, Seattle, WA, Jul. 9–14, 2006, pp. 2067–2071.

[78] W. Mesbah and T. N. Davidson, "Power and resource allocation for orthogonal multiple access relay systems," in *Proc. IEEE Int. Symp. Inf. Theory (ISIT)*, Toronto, Canada, Jul. 6–11, 2008, pp. 2272–2276.

[79] T. M. Cover and J. A. Thomas, *Elements of Information Theory*, 2nd ed. John Wiley & Sons, 2006.

[80] D. Tse and P. Viswanath, *Fundamentals of Wireless Communication*, 1st ed. Cambridge University Press, 2005.

[81] A. Papoulis and S. U. Pillai, *Probability, Random Variables and Stochastic Processes*, 4th ed. McGraw-Hill, 2002.

[82] N. C. Beaulieu, "An infinite series for the computation of the complementary probability distribution function of a sum of independent random variables and its application to the sum of Rayleigh random variables," *IEEE Trans. Commun.*, vol. 38, no. 9, pp. 1463–1474, Sep. 1990.

[83] T. Q. Duong, V. N. Q. Bao, and H.-J. Zepernick, "On the performance of selection decode-and-forward relay networks over Nakagami-m fading channels," *IEEE Commun. Lett.*, vol. 13, no. 3, pp. 172–174, Mar. 2009.

[84] K. Woradit, T. Q. S. Quek, W. Suwansantisuk, H. Wymeersch, L. Wuttisittikulkij, and M. Z. Win, "Outage behavior of selective relaying schemes," *IEEE Trans. Wireless Commun.*, vol. 8, no. 8, pp. 3890–3895, Aug. 2009.

[85] J. Hu and N. C. Beaulieu, "Performance analysis of decode-and-forward relaying with selection combining," *IEEE Commun. Lett.*, vol. 11, no. 6, pp. 489–491, Jun. 2007.

[86] M. Abramowitz and I. A. Stegun, *Handbook of Mathematical Functions with Formula, Graphs, and Mathematical Tables*, 9th ed. Dover Publications, 1970.

[87] A. Goldsmith, *Wireless Communications*, 1st ed. Cambridge University Press, 2005.

[88] A. J. Goldsmith and P. P. Varaiya, "Capacity of fading channels with channel side information," *IEEE Trans. Inf. Theory*, vol. 43, no. 6, pp. 1986–1992, Nov. 1997.

[89] S. Shamai, İ. E. Telatar, and S. Verdú, "Fountain capacity," *IEEE Trans. Inf. Theory*, vol. 53, no. 11, pp. 4372–4376, Nov. 2007.

[90] J. Castura and Y. Mao, "Rateless coding over fading channels," *IEEE Commun. Lett.*, vol. 10, no. 1, pp. 46–48, Jan. 2006.

[91] J. Castura and Y. Mao, "Rateless coding for wireless relay channels," in *Proc. IEEE Int. Symp. Inf. Theory (ISIT)*, Adelaide, Australia, Sep. 4–9, 2005, pp. 810–814.

[92] O. Etesami and A. Shokrollahi, "Raptor codes on binary memoryless symmetric channels," *IEEE Trans. Inf. Theory*, vol. 52, no. 5, pp. 2033–2051, May 2006.

[93] R. Palanki and J. S. Yedidia, "Rateless codes on noisy channels," in *Proc. IEEE Int. Symp. Inf. Theory (ISIT)*, Jun. 27–Jul. 2, 2004, p. 38.

[94] Z. Yang and A. Høst-Madsen, "Rateless coded cooperation for multiple-access channels in the low power regime," in *Proc. IEEE Int. Symp. Inf. Theory (ISIT)*, Seattle, WA, Jul. 9–14, 2006, pp. 967–971.

[95] Y. Liu, "A low complexity protocol for relay channels employing rateless codes and acknowledgment," in *Proc. IEEE Int. Symp. Inf. Theory (ISIT)*, Seattle, WA, Jul. 9–14, 2006, pp. 1244–1248.

[96] X. Liu and T. J. Lim, "Fountain codes over fading relay channels," *IEEE Trans. Wireless Commun.*, vol. 8, no. 6, pp. 3278–3287, Jun. 2009.

[97] J. W. Byers, M. Luby, M. Mitzenmacher, and A. Rege, "A digital fountain approach to reliable distribution of bulk data," in *Proc. ACM SIGCOMM*, Vancouver, BC, Sep. 2–4, 1998, pp. 56–67.

[98] M. Luby, "LT codes," in *Proc. IEEE Symp. Found. of Computer Sci. (FOCS)*, Vancouver, BC, Nov. 16–19, 2002, pp. 271–280.

[99] D. J. C. MacKay, *Information Theory, Inference, and Learning Algorithms*. Cambridge University Press, 2003.

[100] A. Shokrollahi, "Raptor codes," *IEEE Trans. Inf. Theory*, vol. 52, no. 6, pp. 2551–2567, Jun. 2006.

[101] U. Erez, M. D. Trott, and G. W. Wornell, "Rateless coding and perfect rate-compatible codes for Gaussian channels," in *Proc. IEEE Int. Symp. Inf. Theory (ISIT)*, Seattle, WA, Jul. 9–14, 2006, pp. 528–532.

[102] T. E. Hunter and A. Nosratinia, "Coded cooperation under slow fading, fast fading, and power control," in *Proc. Asilomar Conf. Signals, Syst., Comput.*, vol. 1, Pacific Grove, CA, Nov. 3–6, 2002, pp. 118–122.

[103] P. Mitran, H. Ochiai, and V. Tarokh, "Space-time diversity enhancements using collaborative communications," *IEEE Trans. Inf. Theory*, vol. 51, no. 6, pp. 2041–2057, Jun. 2005.

[104] S. M. Alamouti, "A simple transmit diversity technique for wireless communications," *IEEE J. Sel. Areas Commun.*, vol. 16, no. 8, pp. 1451–1458, Oct. 1998.

[105] J. Castura and Y. Mao, "Rateless coding and relay networks," *IEEE Signal Process. Mag.*, vol. 24, no. 5, pp. 27–35, Sep. 2007.

[106] R. M. Corless, G. H. Gonnet, D. E. G. Hare, D. J. Jeffrey, and D. E. Knuth, "On the Lambert W function," *Adv. Comput. Math.*, vol. 5, pp. 329–359, 1996.

[107] A. Bletsas, A. Khisti, D. P. Reed, and A. Lippman, "A simple cooperative diversity method based on network path selection," *IEEE J. Sel. Areas Commun.*, vol. 24, no. 3, pp. 659–672, Mar. 2006.

[108] S. Shamai (Shitz), S. Verdú, and R. Zamir, "Systematic lossy source/channel coding," *IEEE Trans. Inf. Theory*, vol. 44, no. 2, pp. 564–579, Mar. 1998.

[109] A. Bletsas and A. Lippman, "Implementing cooperative diversity antenna arrays with commodity hardware," *IEEE Commun. Mag.*, vol. 44, no. 12, pp. 33–40, Dec. 2006.

[110] S. C. Draper, L. Liu, A. F. Molisch, and J. S. Yedidia, "Routing in cooperative wireless networks with mutual-information accumulation," in *Proc. IEEE Int. Conf. Commun. (ICC)*, Beijing, China, May 19–23, 2008, pp. 4272–4277.

[111] J. Nocedal and S. J. Wright, *Numerical Optimization*. Springer, 1999.

[112] R. L. Burden and J. D. Faires, *Numerical Analysis*, 7th ed. Brooks/Cole, 2001.

Appendix A

Maximum Likelihood Detection in Dual-Hop DF Relaying

In this appendix, the ML detection rule for single-relay DF relaying and the BER under ML detection at the destination are derived. Recall that $r_{\rm SD}$ and $r_{\rm RD}$, given in (2.4) and (2.18), are the baseband equivalent received signals at the destination from the source and relay, respectively. Also, recall the definitions of $x_{\rm SD}$ and $x_{\rm RD}$ given in (2.21) and (2.22). It is verifiable that $\mathrm{Re}\{(x_{\rm SD}, x_{\rm RD})\}$ and $\mathrm{Im}\{(x_{\rm SD}, x_{\rm RD})\}$ are independent functions of b_1 and b_2, and in fact, are sufficient statistics for $(r_{\rm SD}, r_{\rm RD})$ relative to b_1 and b_2, respectively. In the sequel, we determine the ML detection rule for b_1. Thus, we concern ourselves here only with $\mathrm{Re}\{x_{\rm SD}\}$ and $\mathrm{Re}\{x_{\rm RD}\}$ which are given by

$$T_{\rm SD} \triangleq \mathrm{Re}\{x_{\rm SD}\} = \gamma_{\rm SD}\, b_1 + \hat{n}_{\rm SD} \tag{A-1a}$$

and

$$T_{\rm RD} \triangleq \mathrm{Re}\{x_{\rm RD}\} = \gamma_{\rm RD}\, \hat{b}_1 + \hat{n}_{\rm RD} \tag{A-1b}$$

where $\gamma_{\rm SD}$ and $\gamma_{\rm RD}$ are defined in (2.9), and where

$$\hat{n}_{\rm SD} \triangleq \mathrm{Re}\left\{ \frac{g_0^* \sqrt{2\mathcal{E}_{\rm S}}}{N_{\rm SD}}\, n_{\rm SD} \right\} \tag{A-1c}$$

and

$$\hat{n}_{\rm RD} \triangleq \mathrm{Re}\left\{ \frac{g_2^* \sqrt{2\mathcal{E}_{\rm R}}}{N_{\rm RD}}\, n_{\rm RD} \right\} \tag{A-1d}$$

are two independent zero-mean Gaussian RVs with variances γ_{SD} and γ_{RD}, respectively. Therefore, T_{SD} and T_{RD} are conditionally independent, given b_1, and one can write

$$f_{T_{\mathrm{SD}},T_{\mathrm{RD}}|b_1}\left(t_{\mathrm{SD}},t_{\mathrm{RD}}\right)=f_{T_{\mathrm{SD}}|b_1}\left(t_{\mathrm{SD}}\right)\Big[\left(1-P_{\mathrm{e}}^{(\mathrm{SR})}\right)f_{T_{\mathrm{RD}}|\hat{b}_1=b_1}\left(t_{\mathrm{RD}}\right)+P_{\mathrm{e}}^{(\mathrm{SR})}f_{T_{\mathrm{RD}}|\hat{b}_1\neq b_1}\left(t_{\mathrm{RD}}\right)\Big] \tag{A-2}$$

where $f_{T_{\mathrm{SD}},T_{\mathrm{RD}}|\cdot}(\cdot,\cdot)$, $f_{T_{\mathrm{SD}}|\cdot}(\cdot)$, and $f_{T_{\mathrm{RD}}|\cdot}(\cdot)$ are respectively the conditional joint PDF of T_{SD} and T_{RD}, conditional PDF of T_{SD}, and conditional PDF of T_{RD}, and where $P_{\mathrm{e}}^{(\mathrm{SR})}$ is given by (2.19) or (2.27b). Also, the ML detection rule can be written as

$$f_{T_{\mathrm{SD}},T_{\mathrm{RD}}|b_1=+1}\left(t_{\mathrm{SD}},t_{\mathrm{RD}}\right)\underset{-1}{\overset{+1}{\gtrless}}f_{T_{\mathrm{SD}},T_{\mathrm{RD}}|b_1=-1}\left(t_{\mathrm{SD}},t_{\mathrm{RD}}\right). \tag{A-3}$$

Using (A-1)–(A-3) and the mathematical form of the PDF of a real Gaussian RV [50, eq. (2.1–92)] yields the ML detection rule after algebraic simplification as

$$\mathrm{e}^{T_{\mathrm{SD}}}\left[\left(1-P_{\mathrm{e}}^{(\mathrm{SR})}\right)\mathrm{e}^{T_{\mathrm{RD}}}+P_{\mathrm{e}}^{(\mathrm{SR})}\mathrm{e}^{-T_{\mathrm{RD}}}\right]\underset{-1}{\overset{+1}{\lessgtr}}\mathrm{e}^{-T_{\mathrm{SD}}}\left[\left(1-P_{\mathrm{e}}^{(\mathrm{SR})}\right)\mathrm{e}^{-T_{\mathrm{RD}}}+P_{\mathrm{e}}^{(\mathrm{SR})}\mathrm{e}^{T_{\mathrm{RD}}}\right] \tag{A-4}$$

which can be rewritten as

$$\left(1-P_{\mathrm{e}}^{(\mathrm{SR})}\right)\sinh\left(T_{\mathrm{SD}}+T_{\mathrm{RD}}\right)+P_{\mathrm{e}}^{(\mathrm{SR})}\sinh\left(T_{\mathrm{SD}}-T_{\mathrm{RD}}\right)\underset{-1}{\overset{+1}{\lessgtr}}0. \tag{A-5}$$

Expanding the hyperbolic sines in (A-5) and dividing both sides by,

$$\cosh(T_{\mathrm{SD}})\cosh(T_{\mathrm{RD}}) \tag{A-6}$$

gives the ML detection rule (2.28), which is more tractable than (A-5) for BER calculation. Note that if the real parts in (2.28) are replaced with the corresponding imaginary parts, the ML detection rule for the bit b_2 is obtained.

The BER can be written from (2.28) as

$$\begin{aligned}P_{\mathrm{e}}=\left(1-P_{\mathrm{e}}^{(\mathrm{SR})}\right)\Pr\left\{\tanh(T_{\mathrm{SD}})+\left(1-2P_{\mathrm{e}}^{(\mathrm{SR})}\right)\tanh(T_{\mathrm{RD}})<0\,\middle|\,b_1=+1,\hat{b}_1=+1\right\}\\+P_{\mathrm{e}}^{(\mathrm{SR})}\Pr\left\{\tanh(T_{\mathrm{SD}})+\left(1-2P_{\mathrm{e}}^{(\mathrm{SR})}\right)\tanh(T_{\mathrm{RD}})<0\,\middle|\,b_1=+1,\hat{b}_1=-1\right\}\end{aligned} \tag{A-7}$$

where T_{SD} and T_{RD} are defined by (A-1). Assuming that (cf. (2.27b))

$$0<P_{\mathrm{e}}^{(\mathrm{SR})}<0.5 \tag{A-8}$$

and defining

$$p = \tanh^{-1}\left(1 - 2P_{\mathrm{e}}^{(\mathrm{SR})}\right) \tag{A-9}$$

we can show that

$$\Pr\left\{\tanh(T_{\mathrm{SD}}) + \left(1 - 2P_{\mathrm{e}}^{(\mathrm{SR})}\right)\tanh(T_{\mathrm{RD}}) < 0 \,\middle|\, b_1 = +1, \hat{b}_1\right\} =$$
$$F_{T_{\mathrm{SD}}|b_1=+1}(-p) + \int_{-p}^{p} F_{T_{\mathrm{RD}}|\hat{b}_1}\left(-\tanh^{-1}\left(\frac{\tanh x}{\tanh p}\right)\right) f_{T_{\mathrm{SD}}|b_1=+1}(x)\,\mathrm{d}x \tag{A-10}$$

where $F_{T_{\mathrm{SD}}|\cdot}(\cdot)$ denote the conditional CDF of T_{SD}. Combining (A-1), (A-7), and (A-10) yields the final result (2.29) for $0 < P_{\mathrm{e}}^{(\mathrm{SR})} < 0.5$. Eq. (A-7) can be directly invoked for $P_{\mathrm{e}}^{(\mathrm{SR})} = 0$ and $P_{\mathrm{e}}^{(\mathrm{SR})} = 0.5$ to give the respective error probabilities

$$P_{\mathrm{e}} = \Pr\left\{T_{\mathrm{SD}} + T_{\mathrm{RD}} < 0 \,\middle|\, b_1 = +1, \hat{b}_1 = +1\right\} = \mathrm{Q}\left(\sqrt{\gamma_{\mathrm{SD}} + \gamma_{\mathrm{RD}}}\right) \tag{A-11}$$

and

$$P_{\mathrm{e}} = \Pr\left\{T_{\mathrm{SD}} < 0 \mid b_1 = +1\right\} = \mathrm{Q}\left(\sqrt{\gamma_{\mathrm{SD}}}\right). \tag{A-12}$$

Appendix B

Proof of Theorem 2.1

As the communication under study occurs in $2N$ DoFs (see Fig. 2.4), all MI rates are considered to be normalized by $2N$. In other words, the different schemes are compared based on their achievable rates or equivalent SNRs per 2-D symbol or DoF.

Recall that in the DT case, the SD SNR is $\gamma_0/2$. Therefore, based on the decoding margin (2.32), the maximum MI in nats per DoF in this case is given by,

$$\ln\left(1+\frac{1}{\rho}\frac{\gamma_0}{2}\right). \tag{B-1}$$

In AF relaying, the maximum MI between the source and destination is obtained as,

$$\frac{1}{2}\ln\left(1+\frac{1}{\rho}\gamma_{\rm eq}\right) \tag{B-2}$$

where $\gamma_{\rm eq}$ has been given in (2.9). The coefficient $1/2$ in this expression appears because the source uses only half of the available DoFs in the cooperative cases. In the DF relaying case, the relay is required to be capable of successful decoding, which is attainable only if the received value of SNR at the relay exceeds the threshold (2.32). Therefore, the maximum MI between the source and destination in this case is given by,

$$\frac{1}{2}\ln\left(1+\frac{1}{\rho}\min\{\gamma_{\rm SR},\gamma_{\rm SD}+\gamma_{\rm RD}\}\right). \tag{B-3}$$

Now, invoking (2.15)–(2.17) one can write the maximum MI per DoF for DT, AF relaying, and DF relaying cases in the common form

$$I=\frac{1}{2}\ln\left(1+\frac{\Lambda}{\rho}\right) \tag{B-4a}$$

where

$$\Lambda \triangleq \begin{cases} \Lambda_0 \triangleq \gamma_0 + \gamma_0^2/(4\rho), & \text{DT} \\ \Lambda_1 \triangleq \gamma_{\text{eq}}(k), & \text{AF relaying} \\ \Lambda_2 \triangleq \min\left\{k\gamma_1, k\gamma_0 + (1-k)\gamma_2\right\}, & \text{DF relaying} \end{cases}. \tag{B-4b}$$

The remainder of the proof involves solving

$$\Lambda_{\max} = \max_{\substack{k\in(0,1] \\ i\in\{0,1,2\}}} \Lambda_i(k) \tag{B-5}$$

and

$$\operatorname*{argmax}_{\substack{k\in(0,1] \\ i\in\{0,1,2\}}} \Lambda_i(k) \tag{B-6}$$

by scrutinizing different intricate cases, and also obtaining the maximum CG, which, from (2.30) and (B-4), equals

$$\text{CG} = 10\log_{10}\left[\frac{2\rho}{\gamma_0}\left(\sqrt{1+\frac{\Lambda_{\max}}{\rho}}-1\right)\right]. \tag{B-7}$$

First, we establish the first part of the theorem that if $\gamma_2 \leq \Lambda_0$, then relaying is not beneficial; i.e. $\Lambda_{\max} = \Lambda_0$. Note that we can write

$$\gamma_{\text{eq}} = \gamma_{\text{SD}} + \frac{\gamma_{\text{SR}}\gamma_{\text{RD}}}{\gamma_{\text{SR}} + \gamma_{\text{RD}} + 1} \leq \gamma_{\text{SD}} + \gamma_{\text{RD}} \tag{B-8}$$

or

$$\Lambda_1 \leq k\gamma_0 + (1-k)\gamma_2 \tag{B-9}$$

for any power allocation ratio, k. Furthermore, we have

$$\Lambda_2 \leq k\gamma_0 + (1-k)\gamma_2. \tag{B-10}$$

Also, we have obviously that $\gamma_0 \leq \Lambda_0$, which, with the fact that $\gamma_2 \leq \Lambda_0$, gives

$$k\gamma_0 + (1-k)\gamma_2 \leq \Lambda_0 \tag{B-11}$$

for any $0 \leq k \leq 1$. Subsequently, (B-9)–(B-11) yield $\Lambda_i \leq \Lambda_0$ for $i = 1, 2$ and any $k \in [0, 1]$, which implies that $\Lambda_{\max} = \Lambda_0$. Henceforth, we will assume that

$$\gamma_2 > \Lambda_0. \tag{B-12}$$

The parameter L_1 in (2.33) is the unique k for which $k\gamma_0 + (1-k)\gamma_2 = \Lambda_0$; i.e.,

$$L_1\gamma_0 + (1-L_1)\gamma_2 = \Lambda_0. \tag{B-13}$$

It can be observed that given (B-12), we have

$$0 < L_1 < 1 \tag{B-14}$$

and

$$k \leq L_1 \Longleftrightarrow k\gamma_0 + (1-k)\gamma_2 \geq \Lambda_0. \tag{B-15}$$

Also, L_2 in (2.34) is the unique k for which $k\gamma_1 = k\gamma_0 + (1-k)\gamma_2$; i.e.,

$$L_2\gamma_1 = L_2\gamma_0 + (1-L_2)\gamma_2. \tag{B-16}$$

It can be verified that based on (B-12) L_2 is positive but not necessarily less than one. In addition, $k\gamma_1$ is a strictly increasing function of k. However, based on (B-12) we know that $\gamma_2 > \gamma_0$, and therefore, $k\gamma_0 + (1-k)\gamma_2$ is a strictly decreasing function of k. Now, from (B-16) one has

$$\Lambda_2 = \begin{cases} k\gamma_1, & k \leq L_2 \\ k\gamma_0 + (1-k)\gamma_2, & k > L_2 \end{cases} \tag{B-17}$$

and therefore, we obtain

$$\max_k \Lambda_2 = \begin{cases} L_2\gamma_1, & L_2 \leq 1 \\ \gamma_1, & L_2 > 1 \end{cases}. \tag{B-18}$$

Consequently, we have

$$\max_k \Lambda_2 = \Lambda_2\left(k_{\text{opt}}^{(\text{DF})}\right) = k_{\text{opt}}^{(\text{DF})}\gamma_1 \leq k_{\text{opt}}^{(\text{DF})}\gamma_0 + \left(1 - k_{\text{opt}}^{(\text{DF})}\right)\gamma_2 \tag{B-19a}$$

where

$$k_{\text{opt}}^{(\text{DF})} \triangleq \min\{L_2, 1\} \tag{B-19b}$$

is the OPA ratio in the DF relaying case. Note that the inequality in (B-19a) becomes an equality when $L_2 \leq 1$, and a strict inequality otherwise. Meanwhile, making use of (2.2.1) in (2.9), we obtain, after some algebraic manipulations,

$$\max_k \Lambda_1 = \max_k \gamma_{\text{eq}}(k) = \gamma_{\text{eq}}\left(k_{\text{opt}}^{(\text{AF})}\right) = \begin{cases} \gamma_0, & \gamma_0 \geq \gamma_1\gamma_2/(\gamma_1+1) \\ K, & \text{otherwise} \end{cases} \tag{B-20}$$

where $k_{\rm opt}^{(\rm AF)}$, given in (2.2.1), is the OPA ratio in AF relaying, and K is defined by (2.35).

Now, if $L_1 \leq L_2$, we have, from (B-14) and (B-19b),

$$k_{\rm opt}^{(\rm DF)} \geq L_1. \tag{B-21}$$

Therefore, using (B-19a) we can write

$$\max_k \Lambda_2 \leq k_{\rm opt}^{(\rm DF)}\gamma_0 + \left(1 - k_{\rm opt}^{(\rm DF)}\right)\gamma_2 \leq \Lambda_0 \tag{B-22}$$

where the second inequality follows after (B-21) is applied to (B-15). Eq. (B-22) clearly shows that for the case $L_1 \leq L_2$, DF relaying is not the best option and only AF relaying is compared against DT. In this case, if

$$\gamma_0 \geq \frac{\gamma_1\,\gamma_2}{\gamma_1 + 1} \tag{B-23}$$

then one obtains, from (B-20),

$$\max_k \Lambda_1 = \gamma_0 \leq \Lambda_0 \tag{B-24}$$

and Case i in the theorem follows. However, if (B-23) does not hold, we have $\max_k \Lambda_1 = K$ from (B-20). Now, if $K \leq \Lambda_0$, then DT excels. Otherwise, AF relaying is the best option. Also, note that if $K \leq \Lambda_0$, AF relaying is inferior to DT, whether (B-23) holds or not. This concludes the proof for Cases ii and iii.

Now, consider the case $L_1 > L_2$. Recall that (B-12) yields $0 < L_1 < 1$ and $L_2 > 0$. Therefore, in this case the inequalities $0 < L_2 < L_1 < 1$ hold. Then, from (B-19) we obtain $k_{\rm opt}^{(\rm DF)} = L_2$ and

$$\max_k \Lambda_2 = k_{\rm opt}^{(\rm DF)}\gamma_1 = L_2\gamma_1. \tag{B-25}$$

Now, using (B-16) and (B-25) one can concluded that

$$\max_k \Lambda_2 = L_2\gamma_0 + (1 - L_2)\gamma_2. \tag{B-26}$$

Meanwhile, $L_2 < L_1$ yields

$$L_2\gamma_0 + (1 - L_2)\gamma_2 > \Lambda_0 \tag{B-27}$$

after utilizing (B-13) and (B-15). Consequently, we have $\max_k \Lambda_2 > \Lambda_0$, which implies that in the case $L_1 > L_2$, DT must be avoided; the best option is either AF or DF relaying, to be determined next.

If (B-23) does not hold, then we have $\max_k \Lambda_1 = K$ from (B-20). Therefore, from

(B-25), if $K \geq L_2\gamma_1$, AF relaying outperforms DF relaying, and Case iv is obtained. However, if $K < L_2\gamma_1$, AF relaying is inferior. Next, we show that when (B-23) holds, DF relaying is the best option independently of whether $K < L_2\gamma_1$ or not. This completes the proof for Cases v and vi.

If (B-23) holds, we have, from (B-20),

$$\max_k \Lambda_1 = \gamma_0. \tag{B-28}$$

Recall that under (B-12), $k\gamma_0 + (1-k)\gamma_2$ is a strictly decreasing function of k such that

$$L_2\gamma_0 + (1-L_2)\gamma_2 > \gamma_0 \tag{B-29}$$

where we have made use of the fact that $L_2 < 1$. Combining (B-26)–(B-29) gives

$$\max_k \Lambda_2 > \max_k \Lambda_1 \tag{B-30}$$

which means that DF relaying surpasses AF relaying for this case.

Throughout the proof we observed that whenever AF relaying is superior, $\max_k \Lambda_1$ equals K and the OPA ratio is $k_{\text{opt}}^{(\text{AF})}$. Also, if DF relaying is the best option, $\max_k \Lambda_2 = L_2\gamma_1$ and the OPA ratio is $k_{\text{opt}}^{(\text{DF})} = L_2$. Applying $\Lambda_{\max} = K$ and $\Lambda_{\max} = L_2\gamma_1$ to (B-7) gives (2.38) and (2.39), respectively, and the proof of the theorem is concluded.

Appendix C

Proof of Theorem 3.1

If selection AF relaying is optimal, there exists an i for which $\mathbf{e}_i$ is a global solution to (3.16). Then, $\mathbf{e}_i$ is also a local solution, and must satisfy the Karush-Kuhn-Tucker (KKT) conditions [111, Section 12.2]; i.e. we have

$$\nabla f(\mathbf{e}_i) + \boldsymbol{\lambda} = \mathbf{0} \tag{C-1a}$$

where $f(\mathbf{d})$ is the objective function in (3.16) and where

$$\boldsymbol{\lambda} \triangleq (\lambda_1, \cdots, \lambda_M)^{\mathrm{T}} \tag{C-1b}$$

$$\lambda_i = 0 \tag{C-1c}$$

and

$$\lambda_m \geq 0,\, m \neq i. \tag{C-1d}$$

Note that $\boldsymbol{\lambda}$ is a Lagrange vector multiplier for the inequality constraint in the problem. Now, one can observe that

$$\nabla f(\mathbf{d}) = \frac{1}{\mathbf{d}^{\mathrm{T}}\,\acute{\mathbf{D}}\,\mathbf{d}}(\mathbf{A} + \mathbf{A}^{\mathrm{T}})\,\mathbf{d} - \frac{2\,\mathbf{d}^{\mathrm{T}}\mathbf{A}\,\mathbf{d}}{(\mathbf{d}^{\mathrm{T}}\,\acute{\mathbf{D}}\,\mathbf{d})^2}\,\acute{\mathbf{D}}\,\mathbf{d} \tag{C-2}$$

and therefore,

$$\frac{2}{1+|b_i|^2}\,\mathrm{Re}\{a_i\,\mathbf{a}^*\} - \frac{2\,|a_i|^2}{1+|b_i|^2}\,\mathbf{e}_i + [\lambda_1, \cdots, \lambda_{i-1}, 0, \lambda_{i+1}, \cdots, \lambda_M]^{\mathrm{T}} = \mathbf{0} \tag{C-3}$$

where $\lambda_m \geq 0$. Eq. (C-3) shows that for any $j \neq i$, we have

$$\mathrm{Re}\{a_i\,a_j^*\} = -\lambda_j(1+|b_i|^2)/2 \leq 0. \tag{C-4}$$

Substituting for a_i and a_j from (3.9e) concludes the proof.

Appendix D

Proof of Theorem 3.2

First, we introduce the following terminology and prove a lemma.

Definition. Let

$$X \triangleq \{\mathbf{x}_1, \cdots, \mathbf{x}_M\} \tag{D-1}$$

be a set of nonzero vectors in a 2-D plane. The angle between $\mathbf{x}_i$ and $\mathbf{x}_j$, belonging to $[0, \pi]$ by convention, is denoted $\angle(\mathbf{x}_i, \mathbf{x}_j)$. Also, in the set X, the vector $\mathbf{x}_i$ is called *isolated* if there is no other vector in the set making an acute angle with $\mathbf{x}_i$, i.e. if

$$\forall j,\ j \neq i:\ \angle(\mathbf{x}_i, \mathbf{x}_j) \geq \pi/2. \tag{D-2}$$

Lemma. If the phases of the vectors $\mathbf{x}_1, \ldots, \mathbf{x}_M$ in a 2-D plane are independent, each having a uniform distribution over $[0, 2\pi)$,[1] then the probability that none of the vectors is isolated is given by

$$p(M) = \begin{cases} 0, & M = 1 \\ \frac{3}{8}, & M = 3 \\ 1 - M\,2^{1-M} + M\,2^{2-2M}, & M = 2,\ M \geq 4 \end{cases}. \tag{D-3}$$

Proof of the Lemma. Let θ_i denote the phase of $\mathbf{x}_i$, and A_i represent the event that $\mathbf{x}_i$ is isolated. One can write

$$p(M) = 1 - \Pr\left\{\bigcup_{i=1}^{M} A_i\right\} = 1 + \sum_{i=1}^{M} (-1)^i\, S_i \tag{D-4a}$$

[1] Here, the phase of $\mathbf{x}_i$ is the directed angle that $\mathbf{x}_i$ makes with a fixed reference vector that is coplanar with $\mathbf{x}_1, \ldots, \mathbf{x}_M$.

where

$$S_i \triangleq \sum_{1 \le j_1 < \cdots < j_i \le M} \Pr\left\{ \bigcap_{m=1}^{i} A_{j_m} \right\}. \tag{D-4b}$$

Subsequently, we calculate the terms $\Pr\{\bigcap_{m=1}^{i} A_{j_m}\}$ for different values of i. First, we note that

$$\Pr\{A_p\} = \Pr\left\{ \bigcap_{\substack{m=1 \\ m \neq p}}^{M} \left(\angle(\mathbf{x}_m, \mathbf{x}_p) \ge \frac{\pi}{2} \right) \right\} \tag{D-5}$$

$$= \mathrm{E}_{\theta_p}\left\{ \prod_{\substack{m=1 \\ m \neq p}}^{M} \Pr\left\{ \angle(\mathbf{x}_m, \mathbf{x}_p) \ge \frac{\pi}{2} \,\middle|\, \theta_p \right\} \right\} \tag{D-6}$$

$$= \mathrm{E}_{\theta_p}\left\{ \prod_{\substack{m=1 \\ m \neq p}}^{M} \frac{\pi}{2\pi} \right\} = 2^{1-M} \tag{D-7}$$

for $p = 1, \ldots, M$, where $\mathrm{E}_{\theta_p}\{\cdot\}$ denotes expectation over θ_p, and where (D-6) and (D-7) come from the independence and distribution of $\theta_1, \ldots, \theta_M$, respectively. Also, for any unequal p and q in $\{1, \ldots, M\}$, one can write

$$\Pr\{A_p \cap A_q\}$$

$$= \Pr\left\{ \bigcap_{\substack{m=1 \\ m \neq p,q}}^{M} \left[\left(\angle(\mathbf{x}_m, \mathbf{x}_p) \ge \frac{\pi}{2} \right) \bigcap \left(\angle(\mathbf{x}_m, \mathbf{x}_q) \ge \frac{\pi}{2} \right) \right] \bigcap \left(\angle(\mathbf{x}_p, \mathbf{x}_q) \ge \frac{\pi}{2} \right) \right\} \tag{D-8a}$$

$$= \mathrm{E}_{\theta_p,\theta_q}\left\{ \mathbb{I}\left(\angle(\mathbf{x}_p, \mathbf{x}_q) \ge \frac{\pi}{2} \right) \prod_{\substack{m=1 \\ m \neq p,q}}^{M} \Pr\left\{ \left(\angle(\mathbf{x}_m, \mathbf{x}_p) \ge \frac{\pi}{2} \right) \bigcap \left(\angle(\mathbf{x}_m, \mathbf{x}_q) \ge \frac{\pi}{2} \right) \,\middle|\, \theta_p, \theta_q \right\} \right\} \tag{D-8b}$$

$$= \mathrm{E}_{\theta_p,\theta_q}\left\{ \mathbb{I}\left(\angle(\mathbf{x}_p, \mathbf{x}_q) \ge \frac{\pi}{2} \right) \left(\frac{\pi - \angle(\mathbf{x}_p, \mathbf{x}_q)}{2\,\pi} \right)^{M-2} \,\middle|\, \theta_p, \theta_q \right\} \tag{D-8c}$$

$$= \int_{\pi/2}^{3\pi/2} \frac{\mathrm{d}\theta}{2\pi} \left(\frac{|\pi - \theta|}{2\pi} \right)^{M-2} \tag{D-8d}$$

$$= \frac{1}{2^{(2M-3)}\,(M-1)} \tag{D-8e}$$

where $\mathrm{E}_{\theta_p,\theta_q}\{\cdot\}$ denotes expectation over θ_p and θ_q, and where $\mathbb{I}(\cdot)$ is an indicator function such that for event E, $\mathbb{I}(E)$ equals 1 if E occurs, and 0 otherwise. The equalities (D-8b) and (D-8c) result from the independence and uniform distribution of $\theta_1, \ldots, \theta_M$, respectively. Also, (D-8d) is obtained by conditioning on θ_p and taking the expectation over θ_q.

It can be graphically verified that when $M = 3$, all three vectors are isolated if any two

of them are isolated. Therefore, from (D-8), we obtain, for the case of $M = 3$,

$$\Pr\{A_1 \cap A_2 \cap A_3\} = \Pr\{A_1 \cap A_2\} = \frac{1}{2^3 \times 2} = \frac{1}{16}. \tag{D-9}$$

Furthermore, when $M \geq 4$, no more than two vectors can be simultaneously isolated; i.e.,

$$S_i = 0, \quad i \geq 3, \quad M \geq 4. \tag{D-10}$$

Combining (D-4)–(D-10) yields the desired result (D-3) after simplification. ■

Now, let the event that selection AF relaying is outage optimal be denoted E, and the event that

$$\forall i,\ \exists j,\ j \neq i:\ \mathrm{Re}\left\{g_{\mathrm{S}i}\, g_{i\mathrm{D}}\, g_{\mathrm{S}j}^{*}\, g_{j\mathrm{D}}^{*}\right\} > 0 \tag{D-11}$$

be denoted F. Then, according to Theorem 3.1 we have

$$\Pr\{E\} \leq 1 - \Pr\{F\}. \tag{D-12}$$

Let

$$w_m \triangleq g_{\mathrm{S}m}\, g_{m\mathrm{D}} \tag{D-13}$$

for $m = 1, \ldots, M$, and assume that $\mathbf{w}_m$ is the vector representation of w_m in the complex plane. We know that the elements of $\{g_{\mathrm{S}1}, \ldots, g_{\mathrm{S}M}, g_{1\mathrm{D}}, \ldots, g_{M\mathrm{D}}\}$ are independent, each having a uniformly distributed phase over $[0, 2\pi)$. Then, it can be verified that the random vectors $\mathbf{w}_1, \ldots, \mathbf{w}_M$ are independent, each having a uniformly distributed phase over $[0, 2\pi)$. Furthermore, the event F is equivalent to the event that

$$\forall i,\ \exists j,\ j \neq i:\ \angle(\mathbf{w}_i, \mathbf{w}_j) < \pi/2 \tag{D-14}$$

i.e. no $\mathbf{w}_i$ is isolated. Using the result (D-3) of the Lemma and from (D-12), we obtain

$$\Pr\{E\} \leq \begin{cases} 1, & M = 1 \\ \frac{5}{8}, & M = 3 \\ M2^{1-M}(1 - 2^{1-M}), & \text{otherwise} \end{cases}. \tag{D-15}$$

Therefore, as M increases, $\Pr\{E\}$ approaches 0 exponentially, and the proof is concluded.

Appendix E

Average Capacities of DF Relaying Networks for Rayleigh Fading

In this appendix, the derivation steps for the results given in Tables 4.2–4.9 are explained. We assume that in the cases with the SD link, γ_{SD} is exponentially distributed with mean value μ_{SD}, PDF $f_{\mathrm{SD}}(\cdot)$, and CDF $F_{\mathrm{SD}}(\cdot)$. Note that if X is an exponentially distributed RV with mean $\overline{X}$, its PDF, CDF, and MGF are respectively written as

$$f_X(x) = \frac{\mathrm{e}^{-x/\overline{X}}}{\overline{X}}, \qquad x \geq 0 \tag{E-1}$$

$$F_X(x) = 1 - \mathrm{e}^{-x/\overline{X}}, \qquad x \geq 0 \tag{E-2}$$

and

$$M_X(s) = \frac{1}{1 - \overline{X}\, s}, \qquad \mathrm{Re}\{s\} < 1/\overline{X}. \tag{E-3}$$

In the no SD-link case, γ_{SD} is assumed to equal 0 with probability 1 such that (4.59) holds. Also, in the asymmetric case, $\gamma_{\mathrm{S}m}$ and $\gamma_{m\mathrm{D}}$ are exponentially distributed with mean values $\mu_{\mathrm{S}m}$ and $\mu_{m\mathrm{D}}$, and CDFs $F_{\mathrm{S}m}(\cdot)$ and $F_{m\mathrm{D}}(\cdot)$, respectively. In the symmetric case, $\mu_{\mathrm{S}m}$, $\mu_{m\mathrm{D}}$, $F_{\mathrm{S}m}(\cdot)$, and $F_{m\mathrm{D}}(\cdot)$ are denoted μ_{SR}, μ_{RD}, $F_{\mathrm{SR}}(\cdot)$, and $F_{\mathrm{RD}}(\cdot)$, respectively. We also consider the notations and functions $\mu_{\mathrm{S}\mathcal{A}}$, $\mu_{\mathcal{A}\mathrm{D}}$, $P(\cdot,\cdot)$, $\Gamma(\cdot,\cdot)$, $\Gamma(\cdot)$, $\mathcal{I}_m(k,a,b,c,d)$, $\mathcal{I}_m(k,a,b,c)$, $\mathcal{R}(k,\ell,\eta,a,b)$, $\mathcal{R}(\eta,a,b)$, $h(x;\ell,a)$, $g(x;\ell,w,\alpha)$, $\mathcal{S}(x)$, and $\mathcal{T}(\alpha,\beta)$, defined in Section 4.4.2. Next, we investigate the schemes one by one.

E.1 Superimposed Relaying

Observe that the outage probabilities in superimposed relaying with PCC and RC for general fading are given from (4.46) and (4.47) as

$$\Pr\left\{I_{\max}^{(\sup,\,\mathrm{PCC})} < r\right\} = \int_0^{\mathrm{e}^r-1} \mathrm{d}\gamma\; F_{Y\text{-sum}}\!\left(\frac{\mathrm{e}^{2r}}{1+\gamma} - 1 - \gamma\right) f_{\mathrm{SD}}(\gamma) \tag{E-4}$$

and

$$\Pr\left\{I_{\max}^{(\sup,\,\mathrm{RC})} < r\right\} = \int_0^{\frac{\mathrm{e}^{2r}-1}{2}} \mathrm{d}\gamma\; F_{Y-\mathrm{sum}}(\mathrm{e}^{2r} - 1 - 2\gamma)\, f_{\mathrm{SD}}(\gamma) \tag{E-5}$$

where $F_{Y\text{-sum}}(\cdot)$ is the CDF of the summation (4.48). The corresponding average capacities can be obtained from (4.2), (E-4) and (E-5) as

$$\begin{aligned}\overline{I_{\max}^{(\sup,\,\mathrm{PCC})}} &= \int_0^{\infty} \frac{\mathrm{d}u}{u+1}\left[1 - F_{\mathrm{SD}}(u)\right] \\ &\quad + \int_0^{\infty} \mathrm{d}r \int_0^{\mathrm{e}^r-1} \mathrm{d}\gamma \left[1 - F_{Y\text{-sum}}\!\left(\frac{\mathrm{e}^{2r}}{1+\gamma} - 1 - \gamma\right)\right] f_{\mathrm{SD}}(\gamma)\end{aligned} \tag{E-6}$$

and

$$\begin{aligned}\overline{I_{\max}^{(\sup,\,\mathrm{RC})}} &= \int_0^{\infty} \frac{\mathrm{d}u}{2u+1}\left[1 - F_{\mathrm{SD}}(u)\right] \\ &\quad + \int_0^{\infty} \mathrm{d}r \int_0^{\frac{\mathrm{e}^{2r}-1}{2}} \mathrm{d}\gamma \left[1 - F_{Y\text{-sum}}(\mathrm{e}^{2r} - 1 - 2\gamma)\right] f_{\mathrm{SD}}(\gamma).\end{aligned} \tag{E-7}$$

Also, in the no SD-link case, applying (4.59) to (E-4)–(E-7), one obtains, for both PCC and RC cases,

$$\Pr\left\{I_{\max}^{(\sup,\,\mathrm{no\,SD})} < r\right\} = F_{Y\text{-sum}}(\mathrm{e}^{2r} - 1) \tag{E-8}$$

and

$$\overline{I_{\max}^{(\sup,\,\mathrm{no\,SD})}} = \int_0^{\infty} \mathrm{d}r\, \left[1 - F_{Y\text{-sum}}(\mathrm{e}^{2r} - 1)\right]. \tag{E-9}$$

In fact, in the no SD-link case, the superimposed relaying schemes with PCC and RC coincide. This fact can also be verified by inspecting the instantaneous rates achievable in the different schemes given in Table 4.1.

The results (E-4)–(E-9) indicate that to calculate the outage probability and average capacity in superimposed relaying, we need to obtain $F_{Y\text{-sum}}(\cdot)$ first. In the asymmetric case, where μ_{SD}, the $\mu_{\mathrm{S}m}$'s, and the $\mu_{m\mathrm{D}}$'s can have any value except that the $\mu_{m\mathrm{D}}$'s are

unequal, we can write the MGF of the summation (4.48) from (4.55) and (E-3) as

$$\begin{aligned} M_{Y\text{-sum}}(s) &= \prod_{m=1}^{M} \left\{ F_{\mathrm{S}m}(\mathrm{e}^{2r}-1) + \left[1 - F_{\mathrm{S}m}(\mathrm{e}^{2r}-1)\right] M_{m\mathrm{D}}(s) \right\} \\ &= \prod_{m=1}^{M} \left\{ 1 - \mathrm{e}^{(1-\mathrm{e}^{2r})/\mu_{\mathrm{S}m}} + \frac{\mathrm{e}^{(1-\mathrm{e}^{2r})/\mu_{\mathrm{S}m}}}{1-\mu_{m\mathrm{D}}\, s} \right\} \\ &= \prod_{m=1}^{M} \left\{ 1 + \frac{\mu_{m\mathrm{D}}\, \mathrm{e}^{(1-\mathrm{e}^{2r})/\mu_{\mathrm{S}m}}\, s}{1-\mu_{m\mathrm{D}}\, s} \right\} \\ &= A_0 + \sum_{m=1}^{M} \frac{A_m}{1-\mu_{m\mathrm{D}}\, s} \end{aligned} \tag{E-10a}$$

using partial fraction expansion, where

$$A_0 \triangleq \lim_{s\to\infty} M_{Y\text{-sum}}(s) = \prod_{m=1}^{M} \left[1 - \mathrm{e}^{(1-\mathrm{e}^{2r})/\mu_{\mathrm{S}m}}\right] \tag{E-10b}$$

and

$$A_m \triangleq \lim_{s\to 1/\mu_{m\mathrm{D}}} (1-\mu_{m\mathrm{D}}\, s) M_{Y\text{-sum}}(s) = \mathrm{e}^{(1-\mathrm{e}^{2r})/\mu_{\mathrm{S}m}} \prod_{\substack{k=1 \\ k\neq m}}^{M} \left[1 + \frac{\mathrm{e}^{(1-\mathrm{e}^{2r})/\mu_{\mathrm{S}k}}}{\mu_{m\mathrm{D}}/\mu_{k\mathrm{D}} - 1}\right] \tag{E-10c}$$

for $m = 1, \ldots, M$. Taking the inverse Laplace transform of (E-10a), we obtain $f_{Y\text{-sum}}(y)$, the PDF of the summation (4.48), as

$$f_{Y\text{-sum}}(y) = A_0\, \delta(y) + \left[\sum_{m=1}^{M} A_m \frac{\mathrm{e}^{-y/\mu_{m\mathrm{D}}}}{\mu_{m\mathrm{D}}}\right] \mathrm{H}(y) \tag{E-11}$$

where $\delta(\cdot)$ and $\mathrm{H}(\cdot)$ are the Dirac delta and Heaviside step functions, respectively. Therefore, $F_{Y\text{-sum}}(y)$ for $y \geq 0$ can be written, from (E-10) and (E-11), as ($F_{Y\text{-sum}}(y)$ is zero for negative y)

$$F_{Y\text{-sum}}(y) = \sum_{m=0}^{M} A_m - \sum_{m=1}^{M} A_m \mathrm{e}^{-y/\mu_{m\mathrm{D}}} \tag{E-12a}$$

$$= 1 - \sum_{m=1}^{M} \mathrm{e}^{(1-\mathrm{e}^{2r})/\mu_{\mathrm{S}m}} \prod_{\substack{k=1 \\ k\neq m}}^{M} \left[1 + \frac{\mathrm{e}^{(1-\mathrm{e}^{2r})/\mu_{\mathrm{S}k}}}{\mu_{m\mathrm{D}}/\mu_{k\mathrm{D}} - 1}\right] \mathrm{e}^{-y/\mu_{m\mathrm{D}}} \tag{E-12b}$$

where we obtain (E-12b) using the fact that

$$M_{Y\text{-sum}}(0) = \sum_{m=0}^{M} A_m = 1. \tag{E-13}$$

In the symmetric case, we directly use the definition of Y_m given in (4.39) and write

$$F_{Y\text{-sum}}(y) = \sum_{m=0}^{M} \binom{M}{m} F_{\mathrm{SR}}^{M-m}(\mathrm{e}^{2r}-1) \left[1 - F_{\mathrm{SR}}(\mathrm{e}^{2r}-1)\right]^m F_{m\text{-RD}}(y) \tag{E-14}$$

where $F_{m\text{-RD}}(\cdot)$ is the CDF of the sum of m different $\gamma_{i\mathrm{D}}$'s. We define $F_{0\text{-RD}}(y)$ as unity

for any nonnegative y. It is known that the sum of m independent, exponentially distributed RVs with the same mean value has a chi-square distribution with $2m$ degrees of freedom [50, p. 45]. Therefore, we can write

$$F_{m\text{-RD}}(y) = P\left(m, \frac{y}{\mu_{\text{RD}}}\right) = 1 - \mathrm{e}^{-y/\mu_{\text{RD}}} \sum_{k=0}^{m-1} \frac{(y/\mu_{\text{RD}})^k}{k!} \tag{E-15}$$

where $P(\cdot,\cdot)$ is the regularized lower incomplete gamma function [86, eq. 6.5.3].

Now, applying the results (E-12)–(E-15) to (E-4)–(E-9), and using (E-1) and (E-2) for expressing $f_{\text{SD}}(\cdot)$ and $F_{\text{SD}}(\cdot)$, yields the outage probabilities and average capacities in Tables 4.2 and 4.3 after simplification.

E.2 Selection Relaying

The outage probabilities in selection relaying for general fading are given from (4.49) and (4.50) as

$$\Pr\left\{I_{\max}^{(\text{sel, PCC})} < r\right\} = \int_0^{\mathrm{e}^r-1} \mathrm{d}\gamma \prod_{m=1}^{M} F_{Y_m}\left(\frac{\mathrm{e}^{2r}}{1+\gamma} - 1\right) f_{\text{SD}}(\gamma) \tag{E-16}$$

and

$$\Pr\left\{I_{\max}^{(\text{sel, RC})} < r\right\} = \int_0^{\frac{\mathrm{e}^{2r}-1}{2}} \mathrm{d}\gamma \prod_{m=1}^{M} F_{Y_m}(\mathrm{e}^{2r} - 1 - \gamma)\, f_{\text{SD}}(\gamma) \tag{E-17}$$

which give the corresponding average capacities, after being applied to (4.2), as

$$\begin{aligned}\overline{I_{\max}^{(\text{sel, PCC})}} &= \int_0^{\infty} \frac{\mathrm{d}u}{u+1} \left[1 - F_{\text{SD}}(u)\right] \\ &\quad + \int_0^{\infty} \mathrm{d}r \int_0^{\mathrm{e}^r-1} \mathrm{d}\gamma \left[1 - \prod_{m=1}^{M} F_{Y_m}\left(\frac{\mathrm{e}^{2r}}{1+\gamma} - 1\right)\right] f_{\text{SD}}(\gamma)\end{aligned} \tag{E-18}$$

and

$$\begin{aligned}\overline{I_{\max}^{(\text{sel, RC})}} &= \int_0^{\infty} \frac{\mathrm{d}u}{2u+1} \left[1 - F_{\text{SD}}(u)\right] \\ &\quad + \int_0^{\infty} \mathrm{d}r \int_0^{\frac{\mathrm{e}^{2r}-1}{2}} \mathrm{d}\gamma \left[1 - \prod_{m=1}^{M} F_{Y_m}(\mathrm{e}^{2r} - 1 - \gamma)\right] f_{\text{SD}}(\gamma).\end{aligned} \tag{E-19}$$

Also, note that in the no SD-link case, after invoking (4.59), (E-16)–(E-19) reduce to

$$\Pr\left\{I_{\max}^{(\text{sel, no SD})} < r\right\} = \prod_{m=1}^{M} F_{Y_m}(\mathrm{e}^{2r} - 1) \tag{E-20}$$

and

$$\overline{I_{\max}^{(\text{sel, no SD})}} = \int_0^\infty \mathrm{d}r \left[1 - \prod_{m=1}^{M} F_{Y_m}\left(\mathrm{e}^{2r}-1\right)\right] \tag{E-21}$$

for both PCC and RC strategies. This means that here again, like superimposed relaying, the PCC and RC strategies coincide when the SD link is blocked.

All the results (E-16)–(E-21) involve the product $\prod_{m=1}^{M} F_{Y_m}(y)$ which can be simplified as follows. In the asymmetric case,[1] we have, from (4.39b) and (4.54),

$$\begin{aligned}
\prod_{m=1}^{M} F_{Y_m}(y) &= \prod_{m=1}^{M} \Big\{1 - \left[1 - F_{\mathrm{S}m}\left(\mathrm{e}^{2r}-1\right)\right]\left[1 - F_{m\mathrm{D}}(y)\right]\Big\} \\
&= \sum_{\mathcal{A}\subset\{1,\cdots,M\}} (-1)^{|\mathcal{A}|} \prod_{m\in\mathcal{A}} \left[1 - F_{\mathrm{S}m}\left(\mathrm{e}^{2r}-1\right)\right]\left[1 - F_{m\mathrm{D}}(y)\right] \\
&= \sum_{\mathcal{A}\subset\{1,\cdots,M\}} (-1)^{|\mathcal{A}|} \prod_{m\in\mathcal{A}} \mathrm{e}^{(1-\mathrm{e}^{2r})/\mu_{\mathrm{S}m} - y/\mu_{m\mathrm{D}}} \\
&= \sum_{\mathcal{A}\subset\{1,\cdots,M\}} (-1)^{|\mathcal{A}|}\, \mathrm{e}^{(1-\mathrm{e}^{2r})/\mu_{\mathrm{S}\mathcal{A}} - y/\mu_{\mathcal{A}\mathrm{D}}}
\end{aligned} \tag{E-22}$$

where $|\mathcal{A}|$ is the cardinality of $\mathcal{A}$, and where $\mu_{\mathrm{S}\mathcal{A}}$ and $\mu_{\mathcal{A}\mathrm{D}}$ are defined by (4.60) and (4.61). In the symmetric case, (E-22) simply becomes

$$\prod_{m=1}^{M} F_{Y_m}(y) = \sum_{m=0}^{M} \binom{M}{m} (-1)^m\, \mathrm{e}^{m(1-\mathrm{e}^{2r})/\mu_{\mathrm{SR}} - m\,y/\mu_{\mathrm{RD}}}. \tag{E-23}$$

Now, the results for selection relaying given in Tables 4.4 and 4.5 can be derived by applying (E-22) and (E-23) to (E-16)–(E-21) and substituting for $f_{\mathrm{SD}}(\cdot)$ and $F_{\mathrm{SD}}(\cdot)$ from (E-1) and (E-2), and then, simplifying the expressions obtained.

E.3 Orthogonal Relaying

In orthogonal relaying, the outage probabilities for the general fading case can be written from (4.51) and (4.52) as

$$\Pr\left\{I_{\max}^{(\text{ort, PCC})} < r\right\} = \int_0^{\mathrm{e}^{(M+1)r}-1} \mathrm{d}\gamma\; F_{1+Y\text{-prod}}\left(\frac{\mathrm{e}^{(M+1)r}}{1+\gamma}\right) f_{\mathrm{SD}}(\gamma) \tag{E-24}$$

and

$$\Pr\left\{I_{\max}^{(\text{ort, RC})} < r\right\} = \int_0^{\mathrm{e}^{(M+1)r}-1} \mathrm{d}\gamma\; F_{Y\text{-sum}}\left(\mathrm{e}^{(M+1)r} - 1 - \gamma\right) f_{\mathrm{SD}}(\gamma) \tag{E-25}$$

[1] Recall that this case for selection relaying represents the most general scenario, in which μ_{SD}, the $\mu_{\mathrm{S}m}$'s, and the $\mu_{m\mathrm{D}}$'s can independently take any value.

where $F_{1+Y\text{-prod}}(\cdot)$ is the CDF of,

$$\prod_{m=1}^{M}(1+Y_m).$$

Note that we have converted $F_{\ln 1+Y\text{-sum}}(\cdot)$ in (4.51) (which is the CDF of the summation (4.53)) to $F_{1+Y\text{-prod}}(\cdot)$ in (E-24) using the relation

$$F_{\ln 1+Y\text{-sum}}(y) = F_{1+Y\text{-prod}}(\mathrm{e}^{y})$$

for subsequent analytical convenience.

We also write the average capacities in the PCC and RC cases from (4.2), (E-24), and (E-25) as

$$\begin{aligned}\overline{I_{\max}^{(\mathrm{ort,\,PCC})}} &= \frac{1}{M+1}\int_0^{\infty}\frac{\mathrm{d}u}{u+1}\left[1-F_{\mathrm{SD}}(u)\right] \\ &\quad + \int_0^{\infty}\mathrm{d}r\int_0^{\mathrm{e}^{(M+1)r}-1}\mathrm{d}\gamma\left[1-F_{1+Y\text{-prod}}\left(\frac{\mathrm{e}^{(M+1)r}}{1+\gamma}\right)\right]f_{\mathrm{SD}}(\gamma) \qquad \text{(E-26)}\end{aligned}$$

and

$$\begin{aligned}\overline{I_{\max}^{(\mathrm{ort,\,RC})}} &= \frac{1}{M+1}\int_0^{\infty}\frac{\mathrm{d}u}{u+1}\left[1-F_{\mathrm{SD}}(u)\right] \\ &\quad + \int_0^{\infty}\mathrm{d}r\int_0^{\mathrm{e}^{(M+1)r}-1}\mathrm{d}\gamma\left[1-F_{Y\text{-sum}}\left(\mathrm{e}^{(M+1)r}-1-\gamma\right)\right]f_{\mathrm{SD}}(\gamma). \qquad \text{(E-27)}\end{aligned}$$

Further, the corresponding no SD-link expressions for (E-24)–(E-27) are derived, using (4.59), as

$$\Pr\left\{I_{\max}^{(\mathrm{ort,\,no\,SD,\,PCC})} < r\right\} = F_{1+Y\text{-prod}}\left(\mathrm{e}^{(M+1)r}\right) \qquad \text{(E-28)}$$

$$\Pr\left\{I_{\max}^{(\mathrm{ort,\,no\,SD,\,RC})} < r\right\} = F_{Y\text{-sum}}\left(\mathrm{e}^{(M+1)r}-1\right) \qquad \text{(E-29)}$$

$$\overline{I_{\max}^{(\mathrm{ort,\,no\,SD,\,PCC})}} = \int_0^{\infty}\mathrm{d}r\left[1-F_{1+Y\text{-prod}}\left(\mathrm{e}^{(M+1)r}\right)\right] \qquad \text{(E-30)}$$

and

$$\overline{I_{\max}^{(\mathrm{ort,\,no\,SD,\,RC})}} = \int_0^{\infty}\mathrm{d}r\left[1-F_{Y\text{-sum}}\left(\mathrm{e}^{(M+1)r}-1\right)\right]. \qquad \text{(E-31)}$$

Eqs. (E-24)–(E-31) show that calculating the outage probability and average capacity in orthogonal relaying requires knowledge of $F_{1+Y\text{-prod}}(\cdot)$ for the PCC and $F_{Y\text{-sum}}(\cdot)$ for the RC case. In orthogonal relaying, the CDF $F_{Y\text{-sum}}(\cdot)$ for Rayleigh fading is given by (E-12)–(E-15) for the different cases of asymmetric and symmetric links, after $2r$ is replaced with

$(M+1)r$ everywhere (cf. (4.39b)). All the expressions for the RC case given in Tables 4.6–4.9 are derived by applying (E-12)–(E-15) to (E-25), (E-27), (E-29), and (E-31), and simplifying the results. Therefore, we only consider $F_{1+Y\text{-prod}}(\cdot)$ for orthogonal relaying with PCC in the sequel.

It can be observed that no exact closed-form or mathematically tractable solution exists for $F_{1+Y\text{-prod}}(\cdot)$ in the Rayleigh fading case when $M > 1$. However, we can derive tight lower and upper bounds on $F_{1+Y\text{-prod}}(\cdot)$, which, as observed from (E-24), (E-26), (E-28), and (E-30), lead to lower and upper bounds on the outage probability and average capacity of orthogonal relaying with PCC.

Consider k independent, arbitrary, positive RVs X_i. We can write

$$\Big(1+\min_{i=1,\ldots,k} X_i\Big)^k \le \prod_{i=1}^{k}(1+X_i) \le \left(1+\frac{1}{k}\sum_{i=1}^{k} X_i\right)^k \tag{E-32}$$

where the second inequality in (E-32) follows from the arithmetic mean, geometric mean inequality [79, p. 669]. Note that the inequalities (E-32) become equalities when $k = 1$.[2] Then, (E-32) gives the result

$$\Pr\left\{\sum_{i=1}^{k} X_i < k\,x^{1/k} - k\right\} \le \Pr\left\{\prod_{i=1}^{k}(1+X_i) < x\right\} \le 1-\prod_{i=1}^{k}\Big(1-\Pr\Big\{X_i < x^{1/k}-1\Big\}\Big) \tag{E-33}$$

for $x \ge 0$. Now, using the definition of Y_m given in (4.39), we can condition on the values of m for which Y_m is nonzero, and apply (E-33) to the nonzero Y_m's. The result is

$$1-\sum_{\substack{\mathcal{A}\subset\{1,\cdots,M\}\\ \mathcal{A}\neq\varnothing}} \varepsilon(\mathcal{A})\Big[1-F_{\mathcal{A}\text{-RD}}\Big(|\mathcal{A}|\,y^{1/|\mathcal{A}|}-|\mathcal{A}|\Big)\Big] \le$$

$$F_{1+Y\text{-prod}}(y)$$

$$\le 1-\sum_{\substack{\mathcal{A}\subset\{1,\cdots,M\}\\ \mathcal{A}\neq\varnothing}} \varepsilon(\mathcal{A})\prod_{m\in\mathcal{A}}\Big[1-F_{m\text{D}}\Big(y^{1/|\mathcal{A}|}-1\Big)\Big] \tag{E-34a}$$

where $\mathcal{A}^{\text{c}}$ and $|\mathcal{A}|$ are the complement of $\mathcal{A}$ with respect to $\{1,\cdots,M\}$ and cardinality of $\mathcal{A}$, respectively, and where

$$\varepsilon(\mathcal{A}) \triangleq \prod_{m\in\mathcal{A}^{\text{c}}} F_{\text{S}m}\Big(\text{e}^{(M+1)r}-1\Big)\prod_{m\in\mathcal{A}}\Big[1-F_{\text{S}m}\Big(\text{e}^{(M+1)r}-1\Big)\Big] \tag{E-34b}$$

[2]The tightness of the bounds (E-32) is examined for the final resulting lower and upper bounds on the outage probability and average capacity by several numerical examples in Section 4.5.

is the probability that Y_m is nonzero only for $m \in \mathcal{A}$, and where $F_{\mathcal{A}\text{-RD}}(\cdot)$ is the CDF of,

$$\sum_{m\in\mathcal{A}} \gamma_{m\mathrm{D}}. \tag{E-34c}$$

Again, note that the bounds (E-34a) become the exact values when $M = 1$. The bounds are simply specialized to the Rayleigh fading case by substituting for $F_{\mathrm{S}m}(\cdot)$ and $F_{m\mathrm{D}}(\cdot)$ from (E-2). The only remaining unknown is $F_{\mathcal{A}\text{-RD}}(\cdot)$ which can be determined as follows.

In the case of asymmetric links, $F_{\mathcal{A}\text{-RD}}(\cdot)$ can be obtained in a manner very similar to (E-12), by calculating the MGF of the summation (E-34c). The procedure is straightforward with the final result

$$F_{\mathcal{A}\text{-RD}}(y) = 1 - \sum_{m\in\mathcal{A}} \frac{\mathrm{e}^{-y/\mu_{m\mathrm{D}}}}{\prod_{\substack{k\in\mathcal{A}\\k\neq m}} \left(1 - \frac{\mu_{k\mathrm{D}}}{\mu_{m\mathrm{D}}}\right)}. \tag{E-35}$$

In the symmetric case, $F_{\mathcal{A}\text{-RD}}(\cdot)$ becomes the CDF of the sum of $|\mathcal{A}|$ different $\gamma_{m\mathrm{D}}$'s. Therefore, we can write, directly from (E-15),

$$F_{\mathcal{A}\text{-RD}}(y) = P\left(|\mathcal{A}|, \frac{y}{\mu_{\mathrm{RD}}}\right). \tag{E-36}$$

Now, we have the bounds (E-34a) on $F_{1+Y\text{-prod}}(\cdot)$ with $F_{\mathcal{A}\text{-RD}}(\cdot)$ given by (E-35) or (E-36). Applying these bounds to (E-24), (E-26), (E-28), and (E-30), one obtains the results given in Tables 4.6–4.9 for PCC after performing the integrations and simplification.

Appendix F

Maximum Rates in P-1, P-2, and P-3 Under the APC

In this appendix, the derivation details for (5.39)–(5.41) are given. Consider the system model of Section 5.2. As explained in Section 5.6.2, only Gaussian-input channels are considered here for which (5.7e) gives the capacity.

Assume that for a given positive $\mathcal{E}$, the source and relay energies per 2-D DoF are $\mathcal{E}_{\rm S} = p\,\mathcal{E}$ and $\mathcal{E}_{\rm R} = q\,\mathcal{E}$, respectively, where $p > 0$ and $q \geq 0$. Note that based on (5.3)–(5.5) and (5.6), the SD, SR, and RD SNRs become $p\,\gamma_0$, $p\,\gamma_1$, and $q\,\gamma_2$, respectively. Also, using (5.7e), the capacities realized in the SD channel, SR channel, RD channel, and the multiaccess channel from the source and relay to the destination equal $\mathcal{C}(p\,\gamma_0)$, $\mathcal{C}(p\,\gamma_1)$, $\mathcal{C}(q\,\gamma_2)$, and $\mathcal{C}(p\,\gamma_0 + q\,\gamma_2)$, respectively. Therefore, based on the description of P-1, P-2, and P-3 in Section 5.3, when $\mathcal{C}(p\,\gamma_0) \geq \mathcal{C}(p\,\gamma_1)$ or equivalently $\gamma_0 \geq \gamma_1$, all the schemes reduce to DT where the maximum rate is $\mathcal{C}(p\,\gamma_0)$. Henceforth, we assume that

$$\gamma_0 < \gamma_1. \tag{F-1}$$

In the sequel, the protocols are investigated each in turn.

F.1 The P-1 Scheme

Taking steps similar to those leading to (5.14)–(5.17), we obtain

$$H = n_1\,\mathcal{C}(p\,\gamma_1) \tag{F-2}$$

$$H = n_1\,\mathcal{C}(p\,\gamma_0) + (n - n_1)\,\mathcal{C}(p\,\gamma_0 + q\,\gamma_2) \tag{F-3}$$

$$R^{(\text{P-1})} = \frac{H}{n} = \frac{\mathcal{C}(p\,\gamma_0 + q\,\gamma_2)\,\mathcal{C}(p\,\gamma_1)}{\mathcal{C}(p\,\gamma_0 + q\,\gamma_2) + \mathcal{C}(p\,\gamma_1) - \mathcal{C}(p\,\gamma_0)} \tag{F-4}$$

and

$$E^{(\text{P-1})} = \frac{n_1\mathcal{E}_{\text{S}} + (n - n_1)(\mathcal{E}_{\text{S}} + \mathcal{E}_{\text{R}})}{n} = \left[p + q\,\frac{\mathcal{C}(p\,\gamma_1) - \mathcal{C}(p\,\gamma_0)}{\mathcal{C}(p\,\gamma_0 + q\,\gamma_2) + \mathcal{C}(p\,\gamma_1) - \mathcal{C}(p\,\gamma_0)}\right]\mathcal{E}. \tag{F-5}$$

Therefore, the maximum rate can be written as

$$R_{\text{max}}^{(\text{P-1})} = \max_{\substack{p,\,q \\ p>0,\,q\geq 0}} R^{(\text{P-1})} \tag{F-6a}$$

subject to the APC ($E^{(\text{P-1})} = \mathcal{E}$)

$$p + q\,\frac{\mathcal{C}(p\,\gamma_1) - \mathcal{C}(p\,\gamma_0)}{\mathcal{C}(p\,\gamma_0 + q\,\gamma_2) + \mathcal{C}(p\,\gamma_1) - \mathcal{C}(p\,\gamma_0)} = 1. \tag{F-6b}$$

It is clear from (F-6b) and the facts that $p > 0$ and $q \geq 0$, that we should have $p \leq 1$. Next, we show that for any p in $(0, 1]$, there is a unique nonnegative q for which (F-6b) is satisfied. If $p = 1$, then $q = 0$ is trivially the only solution, which corresponds to DT where the relay is not used. Therefore, assume that $p \in (0, 1)$, and consider the expression,

$$\frac{[\mathcal{C}(p\,\gamma_1) - \mathcal{C}(p\,\gamma_0)]\,q}{\mathcal{C}(p\,\gamma_0 + q\,\gamma_2) + \mathcal{C}(p\,\gamma_1) - \mathcal{C}(p\,\gamma_0)} \tag{F-7}$$

for $q \geq 0$. Note that from (F-1), (F-7) is nonnegative. Also, (F-7) is zero at $q = 0$ and approaches ∞ as $q \to \infty$. Also, the derivative of (F-7) with respect to q can be written as,

$$U\left[V + \ln(1 + p\,\gamma_0 + q\,\gamma_2) - \frac{\gamma_2\,q}{1 + p\,\gamma_0 + q\,\gamma_2}\right] \tag{F-8}$$

where U and V are two positive values. Invoking the inequality [86, eq. 4.1.33]

$$(1 + x)\ln(1 + x) \geq x \tag{F-9}$$

which holds for $x > -1$, one can observe that (F-8) is positive for $q \geq 0$. These observations show that (F-7) strictly increases from 0 to ∞ with q. Therefore, a unique q can be obtained for which (F-7) equals $1 - p$ and (F-6b) is satisfied. Now, we proceed to solve (F-6b) for (the unique) q in terms of p when $0 < p < 1$.

After some algebraic manipulations, (F-6b) can be rearranged as

$$-(1 + p\,\gamma_0 + q\,\gamma_2)\,\xi\,\mathrm{e}^{-(1+p\,\gamma_0+q\,\gamma_2)\,\xi} = -\xi\,\mathrm{e}^{-[1+p\,\gamma_0+(1-p)\gamma_2]\,\xi} \tag{F-10}$$

where ξ has been given in (5.39c). Now, consider the Lambert W-function [106], defined

as $W(z)$ for a complex-valued z such that

$$W(z)\,\mathrm{e}^{W(z)} = z. \tag{F-11}$$

The Lambert W-function, like the logarithm function, is a multivalued function that has infinitely many branches. Branch k is denoted $W_k(\cdot)$ for integer k. The principle branch is the zeroth branch, also denoted $W(\cdot)$. The ranges of different branches have been shown in the "W-plane" in Fig. F.1. The range of a branch is the region onto which the branch maps the complex plane. In Fig. F.1, the branch boundaries are represented by heavy solid lines. Each boundary line belongs to the region below it.

Now, note that in (F-10), the negative real-valued expression $-(1 + p\,\gamma_0 + q\,\gamma_2)\,\xi$ becomes a Lambert W-function of the right-hand side expression of the equality. Referring to Fig. F.1, we observe that only Branch -1 and Branch 0 can return negative real-valued numbers, respectively no greater and no smaller than -1. To determine which branch should be employed to solve (F-10), we should examine $(p\,\gamma_0 + q\,\gamma_2 + 1)\,\xi$ to see if it is smaller or greater than 1.

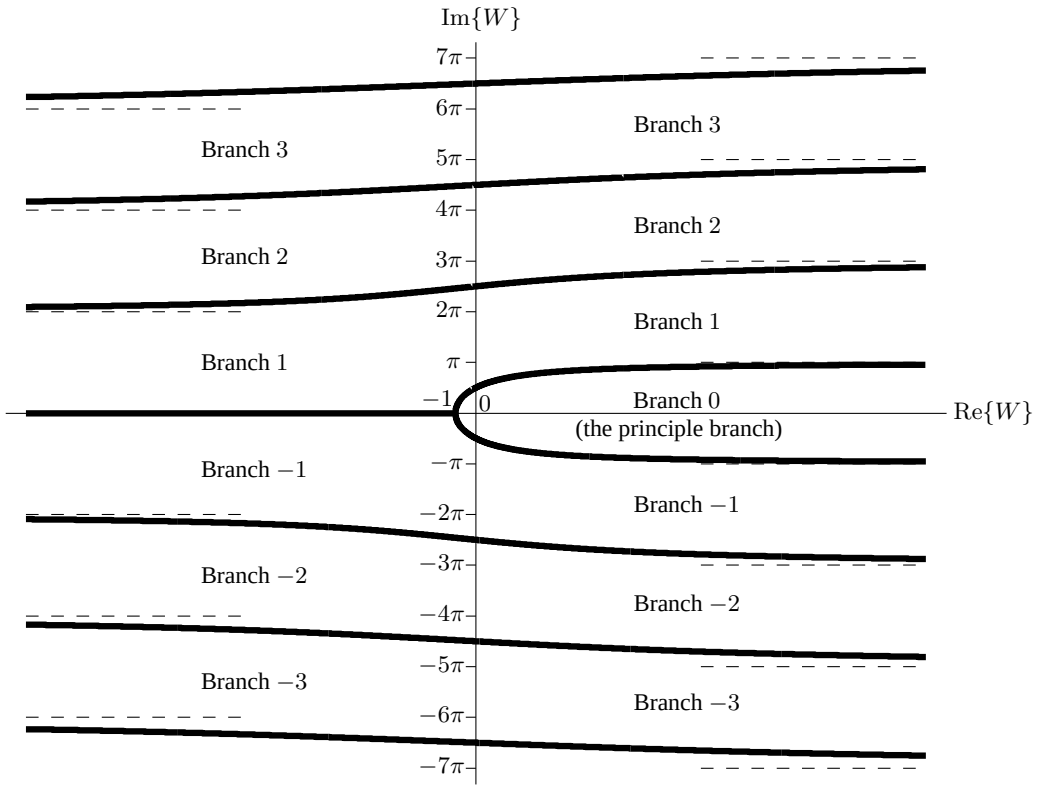

Fig. F.1. The ranges of branches of the Lambert W-function (after [106]).

Substituting for ξ from (5.39c), we can write

$$(1+p\,\gamma_0+q\,\gamma_2)\,\xi = \frac{\mathcal{C}(p\gamma_1)-\mathcal{C}(p\gamma_0)}{(1-p)\gamma_2}\,(1+p\,\gamma_0+q\,\gamma_2) \tag{F-12a}$$

$$= \frac{(1+p\,\gamma_0+q\,\gamma_2)\ln(1+p\,\gamma_0+q\,\gamma_2)}{(p+q-1)\gamma_2} \tag{F-12b}$$

$$> \frac{(1+q\,\gamma_2)\ln(1+q\,\gamma_2)}{q\,\gamma_2} \tag{F-12c}$$

$$\geq 1 \tag{F-12d}$$

where (F-12b) is obtained by rearranging (F-6b), and where (F-12c) comes from the facts that $0<p<1$ and $q>0$. Finally, (F-12d) follows from (F-9). Therefore, we have

$$-(1+p\,\gamma_0+q\,\gamma_2)\,\xi < -1. \tag{F-13}$$

Thus, the function $W_{-1}(\cdot)$ is employed to solve (F-10), which yields

$$q = -\frac{1}{\gamma_2}\left\{\frac{1}{\xi}\mathrm{W}_{-1}\left(-\xi\,\mathrm{e}^{-[1+p\,\gamma_0+(1-p)\gamma_2]\,\xi}\right)+1+p\,\gamma_0\right\}. \tag{F-14}$$

Combining (F-4), (F-6a), (F-14), and the fact that when $p=1$ we have $q=0$, yields the final result (5.39).

F.2 The P-2 Scheme

Following the analysis in Section 5.3.3 while having C_0, C_1, C_2, and C_{m} replaced with $\mathcal{C}(p\,\gamma_0)$, $\mathcal{C}(p\,\gamma_1)$, $\mathcal{C}(q\,\gamma_2)$, and $\mathcal{C}(p\,\gamma_0+q\,\gamma_2)$, respectively, we observe that again point A in Fig. 5.1 is the optimal operating point in Phase II for any given (p,q), and that

$$R_{\max}^{(\text{P-2})} = \max_{\substack{p,\,q\\ p>0,\,q\geq 0}} \frac{\mathcal{C}(p\,\gamma_0+q\,\gamma_2)\,\mathcal{C}(p\,\gamma_1)-\mathcal{C}^2(p\,\gamma_0)}{\mathcal{C}(p\,\gamma_0+q\,\gamma_2)+\mathcal{C}(p\,\gamma_1)-2\,\mathcal{C}(p\,\gamma_0)} \tag{F-15a}$$

subject to the APC

$$p+q\,\frac{\mathcal{C}(p\,\gamma_1)-\mathcal{C}(p\,\gamma_0)}{\mathcal{C}(p\,\gamma_0+q\,\gamma_2)+\mathcal{C}(p\,\gamma_1)-2\,\mathcal{C}(p\,\gamma_0)} = 1. \tag{F-15b}$$

It can be seen from (F-15) that $0<p\leq 1$. We first show that for any p in $(0,1]$, there is a unique nonnegative q satisfying (F-15b). If $p=1$, then $q=0$ is the only solution. Now assume that $p\in(0,1)$, and consider the expression,

$$\frac{[\mathcal{C}(p\,\gamma_1)-\mathcal{C}(p\,\gamma_0)]\,q}{\mathcal{C}(p\,\gamma_0+q\,\gamma_2)+\mathcal{C}(p\,\gamma_1)-2\,\mathcal{C}(p\,\gamma_0)} \tag{F-16}$$

which is 0 and approaches ∞ as $q=0$ and $q\to\infty$, respectively (recall the condition

(F-1)). Also, we can write the derivative of (F-16) with respect to q as

$$D \triangleq U\left[\ln(1+p\,\gamma_0+q\,\gamma_2)+\ln(1+p\,\gamma_1)-2\,\ln(1+p\,\gamma_0)-\frac{\gamma_2\,q}{1+p\,\gamma_0+q\,\gamma_2}\right] \quad \text{(F-17)}$$

where U is a positive value. Now, we have

$$D = U\left[\ln\left(1+\frac{q\,\gamma_2}{1+p\,\gamma_0}\right)+\ln\left(\frac{1+p\,\gamma_1}{1+p\,\gamma_0}\right)-\frac{q\,\gamma_2}{1+p\,\gamma_0+q\,\gamma_2}\right] \quad \text{(F-18a)}$$

$$> U\left[\ln\left(1+\frac{q\,\gamma_2}{1+p\,\gamma_0}\right)-\frac{q\,\gamma_2}{1+p\,\gamma_0+q\,\gamma_2}\right] \quad \text{(F-18b)}$$

$$\geq 0 \quad \text{(F-18c)}$$

where (F-18b) results from (F-1), and where (F-18c) follows directly from (F-9). The results obtained indicate that (F-16) strictly increases from 0 to ∞ with q. Hence, for any $p \in (0,1)$, there is a positive q for which (F-16) equals $1-p$ and (F-15b) is satisfied. Next, we derive q from (F-15b) in terms of p.

Rearranging (F-15b) one obtains an equation similar to (F-10), as

$$-(1+p\,\gamma_0+q\,\gamma_2)\,\xi\,\mathrm{e}^{-(1+p\,\gamma_0+q\,\gamma_2)\,\xi} = -(1+p\,\gamma_0)\,\xi\,\mathrm{e}^{-[1+p\,\gamma_0+(1-p)\gamma_2]\,\xi} \quad \text{(F-19)}$$

where ξ has been given in (5.39c). Eq. (F-19) can be solved like (F-10) using the Lambert W-function. We should only determine that $(1+p\,\gamma_0+q\,\gamma_2)\,\xi$ is smaller or greater than 1. To meet this objective, we write

$$(1+p\,\gamma_0+q\,\gamma_2)\,\xi = \frac{(1+p\,\gamma_0+q\,\gamma_2)[\ln(1+p\,\gamma_0+q\,\gamma_2)-\ln(1+p\,\gamma_0)]}{(p+q-1)\gamma_2} \quad \text{(F-20a)}$$

$$= \frac{(1+p\,\gamma_0)\left(1+\frac{q\,\gamma_2}{1+p\,\gamma_0}\right)\ln\left(1+\frac{q\,\gamma_2}{1+p\,\gamma_0}\right)}{(p+q-1)\gamma_2} \quad \text{(F-20b)}$$

$$\geq \frac{q}{p+q-1} \quad \text{(F-20c)}$$

$$> 1 \quad \text{(F-20d)}$$

where (F-20a) is obtained from (5.39c) and by manipulating (F-19), and where (F-20c) follows from (F-9). Based on (F-20), we use $W_{-1}(\cdot)$ to derive q from (F-19). The result is

$$q = -\frac{1}{\gamma_2}\left\{\frac{1}{\xi}\mathrm{W}_{-1}\left(-(1+p\,\gamma_0)\,\xi\,\mathrm{e}^{-[1+p\,\gamma_0+(1-p)\gamma_2]\,\xi}\right)+1+p\,\gamma_0\right\} \quad \text{(F-21)}$$

which completes the derivation of (5.40).

F.3 The P-3 Scheme

In P-3, like P-1 and P-2, if (F-1) (which is independent of p and q) does not hold, the system reduces to DT. However, unlike P-1 and P-2, even if (F-1) holds, the system reduces to DT if the RD SNR is not larger than the SD SNR (see Section 5.3.4). In fact, under the condition (F-1) we can write, for P-3,

$$p\,\gamma_0 \geq q\,\gamma_2 \iff \text{reversion to DT.} \tag{F-22}$$

First, we show that if $\gamma_0 \geq \gamma_2$, the best P-3 rate under the APC is obtained when $p = 1$ and reversion to DT (based on (F-22)) occurs. Assume that $\gamma_0 \geq \gamma_2$, and consider three schemes S-A, S-B, and S-C, and two positive values p and q. Scheme S-A is a P-3 system with $\mathcal{E}_{\rm S} = p\,\mathcal{E}$ and $\mathcal{E}_{\rm R} = q\,\mathcal{E}$ where $p\,\gamma_0 < q\,\gamma_2$. In S-A, assume that a message of entropy $H_{\rm A}$ is communicated to the destination in Phases I and II with n_1 and n_2 symbols, respectively, and that the short-term average energy equals $\mathcal{E}$. In S-B, the source communicates its message with entropy $H_{\rm B}$ by first transmitting n_1 symbols with energy per symbol $p\,\mathcal{E}$, and then transmitting n_2 symbols with energy per symbol $q\,\mathcal{E}$. It is obvious that the short-term average energy in S-B equals $\mathcal{E}$, the same as that in S-A. Scheme S-C is similar to S-B, with the difference that the source communicates its message with entropy $H_{\rm C}$ by transmitting all n symbols with the same energy per symbol $\mathcal{E}$. Now, it is clear that $H_{\rm A} \leq H_{\rm B}$, as in S-A, n_2 symbols are transmitted with SNR $q\,\gamma_2$, while in S-B, the corresponding SNR is $q\,\gamma_0$. Also, $H_{\rm B} < H_{\rm C}$ as in S-C, all symbols are transmitted with the same energy $\mathcal{E}$. Therefore, $H_{\rm A} < H_{\rm C}$, which shows that P-3 cannot be superior to DT under the APC when $\gamma_0 \geq \gamma_2$. In other words, when $\gamma_0 \geq \gamma_2$, the maximum APC rate of P-3 equals the DT rate, i.e. $\mathcal{C}(\gamma_0)$.

In the following, we assume that not only (F-1) holds, but also we have

$$\gamma_0 < \gamma_2. \tag{F-23}$$

However, $p\,\gamma_0$ may exceed or be exceeded by $q\,\gamma_2$, depending on the values of p and q.

Considering the P-3 scheme depicted in Table 5.1 and performing an analysis similar to that yielding (5.24), we obtain

$$R_{\rm max}^{\rm (P\text{-}3)} = \max_{\substack{p,\,q \\ p>0,\,q\geq 0}} \frac{\mathcal{C}(p\,\gamma_1)\,\mathcal{C}\left(\max\{p\,\gamma_0, q\,\gamma_2\}\right)}{\mathcal{C}(p\,\gamma_1) + \mathcal{C}\left(\max\{p\,\gamma_0, q\,\gamma_2\}\right) - \mathcal{C}(p\,\gamma_0)}. \tag{F-24}$$

where $\max\{\cdot\}$ in the argument of $\mathcal{C}(\cdot)$ is for taking (F-22) into account. The maximization

(F-24) is subject to the APC that the short-term average energy, $E^{(\text{P-3})}$, equals $\mathcal{E}$. Next, we derive an expression for $E^{(\text{P-3})}$ and evaluate the APC.

Consider the example shown in Table 5.1. We obtain, like (5.14) and (5.23),

$$H = n_1\, \mathcal{C}(p\,\gamma_1) \tag{F-25}$$

and

$$H = n_1\, \mathcal{C}(p\,\gamma_0) + (n - n_1)\, \mathcal{C}(q\,\gamma_2). \tag{F-26}$$

Meanwhile, one has

$$E^{(\text{P-3})} = \frac{n_1\, \mathcal{E}_{\text{S}} + (n - n_1)\, \mathcal{E}_{\text{R}}}{n} = \frac{n_1\, p + (n - n_1)\, q}{n}\, \mathcal{E}. \tag{F-27}$$

Now, combining (F-25)–(F-27), and applying (F-22) yields

$$E^{(\text{P-3})} = \begin{cases} \frac{p\,\mathcal{C}(q\,\gamma_2) + q[\mathcal{C}(p\,\gamma_1) - \mathcal{C}(p\,\gamma_0)]}{\mathcal{C}(q\,\gamma_2) + \mathcal{C}(p\,\gamma_1) - \mathcal{C}(p\,\gamma_0)}\, \mathcal{E}, & p\,\gamma_0 < q\,\gamma_2 \\ p\,\mathcal{E}, & p\,\gamma_0 \geq q\,\gamma_2 \end{cases}. \tag{F-28}$$

Therefore, the APC $E^{(\text{P-3})} = \mathcal{E}$ becomes,

$$X \;\text{ or }\; Y \tag{F-29a}$$

where X and Y are two sets of constraints as,

$$X\colon\;\; \frac{p\,\mathcal{C}(q\,\gamma_2) + q[\mathcal{C}(p\,\gamma_1) - \mathcal{C}(p\,\gamma_0)]}{\mathcal{C}(q\,\gamma_2) + \mathcal{C}(p\,\gamma_1) - \mathcal{C}(p\,\gamma_0)} = 1 \;\text{ and }\; p\,\gamma_0 < q\,\gamma_2 \tag{F-29b}$$

and

$$Y\colon\;\; p = 1 \;\text{ and }\; q \leq \frac{\gamma_0}{\gamma_2}. \tag{F-29c}$$

Note that under (F-23), $p = q = 1$ satisfies X and makes the objective function of (F-24) exceed $\mathcal{C}(\gamma_0)$. Using this observation and the fact that if (F-23) does not hold, $R_{\text{max}}^{(\text{P-3})}$ equals $\mathcal{C}(\gamma_0)$, one obtains, from applying (F-29) to (F-24),

$$R_{\text{max}}^{(\text{P-3})} = \begin{cases} \max_{\text{subject to } X} \frac{\mathcal{C}(p\,\gamma_1)\,\mathcal{C}(q\,\gamma_2)}{\mathcal{C}(p\,\gamma_1) + \mathcal{C}(q\,\gamma_2) - \mathcal{C}(p\,\gamma_0)}, & \gamma_0 < \gamma_2 \\ \mathcal{C}(\gamma_0), & \gamma_0 \geq \gamma_2 \end{cases} \tag{F-30}$$

Next, we investigate the pairs (p, q) for which X is satisfied.

Consider the expression,

$$\frac{p\,\mathcal{C}(q\,\gamma_2) + q[\mathcal{C}(p\,\gamma_1) - \mathcal{C}(p\,\gamma_0)]}{\mathcal{C}(q\,\gamma_2) + \mathcal{C}(p\,\gamma_1) - \mathcal{C}(p\,\gamma_0)}. \tag{F-31}$$

It is straightforward to verify by differentiation and using (F-1) and (F-9) that like (F-7) and (F-16), the expression (F-31) for a given p strictly increases from 0 to ∞ with q. Therefore, for a given p, if (F-31) evaluated at $q = p\,\gamma_0/\gamma_2$ is smaller than 1, then a unique q can be found for which X holds. Otherwise, no q can satisfy X. The expression (F-31) evaluated at $q = p\,\gamma_0/\gamma_2$ becomes

$$L(p) \triangleq p\left[\left(1-\frac{\gamma_0}{\gamma_2}\right)\frac{\mathcal{C}(p\,\gamma_0)}{\mathcal{C}(p\,\gamma_1)}+\frac{\gamma_0}{\gamma_2}\right]. \tag{F-32}$$

Now, consider Lemma F.1 which reveals a key fact about $L(p)$.

Lemma F.1. The function

$$f(x) = x\left[(1-c)\frac{\ln(1+ax)}{\ln(1+bx)}+c\right] \tag{F-33}$$

for $0 < a < b$, $0 < c < 1$, and $x > 0$, is an unbounded, strictly increasing function of x.

Proof. We know that $\ln(1+ax)/\ln(1+bx) \to 1$ as $x \to \infty$, by l'Hôpital's rule [86, eq. 3.4.1]. Therefore, $f(x)$ approaches ∞ as $x \to \infty$, which proves part of the lemma. To prove the remainder, first note that the function $(1+x)\ln(1+x)/x$ for $x > 0$, is a strictly increasing function. This can be proved by differentiation and using the inequality $\ln(1+x) < x$ for $x > 0$ [86, eq. 4.1.33]. Using this result and by differentiation, we can show that the function $\ln(1+ax)/\ln(1+bx)$ for $0 < a < b$ and $x > 0$ is a strictly increasing function of x. As $1-c$ and c are both positive, the proof of the lemma is completed. ■

Lemma F.1 indicates that under (F-1), $L(p)$ is a strictly increasing function which increases from 0 to ∞ with p. Therefore, if we assume that p_0 is the (unique) positive root of $L(p)-1$, then only for $p < p_0$ we have $L(p) < 1$ and can find (p, q) that satisfies X.

Before proceeding to derive q in terms of p for $p < p_0$, we examine the value of p_0. First, note that

$$\frac{\gamma_0}{\gamma_1} < \frac{\ln(1+p\,\gamma_0)}{\ln(1+p\,\gamma_1)} < 1 \tag{F-34}$$

where the left inequality is obtained by the fact that $\ln(1+x)/x$ is a strictly decreasing function of x, verifiable by differentiation and using (F-9), and where the right inequality comes from (F-1). Now, combining (F-23), (F-32), and (F-34), and using the fact that $L(p)$ is an increasing function, yields

$$1 < p_0 < \left[\left(1-\frac{\gamma_0}{\gamma_2}\right)\frac{\gamma_0}{\gamma_1}+\frac{\gamma_0}{\gamma_2}\right]^{-1}. \tag{F-35}$$

Employing the bounds in (F-35) and an iterative numerical method such as the bisection method, fixed-point iteration, and Newton's method [112, Chapter 2], one can find p_0 with great accuracy using a few iterations.

Now assume that $0 < p < p_0$. We desire to calculate q in terms of p when

$$\frac{p\,\mathcal{C}(q\,\gamma_2) + q[\mathcal{C}(p\,\gamma_1) - \mathcal{C}(p\,\gamma_0)]}{\mathcal{C}(q\,\gamma_2) + \mathcal{C}(p\,\gamma_1) - \mathcal{C}(p\,\gamma_0)} = 1. \tag{F-36}$$

Rearranging (F-36), we obtain, assuming that $p \neq 1$,

$$-(1+\gamma_2\,q)\,\xi\,\mathrm{e}^{-(1+\gamma_2\,q)\,\xi} = -\xi\,\mathrm{e}^{-(1+\gamma_2)\,\xi} \tag{F-37}$$

where ξ is defined by (5.39c). It can be verified from (F-23) and (F-29b) that when $p = 1$, q equal to 1 is the (only) solution satisfying X. Subsequently, we assume that $p \neq 1$.

Using a branch of the Lambert W-function, we can solve (F-37) to find q like (F-10) and (F-19). We only need to determine which branch is used. We know from the definition of ξ that $\xi > 0$ if $p < 1$ and $\xi < 0$ if $p > 1$. It is observed from the ranges of the branches shown in Fig. F.1 that when $\xi < 0$, the zeroth branch has to be used. However, when $\xi > 0$, it is not readily known if Branch 0 or Branch -1 is the response. To determine that, we should examine $(1+\gamma_2\,q)\,\xi$ to see if it is smaller or greater than 1. We can write

$$(1+\gamma_2\,q)\,\xi = \frac{\ln(1+p\,\gamma_1) - \ln(1+p\,\gamma_0)}{(1-p)\gamma_2}(1+\gamma_2\,q) \tag{F-38a}$$

$$= \frac{\ln(1+\gamma_2\,q)}{(q-1)\gamma_2}(1+\gamma_2\,q) \tag{F-38b}$$

$$> \frac{\ln(1+\gamma_2\,q)}{\gamma_2\,q}(1+\gamma_2\,q) \tag{F-38c}$$

$$> 1 \tag{F-38d}$$

where (F-38a) comes from (5.39c), and where (F-38b) is obtained by manipulating (F-36), and where (F-38d) follows from (F-9). Therefore, Branch -1 has to be used when $p < 1$. Summarizing the results obtained, pairs (p, q) satisfying X, the constraint set given in (F-29b), are characterized by

$$0 < p < p_0 \tag{F-39a}$$

and

$$q = \begin{cases} -\frac{1}{\gamma_2}\left\{\frac{1}{\xi}\mathrm{W}_k\left(-\xi\,\mathrm{e}^{-(1+\gamma_2)\,\xi}\right) + 1\right\}, & p \neq 1 \\ 1, & p = 1 \end{cases} \tag{F-39b}$$

where $k = -1$ and $k = 0$ for $p < 1$ and $p > 1$, respectively. Combining (F-30) and (F-39) gives the final result (5.41).

Appendix G

Expected Values of the Transmission Times in P-n, P-γ, and P-t

In this appendix, the derivation details for (6.18)–(6.23) are given. We investigate the protocols each in turn and obtain the complementary CDFs $\Pr\{T_{\rm S} > t\}$ and $\Pr\{T_{{\rm R}_m} > t\}$ for any t and m. The final results (6.18)–(6.23) can be obtained by applying these complementary CDFs to (6.17). We do not mention the details of the integration (6.17) which leads to (6.18)–(6.23) for conciseness, as this only involves basic change of the order of integration or integration by parts. In the following, $u_{\rm SD}(\cdot)$, $u_{{\rm S}m}(\cdot)$, $u_{m{\rm D}}(\cdot)$, $U_{\rm SD}(\cdot)$, $U_{{\rm S}m}(\cdot)$, and $U_{m{\rm D}}(\cdot)$ are as defined in Section 6.4.1.

G.1 The P-n Scheme

Recall the definitions of $T_{\rm UL}$, the uplink time, $\mathcal{D}(t)$, the set of the indices of decoding relays at time t, and the τ's (6.4), and that L is the parameter of P-n. Based on the protocol, we have, for a given t,

$$\begin{aligned}\Pr\{T_{\rm S} > t\} &= \Pr\{T_{\rm S} > t, T_{\rm UL} > t\} + \Pr\{T_{\rm S} > t, T_{\rm UL} \le t\} \\ &= \Pr\{\tau_{\rm SD} > t, |\mathcal{D}(t)| < L\} \\ &\quad + \Pr\{\tau_{\rm SD} > t, |\mathcal{D}(t)| \ge L, \forall\, m \in \mathcal{D}(t) \colon \tau_{\rm SD} < \tau_{m{\rm D}}\}. \qquad \text{(G-1)}\end{aligned}$$

Now, using the theorem of total probability [81, p. 103], one obtains

$$\Pr\{T_{\rm S} > t\} = [1 - U_{\rm SD}(t)] \sum_{\substack{\mathcal{A} \subset \{1, \cdots, M\} \\ |\mathcal{A}| \le L-1}} \prod_{m \in \mathcal{A}} U_{{\rm S}m}(t) \prod_{m \in \mathcal{A}^{\rm c}} [1 - U_{{\rm S}m}(t)]$$

$$+ \sum_{\substack{\mathcal{A}\subset\{1,\cdots,M\}\\|\mathcal{A}|=L}} \sum_{k\in\mathcal{A}} \int_t^\infty \mathrm{d}x \int_0^t \mathrm{d}y \; u_{\mathrm{SD}}(x)\, u_{\mathrm{S}k}(y)$$

$$\times \prod_{m\in\mathcal{A}} [1 - U_{m\mathrm{D}}(x)] \prod_{\substack{m\in\mathcal{A}\\m\neq k}} U_{\mathrm{S}m}(y) \prod_{m\in\mathcal{A}^{\mathrm{c}}} [1 - U_{\mathrm{S}m}(y)]. \tag{G-2}$$

Variables x and y in (G-2) respectively represent τ_{SD} and $\tau_{\mathrm{S}(L)}$, defined as the time at which the Lth relay decodes.

Next for T_{R_m}, where $m \in \{1, \ldots, M\}$, we need to determine $\Pr\{T_{\mathrm{R}_m} > t\}$ for any given t. First, assume that relay R_m has been selected to transmit in the downlink. Then, from (6.13) we have $T_{\mathrm{R}_m} > t$, or equivalently $T_{\mathrm{DL}} > t$, whenever

$$\frac{T_{\mathrm{UL}}}{\tau_{\mathrm{SD}}} + \frac{t}{\tau_{m\mathrm{D}}} < 1. \tag{G-3}$$

Meanwhile, R_m transmits in the downlink only if it excels among the source and L first decoding relays and if τ_{SD} is greater than $\tau_{\mathrm{S}(L)}$, the decoding time of the L first relays. Combining all these facts, we can write

$$\begin{aligned}
\Pr\{T_{\mathrm{R}_m} > t\} &= \Pr\Big\{ m \in \mathcal{D}(\tau_{\mathrm{S}(L)}), \frac{\tau_{\mathrm{S}(L)}}{\tau_{\mathrm{SD}}} + \frac{t}{\tau_{m\mathrm{D}}} < 1, \tau_{m\mathrm{D}} < \tau_{\mathrm{SD}}, \\
&\qquad \forall\, i \in \mathcal{D}(\tau_{\mathrm{S}(L)}), i \neq m \colon \tau_{m\mathrm{D}} < \tau_{i\mathrm{D}} \Big\} \\
&= \sum_{\substack{\mathcal{A}\subset\{1,\cdots,M\}-\{m\}\\|\mathcal{A}|=L-1}} \sum_{k\in\mathcal{A}\cup\{m\}} \int_t^\infty \mathrm{d}x \int_0^\infty \mathrm{d}y \; u_{m\mathrm{D}}(x)\, u_{\mathrm{S}k}(y) \\
&\quad \times \left[1 - U_{\mathrm{SD}}\left(\max\left\{x, \frac{x\,y}{x-t}\right\}\right)\right] \prod_{i\in\mathcal{A}} [1 - U_{i\mathrm{D}}(x)] \\
&\quad \times \prod_{\substack{i\in\mathcal{A}\cup\{m\}\\i\neq k}} U_{\mathrm{S}i}(y) \prod_{i\in\mathcal{A}^{\mathrm{c}}\cup\{m\}} [1 - U_{\mathrm{S}i}(y)]
\end{aligned} \tag{G-4}$$

where variables x and y represent $\tau_{m\mathrm{D}}$ and $\tau_{\mathrm{S}(L)}$, respectively.

G.2 The P-γ Scheme

Recall that the system parameter here is a threshold SNR denoted γ_{th}. Also, τ_{th} is defined by (6.4) and γ_{th}, such that for example, $\tau_{\mathrm{SD}} < \tau_{\mathrm{th}}$ or $\tau_{m\mathrm{D}} < \tau_{\mathrm{th}}$ means that $\gamma_{\mathrm{SD}} > \gamma_{\mathrm{th}}$ or $\gamma_{m\mathrm{D}} > \gamma_{\mathrm{th}}$, i.e. Node S or Node R_m is AT.

The condition that Node S transmits more than t seconds is that no AT node, except

Node S itself, emerges before t, and that if all relays decode before t while no AT node has been found, Node S has the best link to Node D. Therefore, we have

$$\begin{aligned}\Pr\{T_{\rm S} > t\} &= \Pr\{t < \tau_{\rm SD} < \tau_{\rm th}\} + \Pr\Bigg\{\tau_{\rm SD} > t, \tau_{\rm SD} \geq \tau_{\rm th}, \\ &\qquad \bigcap_{m=1}^{M} \left(\tau_{{\rm S}m} > t \cup \tau_{m{\rm D}} \geq \tau_{\rm th}\right), \\ &\qquad \left[\left(\bigcup_{m=1}^{M} \tau_{{\rm S}m} > t\right) \cup \left(\bigcap_{m=1}^{M} \tau_{m{\rm D}} > \tau_{\rm SD}\right)\right]\Bigg\} \\ &= \max\{U_{\rm SD}(\tau_{\rm th}) - U_{\rm SD}(t), 0\} + [1 - U_{\rm SD}(\max\{t, \tau_{\rm th}\})] \\ &\quad \times \left\{\prod_{m=1}^{M} [1 - U_{{\rm S}m}(t)\, U_{m{\rm D}}(\tau_{\rm th})] - \prod_{m=1}^{M} U_{{\rm S}m}(t)\, [1 - U_{m{\rm D}}(\tau_{\rm th})]\right\} \\ &\quad + \prod_{m=1}^{M} U_{{\rm S}m}(t) \int_{\max\{t,\tau_{\rm th}\}}^{\infty} {\rm d}x\; u_{\rm SD}(x) \prod_{m=1}^{M} [1 - U_{m{\rm D}}(x)] \qquad \text{(G-5)}\end{aligned}$$

where $\cap$ and $\cup$ denote the intersection and union operations and where the integral in (G-5) has been derived by conditioning on $\tau_{\rm SD}$.

To determine $\Pr\{T_{{\rm R}_m} > t\}$, observe that Node ${\rm R}_m$ transmits more than t seconds in either of these two cases; 1) it is AT and

$$\frac{\tau_{{\rm S}m}}{\tau_{\rm SD}} + \frac{t}{\tau_{m{\rm D}}} < 1 \qquad \text{(G-6)}$$

(see (G-3)); 2) all relays decode while no AT node has been found, and ${\rm R}_m$ has the best link to Node D, and

$$\frac{\tau_{{\rm S}(M)}}{\tau_{\rm SD}} + \frac{t}{\tau_{m{\rm D}}} < 1 \qquad \text{(G-7)}$$

where $\tau_{{\rm S}(M)}$ is the time when all relays decode. Based on these facts, one can write

$$\begin{aligned}\Pr\{T_{{\rm R}_m} > t\} &= \Pr\Bigg\{\tau_{\rm SD} \geq \tau_{\rm th}, \tau_{m{\rm D}} < \tau_{\rm th}, \frac{\tau_{{\rm S}m}}{\tau_{\rm SD}} + \frac{t}{\tau_{m{\rm D}}} < 1, \\ &\qquad \bigcap_{\substack{i=1 \\ i\neq m}}^{M} \left(\tau_{{\rm S}i} > \tau_{{\rm S}m} \cup \tau_{i{\rm D}} \geq \tau_{\rm th}\right)\Bigg\} \qquad \text{(G-8a)} \\ &\quad + \Pr\left\{\tau_{\rm th} \leq \tau_{m{\rm D}} < \tau_{\rm SD}, \frac{\tau_{{\rm S}(M)}}{\tau_{\rm SD}} + \frac{t}{\tau_{m{\rm D}}} < 1, \min_{\substack{i=1,\cdots,M \\ i\neq m}} \tau_{i{\rm D}} > \tau_{m{\rm D}}\right\} \qquad \text{(G-8b)}\end{aligned}$$

$$= \int_0^\infty \mathrm{d}x \int_t^{\max\{t,\tau_{\rm th}\}} \mathrm{d}y \; u_{{\rm S}m}(x)\, u_{m{\rm D}}(y) \left[1 - U_{\rm SD}\left(\max\left\{\tau_{\rm th}, \frac{x\,y}{y-t}\right\}\right)\right]$$

$$\times \prod_{\substack{i=1 \\ i\neq m}}^{M} \left[1 - U_{{\rm S}i}(x)\, U_{i{\rm D}}(\tau_{\rm th})\right] \tag{G-8c}$$

$$+ \int_{\max\{t,\tau_{\rm th}\}}^\infty \mathrm{d}x \int_{\max\{t,\tau_{\rm th}\}}^{x} \mathrm{d}y \; u_{\rm SD}(x)\, u_{m{\rm D}}(y)$$

$$\times \prod_{i=1}^{M} U_{{\rm S}i}\left(x\left(1 - \frac{t}{y}\right)\right) \prod_{\substack{i=1 \\ i\neq m}}^{M} \left[1 - U_{i{\rm D}}(y)\right] \tag{G-8d}$$

where the summands (G-8c) and (G-8d) are respectively obtained from (G-8a) and (G-8b) by conditioning on $\tau_{{\rm S}m}$ and $\tau_{m{\rm D}}$, and on $\tau_{\rm SD}$ and $\tau_{m{\rm D}}$.

G.3 The P-t Scheme

In P-t, Node S transmits more than t seconds, for a given t, if one of the following cases happens. 1) We have $\tau_{\rm SD} \leq t_0$, which means that the protocol reduces to DT (see the proof of Lemma 6.1), and we have $\tau_{\rm SD} > t$, which means that Node D needs to receive more than t seconds from Node S to decode. 2) We have $\max\{t, t_0\} < \tau_{\rm SD} \leq t + t_0$. In this case, Node S transmits to Node D more than t seconds only if no relay qualifies as the downlink node until $\tau_{\rm SD} - t_0$. Recalling (6.11), one observes that this happens when $\Theta_m(\tau_{\rm SD} - t_0) > t_0$, where $\Theta_\cdot(\cdot)$ is given by (6.11), or equivalently $\tau_{m{\rm D}} > \tau_{\rm SD}$, for any m. 3) The condition $\max\{t, t_0\} > t + t_0$ holds. In this case, for any $m \in \mathcal{D}(t)$ we should have $\Theta_m(t) > t_0$. This means that no decoding relay qualifies for the downlink transmission prior to t. Also, if $\mathcal{D}(t) = \{1, \ldots, M\}$, Node S should have the best link to Node D. Now, we can write, from these three cases,

$$\begin{aligned}
\Pr\{T_{\rm S} > t\} &= \Pr\{t < \tau_{\rm SD} \leq t_0\} \\
&\quad + \Pr\left\{\max\{t, t_0\} < \tau_{\rm SD} \leq t + t_0, \bigcap_{m=1}^{M} \left(\tau_{{\rm S}m} > \tau_{\rm SD} - t_0 \cup \tau_{m{\rm D}} > \tau_{\rm SD}\right)\right\} \\
&\quad + \Pr\left\{\tau_{\rm SD} > t + t_0, \bigcap_{m=1}^{M} \left(\tau_{{\rm S}m} > t \cup \left(1 - \frac{t}{\tau_{\rm SD}}\right)\tau_{m{\rm D}} > t_0\right), \right. \\
&\qquad \left. \left(\tau_{{\rm S}(M)} > t \cup \min_{m\in\{1,\cdots,M\}} \tau_{m{\rm D}} > \tau_{\rm SD}\right)\right\}
\end{aligned}$$

$$= \max\{U_{\mathrm{SD}}(t_0) - U_{\mathrm{SD}}(t), 0\}$$

$$+ \int_{\max\{t,t_0\}}^{t+t_0} \mathrm{d}x \; u_{\mathrm{SD}}(x) \prod_{m=1}^{M} \left[1 - U_{\mathrm{S}m}(x - t_0)\, U_{m\mathrm{D}}(x)\right]$$

$$+ \int_{t+t_0}^{\infty} \mathrm{d}x \; u_{\mathrm{SD}}(x) \Bigg\{ \prod_{m=1}^{M} \left[1 - U_{\mathrm{S}m}(t)\, U_{m\mathrm{D}}\left(\frac{t_0\, x}{x - t}\right)\right]$$

$$- \prod_{m=1}^{M} U_{\mathrm{S}m}(t) \left[U_{m\mathrm{D}}(x) - U_{m\mathrm{D}}\left(\frac{t_0\, x}{x - t}\right)\right] \Bigg\}. \tag{G-9}$$

Regarding relay transmissions and to calculate $\mathrm{E}\{T_{\mathrm{R}_m} > t\}$, first recall from (6.11) that if Node S transmits t seconds and then Node R_m substitutes for Node S, it takes

$$\Theta_m(t) = \left(1 - \frac{t}{\tau_{\mathrm{SD}}}\right) \tau_{m\mathrm{D}} \tag{G-10}$$

seconds more until Node D decodes. Let t_m be defined as the time t at which $\Theta_m(t) = t_0$; i.e.,

$$t_m \triangleq \left(1 - \frac{t_0}{\tau_{m\mathrm{D}}}\right) \tau_{\mathrm{SD}}. \tag{G-11}$$

Also, note that $\tau_{\mathrm{S}m}$ is the time at which R_m can decode. Therefore, based on the protocol description in Section 6.3,

$$T_{\mathrm{UL}}^{(\mathrm{R}_m)} \triangleq \max\{\tau_{\mathrm{S}m}, t_m\} \tag{G-12}$$

is the time at which R_m qualifies as a candidate for the downlink transmission. Meanwhile,

$$T_{\mathrm{UL}}^{(\mathrm{S})} \triangleq \max\{0, \tau_{\mathrm{SD}} - t_0\} \tag{G-13}$$

is the time at which Node S becomes qualified.

Combining all these facts, Node R_m becomes the downlink transmitter in either of these following two cases. 1) The time $T_{\mathrm{UL}}^{(\mathrm{R}_m)}$ is the smallest among all the $T_{\mathrm{UL}}^{(X)}$'s where $X \in \{\mathrm{S}, \mathrm{R}_1, \cdots, \mathrm{R}_M\}$, and not all relays decode before $T_{\mathrm{UL}}^{(\mathrm{R}_m)}$. In this case, the uplink time equals $T_{\mathrm{UL}}^{(\mathrm{R}_m)}$ and the downlink time is $\Theta_m\Big(T_{\mathrm{UL}}^{(\mathrm{R}_m)}\Big)$. 2) All relays decode before $T_{\mathrm{UL}}^{(\mathrm{R}_m)}$, and we have that $T_{\mathrm{UL}}^{(\mathrm{R}_m)} < T_{\mathrm{UL}}^{(\mathrm{S})}$ and that R_m has the best link to Node D among the relays. In this case, the uplink and downlink times are given by $\tau_{\mathrm{S}(M)}$ and $\Theta_m\big(\tau_{\mathrm{S}(M)}\big)$, respectively, where $\tau_{\mathrm{S}(M)}$ is the time that the last relay decodes. Now, based on these observations and using (6.11), (G-13), and (G-12), we can write

$$\Pr\{T_{\mathrm{R}_m} > t\} = \Pr\Bigg\{T_{\mathrm{UL}}^{(\mathrm{R}_m)} < \tau_{\mathrm{SD}} - t_0,\, T_{\mathrm{UL}}^{(\mathrm{R}_m)} \leq \tau_{\mathrm{S}(M)},\, \Theta_m\Big(T_{\mathrm{UL}}^{(\mathrm{R}_m)}\Big) > t,$$

$$\bigcap_{\substack{i=1\\ i\neq m}}^{M}\left(\tau_{\mathrm{S}i} > T_{\mathrm{UL}}^{(\mathrm{R}_m)} \cup \Theta_i\Big(T_{\mathrm{UL}}^{(\mathrm{R}_m)}\Big) > t_0\right)\Bigg\}$$

$$+\Pr\left\{\tau_{\mathrm{S}(M)} < T_{\mathrm{UL}}^{(\mathrm{R}_m)} < \tau_{\mathrm{SD}} - t_0,\, \Theta_m\Big(\tau_{\mathrm{S}(M)}\Big) > t,\, \min_{m\in\{1,\cdots,M\}} \tau_{m\mathrm{D}} = \tau_{m\mathrm{D}}\right\}$$

$$=\Pr\left\{\tau_{\mathrm{S}m} > \tau_{\mathrm{SD}}\left(1-\frac{t_0}{\tau_{m\mathrm{D}}}\right), \tau_{\mathrm{S}m} < \tau_{\mathrm{SD}} - t_0, \frac{\tau_{\mathrm{S}m}}{\tau_{\mathrm{SD}}} + \frac{t}{\tau_{m\mathrm{D}}} < 1,\right.$$

$$\left.\bigcap_{\substack{i=1\\ i\neq m}}^{M}\left(\tau_{\mathrm{S}i} > \tau_{\mathrm{S}m} \cup \tau_{i\mathrm{D}} > \frac{t_0}{1-\frac{\tau_{\mathrm{S}m}}{\tau_{\mathrm{SD}}}}\right)\right\}$$

$$+\Pr\left\{\tau_{\mathrm{S}m} \le \tau_{\mathrm{SD}}\left(1-\frac{t_0}{\tau_{m\mathrm{D}}}\right) \le \tau_{\mathrm{S}(M)},\, \tau_{M\mathrm{D}} < \tau_{\mathrm{SD}},\, t < t_0,\right.$$

$$\left.\bigcap_{\substack{i=1\\ i\neq m}}^{M}\left(\tau_{\mathrm{S}i} > \tau_{\mathrm{SD}}\left(1-\frac{t_0}{\tau_{m\mathrm{D}}}\right) \cup \tau_{i\mathrm{D}} > \tau_{m\mathrm{D}}\right)\right\}$$

$$+\Pr\left\{\tau_{\mathrm{SD}}\left(1-\frac{\max\{t,t_0\}}{\tau_{m\mathrm{D}}}\right) > \tau_{\mathrm{S}(M)},\, \tau_{m\mathrm{D}} = \min_{i\in\{1,\cdots,M\}} \tau_{i\mathrm{D}} < \tau_{\mathrm{SD}}\right\}$$

$$=\int_{t_0}^{\infty}\mathrm{d}x\int_{0}^{x-t_0}\mathrm{d}y\; u_{\mathrm{SD}}(x)\, u_{\mathrm{S}m}(y)\, \max\left\{U_{m\mathrm{D}}\left(\frac{t_0\, x}{x-y}\right) - U_{m\mathrm{D}}\left(\frac{t\, x}{x-y}\right), 0\right\}$$

$$\times\prod_{\substack{i=1\\ i\neq m}}^{M}\left[1-U_{\mathrm{S}i}(y)\, U_{i\mathrm{D}}\left(\frac{t_0\, x}{x-y}\right)\right]$$

$$+\int_{t_0}^{\infty}\mathrm{d}x\int_{t_0}^{x}\mathrm{d}y\; u_{\mathrm{SD}}(x)\, u_{m\mathrm{D}}(y)\, U_{\mathrm{S}m}\left(x\left(1-\frac{t_0}{y}\right)\right)$$

$$\times\left\{\prod_{\substack{i=1\\ i\neq m}}^{M}\left[1-U_{\mathrm{S}i}\left(x\left(1-\frac{t_0}{y}\right)\right)\, U_{i\mathrm{D}}(y)\right] - \prod_{\substack{i=1\\ i\neq m}}^{M} U_{\mathrm{S}i}\left(x\left(1-\frac{t_0}{y}\right)\right)\left[1-U_{i\mathrm{D}}(y)\right]\right\}$$

$$+\int_{\max\{t,t_0\}}^{\infty}\mathrm{d}x\int_{\max\{t,t_0\}}^{x}\mathrm{d}y\; u_{\mathrm{SD}}(x)\, u_{m\mathrm{D}}(y)$$

$$\times\prod_{i=1}^{M} U_{\mathrm{S}i}\left(x\left(1-\frac{\max\{t,t_0\}}{y}\right)\right)\prod_{\substack{i=1\\ i\neq m}}^{M}\left[1-U_{i\mathrm{D}}(y)\right] \tag{G-14}$$

where the second equality is obtained after separately considering the two cases of $\tau_{\mathrm{S}m} > t_m$ and $\tau_{\mathrm{S}m} \le t_m$ (see (G-13) and (G-12)), and where the third equality is obtained by conditioning on τ_{SD}, $\tau_{\mathrm{S}m}$, and $\tau_{m\mathrm{D}}$.